

# **Topology and Telechelic Functionality Control in Polyester Design**

Gozde Ipek Ozturk

Dissertation submitted to the faculty of the Virginia Polytechnic Institute and State  
University in partial fulfillment of the requirements for the degree of

Doctor of Philosophy  
In  
Macromolecular Science and Engineering

Timothy E. Long, Committee Chair  
Judy S. Riffle, Committee Member  
Richard Turner, Committee Member  
Garth Wilkes, Committee Member  
Robert B. Moore, Committee Member

May 29, 2009  
Blacksburg, Virginia

Keywords: Polyester, Topology, Polycondensation, Michael Addition, Adhesion

Copyright 2009, Gozde I. Ozturk

# Topology and Telechelic Functionality Control in Polyester Design

Gozde I. Ozturk

## ABSTRACT

Research efforts have focused on synthesis of linear, long-chain branched, and novel crosslinked polyesters for applications spanning from pressure sensitive adhesives to biomedical applications. Altering polymer topology and functionality using different synthetic strategies was enabled tailoring the thermomechanical, rheological, and adhesive properties of polyesters. The synthesis and characterization of linear, long-chain branched, and crosslinked networks are described focusing on the structure-property relationships.

Aliphatic low- $T_g$  polyesters with linear and long-chain branched topology were synthesized using melt polycondensation for pressure sensitive adhesive applications. Relationships between molecular weight, polymer composition, and adhesive performance were investigated. Melt rheological studies and the characterization of adhesive properties indicated that adhesive performance was enhanced with increasing molecular weight. Moreover, a series of long-chain branched low- $T_g$  polyester were investigated to determine the influence of branching and molecular weight. Tailoring the degree of branching enabled the control of rheological and adhesive properties. Characterization of adhesive properties revealed that long-chain branched polymers displayed an enhanced cohesive strength. In addition, utilization of different comonomer compositions allowed tailoring thermal and adhesive properties of low- $T_g$  polyesters over a wide range.

Biodegradable networks were synthesized for the first time using base-catalyzed Michael addition of acetoacetate functionalized polyesters with acrylates. Linear and star-shaped poly( $\epsilon$ -caprolactone) (PCL) oligomers with different molecular weights were functionalized and crosslinked. Thermomechanical properties were evaluated as a function of precursor molecular weight and crosslink density. The glass transition temperature and the extent of crystallinity of the networks were dependent on the molecular weight of the PCL segment. Moreover, dynamic mechanical analysis (DMA) indicated that molecular weight of the oligomeric precursors influenced the plateau modulus of the networks as a result of the differences in crosslink density of the networks. In addition, covalently crosslinked networks were synthesized from Michael addition reaction of acetoacetate-functional oligomeric poly(trimethylene succinate)s and poly(trimethylene adipate)s with neopentylglycol diacrylate. The oligomeric polyesters with telechelic hydroxyl functionality were synthesized from renewable monomers, adipic acid, succinic acid, and 1,3-propanediol using melt polycondensation. The molecular weights of the precursors were varied systematically to probe the influence of molecular weight on thermomechanical properties of the networks. The extent of crystallinity and mechanical properties were dependent on the molecular weight of the oligomeric polyester precursors which also controlled crosslink density. Moreover, Michael addition chemistry was utilized to crosslink low- $T_g$  polyesters to improve cohesive strength for PSA applications. In order to determine the influence of temperature and catalyst levels, crosslinking reactions were monitoring using measurement of loss and storage moduli during the reaction. Networks having different

levels of gel fractions were investigated to elucidate the influence of degree of crosslinking on thermomechanical and adhesive properties of low- $T_g$  polyesters.

## **Table of Contents**

<b>Chapter 1: Introduction</b> .....	1
1.1 Dissertation overview.....	1
<b>Chapter 2: Literature Review</b> .....	4
2.1 Abstract.....	4
2.2 Scientific rationale and perspective.....	4
2.3 Thermoplastic elastomers.....	6
2.3.1 Polyurethanes.....	9
2.3.1.1 Poly(ester urethane)s.....	14
2.3.1.2 Poly(ether urethane)s.....	17
2.3.2 Polyesters.....	19
2.3.2.1 Poly(ether ester)s.....	22
2.3.2.1 Block polyesters.....	23
2.3.3 Polyamides.....	25
2.3.3.1 Poly(ether amide)s.....	26
2.3.3.2 Poly(ester amide)s.....	28
2.4 Thermoset elastomers.....	30
2.4.1 UV crosslinking.....	31
2.4.2 Polymerization of multifunctional groups.....	36
2.4.3 Michael addition.....	38
2.5 Conclusions.....	41
2.6 Acknowledgements.....	42
2.7 References.....	42

<b>Chapter 3: Melt synthesis and characterization of aliphatic low-<math>T_g</math> polyesters as pressure sensitive adhesives</b> .....	48
3.1 Abstract.....	48
3.2 Introduction.....	49
3.3 Experimental.....	51
3.3.1 Materials.....	51
3.3.2 Polymer characterization.....	52
3.3.3 Synthesis of low- $T_g$ polyesters.....	53
3.3.4 Characterization of adhesive properties.....	53
3.3.4.1 180 ° Peel testing .....	54
3.3.4.2 Loop tack and rolling ball tack.....	54
3.3.4.3 Holding power.....	54
3.4 Results and Discussion.....	55
3.5 Conclusions.....	64
3.6 Acknowledgements.....	65
3.7 References.....	65
<b>Chapter 4: Influence of long-chain branching on adhesive properties of aliphatic low-<math>T_g</math> polyesters</b> .....	68
4.1 Abstract.....	68
4.2 Introduction.....	69
4.3 Experimental.....	73
4.3.1 Materials.....	73
4.3.2 Characterization.....	73

4.3.3 Adhesive Testing .....	74
4.3.3.1 180 ° Peel testing .....	75
4.3.3.2 Holding power.....	75
4.3.4 Synthesis of low-T <sub>g</sub> polyesters.....	75
4.3.5 Synthesis of long-chain branched low-T <sub>g</sub> polyesters in the presence of.....	
monofunctional monomers.....	76
4.4 Results and Discussion.....	79
4.5 Conclusions.....	88
4.6 Acknowledgements.....	89
4.7 References.....	89
<b>Chapter 5: Melt synthesis and characterization of aliphatic copolyesters for pressure sensitive adhesive applications.....</b>	<b>89</b>
5.1 Abstract.....	89
5.2 Introduction.....	89
5.3. Experimental.....	94
5.3.1 Materials .....	94
5.3.2 Synthesis of low-T <sub>g</sub> polyesters .....	94
5.3.3 Synthesis of low-T <sub>g</sub> polyesters in the presence of comonomers.....	95
5.3.4 Characterization.....	98
5.3.5 Characterization of adhesive properties.....	98
5.3.5.1 180 ° Peel testing .....	98
5.3.5.2 Holding power.....	99
5.4 Results and Discussion.....	99

5.5 Conclusions.....	108
5.6 Acknowledgements.....	109
5.7 References.....	109
<b>Chapter 6: Michael addition crosslinking of poly(caprolactone)s.....</b>	<b>110</b>
6.1 Abstract.....	110
6.2 Introduction.....	111
6.3 Experimental.....	116
6.3.1 Materials .....	116
6.3.2 Characterization .....	116
6.3.3 Synthesis of acetoacetate-functionalized poly(caprolactone) .....	
(PCL bisAcAc).....	118
6.3.4 Synthesis of poly(caprolactone) networks: crosslinking reactions.....	118
6.4 Results and Discussion.....	119
6.4.1 Synthesis of acetoacetate-functionalized poly(caprolactone) .....	
(PCL bisacac) .....	119
6.4.2 Crosslinking of PCL bisacetoacetate and neopentyl glycol diacrylate .....	126
6.5 Conclusions.....	141
6.6 Acknowledgements.....	142
6.7 References.....	141
<b>Chapter 7: Michael addition crosslinking of acetoacetate-functionalized poly(trimethylene adipate)s and poly(trimethylene succinate)s.....</b>	<b>144</b>
7.1 Abstract.....	144
7.2 Introduction.....	145

7.3. Experimental.....	149
7.3.1 Materials .....	149
7.3.2 Characterization .....	149
7.3.3 Synthesis of oligomeric polyester polyols.....	150
7.3.4 Acetoacetate end-functionalization of polyesters polyols .....	151
7.3.5 Synthesis of crosslinked networks .....	151
7.4 Results and discussion.....	152
7.4.1 Synthesis of hydroxyl telechelic polyesters .....	152
7.4.2 Synthesis of acetoacetate-functionalized polyesters.....	154
7.4.3 Network synthesis.....	164
7.5 Conclusions.....	173
7.6 Acknowledgements.....	173
7.7 References.....	174
<b>Chapter 8: Crosslinking of aliphatic low-<math>T_g</math> polyesters for adhesive and coating applications.....</b>	<b>176</b>
8.1 Abstract.....	176
8.2 Introduction.....	176
8.3. Experimental.....	179
8.3.1 Materials .....	179
8.3.2 Characterization .....	179
8.3.3 Synthesis of oligomeric low- $T_g$ polyester polyols .....	180
8.3.4 Acetoacetate end-functionalization of oligomeric low- $T_g$ polyesters.....	181
8.3.5 Synthesis of crosslinked networks .....	181

8.4 Results and discussion.....	182
8.5 Conclusions.....	192
8.6 Acknowledgements.....	193
8.7 References.....	193
<b>Chapter 9: Overall conclusions.....</b>	<b>195</b>
<b>Chapter 10: Suggested future work.....</b>	<b>199</b>
10.1 Synthesis of low- $T_g$ polyesters for PSA applications.....	199
10.2 Synthesis of polyester based Michael addition networks.....	200
10.3 UV-curing of Michael Addition Networks .....	202
10.4 References.....	207

## List of Figures

Figure 2.1. Schematic representation of a TPU.....	6
Figure 2.2. Examples of polyethers a) poly(ethylene oxide), b) poly(tetramethylene oxide), and c) poly(propylene oxide).....	8
Figure 2.3. Chemical structures of crystallizable soft segments a) poly(caprolactone) and b) poly(butylene adipate).....	9
Figure 2.4. Synthesis of degradable hard block from 1,4-butanediol and L-lysine diisocyanates.....	11
Figure 2.5. Chemical structures of polyurethanes synthesized from threitol, arabinitol, and xylitol. ....	12
Figure 2.6. Chemical structures of commonly utilized polyester based soft segments....	14
Figure 2.7. Synthetic scheme for synthesis of novel oligomeric polyols.....	15
Figure 2.8. Coupling of 4-hydroxybenzaldehyde spacer to hydrolyzable phosphate linkage and attachment of <i>p</i> -aminosalicylic acid to the spacer.....	16
Figure 2.9. Synthesis of highly branched poly(ester urethane)s via $A_2 + B_3$ polymerization.....	17
Figure 2.10. The chemical structure of polyisoprenol.....	19
Figure 2.11. Synthesis of PET-PCL block copolymer.....	24
Figure 2.12. Chemical structures of the soft segments and hard of poly(ether ester amide)s.....	29
Figure 2.13. Synthetic scheme for synthesis of poly(ester amide) from 1,3-diamino-2-hydroxy-propane with glycerol, D,L-threitol, and sebacic acid.....	30
Figure 2.14. Photopolymerization via (a) photocleavage and (b) hydrogen abstraction..	32
Figure 2.15. Synthesis of star-shaped poly(lactide) containing fumarate functionality....	34
Figure 2.16. Chemical structure of multifunctional lactic acid oligomer with poly(ethylene glycol) core.....	35
Figure 2.17. Synthesis of degradable crosslinkers.....	36
Figure 2.18. (a) Chemical structures of gluconolactone and citric acids. (b) Structure of post-polymerization product.....	37
Figure 2.19. Mechanism of carbon-Michael addition reaction.....	39

Figure 2.20. Crosslinking of poly(caprolactone) bisacetoacetate with NPGDA in the presence of DBU.....	41
Figure 3.1. <sup>1</sup> H NMR of linear DMCD-DEG based polyester.....	57
Figure 3.2. Dynamic mechanical analysis of molecular weight series.....	61
Figure 3.3. Tack properties of molecular weight series measured with rolling ball and loop tack techniques.....	62
Figure 3.4. Peel and shear properties of molecular weight series.....	64
Figure 4.1. Effect of molecular weight on adhesive properties.....	70
Figure 4.2. Four-quadrant viscoelastic window concept proposed by Yang and Chang..	71
Figure 4.3. Temperature sweep of linear and branched polyesters.....	82
Figure 4.4. Peel strength and holding power properties of linear and low-T <sub>g</sub> polyesters	83
Figure 4.5. <sup>1</sup> H NMR of dodecylester endcapped long-chain branched polyester.....	84
Figure 4.6. <sup>1</sup> H NMR of poly(propylene glycol) monobutyl ether endcapped long-chain branched polyester. ....	86
Figure 4.7. Viscoelastic window of linear and long-chain branched polyesters.....	88
Figure 5.1. Dynamic mechanical analysis of polyesters having various amounts of 1,4-butanediol.....	101
Figure 5.2. Peel strength results of low-T <sub>g</sub> copolyester containing different amounts of 1,4-butanediol.....	103
Figure 5.3. Holding power results of copolymers containing different amounts of 1,4-butanediol.....	103
Figure 5.4. Temperature dependence of copolyesters having different amounts of 1,4-cyclohexanedimethanol.....	105
Figure 5.5. Peel strength results of copolyesters containing different amounts of ..... CHDM.....	106
Figure 5.6. Holding power results of copolyesters containing different amounts of CHDM.....	107
Figure 5.7. Influence of diol type on holding power of low-T <sub>g</sub> polyesters containing a) 100 mol% DEG, b) 15 mol% 1,4-butanediol, and c) 25 mol% CHDM.....	108
Figure 6.1. <sup>1</sup> H NMR spectra of acetoacetate functionalized poly(caprolactone) (PCL bisacac) .....	121

Figure 6.2. MALDI-TOF MS of a) acetoacetate-functionalized poly(caprolactone) (PCL bisAcAc) and b) poly(caprolactone) diol.....	122
Figure 6.3. Comparison of SEC refractive index trace of PCL diol and PCL bisacetoacetate.....	124
Figure 6.4. Stacked <i>in situ</i> FTIR spectra of crosslinking of PCL bisAcAc with neopentyl glycol diacrylate showing 810 cm <sup>-1</sup> .....	128
Figure 6.5. Thermogravimetric analysis of PCL precursors and networks.....	129
Figure 6.6. DSC analysis of networks from crosslinking of NPGDA with PCL bisacetoacetate a) 4000, b) 2000, and c) 1000 g/mol.....	130
Figure 6.7. DSC of PCL(1K)-NPGDA networks a) after 1 week of storage b) after 2 months of storage.....	131
Figure 6.8. DMA of networks with varying PCL molecular weight.....	133
Figure 6.9. Tensile testing of PCL networks.....	135
Figure 6.10. Comparison of SEC refractive index trace of PCL diol and PCL bisacetoacetate.....	136
Figure 6.11. Thermogravimetric analysis of PCL triol and the corresponding network..	137
Figure 6.12. DSC analysis of PCL networks from crosslinking of NPGDA with a) PCL bisacetoacetate and b) PCL trisacetoacetate.....	138
Figure 6.13. DMA analysis of PCL networks from crosslinking of NPGDA with a) PCL bisacetoacetate and b) PCL trisacetoacetate.....	139
Figure 6.14. Swelling properties of PCL networks in THF. ....	146
Figure 7.1. <sup>1</sup> H NMR spectroscopy comparison of a) poly(trimethylene adipate) diol and b) poly(trimethylene adipate) bisacac.....	156
Figure 7.2. SEC RI detector traces of a) poly(trimethylene adipate) diol and b) poly(trimethylene adipate) bisacac.....	158
Figure 7.3. MALDI-TOF MS comparison of poly(trimethylene adipate) diol and poly(trimethylene adipate) bisacac.....	160
Figure 7.4. MALDI-TOF MS comparison of poly(trimethylene succinate) diol and poly(trimethylene succinate) bisacac.....	161
Figure 7.5. DSC of poly(trimethylene succinate) diol oligomers with molecular weights of a) 1000, b) 2000, and c) 4000 g/mol.....	163

Figure 7.6. DSC of poly(trimethylene adipate) diol oligomers having molecular weight of a) 1000, b) 2000, and c) 4000 g/mol.....	165
Figure 7.7. DSC analysis of networks synthesized from NPGDA and poly(trimethylene adipate) 4000 g/mol after a) two days and b) after two months.....	168
Figure 7.8. DSC comparison of poly(trimethylene adipate)-NPG networks.....	169
Figure 7.9. DMA of networks synthesized from NPGDA and poly(trimethylene adipate) 4000 g/mol after a) two days b) after two months.....	171
Figure 7.10. DMA of networks synthesized from NPGDA and poly(trimethylene adipate) a) 1000 b) 2000, and c) 4000 g/mol.....	172
Figure 8.1. <sup>1</sup> H NMR spectroscopy comparison of polyester polyol synthesized from polycondensation of CHDA and DEG.....	184
Figure 8.2. <sup>1</sup> H NMR spectra of polyester polyol a) after and b) before transacetoacetylation.....	186
Figure 8.3. SEC RI detector traces of polyester polyol a) after and b) before transacetoacetylation.....	187
Figure 8.4. DSC analysis of (a) polyester precursor and the networks synthesized from NPGDA and acetoacetate-functionalized low-T <sub>g</sub> polyester having gel fractions of (b) 10, c) 60, and d) 80%.....	189
Figure 8.5. Dependence of T <sub>g</sub> of the networks on gel fraction.....	190
Figure 8.6. Rheological analysis of crosslinking at 40 °C.....	191
Figure 8.7. Rheological analysis of crosslinking at 40 °C using a) 0.75, b) 0.05, and c) 0.025 wt% DBU catalyst.....	192
Figure 10.1. Chemical structure of dimethyl-5-sulfoisophthalate sodium salt.....	199
Figure 10.2. Chemical structure of poly(ethylene glycol) diacrylate.....	201
Figure 10.3. Synthesis of Michael addition oligomer.....	203
Figure 10.4. Proposed mechanism for formation of radical species upon UV exposure of a of Michael addition oligomer.....	204
Figure 10.5. DSC analysis of Michael addition oligomer a) neat oligomer (before UV radiation) and b) after UV radiation .....	206

## List of Schemes

Scheme 3.1. Synthesis of linear low- $T_g$ polyester via melt polycondensation.....	56
Scheme 4.1. Synthesis of long-chain branched low- $T_g$ polyester in the presence of 1-dodecanol.....	77
Scheme 4.2. Synthesis of long-chain branched low- $T_g$ polyester in the presence of poly(propylene glycol) monobutyl ether.....	78
Scheme 5.1. Synthetic scheme for polycondensation of DMCD and DEG.....	95
Scheme 5.2. Polycondensation of dimethyl-1,4-cyclohexanedicarboxylate (DMCD), diethylene glycol (DEG), and 1,4-cyclohexanedimethanol (CHDM).....	96
Scheme 5.3. Polycondensation of dimethyl-1,4-cyclohexanedicarboxylate (DMCD), diethylene glycol (DEG), and 1,4-butanediol.....	97
Scheme 6.1. Mechanism of carbon-Michael addition reaction of acetoacetates and acrylates.....	114
Scheme 6.2. Synthesis of bisacetoacetate functionalized poly(caprolactone).....	119
Scheme 6.3. Crosslinking of poly(caprolactone) bisacetoacetate with neopentyl glycol diacrylate.....	127
Scheme 7.1. Mechanism of Michael addition reaction.....	147
Scheme 7.2. Synthesis of poly(trimethylene adipate) and poly(trimethylene succinate) ..... Diol .....	152
Scheme 7.3. Transacetoacetylation of poly(trimethylene adipate) diol.....	155
Scheme 8.1. Synthesis of oligomeric low- $T_g$ polyester polyol from polycondensation of CHDA and DEG.....	183
Scheme 8.2. Acetoacetate functionalization of low- $T_g$ polyols.....	186
Scheme 8.3. Crosslinking of acetoacetate-functionalized low- $T_g$ polyester with NPGDA in the presence of DBU.....	188

## List of Tables

Table 3.1. Summary of thermal analysis results (DMAP: dimethyl adipate, DMCD: 1,4-dimethyl cyclohexanedicarboxylate, DEG: diethylene glycol, and TEG: triethylene glycol). .....	58
Table 3.2. Summary of molecular weight and peel properties of linear low- $T_g$ polyesters .....	58
Table 3.3. Thermal analysis and SEC results of DMCD and DEG based low- $T_g$ polyesters having various molecular weights.....	59
Table 4.1. Summary of molecular weight of linear and long-chain branched low- $T_g$ polyesters.....	81
Table 4.2. Summary of molecular weight and compositional properties of linear and long-chain branched low- $T_g$ polyesters.....	87
Table 5.1. Summary of thermal, compositional, and molecular weight characterization of copolyesters containing 1,4-butanediol.....	100
Table 5.2. Summary of thermal, compositional, and molecular weight characterization of copolyesters containing CHDM.....	104
Table 6.1. Molecular weight characterization of PCL diol and PCL bisacetoacetate precursors using $^1\text{H}$ NMR, hydroxyl-end titration, and MALDI-TOF MS.....	125
Table 6.2. Glass transition temperatures, melting point, heat of fusion, and crystallinity of the networks.....	131
Table 6.3. Summary of tensile data for PCL bisacetoacetate-NPG based networks.....	135
Table 7.1. Molecular weight data of poly(trimethylene adipate) measured using $^1\text{H}$ NMR spectroscopy, MALDI-TOF MS, and base titration.....	154
Table 7.2. Molecular weight data of poly(trimethylene succinate) measured using $^1\text{H}$ NMR spectroscopy, MALDI-TOF MS, and base titration.....	154
Table 7.3. Glass transition temperatures, melting point, and heat of fusion of poly(trimethylene succinate) diol oligomers.....	163
Table 7.4. Glass transition temperatures, melting point, and heat of fusion of poly(trimethylene adipate) diol oligomers.....	165
Table 8.1. Summary of molecular weight and thermal characterization of low- $T_g$ polyols.....	185

## Acknowledgements

I would like to thank my advisor, Prof. Timothy E. Long, for his encouragement, guidance, and tremendous support throughout my graduate career. I would like to thank all my committee members, Prof. Judy S. Riffle, Prof. S. Richard Turner, Prof. Garth Wilkes, Prof. Robert B. Moore, and Prof. Brian Love for their support and guidance.

I would like to thank various people including Millie Ryan, Tammy Jo Hiner, and Mary Jane Smith for their assistance over the years. I would like to especially thank to Laurie Good for not only editing my papers but also for her friendship. I would like to thank Vicki Long for training me on several instruments and for her support over the years. I acknowledge the funding sources for my research, including Eastman Chemical Company and MAP MURI. I would like to particularly thank to A.J. Pasquale, Jeremy Lizotte, Emmet O'Brien, Mark Peters, and Peter Miller at Chemical Company for their collaboration and technical support during my graduate studies and my internship at Eastman Chemical Company labs at Kingsport, TN.

I would like to recognize all Long group members, particularly my colleagues Brian Mather, Afia Karikari, Kalpana Viswanathan, Tomonori Saito, Ann Fornof, Sharlene Williams, Shijing Cheng, Mana Tamami, Emily Anderson, John Layman, Rebecca Huyck, Matthew Cashion, Renlong Gao, and Nancy Zhang. I would particularly like to thank my colleague, Serkan Unal for his mentorship, guidance, and support during my graduate studies. In addition, my thanks especially go to my friends Dr.Selen Olgun and Gulden Sonaer for their friendship and support starting from the first day I met them.

I cannot thank enough to my family for everything they did for me. My parents, Erol and Serap Ozturk, and my brothers, Gorkem and Anil Ozturk always supported me

and believed in me from the first day. Finally, I would like to thank my fiancé, Ufuk Karabiyik for his support, patience, love, and encouragement during everyday of my graduate life.

# Chapter 1: Introduction

## 1.1 Dissertation Overview

Polyesters offer versatile physical and chemical properties for a variety of applications. Changing the molecular structure of polyesters permits tailoring thermomechanical properties and biodegradation behavior. Polyesters are promising biodegradable polymers due to susceptibility of the ester bond to hydrolysis, predictable biodegradation kinetics, and potential to tailor the polymer composition to adjust physical properties for specific applications. However, some applications require unique thermal and physical properties. Research objectives will address tailoring thermomechanical, rheological, and adhesive properties of a variety of aliphatic polyesters through controlling the topology and functionality.

In this dissertation, aliphatic polyesters were investigated for applications varying from pressure sensitive adhesives to biodegradable networks for biomedical applications. This research examined synthesis and characterization of aliphatic polyesters having linear, long-chain branched, and crosslinked topologies. The second chapter is a literature survey related to the synthesis of elastomers, factors influencing biodegradation behavior, and recent trends to alter polymer properties through controlling the polymer architecture.

The research efforts focused on utilizing environmentally friendly, solvent-free melt polycondensation technique to synthesize polyesters with linear and long-chain branched topology. The third chapter describes the synthesis of linear aliphatic polyesters having low glass transition temperatures ( $T_g$ s) for pressure sensitive adhesive (PSA) applications. Polymerization of isomeric mixtures of dimethyl-1,4-cyclohexane

dicarboxylate (DMCD) and diethylene glycol (DEG) in the melt phase generated a series of linear low- $T_g$  polyesters with suitable viscoelastic, thermal and adhesive properties for room temperature PSA applications. Relationship between molecular weight and adhesive performance was investigated. The fourth chapter describes the synthesis and characterization of long-chain branched low- $T_g$  polyesters having a chemical composition similar to linear analogs. Incorporation of low levels of branching was explored to investigate the influence of long-chain branching on melt rheology and adhesive properties. Long-chain branched topology (LCB) was attained using a trifunctional monomer, trimethyl-1,3,5-benzene tricarboxylate (TMT). Polymers with varying degrees of branching were synthesized using different levels of TMT. Synthesis of long-chain branched polyesters in the presence of monofunctional alcohols avoided gel formation at higher conversions. Adhesive performance was investigated as a function of branching and molecular weight.

The fifth chapter describes the synthesis of linear low- $T_g$  polyesters from melt polycondensation of DMCD with various diols including DEG, 1,4-butanediol, and 1,4-cyclohexanedimethanol (CHDM) at different molar ratios. Polyesters having various compositions were synthesized to investigate the influence of molecular structure on thermomechanical properties and cohesive strength for adhesive applications. The adhesive properties were evaluated as a function of comonomer ratio.

The sixth chapter focuses on the synthesis of poly(caprolactone) (PCL) based networks from Michael addition of acetoacetate-functional oligomeric PCLs with neopentyl glycol diacrylate. Linear and star-shaped oligomeric PCL precursors with varying molecular weights were crosslinked with acrylate monomers.

Thermomechanical properties of the networks were analyzed to investigate the influence of molecular weight between crosslink points. The seventh chapter focuses on synthesis of covalently crosslinked networks from reaction of acetoacetate-functional oligomeric poly(trimethylene succinate)s and poly(trimethylene adipate)s with neopentylglycol diacrylate using Michael addition chemistry. The influence of precursor molecular weight on the thermomechanical properties was investigated.

The eighth chapter describes crosslinking of oligomeric low- $T_g$  polyesters to for PSA and coatings applications. Low- $T_g$  polyesters with telechelic acetoacetate functionalities were crosslinked with acrylates using Michael addition. Relationship between catalyst concentrations and crosslinking time was investigated using rheological analysis. The ninth chapter summarizes the conclusions and the tenth chapter describes the potential future work.

## **Chapter 2: Literature Review: Biodegradable Elastomers**

**Partially taken from:** Ozturk, G.I.; Long, T.E. “Biodegradable Elastomers”, Review article in progress, 2009.

### **2.1 Abstract**

Biodegradable polymers have been widely utilized in a variety of biomedical applications.<sup>1-3</sup> There is growing interest in tailoring polymer topologies using covalent crosslinking<sup>4,5,6</sup> and branching<sup>7</sup> to alter mechanical properties and degradation rates for different types of biomedical applications. In addition, elastomeric biodegradable polymers have attracted attention due to the need for soft materials in biomedical applications, particularly in tissue engineering applications. Biodegradable elastomers have been synthesized as thermosets<sup>5,6</sup> and thermoplastic<sup>8-11</sup> elastomers. Several synthetic methods have been utilized to control the thermomechanical properties and degradation behavior of elastomers to provide structural support, flexibility, and tunable degradation rates for diverse applications. This review focuses on a variety of synthetic methodologies to produce biodegradable elastomers, as well as the influence of topology on the physical properties of thermoset and thermoplastic elastomers.

### **2.2 Scientific Rationale and Perspective**

Several studies have investigated tailoring the biodegradation rates<sup>7,12</sup> and mechanical properties<sup>13</sup> of biodegradable polymers through altering their topology for use in different biomedical applications. Literature reports<sup>14</sup> have also described the viscosity, morphology, thermal stability, and mechanical properties of a number of biodegradable polymers that were modified by covalent crosslinking<sup>5,6</sup> and branching.<sup>7</sup> Moreover, there is a well-established literature<sup>14</sup> demonstrating that branched polymers

exhibit significantly different physical properties compared to linear polymers having similar weight-average molecular weights. Several studies<sup>15-19</sup> on polymer structure-property relationships reported that branched polymers exhibit unique thermal, rheological, and solution properties due to the presence of a large number of end groups. Branched polymers such as dendrimers, hyperbranched polymers, long-chain branched polymers, and star-shaped<sup>20</sup> polymers have been extensively investigated to probe the influence of the degree of branching, the length of the branches (i.e. long and short-chain branching), and the polymer architecture on thermal, mechanical, and drug release properties in biomedical applications.<sup>21</sup>

Although biodegradable polymers with linear and branched topology have been utilized in several biomedical applications, most are not suitable for soft tissue engineering applications due to their high modulus and low elongation properties. In particular, tissue and vascular engineering require polymers with high elasticity and low modulus that resemble the surrounding tissue.<sup>22,23</sup> There is a need for flexible and soft polymers in tissue engineering applications to reduce the likelihood of tissue irritation. Biodegradable elastomers show potential for such uses since they offer balanced mechanical strength, flexibility, and biodegradability. And in fact, such materials have been synthesized as thermoplastic or thermoset elastomers for applications that require flexible polymers with tunable degradation and release rates.<sup>23</sup> The flexibility and mechanical strength of thermoset elastomers are attained from incorporation of different degrees of crosslinking and controlling the molecular weight between crosslink points.<sup>24</sup> Additionally, the phase separated morphology of the block copolymers provides the elasticity for thermoplastic elastomers. Altering the composition of each block permits

control over hydrophilicity and degradation behavior. As discussed below, several synthetic strategies facilitate control of the overall physical and chemical properties of biodegradable thermoset and thermoplastic elastomers. This review also examines the influence of topology on mechanical properties and degradation behavior.

### 2.3 Thermoplastic Elastomers

Thermoplastic elastomers (TPEs) are utilized in a number of biomedical applications due to their biocompatibility and excellent mechanical properties.<sup>25,26</sup> Thermoplastic elastomers are phase separated block polymers that contain a hard crystalline segment and a soft rubbery phase with a low glass transition temperature (Figure 2.1).<sup>26</sup> The elasticity of thermoplastic elastomers is due to the microphase separated morphology of the hard and soft domains. The amorphous soft phase provides the elasticity, whereas the crystalline hard segment acts as a physical crosslinking point and contributes to improved mechanical strength. The presence of a crystalline phase results in heterogeneous biodegradation and the loss of mechanical strength in a non-linear fashion. Therefore, utilizing biodegradable thermoplastic elastomers has limitations in biomedical applications such as drug delivery, which requires controlled degradation behavior.

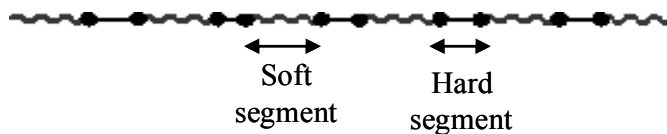


**Figure 2.1.** Schematic representation of a TPU.

Many factors influence the phase separation of the soft and hard blocks, including the molecular weight and glass transition temperature of each block.<sup>26</sup> Moreover, the

miscibility of the two phases influences the resulting phase separated morphology. Other variables such as the weight percent and length of the soft segments also play a role in the phase separation behavior of the blocks. The phase separation of the hard and soft block controls the mechanical properties and the degradation behavior of thermoplastic elastomers. As such, it is critical to characterize the phase separated morphology of these materials, which was achieved using thermal characterization and X-ray scattering techniques. Moreover, transmission electron microscopy (TEM) and atomic force microscopy (AFM) provided detailed information on the morphology of the phase separated thermoplastic elastomers, while tapping-mode AFM was utilized to characterize topography, height and phase information, and local stiffness.<sup>26</sup>

In the literature,<sup>26</sup> a variety of thermoplastic elastomers have been synthesized from segmented poly(ether ester)s, poly(ester urethane)s, poly(ether urethane)s, poly(ester amide)s, and poly(ether amide)s. The degradation behavior of TPEs is highly dependent on chemical composition and the ratio of the hard and soft blocks. A variety of hydrophilic soft segments and hydrophobic hard segments have been utilized in the synthesis of thermoplastic elastomers to control the degradation behavior and physical properties. Hydrophilic polyethers such as poly(ethylene glycol) (PEG), poly(propylene glycol) (PPG), and poly(tetramethylene oxide) (PTMO) have been used in the synthesis of thermoplastic elastomers to enhance hydrophilicity and water uptake (Figure 2.2).<sup>26,27</sup> Poly(ethylene oxide) (PEO) is commonly used as a soft hydrophilic segment in biodegradable thermoplastic poly(ether ester)s and poly(ester urethane)s. Unfortunately, the oxidative instability of PEO upon exposure to light under ambient conditions limits its use in several applications.<sup>28</sup> In comparison, polyester-based soft segments are prone

to hydrolytic and enzymatic degradation due to the presence of hydrolyzable ester groups.<sup>29</sup> Therefore, polyester polyols are preferred for the synthesis of thermoplastic elastomers for applications that require adjustable biodegradation rates. Moreover, the chemical composition of the hard segments can be modified to enhance the degradation behavior of thermoplastic elastomers, while varying the ratio of hard and soft segments and the molecular weight of each segment allows one to control phase separation. Thus, careful selection of the soft and hard segments facilitates control of the thermomechanical properties and biodegradation behavior of thermoplastic elastomers.

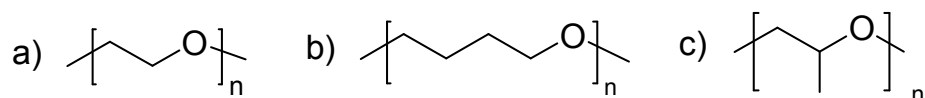


**Figure 2.2.** Examples of polyethers a) poly(ethylene oxide), b) poly(tetramethylene oxide), and c) poly(propylene oxide).

Triblock copolymers containing a poly(isobutylene) soft segment and poly(styrene) based hard segment are important examples of TPEs. Specifically, triblock poly(styrene-*b*-isobutylene-*b*-styrene)<sup>30</sup> copolymers have been utilized in biomedical applications such as drug-releasing coatings on coronary stents<sup>31</sup> (Taxus<sup>®</sup>, Translute<sup>™</sup>).<sup>32</sup> These elastomers have mechanical properties and biocompatibility resembling silicone and poly(urethane)s; however, their utilization is limited to long-term applications due to their poor biodegradability. The literature<sup>23</sup> reports other types of TPEs such as thermoplastic poly(urethane)s (TPUs) and poly(ester ether)s as important classes of biodegradable thermoplastic elastomers. The synthetic methodologies, mechanical properties, and potential applications of polyurethane, polyester, and polyamide based thermoplastic elastomers are discussed in the following sections.

### 2.3.1 Polyurethanes

Thermoplastic polyurethanes (TPUs), which represent an important class of thermoplastic elastomers, are segmented polyurethanes that consist of alternating segmented hard and soft blocks.<sup>27</sup> The microphase separation of the hard and soft segments results in exceptional mechanical properties.<sup>25</sup> TPUs have been utilized in a number of biomedical applications due their excellent mechanical properties and biocompatibility.<sup>8,10,25,33-35</sup> For example, TPUs have been used in applications that include heart valves,<sup>36</sup> pacemakers, drug delivery systems,<sup>37</sup> catheters, and scaffolds.<sup>25,38</sup>

The use of soft segments with various chemical compositions facilitates the precise tailoring of biodegradation rates over a broad range. Moreover, changing the hard and soft segment block length permits manipulation of the phase separated morphology and resulting mechanical properties.<sup>23,39</sup> Sonnenschein<sup>40</sup> demonstrated improvement of mechanical properties upon incorporation of a mixture of soft phases that contain a crystallizable diol and an amorphous segment (Figure 2.3). The presence of crystallinity in the soft phase results in significant enhancement in the modulus, however it leads to heterogeneous degradation. Conversely, tailoring the thermomechanical properties of the segmented TPUs using varying mole ratios and molecular weights of soft segments enables one to control mechanical properties while maintaining homogeneous degradation.

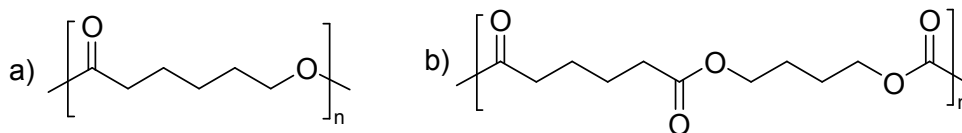


**Figure 2.3.** Chemical structures of crystallizable soft segments a) poly(caprolactone) and b) poly(butylene adipate).

Changing the chemistry of the hard and soft segments can be used to modify degradation behavior to suit the specific application example, several studies<sup>8,41</sup> reported utilizing polyester soft segments for synthesizing biodegradable TPUs. Moreover, incorporating degradable hard segments is important for enhancing the biodegradation of TPUs. Hard segments have been commonly synthesized from reactions of diisocyanates with chain extenders such as 1,4-butanediol. However, aromatic diisocyanates cannot be utilized in the synthesis of poly(urethane)s for biomedical applications due to their toxic degradation. In contrast, aliphatic diisocyanates such as 1,6-hexamethylene diisocyanates and 1,4-butane diisocyanate are non-toxic alternatives that provide biocompatibility. In addition, L-lysine diisocyanates<sup>10,33</sup> were utilized in synthesis of hard segments since their degradation products are biocompatible (Figure 2.4). Hettrich et al.<sup>41</sup> reported the synthesis of diisocyanates from several amino including glycine, alanine, leucine, and phenyl alanin to overcome problems associated with toxic aromatic diisocyanates. Moreover, the synthesis of degradable chain extenders from D,L-lactic acid and ethylene glycol have provided enhanced degradation.<sup>8</sup>

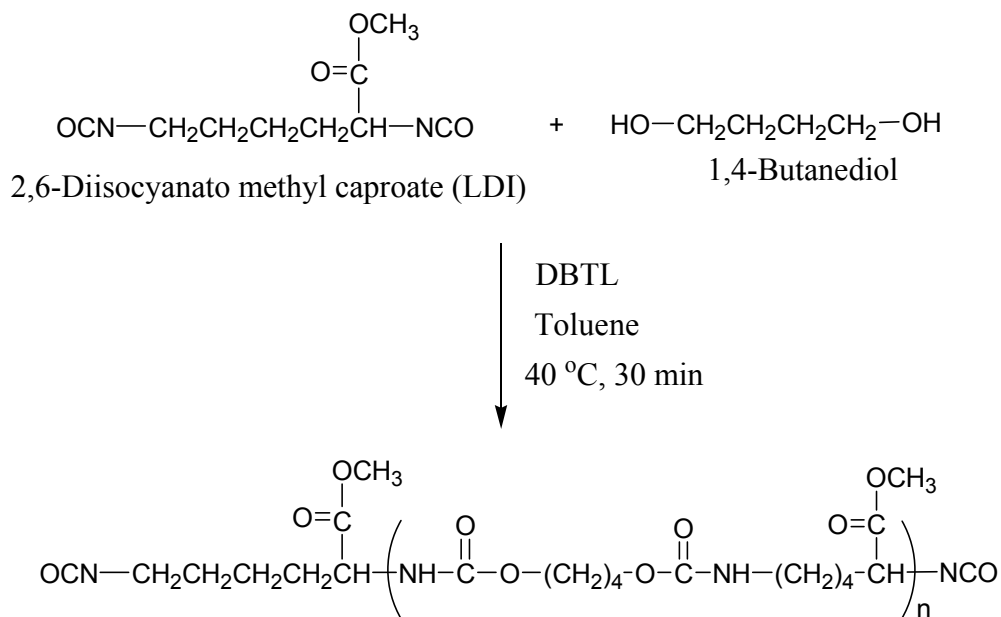
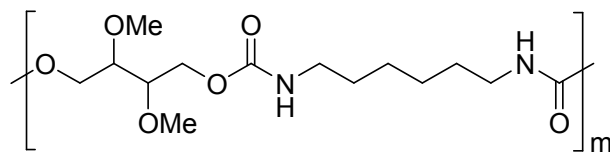


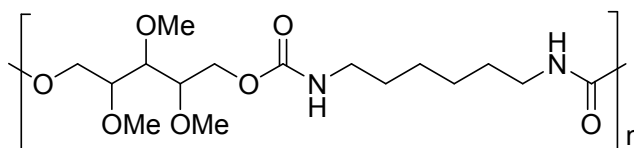
**Figure 2.4.** Synthesis of degradable hard block from 1,4-butanediol and L-lysine diisocyanates.<sup>10</sup>

Even though the incorporation of degradable hard segment has been effectively used to enhance biodegradation, several studies reported that the biodegradation behavior of TPUs is highly dependent on the composition of and the hydrophilicity of the soft phase. Incorporation of various polyols including polyethers, polyesters, and polycarbonates have been utilized in the synthesis of TPUs.<sup>9,33,42</sup> Poly(caprolactone) (PCL), poly(lactic acid) (PLA), and their copolyesters are commonly used as soft segments. In addition, the synthesis of TPUs using a mixture of polyols such as poly(propylene glycol) (PPG), poly(tetramethylene glycol) (PTMEG), and poly(ethylene oxide) have been investigated in the literature.<sup>40</sup> Moreover, the literature<sup>43</sup> describes the synthesis of polyurethanes from sugar-derived monomers to investigate the influence of labile bonds on biodegradation behavior. De Paz et al.<sup>44</sup> investigated the synthesis of poly(urethane)s using threitol, arabinitol, and xylitol, in comparison to poly(urethane)s

synthesized from 1,4-butanediol. The results revealed that sugar-containing poly(urethane)s exhibited enhanced hydrophilicity. Moreover, hydrolytic degradation was highly dependent on the size of the alditol unit (Figure 2.5).



L and D threitol-HMDI



L arabinitol and xylitol-HMDI

**Figure 2.5.** Chemical structures of polyurethanes synthesized from threitol, arabinitol, and xylitol.<sup>44</sup>

Poly(urethane)-based thermoplastic elastomers are categorized as poly(ether urethane)s or poly(ester urethane)s, depending on the composition of the soft segment. The literature reports that poly(ester urethane)s possess superior mechanical properties and better resistance to oxidation compared to poly(ether urethane)s. Conversely, poly(ether urethane)s exhibit better hydrolytic stability and functionality at low temperatures. Poly(ester urethane)s degrade *in-vivo* through hydrolytic chain scission of the ester and urethane linkages, while polyether segments are hydrolytically stable and prone to oxidative attack. Therefore, mixtures of polyester and polyether polyols have been utilized in synthesizing TPUs with adaptable degradation and hydrophilic properties. Moreover, *in-vivo* degradation behavior of TPUs depends on the presence of cell enzymes, peroxides, metal ions, and the formation of carboxylic groups. Biomedical

factors such as calcification and the resulting stress on an implant also play a significant role in the *in-vivo* degradation of TPUs used in scaffold applications. Thoma et al.,<sup>45</sup> for example, demonstrated that poly(ether urethane)s are more susceptible to calcification due to preferential interaction of the polyether soft segment with the calcium ion. Gorna et al.<sup>46</sup> showed how the synthesis of poly(urethane)s from a mixture of PCL and PPG-PEO polyols could be used to control the hydrophilicity and the calcification of implants. In addition to polyester and polyether-based soft segments, poly(dimethyl siloxane)-based soft segments<sup>47</sup> have been widely utilized in synthesizing segmented polyurethanes. PDMS-based soft segments offer several advantages in terms of hemocompatibility, thermal, and oxidative resistance.<sup>39,47</sup>

Biodegradable polyurethanes have been fabricated using a variety of techniques including leaching, solvent casting, and molding to form porous structures. Recently, electrospinning of biodegradable polymers has been utilized as an effective technique to form uniform fibers with sub-micron diameters to fabricate scaffolds for tissue engineering. There is a well established literature<sup>19,48-50</sup> demonstrating the electrospinning of various polymers for a number of applications. For example, electrospinning poly(ester urethane)s in the presence of biomacromolecules such as collagen, growth factors, and proteins has been used to fabricate scaffolds for soft tissue engineering applications.<sup>49,51</sup> Stankus et al.<sup>52</sup> showed that electrospinning a mixture of poly(ester urethane)ureas with different levels of collagen enhanced cell adhesion in the scaffold structure.

### 2.3.1.1 Poly(ester urethane)s

Poly(ester urethane)s are utilized in several biomedical applications as biodegradable elastomeric materials.<sup>25</sup> Degradable polyester soft segments have been commonly used in synthesizing TPUs for temporary implant applications due to the ability to control their degradations rates. Polyester polyols such as PCL, poly(butylene adipate)s,<sup>29</sup> poly(ethylene adipate), poly(butylene succinate)s, and their copolyesters<sup>42</sup> have been widely used as soft segments (Figure 2.6).<sup>10</sup> Several researchers<sup>42,53</sup> utilized copolyesters and mixture of polyester polyols as soft segments in the synthesis of TPUs to prevent the formation of crystallinity in the soft phase and to enhance mechanical properties without compromising important biodegradation properties.

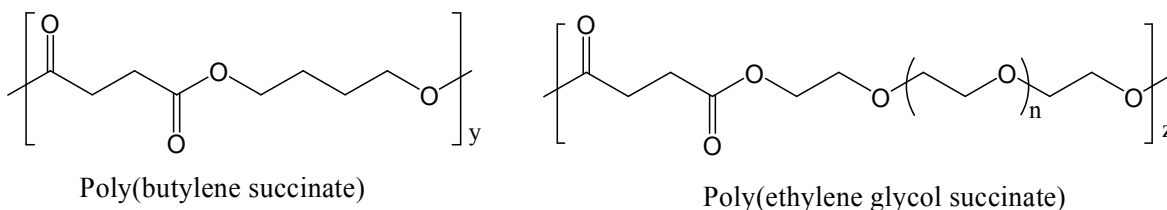


**Figure 2.6.** Chemical structures of commonly utilized polyester based soft segments.

PCL polyols have been commonly used as soft segments for the synthesis of biodegradable poly(ester urethane)s. A PCL segment with a high molecular weight is required to achieve microphase separated morphology. However, the synthesis of TPUs utilizing high molecular weight PCL polyols is limited due to crystallinity. Conversely, at molecular weights lower than 2000 g/mol the crystallinity is suppressed.<sup>27</sup> To address problems of crystallinity, several studies<sup>9,54,55</sup> investigated the synthesis of TPUs from copolyesters of PCL. Wang et al.<sup>9</sup> demonstrated the synthesis of poly(ester urethane)s using a random copolymer of L-lactide and  $\epsilon$ -caprolactone. This study showed that utilizing poly(caprolactone-*co*-lactide) random copolymers as the soft segment enhanced

the ability to adjust the modulus and elongation properties of the thermoplastic elastomers. Pierce et al.<sup>53</sup> synthesized poly(ester urethane)s using a novel amorphous polyester soft segment (Figure 2.7). The resulting poly(ester urethane)s exhibited very fast degradation behavior with a linear degradation profile. Moreover, poly(hydroxyl alkananoate)-based polyols have been utilized in synthesizing thermoplastic poly(ester urethane)s.<sup>56,57</sup> Chen et al.<sup>56</sup> described the synthesis of biodegradable and tissue compatible poly(ester urethane)s from a poly(3-hydroxybutyrate-*co*-4-hydroxybutyrate).

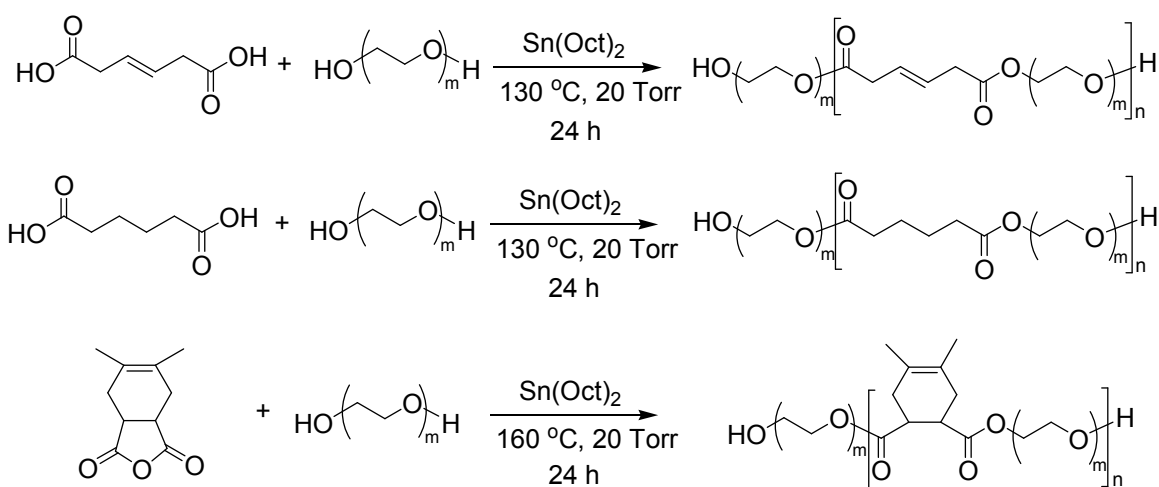


**Figure 2.7.** Synthetic scheme for synthesis of novel oligomeric polyols reported by Pierce.<sup>53</sup>

In poly(ester urethane)s, the presence of ester groups on the soft segment results in hydrolytic degradation through bulk erosion as a result of chain scission.<sup>58</sup> Literature reports<sup>8,10</sup> have detailed how ester groups hydrolyze faster compared to urethane linkages, while the degradation of hard segment is enhanced by incorporating hydrolyzable chain extenders. For example, Tatai et al.<sup>8</sup> demonstrated that incorporation of lactic acid and ethylene glycol-based degradable chain extenders could dramatically enhance biodegradation. In addition to using polyester polyols, orthoester diols were

utilized to introduce labile linkages and enhance biodegradation behavior. Dahiyat et al.<sup>59</sup> demonstrated that incorporating a hydrolyzable phosphoester group in the chain extender enhanced biodegradation. Moreover, the presence of hydrolyzable phosphate linkages on the polymer backbone enabled covalent attachment of drugs as pendant groups (Figure 2.8). In addition, Hassan et al.<sup>10</sup> described the synthesis of biodegradable poly(ester urethane)s using a degradable hard segment based on L-lysine diisocyanate and 1,4-butanediol.

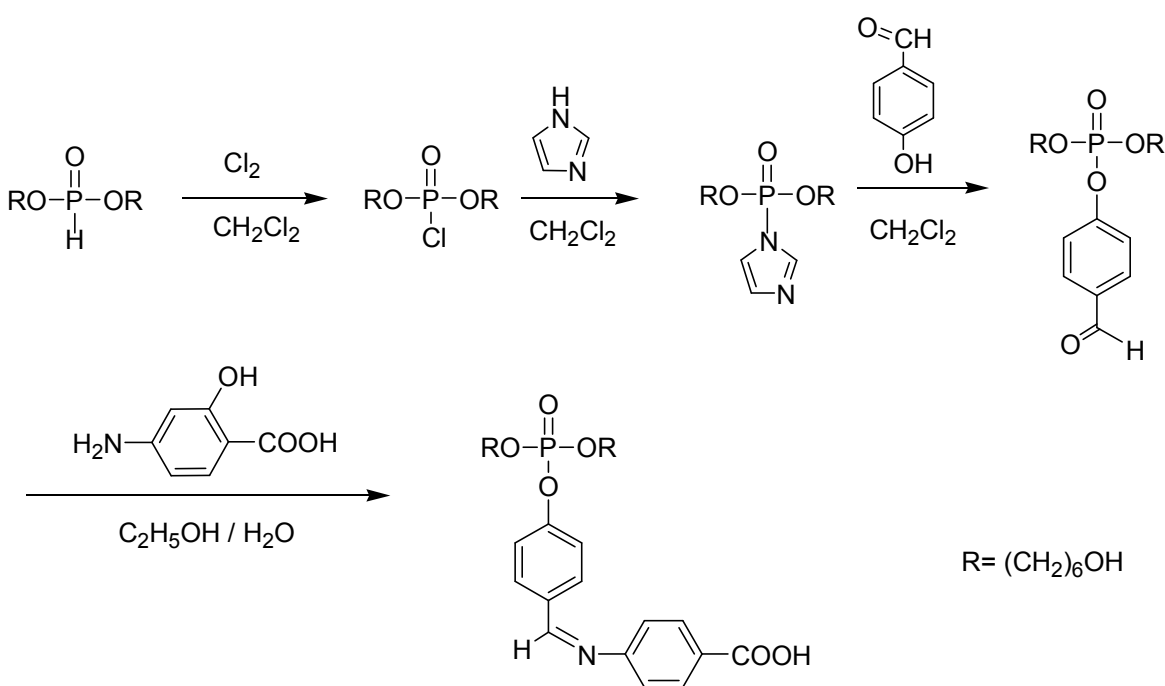


**Figure 2.8.** Coupling of 4-hydroxybenzaldehyde spacer to hydrolyzable phosphate linkage and attachment of *p*-aminosalicylic acid to the spacer.<sup>59</sup>

In addition to investigation of TPUs with linear topology, polyurethane elastomers containing segmented hyperbranched polyesters were investigated to probe the influence of branching on thermomechanical and degradation behavior.<sup>60</sup> Unal et al.<sup>61</sup> investigated the synthesis of segmented highly branched poly(ester urethane)s using an  $\text{A}_2 + \text{B}_3$  approach (Figure 2.9). TPUs with highly branched topology were synthesized

from the reaction of a trifunctional PCL polyol (oligomeric B<sub>3</sub> monomer) and an isocyanate functionalized 1,4-butanediol (A<sub>2</sub> monomer). This study demonstrated that the molecular weight of the oligomeric B<sub>3</sub> segment determined the distance between each branch point. The reaction of branched PCL yielded an amorphous morphology, whereas their linear counterparts with similar molecular weights were semicrystalline. Moreover, the presence of branching resulted in an increased number of functional end groups which enabled the synthesis of networks with high gel fractions (~92% gel content).

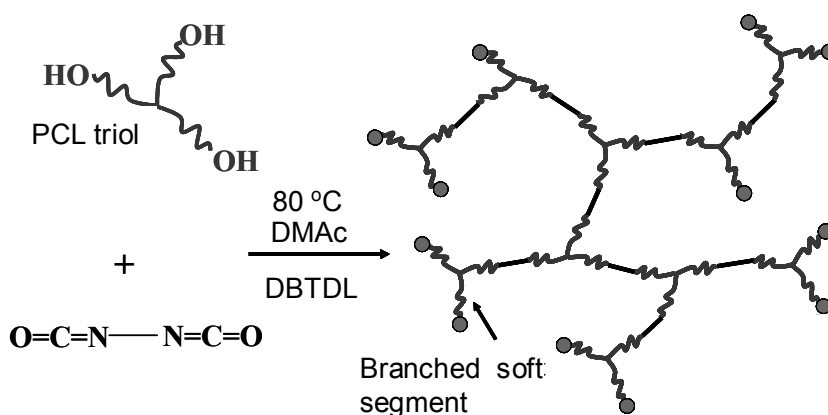


**Figure 2.9.** Synthesis of highly branched poly(ester urethane)s via A<sub>2</sub> + B<sub>3</sub> polymerization.

### 2.3.1.2 Poly(ether urethane)s

Poly(ether urethane)s are typically utilized in biomedical applications that require enhanced biostability. Polyether polyols including PEG, PPG, and PTMO have been commonly utilized as soft segments for synthesis of poly(ether urethane)s. According to the literature<sup>39</sup> poly(ether urethane)s are hydrolytically stable, while polyether-based soft segments are prone to oxidative degradation. In light of these findings, several studies investigated the incorporation of reduced levels of polyether soft segments to reduce oxidative susceptibility.<sup>62</sup> Several studies<sup>36,63</sup> reported that complexation of TPUs with

calcium ions is more pronounced in poly(ether urethane)s, and that the molecular weight of the polyether segment influences the efficiency of calcium binding. Chou et al.<sup>63</sup> showed that incorporating gold and silver nanoparticles improved thermomechanical properties and the biostability of poly(ether urethane)s. Investigation of *in-vivo* degradation of a series of poly(ether urethane)s containing silver and gold nanoparticles using SEM, microscopy, and FTIR indicated that incorporation of silver and gold nanoparticles enhanced biostability and inhibited oxidation. The enhanced biostability was attributed to free-radical scavenging of the silver and gold nanoparticles. Moreover, Schubert et al.<sup>28</sup> demonstrated how incorporating vitamin E could prevent oxidation in poly(ether urethane) based implants. Moreover, Gorna et al.<sup>46</sup> were able to control the hydrophilicity of segmented polyurethanes using a mixture of polyester and polyether polyols. This study demonstrated that incorporating various ratios of hydrophilic Pluronic<sup>®</sup> and hydrophobic PCL segment influenced water absorption and polymer degradation.

A microphase separated morphology of the hard and soft phase and the presence of hydrogen bonding sites enhances the mechanical properties of TPUs. Importantly, the mechanical properties of TPUs can be tailored to be either rigid or elastic depending on the end use.<sup>27</sup> In addition, changing the chemistry of the soft segment enables one to modify the TPUs to be hydrophilic, hydrophobic or amphiphilic depending on the anticipated application.<sup>64</sup> Fromstein et al.<sup>65</sup> investigated the synthesis of poly(urethane)s from a mixture of PCL and PEO. They showed that poly(urethane)s with higher levels of PEO soft segments displayed enhanced hydrophilicity and reduced extension. Gorna et al.<sup>46</sup> showed that synthesizing polyurethanes from a mixture of PCL and PPG-PEO

polyols facilitated the control of hydrophilicity and slowed the calcification of the implants. In addition to polyester- and polyether-based soft segments, poly(dimethyl siloxane)-based soft segments<sup>47</sup> have been widely utilized in the synthesis of segmented polyurethanes. PDMS-based soft segments offer several advantages in terms of hemocompatibility, thermal, and oxidative resistance.

Additionally, incorporating biologically active molecules on the polymer chain or as pendant groups has been shown to enhance the interaction of the polymer with surrounding cells. For example, Gogolewski et al.<sup>34</sup> demonstrated that isosorbide containing polyurethanes exhibited enhanced interactions with cells and tissues. Moreover, the addition of biologically active polyisoprenol to the polyurethane backbone was shown to facilitate the interaction of the polymer with surrounding cell and tissues (Figure 2.10).<sup>66</sup>

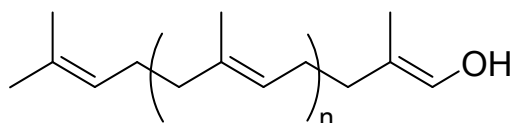


**Figure 2.10.** The chemical structure of polyisoprenol.<sup>66</sup>

### 2.3.2 Polyesters

Biodegradable aliphatic polyesters such as poly(caprolactone)s,<sup>11</sup> poly(lactide)s,<sup>67</sup> poly(glycolide)s, and their copolymers<sup>68</sup> are important classes of polymers that have been widely utilized in drug delivery, tissue engineering, and medical implants. However, use of these polyesters in certain applications is hindered due to their low glass transition temperatures, which negatively impacts mechanical properties. Aromatic groups are usually incorporated to improve overall mechanical properties; however the presence of aromatic units results in reduced biodegradation. To overcome this drawback, segmented

block copolyesters with phase separated morphology were synthesized with improved mechanical properties and enhanced biodegradability.<sup>23</sup> Moreover, several multiblock polyesters with adjustable mechanical and biodegradation properties were investigated for their potential as biodegradable thermoplastic elastomers for a number of applications.<sup>23,69-71</sup>

Polyester-based thermoplastic elastomers are synthesized as multiblock copolyesters and segmented polyesters such as poly(ether ester)s. Polyester thermoplastic elastomers are composed of a crystalline or high  $T_g$  hard phase and a rubbery soft phase. The difference in the miscibility of the two segments results in a phase separated morphology.<sup>23</sup> The first examples of thermoplastic polyester elastomers reported in the literature were synthesized from poly(ethylene terephthalate) and poly(ethylene ether)s.<sup>72</sup> Hytrel<sup>®</sup> is an example of a commercial thermoplastic poly(ether ester) elastomer that has been widely utilized in several applications. The literature<sup>23</sup> describes several different polyester and polyether blocks of varying molecular weights and compositions that have been tailored to improve their mechanical properties. Additionally, a number of studies<sup>73-76</sup> have explored the relationship between the chemical composition, molecular weight, and thermal properties of hard and soft segments with respect to the mechanical and degradation properties of thermoplastic elastomers.

Aliphatic polyesters such as poly(glycolic acid), poly(lactic acid), and poly( $\epsilon$ -caprolactone) are typically synthesized from ring opening polymerization of cyclic glycolide, lactide,  $\epsilon$ -caprolactone using a variety of initiators including tetraphenyl tin, stannous octanoate, aluminum isopropoxide. Cytotoxicity of the initiator is a concern for

biomedical applications. Therefore, an FDA approved, stannous octanoate, is commonly used to activate the ring opening polymerization of lactones for medical applications. Moreover, zinc powder is another alternative nontoxic catalyst.<sup>77,78</sup>

Polycondensation is another method to synthesize biodegradable aliphatic polyesters. The synthesis of polyesters using polycondensation method may result in formation of cyclic groups due to cyclization reactions.<sup>77</sup> Reactions of difunctional monomers such as diacid and diols or diesters and diols produce linear polyesters; however formation of cyclic products also takes place as a result of intramolecular reactions.<sup>14</sup> During polycondensation reaction, the monomers react with each other and forms dimers and trimers. As the oligomers are produced, the intramolecular reactions take place and cyclics are produced as a result of intramolecular cyclization. Literature<sup>79</sup> indicates in polycondensation reactions cyclization competes with linear polymer formation. When the polymerization is carried out in solution, there is a tendency to form cyclic oligomers due to cage effect.<sup>77</sup> During synthesis of polyesters using solution polymerization formation of cyclic macromolecules are observed at dilute conditions. Moreover, literature studies<sup>79</sup> reported that reaction of multifunctional monomers results in cyclization during polymerization and influences the gel points. In particular, Kricheldorf et al.<sup>79</sup> demonstrated that cyclization reactions takes place during polymerization of A<sub>2</sub> and B<sub>3</sub> and cyclic groups are commonly present in the final product. Moreover, the flexibility of a polymer chain has a significant influence on cyclic formation. The literature<sup>79</sup> reports formation of cyclics depending on polymer conformation for synthesis of several polymers.

### 2.3.2.1 Poly(ether ester)s

Poly(ether ester)s are synthesized from poly(alkylene oxide)s and polyester segments with varying compositions and molecular weights.<sup>80,81</sup> The amorphous polyether segment acts as a soft segment, while the semicrystalline polyester segment with high  $T_g$  serves as the hard segment that reinforces mechanical properties. The difference between the molecular weight of the polyether-based soft segment and the hard phase results in phase separation. Poly(tetramethylene oxide) (PTMO), poly(ethylene oxide) (PEO), poly(propylene oxide), poly(butylene succinate), and poly(caprolactone) are several examples of soft segments that are commonly utilized in the synthesis of thermoplastic polyester elastomers. Since PEG is non-toxic, non-antigenic, and non-immunogenic, it has been commonly used to synthesize biodegradable thermoplastic elastomers with enhanced biocompatibility and biodegradability.<sup>80,81</sup> Moreover, PTMO is typically used as soft segments in several thermoplastic elastomers including commercial polyester-based thermoplastic elastomers such as Hytrel<sup>®</sup>. Due to the fact that the crystallization behavior of PTMO is highly dependent on molecular weight, it is prone to crystallization at molecular weights greater than 1500 g/mol. Therefore, copolymer blends of PTMO and PEO or PPG have been commonly utilized to retard crystallinity in the soft phase.<sup>26</sup> PEG has been widely used to synthesize hydrophilic polyester block copolymers for biomedical applications.<sup>82</sup> Pepic et al.<sup>81</sup> synthesized poly(ether ester)-based thermoplastic elastomers from poly(butylene succinate) based hard segment and PEG based soft segment. Moreover, Albertsson et al.<sup>73</sup> synthesized poly(ether ester)s from the polycondensation of poly(ethylene succinate) with PEG. Nagata et al.<sup>82</sup> reported several examples of thermoplastic elastomers

containing PEG as the soft phase. Investigations of poly(butylene succinate) and PEG-based thermoplastic elastomers showed that incorporating PEG soft segment increased hydrophilicity and significantly enhanced hydrolytic degradation behavior. Although the molar ratio and molecular weight of the PEG segment significantly enhanced water absorption of the copolymer, enzymatic degradation was reduced slightly. Increasing PEG molecular weight reduced the number of ester linkages along the polymer backbone, which resulted in reduced weight loss. Nagata et al.<sup>83</sup> also showed that incorporation of dicarboxylic acids such as adipic acid enhanced the enzymatic degradation of the segmented copolyesters. These results confirmed that degradation was not only controlled by only the amount of water absorption, but also by the amount of ester linkages along the copolyester backbone. PBSu-*co*-PEG copolymers exhibited an enhanced hydrolytic degradation rate with increased PEG content due to reduced melting temperature ( $T_m$ ) and crystallinity. However, the presence of PEG units reduced the tensile strength and elongation.

### **2.3.2.2 Block polyesters**

Polyester thermoplastic elastomers are also synthesized as diblock or multiblock polyesters. The mechanical properties and biodegradation behavior of these materials highly depend on the chemical composition and molecular weight of each block. Therefore, modifying either or both of these components using a variety of different polyester compositions means that thermomechanical properties can be easily tailored to achieve desired properties.

Several researchers described the synthesis of thermoplastic elastomers from a number of polyesters where each segment impacted biodegradation or mechanical

strength.<sup>75,76</sup> For example, several block copolyesters were synthesized from PLA, PCL, and poly(3-hydroxybutyrate)s.<sup>23</sup> Ye et al.<sup>84</sup> reported the synthesis of thermoplastic elastomers from PLA-PCL diblock copolymers, wherein the PLA segment provided degradability and the PCL segment provided permeability to drugs. Witt et al.<sup>76</sup> showed that aromatic polyesters such as poly(butylene terephthalate) and poly(ethylene terephthalate) are not biodegradable. In contrast, copolymerization with aliphatic esters and ethers resulted in biodegradation during contact with biological environments.<sup>75,76,85,86</sup> Copolymers of PET-containing aliphatic units have been reported to biodegrade depending on the level of aromatic content.<sup>82,87</sup> Witt et al.<sup>88</sup> also showed that aromatic oligomers containing one or two terephthalate units degrade and metabolize rapidly, while the longer aromatic sequences remain almost unaffected. Tang et al.<sup>89</sup> showed that the copolymerization of PET with glycolic acid and lactic acid produces biodegradable copolyesters. The synthesis of PET-*co*-PHB, PET-*co*-PBSu, and PET-*co*-PCL are examples of aliphatic-aromatic polyesters (Figure 2.11).

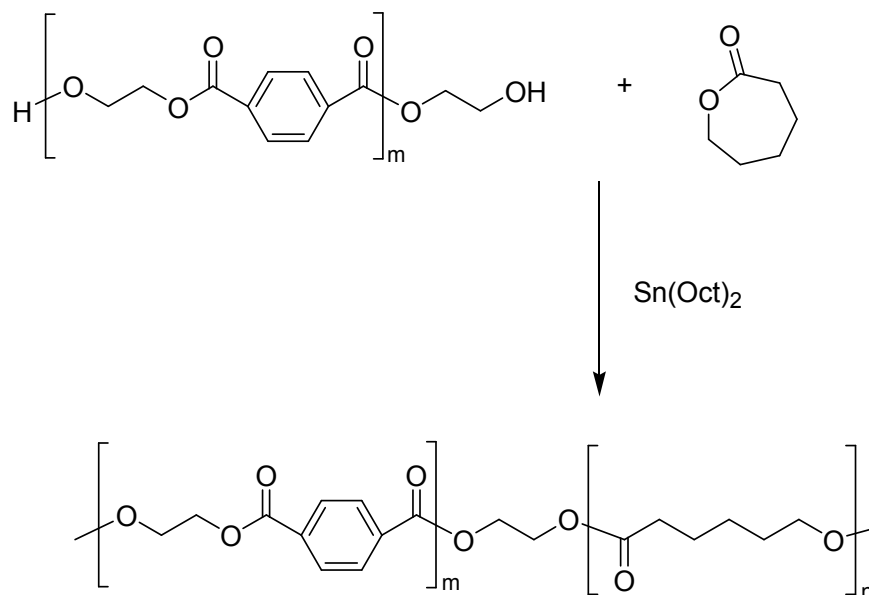


**Figure 2.11.** Synthesis of PET-PCL block copolymer.<sup>89</sup>

Cohn et al.<sup>11</sup> synthesized thermoplastic elastomers from PLLA and PCL-based multiblock copolymers. The presence of the hard PLLA block and the PCL-based soft block resulted in phase separation and therefore enhanced elastomeric properties. Moreover, Miyamoto et al.<sup>90</sup> synthesized ABA triblock copolymers from PHB as the soft segment and poly(L-lactide) based hard segment. The study showed that controlling the hard and soft segment ratio enabled synthesis of biodegradable elastomer with tunable mechanical properties. Wanamaker et al.<sup>71</sup> synthesized thermoplastic elastomers from poly(lactide)-poly(menthite)-poly(lactide) based ABA triblock. The midblock was synthesized from a renewable polyester, poly(menthite), while an amorphous polyester with a  $T_g$  of  $-25\text{ }^\circ\text{C}$  served as the soft phase. The microphase separation of the blocks resulted in elastomeric properties. Moreover, degradation studies indicated that the elastomeric properties were retained upon degradation for up to 21 weeks.

Moreover, biodegradable polymers with branched topology have been investigated in detail with respect to the influence of branch points on thermomechanical and rheological properties.<sup>14</sup> Several studies have investigated how branching can be used to tailor the mechanical properties of thermoplastic elastomers that contain polyester blocks.<sup>7,12,16,17</sup> Branched polymers exhibit smaller hydrodynamic radius and lower viscosities compared to linear polymers of similar molecular weight.<sup>14</sup> The star-shaped block copolyester display significantly different swelling, morphology, and drug release profiles compared to linear analogs.<sup>20,91</sup> Choi et al.<sup>91</sup> investigated star-shaped block copolyesters containing PEO-PLLA and PEO-PCL segments. Their results showed that the presence of branching lowered the melting point and reduced the phase separation of the block copolymer. The use of high molecular weight PEO in drug delivery was

limited due to its high hydrodynamic volume and the difficulty in eliminating it from the kidney. However, star-shaped copolyesters containing PEO displayed lower hydrodynamic volume and were appropriate for use with high molecular weight PEO segments.

### **2.3.3 Polyamides**

Polyamides possess strong intermolecular hydrogen bonding which results in highly ordered structures.<sup>2</sup> Several literature reports have investigated incorporation of ester linkages to improve flexibility and enhance biodegradation behavior of polyamides.<sup>92-94</sup> The literature also describes several examples of poly(ester amide)s and poly(ether amide)s as biodegradable thermoplastic elastomers.<sup>92-97</sup> The thermomechanical properties of poly(ether amide)s and poly(ester amide)s depend on chemical composition and the length of both the polyamide hard segment and the polyether or polyester-based soft segment.<sup>95,98</sup> The hard segment dictates the melting point and processing temperature, while the soft segment determines the flexibility of the elastomer.<sup>99</sup> Polyester-based soft segments are susceptible to hydrolysis, whereas the polyether segments are hydrolytically stable. However, as discussed earlier, the polyether segments are not oxidatively stable.

#### **2.3.3.1 Poly(ether amide)s**

Poly(ether amide)s are a class of thermoplastic elastomers that contain polyether soft segment and polyamide based hard segments.<sup>2,99</sup> As reported in the literature,<sup>99</sup> the discovery of tetraalkoxide catalysts enabled the synthesis of high molecular weight poly(ether amide)s and promoted the development of the first commercial example of poly(ether amide), PEBA<sup>®</sup>X, which is commonly used for biomedical applications.<sup>26</sup>

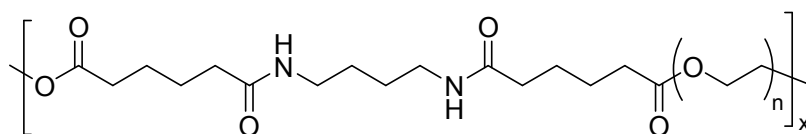
Poly(ether amide)-based thermoplastic elastomers are composed of soft polyether segments such as PPG and PTMO and a polyamide-based hard segment. Controlling the chemistry and the ratio of the polyether and polyamide segments facilitates control of mechanical properties.<sup>100</sup> For example, in poly(ether ester amide)s, the presence of the poly(ether) unit provides the biocompatibility, whereas the polyester segment supplies the biodegradable component. Moreover, the presence of hydrogen bonding in the amide unit enhances mechanical properties.

Poly(ether amide)s are synthesized from melt polycondensation of carboxylic acid functional amide blocks and polyether polyols. The literature features studies that utilize a variety of polyamide segments such as nylon 6, nylon 11, and nylon 12 as the hard segments.<sup>97</sup> PTMO-, PPG-, and PEO-based soft segments with various molecular weights have been used in synthesizing poly(ether amide)s.<sup>98</sup> Yu et al.<sup>97</sup> showed that block length significantly influenced the resulting microphase separated morphology and crystallinity of the hard phase. Their results confirmed that short block segments resulted in the formation of fringed micelle semicrystalline polyamide segment, whereas longer segments led to the formation of chain folded crystals. Characterization of the microstructure using SAXS confirmed that increased hard segment length resulted in the formation of crystals that followed a chain-folding mechanism. Sheth et al.<sup>98</sup> published a detailed investigation of a series of nylon 12 and PTMO-based poly(ether amide)s having different hard segment content. The influence of segment length on morphology was investigated using DMA, DSC, AFM, SAXS, and WAXS. Their study concluded that the polyamide segment and the thermal history of the samples influenced the morphology of the poly(ether amide). The overall crystallinity of the samples was reported to

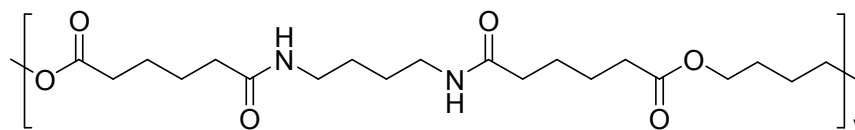
increase with polyamide content. Ukielski et al.<sup>96</sup> reported the synthesis of multiblock elastomers based on terpolymers of poly(tetramethylene terephthalate)-*b*-poly(oxytetramethylene)-*b*-poly(dodecanolactam)s. The terpolymer was synthesized from the melt polycondensation of  $\alpha,\omega$ -dihydroxy poly(butylene terephthalate),  $\alpha,\omega$ -dihydroxy poly(oxytetramethylene), and  $\alpha,\omega$ -dicarboxy oligo(dodecanolactam). This study confirmed that the phase separation of the multiblock copolymer was highly dependent on the molecular weight of each segment.

### 2.3.3.2 Poly(ester amide)s

Biodegradable poly(ester amide)s containing various polyester blocks have been reported in the literature. For example, the synthesis of poly(ester amide)s containing poly( $\epsilon$ -caprolactone) blocks has been of interest for biomedical applications including drug delivery systems, resorbable sutures, temporary implants.<sup>92,94</sup> Kozłowska et al.<sup>93</sup> investigated the synthesis of poly(ester amide) based elastomers from polycondensation of 1,4-butanediol, dimerized fatty acid and oligo( $\epsilon$ -caprolactam) with varying soft segment content. As the researchers showed, the thermomechanical properties changed significantly depending on the ratio of the hard and soft segment. Deschamps et al.<sup>95</sup> described the synthesis of poly(ether ester amide) copolymers for tissue engineering applications (Figure 2.12). The hydrophilicity of the segmented poly(ether ester amide) and the biocompatibility was adjusted as the ratio and the block length of the polyester and the polyether segment were varied over a broad range. Moreover, Barbato et al.<sup>101</sup> reported the synthesis of segmented poly(ether ester amide)s composed of poly( $\epsilon$ -caprolactone) and hydrophilic diamines for drug delivery applications.



PEO containing soft segment



Hard segment

**Figure 2.12.** Chemical structures of the soft segments and hard of poly(ether ester amide)s.<sup>95</sup>

Bettinger et al.<sup>102</sup> reported the synthesis of novel poly(ester amide)-based biodegradable elastomers from a copolymerization of 1,3-diamino-2-hydroxy-propane with glycerol, D,L-threitol, and sebacic acid (Figure 2.13). The resulting polymers, poly(1,3-diamino-2-hydroxypropane-*co*-polyol sebacate)s, were crosslinked through the formation of ester and amide bonds. *In-vivo* and *in-vitro* characterization studies indicated that these networks were suitable for fabrication of resorbable scaffolds for tissue engineering and drug delivery.

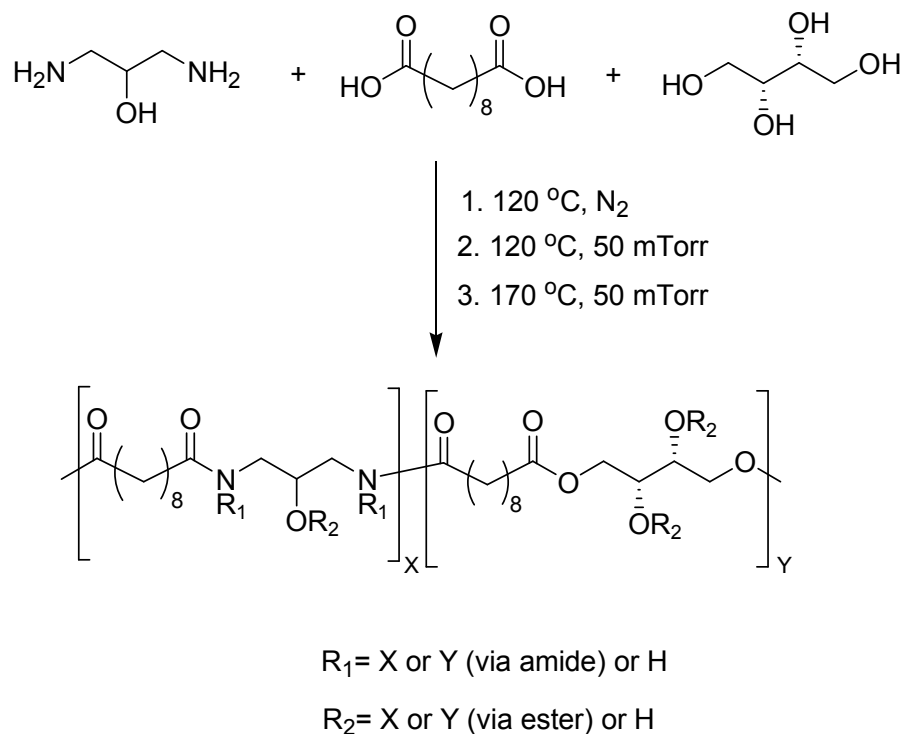


**Figure 2.13.** Synthetic scheme for synthesis of poly(ester amide) from 1,3-diamino-2-hydroxy-propane with glycerol, D,L-threitol, and sebacic acid.<sup>102</sup>

## 2.4 Thermoset Elastomers

Thermoset elastomers are chemically crosslinked networks.<sup>23</sup> Due to the ability to modify the biodegradation rates, morphology, and physical properties of these materials, they have significant potential for biomedical applications. For example, enhanced mechanical properties can be achieved through chemical crosslinking using various synthetic techniques. Currently, certain biodegradable amorphous and semicrystalline polymers such as poly(caprolactone), poly(D,L-lactide), and poly(lactide-*co*-glycolide), which are commonly used for several biomedical applications, are brittle at physiological temperature because of their crystallinity and hydrophobicity.<sup>2,5,6</sup> Main difficulty in use of these polymers in biomedical applications arises from the crystallinity and hydrophobic nature of these polymers. The presence of crystallinity results in

reduced biodegradation rates due to hindered water penetration through the material and the reduced accessibility of hydrolytically labile bonds. Because the presence of crystallinity is detrimental for soft tissue and drug delivery applications, chemically crosslinking of these polymers to avoid crystallinity offers several important advantages over the use of more brittle thermoplastic elastomers. Moreover, controlling crosslink density enables control over drug loading capacity and release property.<sup>103</sup> Since the mechanical properties of these biodegradable networks can also be modified to mimic the surrounding tissue, they are highly suitable for soft tissue applications.<sup>23</sup>

Biodegradable thermoset elastomers have been synthesized from the crosslinking<sup>23</sup> of poly(caprolactone)s, poly(butylene succinate)s, poly(lactide)s, and poly(glycolide)s. Mechanical properties and biodegradation rates can be tailored through controlled crosslink density and crystallinity. In the literature, biodegradable polymers have been crosslinked using benzoyl peroxide,<sup>104</sup> UV-curing, and post-polymerization techniques.<sup>105-108</sup> In terms of viable biological applications, crosslinking biodegradable polymers at physiological temperatures and pH in the absence of toxic monomers, catalysts, and organic solvents is particularly important. Recently, Michael addition reactions have been investigated as a novel means for synthesizing chemically crosslinked networks.<sup>109-112</sup> Such reactions offer potential due to the absence of solvents, byproducts, and the ability to achieve room temperature crosslinking.

#### **2.4.1 UV-crosslinking**

The photo-initiated crosslinking or UV-crosslinking of polymers is a commonly utilized technique to synthesize biodegradable networks. UV-crosslinking is a rapid, effective and well-controlled curing technique that is performed at physiological

temperatures in the presence of a light source and appropriate photoinitiators. The process produces minimum heat production which is critical for loading of thermosensitive drugs and proteins.<sup>103</sup> Photopolymerization has been utilized extensively for many applications including membranes, hydrogels,<sup>113</sup> adhesion barriers, *in-situ* crosslinkable adhesives, and scaffold structures<sup>114</sup> to synthesize biodegradable thermosets.<sup>23</sup>

As indicated, UV-crosslinking takes place in the presence of a photoinitiator that produces a radical initiating species through the absorption of light at a specific wavelength. Radical photopolymerization takes place via photocleavage, hydrogen abstraction, and cationic photopolymerization (Figure 2.14). In biomedical applications, photoinitiators are selected based on biocompatibility, cytotoxicity, and stability. For example, cationic photoinitiators are not used due to the formation of protonic acids.

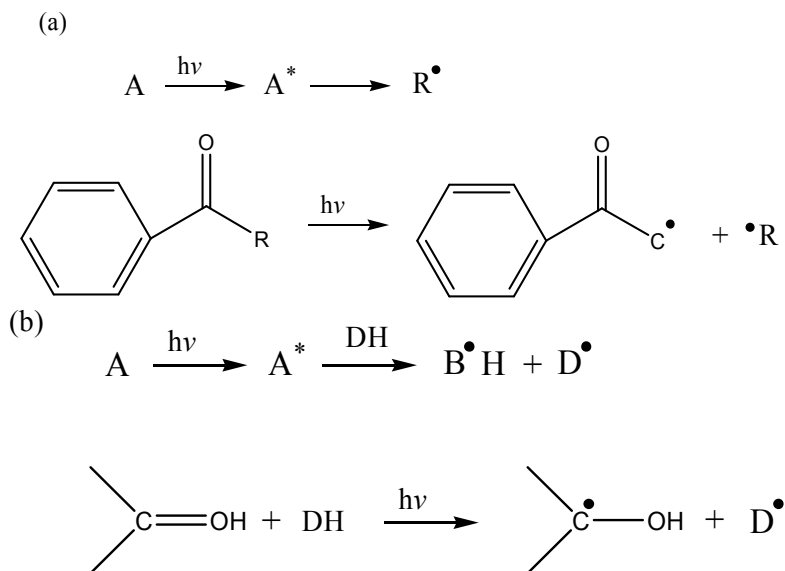


**Figure 2.14.** Photopolymerization via (a) photocleavage and (b) hydrogen abstraction.<sup>113</sup>

A number of polymers have been end-functionalized with photo-polymerizable groups such as acrylate and methacrylate groups using a reaction of a hydroxyl end-group with an acyl chloride derivative of an unsaturated methacrylate.<sup>103,115-117</sup> Other functional groups such as styryl, coumarin, and phenylazide<sup>118</sup> are also used as photo-polymerizable groups.<sup>117</sup> The photocrosslinking of polymers containing coumarin and phenylazide end groups takes place in the absence of a photoinitiator. Matsuda et al.<sup>118</sup> reported the photocrosslinking of PCL with trimethylene carbonate containing coumarin<sup>119</sup> and phenylazide end groups. Despite its lower reactivity, the photopolymerization of fumarate containing polymers<sup>120</sup> are preferred over acrylate functionalized polymers for use in *in-situ* biomedical applications due to the biocompatibility of reaction byproducts.<sup>121</sup> Poly(propylene fumarate), a well studied biodegradable and crosslinkable polymer, has its biodegradation products as propylene glycol and fumaric acid, both of which are biocompatible. Grijpma et al.<sup>116</sup> reported the synthesis of biodegradable networks from the photocrosslinking of fumaric acid functionalized lactide, caprolactone based polyesters, and linear and star-shaped oligomers (Figure 2.15). Networks with gel fractions up to 96% were reported.

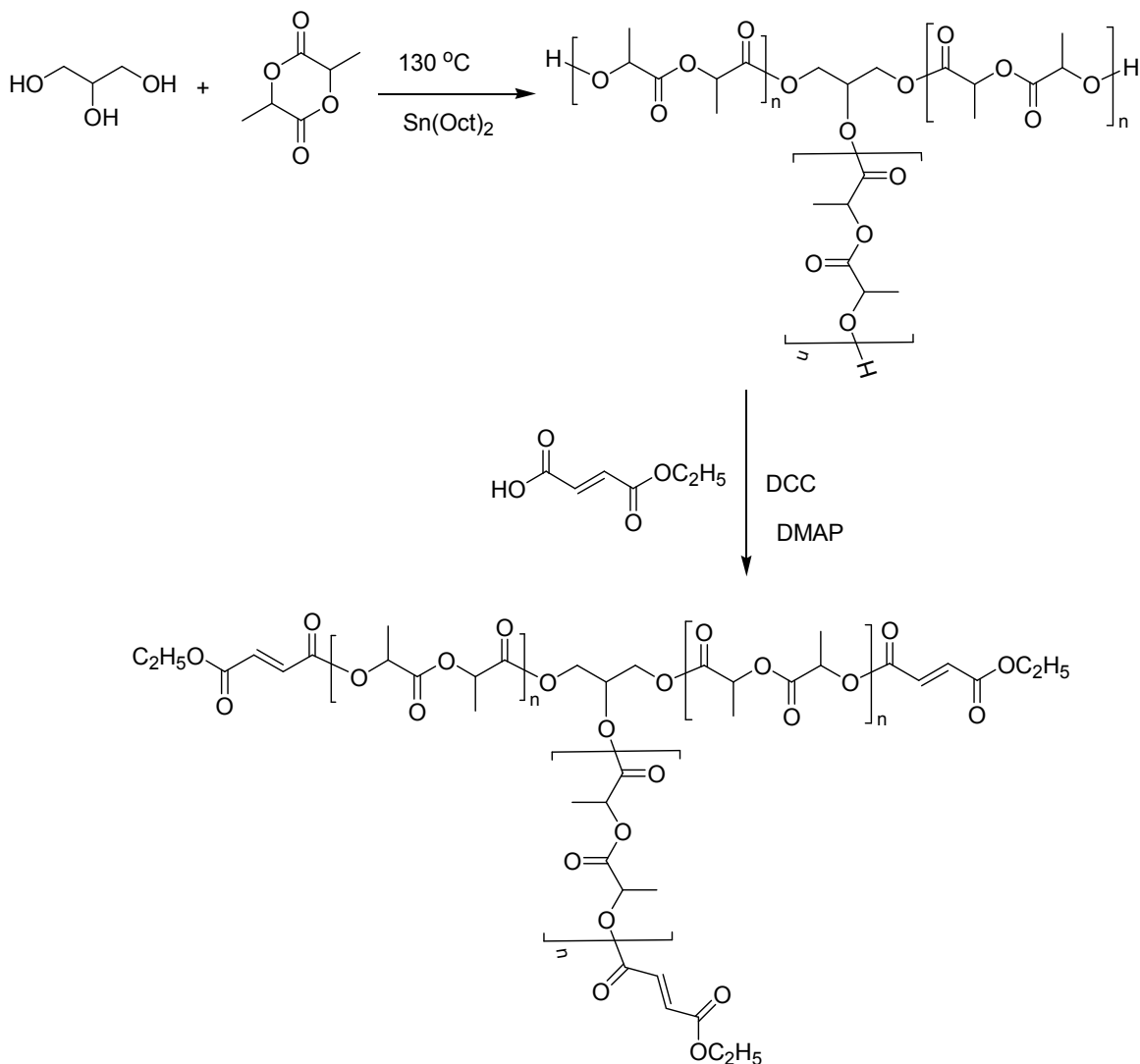


**Figure 2.15.** Synthesis of star-shaped poly(lactide) containing fumarate functionality.

Burdick et al.<sup>114</sup> demonstrated synthesis of lactic acid oligomer with low molecular weight ethylene glycol cores to form *in-situ* degradable networks for orthopedic applications (Figure 2.16). Their study showed that the degradation of the networks were highly dependent on the hydrophobicity of the monomers. In another study, Burdick et al.<sup>122</sup> investigated the synthesis of poly(glycerol sebacate)-based networks using UV-curing as an alternative to the polycondensation of multifunctional monomers. Since crosslinking poly(glycerol sebacate) using polycondensation requires

high temperatures, it is not suitable for *in-vivo* crosslinking applications. However, they demonstrated that UV-crosslinking acrylate functionalized poly(glycerol sebacate)s take place at lower temperatures.

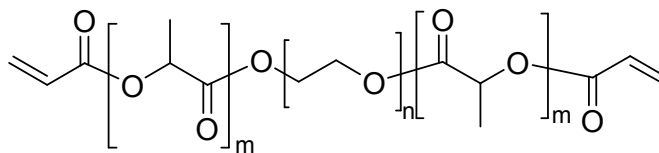


**Figure 2.16.** Chemical structure of multifunctional lactic acid oligomer with poly(ethylene glycol) core.<sup>114</sup>

In addition to UV-crosslinking of biodegradable polymers with linear topology, the crosslinking of star-shaped polymers was used to study the influence of topology on the crosslink density of the resulting network.<sup>115,107</sup> Star-shaped polyesters were synthesized from ring opening polymerization in the presence of glycerol based trifunctional initiator. In related studies, Amsden et al.<sup>103,123</sup> investigated the photocrosslinking of methacrylated star-shaped poly(caprolactone-*co*-D,L-lactide) in comparison to linear analogs. The researchers showed that the star-shaped precursors displayed a reduced viscosity compared to their linear analogues, which is beneficial in applications where the polymer is injected and cured *in-situ*. Characterization of *in-vivo* and *in-vitro* degradation behaviors revealed that crosslink density significantly influenced degradation mechanisms.<sup>124</sup> Moreover, tailoring the number of arms of the star-shaped prepolymer permitted control of the final properties of the networks.

Controlling the degradation rate of thermoset elastomers is important for a number of biomedical applications. For polymer networks with high crosslink densities, the diffusion of water and enzymes is reduced; therefore resistance to hydrolysis is greater. Conversely, crosslinked polymer networks degrade more rapidly compared to

their linear analogues due to the difference in extent of crystallinity. As crosslinked polymers degrade through random chain scission, the polymer strength, crosslink density, and weight all decrease. However, in contrast to linear polymers, crosslinked polymers degrade at a slower rate, meaning that their mechanical properties decrease gradually instead of failing catastrophically. Moreover, to attain crosslink networks with different biodegradation behaviors, biodegradable and non-biodegradable crosslinkers and biodegradable units are placed on a crosslink point or on the polymer backbone. Thomas et al.<sup>125</sup> demonstrated the selective synthesis of symmetrical degradable lactate and glycolate ester based crosslinkers in order to control degradation rates (Figure 2.17). Specifically, these crosslinkers show promise for use in synthesizing biodegradable networks with adjustable degradation rates for drug delivery implants, and as biodegradable scaffolds for tissue engineering applications.

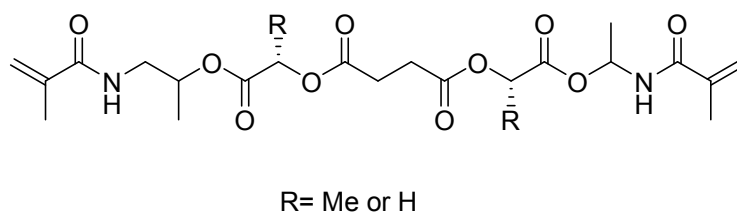


**Figure 2.17.** Synthesis of degradable crosslinkers.<sup>125</sup>

#### 2.4.2 Polymerization of multifunctional monomers

The synthesis of biodegradable networks based on renewable monomers such as gluconolactone and citric acid have received considerable attention due to issues of sustainability.<sup>6,126</sup> Gluconolactone and citric acid, whose structures are shown in Figure 2.18, are both produced from natural resources. An esterification reaction of the two monomers results in crosslinking at higher reaction conversions due to multiple

carboxylic acid and hydroxyl functionalities. Tsutsumi et al.<sup>126</sup> demonstrated the synthesis of prepolymers from the melt polycondensation of gluconolactone with citric acid at 165 °C for 3 h under nitrogen. The prepolymers were subsequently cast on an aluminum substrate from solution in THF and heated at room temperature for 2 h and at 65 °C for 2 h. The resulting films were post-polymerized at 180 °C for 3 h. Post-polymerization between the carboxyl and the hydroxyl groups generated a crosslinked network. Tsutsumi and Nagata<sup>127</sup> also synthesized poly(caprolactone)-based elastomeric networks from a post-polymerization of poly(caprolactone)-based precursors. The prepolymers were synthesized from the melt polycondensation of poly(caprolactone) and multifunctional acids, such as tricarballic acid and *meso*-1,2,3,4-butanetetracarboxylic acid. The films were cast from prepolymers and post-polymerized at 260 °C under nitrogen.

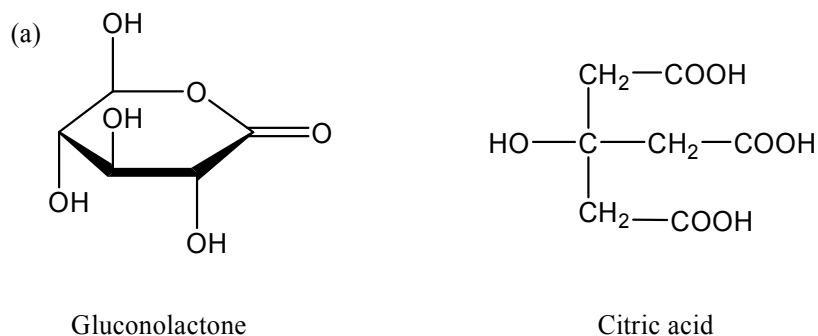


**Figure 2.18.** (a) Chemical structures of gluconolactone and citric acids. (b) Structure of post-polymerization product.

Studies have also detailed the use of poly(diols citrate) as a biocompatible, biodegradable polyester.<sup>106,128</sup> The multi-acid functionality on the citrate group enables the crosslinking of poly(diols citrate)s upon post-polycondensation. In the literature, several polyester elastomers have been synthesized via a polycondensation reaction of

citric acid with 1,8-octanediol and glycerol.<sup>106,128,129</sup> All these elastomeric materials show promise for use in biomedical applications due to their biocompatibility, biodegradability, support for cell adhesion, proliferation, and their anticoagulant properties.<sup>128</sup> Moreover, these polymers have been shown to demonstrate differentiation of endothelial cells and reduction of platelet adsorption. Zhang et al.<sup>128</sup> utilized poly(diols-citrate)-based polyester elastomers as substrates for the immobilization of plasmids and cellular transfection. Their results demonstrated that the elastomers are promising materials for use in substrate-mediated gene delivery. This study also verified the importance of the duration of post-polymerization, since crosslink density depends on the conversion of the reaction. Specifically, longer polymerization times were shown to enhance tensile strength and lower degradation rates due to increased crosslink density. *In-vivo* and *in-vitro* studies confirmed that these networks show potential for use as scaffold materials. Moreover, the presence of unreacted carboxyl or hydroxyl groups on the elastomers offers potential for post-modification of the networks using proteins and peptides. Yang et al.<sup>106</sup> showed that these polymers can be engineered into various shapes and that tensile properties can be tailored to mimic the properties of the surrounding tissue. Moreover, good fatigue resistance and deformation recovery was reported. In another study, citric acid was reacted with isosorbide to synthesize renewable polyester elastomers for coating applications.<sup>130</sup>

### **2.4.3 Michael Addition**

*In-situ* crosslinking is important for applications such as scaffolding and medical adhesives. *In-vivo* applications require *in-situ* crosslinking of polymers at physiological temperatures and pH, and in the absence of toxic monomers, byproducts, and solvents.

Recently, the Michael addition reaction<sup>131</sup> was utilized in chemical crosslinking of a variety of polymers for thermoset applications. Michael addition enables crosslinking of polymers at room temperature without the use of organic solvents (Figure 2.19). Long et al.<sup>109-112</sup> demonstrated successful application of Michael addition to synthesize covalently crosslinked networks with high gel fractions. Controlling the chemistry of the donor or acceptor type precursors facilitated the incorporation of hydrophilic units into the network. Williams et al.<sup>109,112</sup> demonstrated that the hydroxyl functionality is readily derivatized with acetoacetate groups using transacetoacetylation in the bulk. Therefore, Michael addition is promising for crosslinking several hydroxyl telechelic polymers including poly(caprolactone), poly(alkyl succinate)s, and poly(alkyl adipate)s. Moreover, Michael addition shows potential as a synthetic route for synthesizing biodegradable polyester networks with controllable thermomechanical properties and biodegradability.

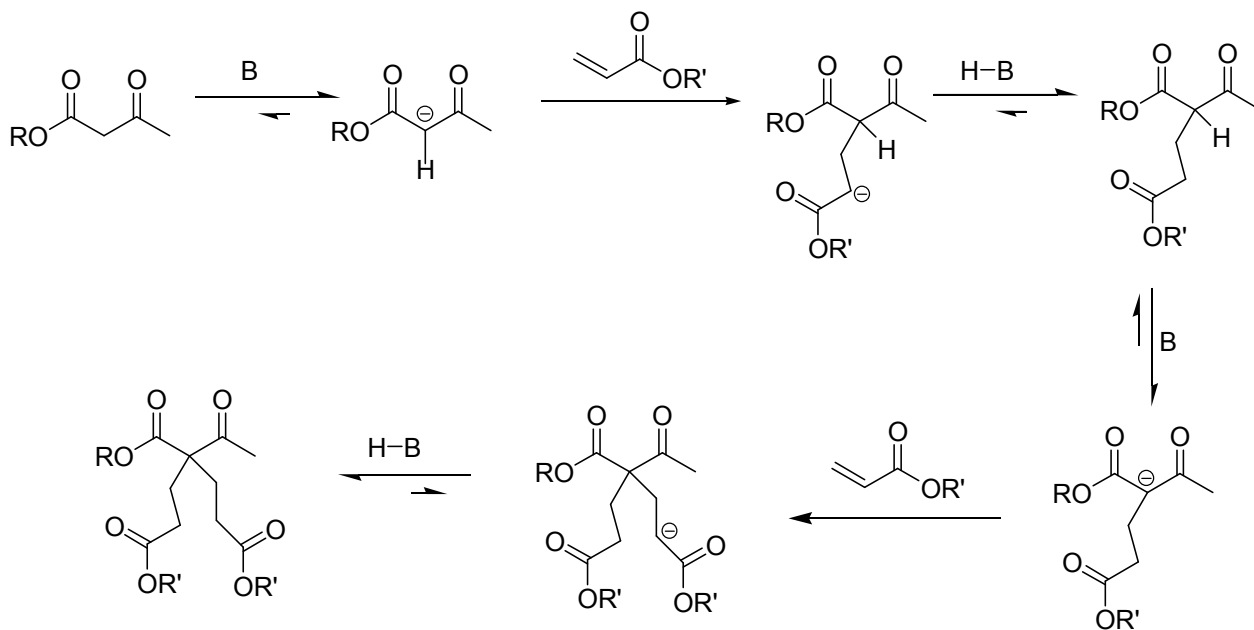


**Figure 2.19.** Mechanism of carbon-Michael addition reaction.

Recently, our research group reported the crosslinking of acetoacetate functionalized oligomeric poly(caprolactone)s with varying molecular weights to form

networks with high gel fractions (Figure 2.22).<sup>133</sup> The crosslinking of oligomeric poly(caprolactone)s of various molecular weights permitted us to adjust crosslink density, crystallinity, and consequently the final thermomechanical properties. Moreover, the incorporation of diacrylates such as poly(ethylene glycol) diacrylates with varying molecular weights enabled us to tailor the hydrophilicity of the networks.

Moreover, covalently crosslinked biodegradable networks were synthesized from the Michael addition reaction of acetoacetate-functional oligomeric poly(trimethylene succinate)s and poly(trimethylene adipate)s with neopentylglycol diacrylate. The resulting oligomeric polyesters with telechelic hydroxyl functionality were synthesized from renewable monomers, adipic and succinic acid, using a solvent-free melt polycondensation method. The molecular weight of the polyols was varied systematically to probe the influence of molecular weight on the thermomechanical properties of the networks. Acetoacetate-functionalized polyesters were reacted with neopentyl glycol diacrylate in the presence of an organic base catalyst at room temperature and networks with high gel contents (> 90%) were obtained. Characterization of the thermomechanical properties revealed the influence of oligomeric polyester molecular weight on crystallinity and the glass transition temperature of the resulting networks. DSC and DMA analyses showed that the extent of crystallinity was dependent on the precursor molecular weight, which also controlled the crosslink density of the networks.

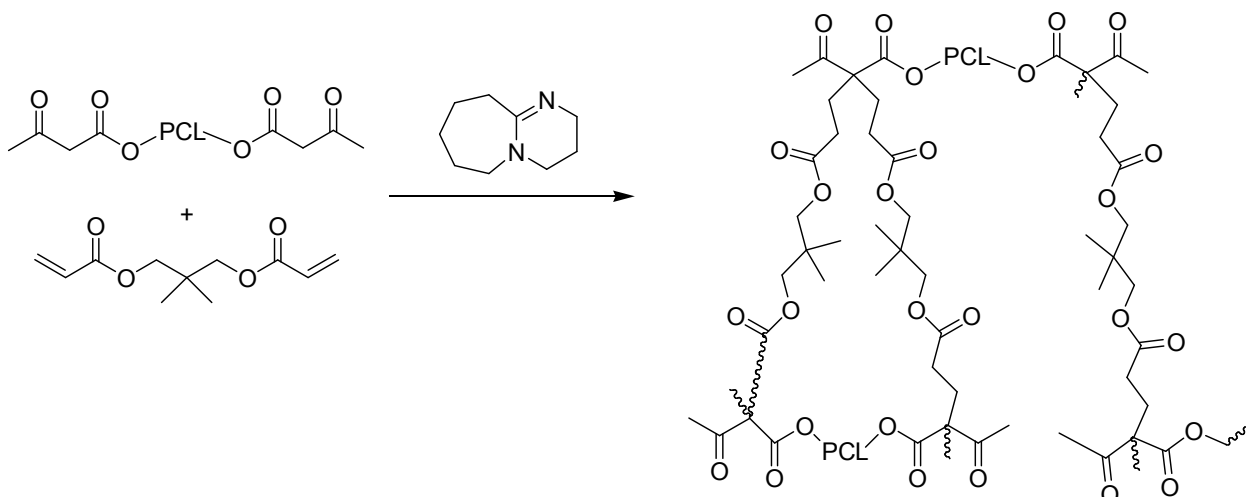


**Figure 2.20.** Crosslinking of poly(caprolactone) bisacetoacetate with NPGDA in the presence of DBU.

## 2.5 Conclusions

This review focused synthetic methodologies to synthesize biodegradable elastomers thermoset and thermoplastic elastomers in addition to thermomechanical properties and degradation behavior. The ability of biodegradable elastomers to selectively degrade in contact with living tissues or the external environment expands their potential applications, as well as stimulates further research on achieving controlled degradation for specific applications, especially in the biomedical arena. Thermoset and thermoplastic elastomers derived from polyesters, polyurethanes and polyamides have been widely studied and their degradation mechanisms have been investigated in detail. However, further investigations are needed in order to develop novel elastomers with controllable degradation behaviors and improved mechanical properties, particularly through modification of topology and functionality.

## 2.6 Acknowledgements

The authors would like to acknowledge Laurie Good for manuscript editing.

## 2.7 References

1. Nair, L. S.; Laurencin, C. T., *Prog. Polym. Sci.* **2007**, *32* (8-9), 762-798.
2. Okada, M., *Prog. Polym. Sci.* **2002**, *27* (1), 87-133.
3. Williams, D. F. In *On the mechanisms of biocompatibility*, 2006; Elsevier Science: 2008; pp 2941-2953.
4. D'Haene, P.; Remsen, E. E.; Asrar, J., *Macromolecules* **1999**, *32* (16), 5229-5235.
5. Horna, D.; Semino, C. E.; Agullo, N.; Borros, S., *Afinidad* **2007**, *64*, 404-414.
6. Tsutsumi, N.; Kono, Y.; Oya, M.; Sakai, W.; Nagata, M., *Clean-Soil Air Water* **2008**, *36* (8), 682-686.
7. Breitenbach, A.; Li, Y. X.; Kissel, T. In *Branched biodegradable polyesters for parenteral drug delivery systems*, 5th Symposium on Controlled Drug Delivery, Noordwijk Aan Zee, Netherlands, Apr 01-03; Elsevier Science Noordwijk Aan Zee, Netherlands, 1998; pp 167-178.
8. Tatai, L.; Moore, T. G.; Adhikari, R.; Malherbe, F.; Jayasekara, R.; Griffiths, I.; Gunatillake, P. A., *Biomaterials* **2007**, *28* (36), 5407-5417.
9. Wang, W.; Peng, P.; Yu, H.; Chen, X.; Jing, X., *J. Polym. Sci., Part A: Polym. Chem.* **2006**, *44* (19), 5505-5512.
10. Hassan, M. K.; Mauritz, K. A.; Storey, R. F.; Wiggins, J. S., *J. Polym. Sci., Part A: Polym. Chem.* **2006**, *44* (9), 2990-3000.
11. Cohn, D.; Salomon, A. F., *Biomaterials* **2005**, *26* (15), 2297-2305.
12. Dailey, L. A.; Wittmar, M.; Kissel, T. In *The role of branched polyesters and their modifications in the development of modern drug delivery vehicles*, 8th European Symposium on Controlled Drug Delivery, Elsevier Science Bv: Noordwijk, 2004; pp 137-149.
13. Han, Y. K.; Um, J. W.; Im, S. S.; Kim, B. C., *J. Polym. Sci., Part A: Polym. Chem.* **2001**, *39* (13), 2143-2150.
14. McKee, M. G.; Unal, S.; Wilkes, G. L.; Long, T. E., *Prog. Polym. Sci.* **2005**, *30* (5), 507-539.
15. Lin, Q.; Unal, S.; Fornof, A. R.; Yilgor, I.; Long, T. E., *Macromol. Chem. Phys.* **2006**, *207* (6), 576-586.
16. Unal, S.; Oguz, C.; Yilgor, E.; Gallivan, M.; Long, T. E.; Yilgor, I., *Polymer* **2005**, *46* (13), 4533-4543.
17. Unal, S.; Lin, Q.; Mourey, T. H.; Long, T. E., *Macromolecules* **2005**, *38* (8), 3246-3254.
18. Sheth, J. P.; Unal, S.; Yilgor, E.; Yilgor, I.; Beyer, F. L.; Long, T. E.; Wilkes, G. L., *Polymer* **2005**, *46* (23), 10180-10190.
19. McKee, M. G.; Park, T.; Unal, S.; Yilgor, I.; Long, T. E., *Polymer* **2005**, *46* (7), 2011-2015.
20. Karikari, A. S.; Edwards, W. F.; Mecham, J. B.; Long, T. E., *Biomacromolecules* **2005**, *6* (5), 2866-2874.

21. Kim, E. K.; Bae, J. S.; Im, S. S.; Kim, B. C.; Han, Y. K., *J. Appl. Polym. Sci.* **2001**, *80* (9), 1388-1394.
22. Yow, K. H.; Ingram, J.; Korossis, S. A.; Ingham, E.; Homer-Vanniasinkam, S., *British Journal of Surgery* **2006**, *93* (6), 652-661.
23. Amsden, B. G., *Expert Opin. Drug Deliv.* **2008**, *5* (2), 175-187.
24. Liu, Q. Y.; Tan, T. W.; Weng, J. Y.; Zhang, L. Q., *Biomed. Mater.* **2009**, *4* (2), 9.
25. Lamba NMK, W. K., Cooper SL, *Polyurethanes in Biomedical Applications*. Boca Raton: CRC Press, 1998.
26. Walker, B. M. R., C. P., *Handbook of Thermoplastic Elastomers*. Van Nostrand Reinhold: New York, 1988.
27. Hepburn, C., *Polyurethane Elastomers*. Elsevier Science Publishers, New York, 1992.
28. Schubert, M. A.; Wiggins, M. J.; DeFife, K. M.; Hiltner, A.; Anderson, J. M., *J. Biomed. Mater. Res.* **1996**, *32* (4), 493-504.
29. Dupret, I.; David, C.; Colpaert, M.; Loutz, J. M.; Vander Wauven, C., *Macromol. Chem. Phys.* **1999**, *200* (11), 2508-2518.
30. Puskas, J. E.; El Fray, M.; Tomkins, M.; Dos Santos, L. M.; Fischer, F.; Altstadt, V., *Polymer* **2009**, *50* (1), 245-249.
31. Pinchuk, L.; Wilson, G. J.; Barry, J. J.; Schoephoerster, R. T.; Parel, J. M.; Kennedy, J. P., *Biomaterials* **2008**, *29* (4), 448-460.
32. Kamath, K. R.; Barry, J. J.; Miller, K. M., *Adv. Drug Deliver. Rev.* **2006**, *58* (3), 412-436.
33. Guan, J. J.; Sacks, M. S.; Beckman, E. J.; Wagner, W. R., *J. Biomed. Mater. Res.* **2002**, *61* (3), 493-503.
34. Gogolewski, S.; Gorna, K.; Zaczynska, E.; Czary, A., *J. Biomed. Mater. Res. Part A* **2008**, *85A* (2), 456-465.
35. Adhikari, R.; Gunatillake, P. A.; Griffiths, I.; Tatai, L.; Wickramaratna, M.; Houshyar, S.; Moore, T.; Mayadunne, R. T. M.; Field, J.; McGee, M.; Carbone, T., *Biomaterials* **2008**, *29* (28), 3762-3770.
36. Thomas, V.; Jayabalan, M., *J. Biomed. Mater. Res. Part A* **2009**, *89A* (1), 192-205.
37. Reddy, T. T.; Hadano, M.; Takahara, A. In *Controlled release of model drug from biodegradable segmented polyurethane ureas: Morphological and structural features*, Wiley, 2006; pp 241-249.
38. Gogolewski, S.; Gorna, K., *J. Biomed. Mater. Res. Part A* **2007**, *80A* (1), 94-101.
39. Anderson, J. M.; Hiltner, A.; Wiggins, M. J.; Schubert, M. A.; Collier, T. O.; Kao, W. J.; Mathur, A. B., *Polym. Int.* **1998**, *46* (3), 163-171.
40. Sonnenschein, M. F.; Lysenko, Z.; Brune, D. A.; Wendt, B. L.; Schrock, A. K., *Polymer* **2005**, *46* (23), 10158-10166.
41. Hettrich, W.; Becker, R., *Polymer* **1997**, *38* (10), 2437-2445.
42. Kylma, J.; Seppala, J. V., *Macromolecules* **1997**, *30* (10), 2876-2882.
43. Marin, R.; de Paz, M. V.; Ittobane, N.; Galbis, J. A.; Munoz-Guerra, S., *Macromol. Chem. Phys.* **2009**, *210* (6), 486-494.
44. De Paz, M. V.; Marin, R.; Zamora, F.; Hakkou, K.; Alla, A.; Galbis, J. A.; Munoz-Guerra, S., *J. Polym. Sci., Part A: Polym. Chem.* **2007**, *45* (17), 4109-4117.

45. Thoma, R. J., Tan, F. R., Phillips, R. E., *J. Biomater. Appl.* **1988**, *3*, 180-206.
46. Gorna, K.; Gogolewski, S., *Polym. Degrad. Stabil.* **2002**, *75* (1), 113-122.
47. Simmons, A.; Hyvarinen, J.; Poole-Warren, L., *Biomaterials* **2006**, *27* (25), 4484-4497.
48. Guelcher, S. A., *Tissue Eng. Part B-Rev.* **2008**, *14* (1), 3-17.
49. Hong, Y.; Fujimoto, K.; Hashizume, R.; Guan, J. J.; Stankus, J. J.; Tobita, K.; Wagner, W. R., *Biomacromolecules* **2008**, *9* (4), 1200-1207.
50. Rockwood, D. N.; Woodhouse, K. A.; Fromstein, J. D.; Chase, D. B.; Rabolt, J. F., *J. Biomater. Sci.-Polym. Ed.* **2007**, *18* (6), 743-758.
51. Henry, J. A.; Simonet, M.; Pandit, A.; Neuenschwander, P., *J. Biomed. Mater. Res. Part A* **2007**, *82A* (3), 669-679.
52. Stankus, J. J.; Guan, J. J.; Wagner, W. R., *J. Biomed. Mater. Res. Part A* **2004**, *70A* (4), 603-614.
53. Pierce, B. F.; Brown, A. H.; Sheares, V. V., *Macromolecules* **2008**, *41* (11), 3866-3873.
54. Storey, R. F.; Wiggins, J. S.; Puckett, A. D., *J. Polym. Sci., Part A: Polym. Chem.* **1994**, *32* (12), 2345-2363.
55. Asplund, B.; Aulin, C.; Bowden, T.; Eriksson, N.; Mathisen, T.; Bjursten, L. M.; Hilborn, J., *J. Biomed. Mater. Res. Part B* **2008**, *86B* (1), 45-55.
56. Chen, Z.; Cheng, S.; Xu, K., *Biomaterials* **2009**, *30* (12), 2219-2230.
57. Saad, B.; Hirt, T. D.; Welte, M.; Uhlschmid, G. K.; Neuenschwander, P.; Suter, U. W., *J. Biomed. Mater. Res.* **1997**, *36* (1), 65-74.
58. Santerre, J. P.; Woodhouse, K.; Laroche, G.; Labow, R. S., *Biomaterials* **2005**, *26* (35), 7457-7470.
59. Dahiyat, B. I.; Posadas, E. M.; Hirosue, S.; Hostin, E.; Leong, K. W., *Reactive Polymers* **1995**, *25* (2-3), 101-109.
60. Zhang, J.; Hu, C. P., *Eur. Polym. J.* **2008**, *44* (11), 3708-3714.
61. Unal, S.; Ozturk, G.; Sisson, K.; Long, T. E., *J. Polym. Sci., Part A: Polym. Chem.* **2008**, *46* (18), 6285-6295.
62. Griesser, H. J., *Polym. Degrad. Stabil.* **1991**, *33* (3), 329-354.
63. Chou, C. W.; Hsu, S. H.; Wang, P. H., *J. Biomed. Mater. Res. Part A* **2008**, *84A* (3), 785-794.
64. Thoma, R. J.; Phillips, R. E., *J. Biomed. Mater. Res.* **1987**, *21* (4), 525-530.
65. Fromstein, J. D.; Woodhouse, K. A., *J. Biomater. Sci.-Polym. Ed.* **2002**, *13* (4), 391-406.
66. Walinska, K.; Iwan, A.; Gorna, K.; Gogolewski, S., *J. Mater. Sci.-Mater. Med.* **2008**, *19* (1), 129-135.
67. Venkatraman, S.; Boey, F.; Lao, L. L., *Progress in Polymer Science* **2008**, *33* (9), 853-874.
68. Nguyen, J.; Steele, T. W. J.; Merkel, O.; Reul, R.; Kissel, T., *Journal of Controlled Release* **2008**, *132* (3), 243-251.
69. Sipos, L.; Zsuga, M.; Deak, G., *Macromol. Rapid Comm.* **1995**, *16* (12), 935-940.
70. Ba, C. Y.; Yang, J.; Hao, Q. H.; Liu, X. Y.; Cao, A., *Biomacromolecules* **2003**, *4* (6), 1827-1834.
71. Wanamaker, C. L.; Tolman, W. B.; Hillmyer, M. A., *Biomacromolecules* **2009**, *10* (2), 443-448.

72. Coleman, D., *J. Polym. Sci.* **1954**, *14* (73), 15-28.
73. Albertsson, A. C.; Ljungquist, O., *J. Macromol. Sci. Chem.* **1986**, *A23* (3), 411-422.
74. Nagata, M.; Kiyotsukuri, T., *Eur. Polym. J.* **1994**, *30* (11), 1277-1281.
75. Soni, R. K.; Soam, S.; Dutt, K., *Polym. Degrad. Stabil.* **2009**, *94* (3), 432-437.
76. Witt, U.; Yamamoto, M.; Seeliger, U.; Muller, R. J.; Warzelhan, V., *Angew. Chem.-Int. Edit.* **1999**, *38* (10), 1438-1442.
77. Semlyen, J. A., *Large Ring Molecules*. Wiley: New York, 1996.
78. Domb, A. J. K., J., Wiseman, D. M., *Handbook of Biodegradable Polymers*. Harwood Academic Publishers, Amsterdam, 2007.
79. Kricheldorf, H. R.; Rabenstein, M.; Maskos, M.; Schmidt, M., *Macromolecules* **2001**, *34* (4), 713-722.
80. Cohn, D.; Hotovely-Salomon, A., *Polymer* **2005**, *46* (7), 2068-2075.
81. Pepic, D.; Zagar, E.; Zigon, M.; Krzan, A.; Kunaver, M.; Djonla, J., *Eur. Polym. J.* **2008**, *44* (3), 904-917.
82. Nagata, M.; Kiyotsukuri, T.; Takeuchi, S.; Tsutsumi, N.; Sakai, W., *Polymer International* **1997**, *42* (1), 33-38.
83. Nagata, M.; Kiyotsukuri, T.; Minami, S.; Tsutsumi, N.; Sakai, W., *Eur. Polym. J.* **1997**, *33* (10-12), 1701-1705.
84. Ye, L.; Gao, P.; Zhao, Y. M.; Feng, Z. G.; Bai, Y.; Wu, F., *J. Appl. Polym. Sci.* **2008**, *109* (3), 1955-1961.
85. Kint, D.; Munoz-Guerra, S., *Polymer International* **1999**, *48* (5), 346-352.
86. Waris, E.; Ashammakhi, N.; Lehtimaki, M.; Tulamo, R. M.; Tormala, P.; Kellomaki, M.; Konttinen, Y. T., *Biomaterials* **2008**, *29* (16), 2509-2515.
87. Marten, E.; Muller, R. J.; Deckwer, W. D., *Polym. Degrad. Stabil.* **2005**, *88* (3), 371-381.
88. Muller, R. J.; Witt, U.; Rantze, E.; Deckwer, W. D. In *Architecture of biodegradable copolyesters containing aromatic constituents*, Symposium H on Biodegradable Polymers and Macromolecules, France, Elsevier, France, 1997; pp 203-208.
89. Tang, W. M.; Murthy, N. S.; Mares, F.; McDonnell, M. E.; Curran, S. A., *J. Appl. Polym. Sci.* **1999**, *74* (7), 1858-1867.
90. Hiki, S.; Miyamoto, M.; Kimura, Y., *Polymer* **2000**, *41* (20), 7369-7379.
91. Choi, Y. R.; Bae, Y. H.; Kim, S. W., *Macromolecules* **1998**, *31* (25), 8766-8774.
92. Bezemer, J. M.; Weme, P. O.; Grijpma, D. W.; Dijkstra, P. J.; van Blitterswijk, C. A.; Feijen, J., *J. Biomed. Mater. Res.* **2000**, *52* (1), 8-17.
93. Kozłowska, A.; Ukielski, R., *Eur. Polym. J.* **2004**, *40* (12), 2767-2772.
94. Maglio, G.; Palumbo, R.; Rachiero, G. P.; Vignola, M. C., *Macromolecular Bioscience* **2002**, *2* (6), 293-297.
95. Deschamps, A. A.; van Apeldoorn, A. A.; de Bruijn, J. D.; Grijpma, D. W.; Feijen, J., *Biomaterials* **2003**, *24* (15), 2643-2652.
96. Ukielski, R.; Lembicz, F.; Majszczyk, J., *Angew. Makromol. Chem.* **1999**, *271*, 53-60.
97. Yu, Y. C.; Jo, W. H.; Lee, M. S., *J. Appl. Polym. Sci.* **1997**, *64* (11), 2155-2163.
98. Sheth, J. P.; Xu, J. N.; Wilkes, G. L., *Polymer* **2003**, *44* (3), 743-756.

99. Fakirov, S., *Handbook of Condensation Thermoplastic Elastomers*. Wiley, Weinheim, 2005.
100. Park, C.; Kim, E. Y.; Yoo, Y. T.; Im, S. S., *J. Appl. Polym. Sci.* **2003**, *90* (10), 2708-2714.
101. Barbato, F.; Rotonda, M. I. L.; Maglio, G.; Palumbo, R.; Quaglia, F., *Biomaterials* **2001**, *22* (11), 1371-1378.
102. Bettinger, C. J.; Bruggeman, J. P.; Borenstein, J. T.; Langer, R. S., *Biomaterials* **2008**, *29* (15), 2315-2325.
103. Amsden, B. G.; Misra, G.; Gu, F.; Younes, H. M., *Biomacromolecules* **2004**, *5* (6), 2479-2486.
104. Teramoto, N.; Ozeki, M.; Fujiwara, I.; Shibata, M., *J. Appl. Polym. Sci.* **2005**, *95* (6), 1473-1480.
105. Nagata, M.; Tanabe, T.; Sakai, W.; Tsutsumi, N., *Polymer* **2008**, *49* (6), 1506-1511.
106. Yang, J.; Webb, A. R.; Pickerill, S. J.; Hageman, G.; Ameer, G. A., *Biomaterials* **2006**, *27* (9), 1889-1898.
107. Nagata, M.; Kanechika, M.; Saka, W.; Tsutsumi, N., *J. Polym. Sci., Part A: Polym. Chem.* **2002**, *40* (24), 4523-4529.
108. Helminen, A.; Korhonen, H.; Seppala, J. V., *Polymer* **2001**, *42* (8), 3345-3353.
109. Williams, S. R.; Mather, B. D.; Miller, K. M.; Long, T. E., *J. Polym. Sci., Part A: Polym. Chem.* **2007**, *45* (17), 4118-4128.
110. Mather, B. D.; Williams, S. R.; Long, T. E., *Macromol. Chem. Phys.* **2007**, *208* (18), 1949-1955.
111. Mather, B. D.; Miller, K. M.; Long, T. E., *Macromol. Chem. Phys.* **2006**, *207* (15), 1324-1333.
112. Williams, S. R.; Miller, K. M.; Long, T. E., *Prog. React. Kinet. Mec.* **2007**, *32* (4), 165-194.
113. Nguyen, K. T.; West, J. L., *Biomaterials* **2002**, *23* (22), 4307-4314.
114. Burdick, J. A.; Philpott, L. M.; Anseth, K. S., *J. Polym. Sci., Part A: Polym. Chem.* **2001**, *39* (5), 683-692.
115. Karikari, A. S.; Williams, S. R.; Heisey, C. L.; Rawlett, A. M.; Long, T. E., *Langmuir* **2006**, *22* (23), 9687-9693.
116. Grijpma, D. W.; Hou, Q. P.; Feijen, J., *Biomaterials* **2005**, *26* (16), 2795-2802.
117. Matsuda, T.; Mizutani, M., *Macromolecules* **2000**, *33* (3), 791-794.
118. Mizutani, M.; Arnold, S. C.; Matsuda, T., *Biomacromolecules* **2002**, *3* (4), 668-675.
119. Mizutani, M.; Matsuda, T., *Biomacromolecules* **2002**, *3* (2), 249-255.
120. Fisher, J. P.; Tirnmer, M. D.; Holland, T. A.; Dean, D.; Engel, P. S.; Mikos, A. G., *Biomacromolecules* **2003**, *4* (5), 1327-1334.
121. Hou, Q.; Grijpma, D. W.; Feijen, J. In *Preparation of hydrogels by photocrosslinking of fumaric acid monoethyl ester (FAME) functionalized oligomers*, 8th European Symposium on Controlled Drug Delivery, Elsevier Science, Netherlands, 2004; pp 335-337.
122. Ifkovits, J. L.; Padera, R. F.; Burdick, J. A., *Biomed. Mater.* **2008**, *3* (3).
123. Younes, H. M.; Bravo-Grimaldo, E.; Amsden, B. G. B. G., *Biomaterials* **2004**, *25* (22), 5261-5269.

124. Amsden, B. G.; Tse, M. Y.; Turner, N. D.; Knight, D. K.; Pang, S. C., *Biomacromolecules* **2006**, *7* (1), 365-372.
125. Thomas, A. A.; Kim, I. T.; Kiser, P. F., *Tetrahedron Lett.* **2005**, *46* (51), 8921-8925.
126. Tsutsumi, N.; Oya, M.; Sakai, W., *Macromolecules* **2004**, *37* (16), 5971-5976.
127. Nagata, M.; Kato, K.; Sakai, W.; Tsutsumi, N., *Macromolecular Bioscience* **2006**, *6* (5), 333-339.
128. Zhang, X. Q.; Tang, H. H.; Hoshi, R.; De Laporte, L.; Qiu, H. J.; Xu, X. Y.; Shea, L. D.; Ameer, G. A., *Biomaterials* **2009**, *30* (13), 2632-2641.
129. Djordjevic, I.; Choudhury, N. R.; Dutta, N. K.; Kumar, S., *Polymer* **2009**, *50* (7), 1682-1691.
130. Noordover, B. A. J.; van Staalduinen, V. G.; Duchateau, R.; Koning, C. E.; van Benthem, R.; Mak, M.; Heise, A.; Frissen, A. E.; van Haveren, J., *Biomacromolecules* **2006**, *7* (12), 3406-3416.
131. Mather, B. D.; Viswanathan, K.; Miller, K. M.; Long, T. E., *Prog. Polym. Sci.* **2006**, *31* (5), 487-531.
132. Metters, A.; Hubbell, J., *Biomacromolecules* **2005**, *6* (1), 290-301.
133. Ozturk, G. L., T.E., *J. Polym. Sci., Part A: Polym. Chem.* **2009**, Submitted.

## **Chapter 3: Melt Synthesis and Characterization of Aliphatic Low- $T_g$ Polyesters as Pressure Sensitive Adhesives**

**From:** Ozturk, G.I.; Pasquale, A.J.; Long, T.E. *Journal of Adhesion*, submitted, 2009.

### **3.1 Abstract**

Low- $T_g$  Polyesters, which are readily synthesized in the absence of solvent, are excellent candidates for a new generation of pressure sensitive adhesives (PSAs) due to their low cost and potential biodegradability. In this study, linear, all-aliphatic polyesters with low glass transition temperatures ( $T_g$ ) were synthesized using a solvent-free, environmentally friendly melt polycondensation methodology. Polyesters of various compositions were synthesized from different diol and diester monomers to adjust the glass transition temperature and achieve optimum adhesive properties. Melt polycondensation of an isomeric mixture of dimethyl-1,4-cyclohexane dicarboxylate (DMCD), dimethyl adipate (DMAP), diethylene glycol (DEG), and triethylene glycol (TEG) generated a series of linear low- $T_g$  polyesters. The synthesized polyesters were characterized using size exclusion chromatography (SEC), differential scanning calorimetry (DSC), and  $^1\text{H}$  NMR spectroscopy. The frequency and temperature dependent properties of the low- $T_g$  polyesters were characterized using dynamic mechanical analysis (DMA). The adhesive performance of the polymers was evaluated using tack, peel, and shear strength measurements at ambient humidity and temperature. The low- $T_g$  polyesters exhibited peel and tack properties comparable to commercial acrylic adhesives.

## 3.2 Introduction

Pressure sensitive adhesives (PSA) represent a class of adhesives that adhere to a surface upon application of light pressure.<sup>1</sup> PSAs are utilized as self-adhesive labels, double-sided tapes, packaging tapes, and in biomedical applications such as drug loaded adhesive patches.<sup>1-3</sup> Acrylic copolymers,<sup>4-6</sup> styrene-isoprene-styrene (SIS) block copolymers,<sup>7</sup> styrene-butadiene-styrene (SBS) block copolymers,<sup>8</sup> styrene-butadiene rubber (SBR),<sup>9</sup> and polysiloxane<sup>10</sup> based polymers are important families of polymers that are commonly used for PSA applications. In addition, a recent study describes the incorporation of carbon nanotubes and fullerenes<sup>11</sup> to improve the adhesive properties of PSAs.

The performance of adhesives strongly depends on the viscoelastic properties of polymers.<sup>12</sup> PSAs must possess a balanced combination of viscous and elastic properties, for good pressure sensitive adhesive performance. Chang et al.<sup>13,14</sup> demonstrated the four-quadrant viscoelastic window concept to classify different types of PSAs using dynamic storage and loss modulus measured at frequencies of  $10^{-2}$  and  $10^2$  rad/sec, which corresponds to the time scale for bonding and debonding in an adhesive. A low glass transition temperature is another important property associated with polymers for PSA applications. It was shown, for example, that the  $T_g$  of polymers that are intended for use in PSA applications at room temperature generally falls between -20 and -60 °C.<sup>1</sup>

Tack, peel, and shear strength typically define the basic performance of a PSA. Tack corresponds to an adhesive's ability to adhere quickly to a surface and its resistance to separation after short contact time.<sup>15,16</sup> Tack is highly dependent on the modulus of the polymer; therefore, adjusting the composition and molecular weight of a polymer enables

one to regulate tack for specific applications.<sup>17</sup> Moreover, tack not only depends on the bulk property of the polymer, but also on the surface energy of the adhesive and adherend surface.<sup>17,18</sup> Peel strength corresponds to the ability of an adhesive to resist removal from a surface upon peeling at a certain angle from the substrate. Peel strength is not a direct measure of the bond strength, but rather the sum of the energy needed to break the bond and deform the backing material and the adhesive. Shear strength represents an adhesive's ability to resist flow as shearing forces are applied and measured in a static manner. Song et al.<sup>19</sup> characterized adhesion behavior of polymers using a combinatorial approach. Literature<sup>1</sup> reports that the molecular weight distribution of the polymer influences both resistance to peel and resistance to shear. Additives such as tackifiers and plasticizers are commonly incorporated into PSA formulations to adjust  $T_g$  and viscoelastic properties.

In the literature, new types of polymers were investigated for use as novel PSAs and to improve the adhesive properties of existing polymers.<sup>20</sup> More recently, Crosby et al.<sup>21,22</sup> studied patterned adhesives to investigate the influence of surface patterns on adhesion of elastomeric interfaces. In addition, a recent study described incorporation of carbon nanotubes and fullerenes<sup>11</sup> to improve the adhesive properties of PSAs. Moreover, incorporation of varying degrees of crosslinking using UV-curing<sup>23</sup> resulted in balanced tack, peel and shear strength; hence improved the performance.<sup>24,25</sup> Incorporating hydrogen bonding represents an alternative method for improving the adhesive properties of polymers. Improved peel strength, tack, and cohesive strength were achieved upon incorporation of acrylic acid units, since they are able to hydrogen bond to other acrylic acid groups.<sup>26</sup> Recently, new families of PSAs have been derived

from the existing synthetic processes and addressed reduced availability of conventional raw materials.<sup>27-29</sup> For example, polyesters are viable candidates for a new generation of PSAs due to their low cost and potential biodegradability.<sup>30</sup> Polymerization involving a solvent-free melt phase also offers environmental benefits and volatile organic solvents are eliminated from the reaction system.<sup>31,32</sup> Moreover, polyester-based adhesives degrade in a more environmentally friendly manner due to the presence of hydrolyzable ester bonds on the polymer backbone.<sup>30</sup> Incorporating comonomers and tailoring the topology of the polyesters facilitate efficient modification of both their thermomechanical properties and hydrolytic stability.<sup>31-34</sup> The diester monomer, DMCD, used in this study, is commonly utilized to synthesize polyesters and polyamides. Moreover, the influence of the *cis* and *trans* ratios of DMCDs on polymer properties was also investigated partially in response to an earlier study<sup>35,36</sup> that confirmed that the ratio of *cis* and *trans* isomers in a polymer composition affected the physical properties of the resulting polymer. Specifically, the *trans* isomer produces a more crystalline structure compared to the *cis* isomer.<sup>37</sup> Conversely, the *cis* isomer is less symmetrical and introduces kinks into the polymer backbone; therefore it reduces the crystallinity of the polymer.<sup>38</sup> The UV-stability of this monomer also enables the utilization of DMCD-based polyesters for coatings and outdoor applications where UV radiation has a detrimental effect on the mechanical properties.<sup>39</sup>

The current research investigated the synthesis of linear all-aliphatic polyesters for PSA performance. A series of low- $T_g$  polyesters for use as pressure sensitive adhesives was synthesized to determine the dependence of viscoelastic properties on temperature and frequency. In this study, careful selection of the comonomer composition enabled us

to tailor the glass transition temperature over a broad range. The dependence of adhesive properties on molecular weight and composition was analyzed in detail using differential scanning calorimetry (DSC),  $^1\text{H}$  NMR spectroscopy, and adhesive testing methods.

### **3.3 Experimental**

#### **3.3.1 Materials**

Dimethyl adipate (DMAP), diethylene glycol (DEG), triethylene glycol (TEG), titanium tetraisopropoxide (99%), and toluene were purchased from Aldrich. Dimethyl-1,4-cyclohexane dicarboxylate (DMCD, 5/95 *cis/trans* mixture) was donated by Eastman Chemical Company. All reagents and solvents were used as received without further purification.

#### **3.3.2 Polymer characterization**

Molecular weight was determined at 40 °C in THF (HPLC grade) using polystyrene standards on a Waters size exclusion chromatograph (SEC) equipped with 3 in-line PLgel 5  $\mu\text{m}$  MIXED-C columns with an autosampler, a 410 RI detector, a Viscotek 270 dual detector, and an in-line Wyatt Technologies miniDawn multiple angle laser light scattering (MALLS) detector.  $^1\text{H}$  NMR analyses were performed on a Varian Unity 400 spectrometer at 400 MHz in  $\text{CDCl}_3$ . Thermal analysis using a TA Instruments DSC determined thermal transition temperatures at a heating rate of 10 °C/min under nitrogen; all reported values were obtained from the second heating cycle. Dynamic mechanical analysis (DMA) conducted using 8 mm plates at an auto-strain of 0.5 to 5%, ramp rate of 6 °C/min, and frequency of 10 rad/sec.

### 3.3.3 Synthesis of linear low- $T_g$ polyesters

Diester monomer (DMCD or DMAP) and 50 mol% excess diol (DEG or TEG) were charged to a 250-mL, round-bottomed flask equipped with a mechanical stirrer, nitrogen inlet, and condenser. Titanium tetraisopropoxide (60 ppm  $Ti(OR)_4$ ) catalyst was added to facilitate transesterification. The flask was degassed three times using vacuum and nitrogen flush and subsequently heated to 200 °C. The reaction proceeded under nitrogen atmosphere at 200 °C for 2 h and the temperature was raised to 220 °C over 3 h. Vacuum (0.1 to 0.2 mm Hg) was gradually applied for 2 h at 250 °C. The reaction products were characterized without further purification.

### 3.3.4 Characterization of adhesive properties

Samples were prepared from solution casting of the polymer solutions (30 wt% in toluene) on poly(ethylene terephthalate) (Mylar<sup>®</sup>) backing material. Coated films were dried at room temperature for 10 min and subsequently dried in a convection oven at 80 °C for 30 min and ramped to 120 °C for 5 min. The coating weight of each film specimen was measured prior to adhesive testing, with a coating weight of 20 g/m<sup>2</sup> targeted for each sample. In addition to solvent casting, the excellent thermal stability of the polyesters enabled melt coating of polymers onto a Mylar<sup>®</sup> substrate. The surfaces of stainless steel substrates were carefully cleaned with acetone prior to peel, tack, and holding power tests. All the samples were stored under controlled temperature (22 °C) and humidity (50% R.H.) conditions prior to testing.

#### **3.3.4.1 180° Peel testing**

Peel strength of all samples was measured as follows. Strips of 2.54 cm width were cut from the polymer coated Mylar<sup>®</sup> films and the coating weight of the each strip was measured. Upon application of the specimen onto a stainless steel substrate, a 2-kg roller was passed over the sample two times under its own weight before each peel test. The specimen strip was peeled from a stainless steel substrate at an angle of 180° and at a speed of 300 mm/min.<sup>40</sup> The reported results represent an average of five specimens.

#### **3.3.4.2 Loop tack and rolling ball tack**

Rolling ball tack experiments were performed using a 7/16" diameter steel ball and a 2.54 cm x 2.54 cm strip of tape.<sup>41</sup> Loop tack was measured using a ChemInstruments loop tack tester at a cross-head displacement rate of 300 mm/min.<sup>42</sup> Low-T<sub>g</sub> polyester coated Mylar<sup>®</sup> film was brought into contact with a stainless steel surface area (2.54 cm x 2.54 cm). The maximum force per width of the specimen was recorded at a dwell time of 1 second.

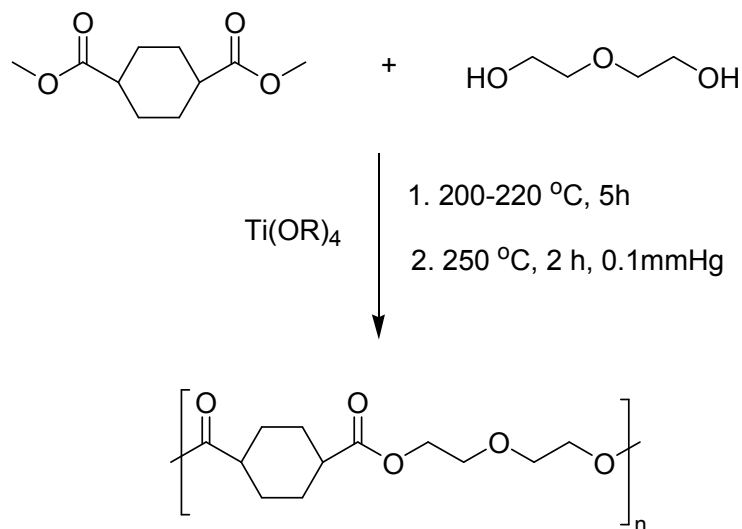
#### **3.3.4.3 Holding power**

Resistance-to-shear was measured as the time required for a specific area of polymer to fail under continuous applied force.<sup>43</sup> Polymer films were cut into strips and a 2.54 cm x 2.54 cm square of the specimen was placed onto a stainless steel panel. A 2-kg roller was passed over the sample two times under its own weight before each test. A clamp was placed on the free end of the specimen ensuring that the clamp extended evenly across the width and was properly aligned to uniformly distribute the load. The specimen was then placed in the test stand and a 1-kg weight was applied to the clamp. The elapsed time during which the specimen completely separated from the test panel

was recorded. Holding power was tested at controlled room temperature and humidity. The reported values represent an average of five tests.

### 3.4 Results and Discussion

The synthesis of solvent-free, water-based acrylic PSAs has become increasingly important because of their environmental advantages.<sup>44</sup> In this study, all linear low- $T_g$  polyesters were also synthesized using an environmentally friendly, solvent-free melt-polycondensation reaction (Scheme 3.1). DMCD was reacted with DEG to form an oligomeric precursor, which underwent subsequent polycondensation to produce high molecular weight polyesters when excess diethylene glycol and methanol were removed under vacuum. Titanium isopropoxide was used as the transesterification catalyst. The transesterification of DMCD and DEG was conducted at 200-220 °C with removal of the methanol. Polycondensation of the oligomers occurred at a higher temperature under vacuum to remove the DEG byproduct. The diester monomer, 1,4-dimethyl cyclohexanedicarboxylate was composed of a mixture of 90% *trans* and 10% *cis* isomers. The *cis* to *trans* ratio in the starting monomer and the polymer was calculated from the integration of the corresponding peaks in <sup>1</sup>H NMR spectrum. Moreover, a series of low- $T_g$  polyesters were synthesized from melt polycondensation of DMAP with DEG or TEG.



**Scheme 3.1.** Synthesis of linear low- $T_g$  polyester via melt polycondensation.

The thermal properties and molecular weight of DMCD, DMAP, DEG, and TEG based low- $T_g$  polyesters are summarized in Table 3.1. The glass transition temperatures of the low- $T_g$  polyesters ranged from  $-49$  to  $-18$   $^\circ\text{C}$  depending on the monomer used in the synthesis. Low- $T_g$  polyesters based on DMCD were characterized using  $^1\text{H}$  NMR spectroscopy to determine the ratio of *cis* to *trans* isomers in the synthesized polymers. This was calculated using the integration of the peaks corresponding to the *cis* and *trans* protons in the cyclohexane ring (Figure 3.1).  $^1\text{H}$  NMR resonances for the cycloaliphatic protons in the cyclohexane dicarboxylate residue were identified at the 2.8-1.5 ppm region. The calculation of the areas under the peaks, which correspond to the *cis* and *trans* cyclohexanedicarboxylate isomer, indicated that the *cis* to *trans* ratio did not change after polycondensation. In the literature, however, studies have indicated that the *cis* to *trans* ratio changes under certain reaction conditions.<sup>36</sup>

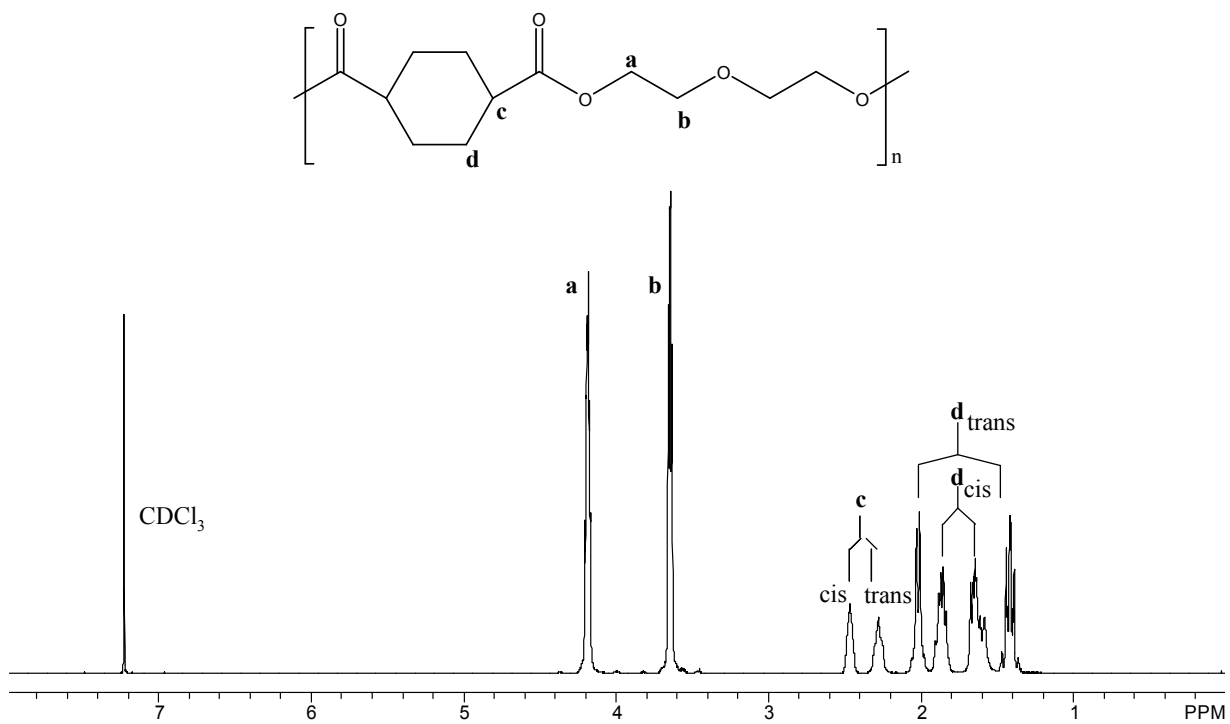


**Figure 3.1.** <sup>1</sup>H NMR of linear DMCD-DEG based polyester.

**Table 3.1.** Summary of thermal analysis results (DMAP: dimethyl adipate, DMCD: 1,4-dimethyl cyclohexanedicarboxylate, DEG: diethylene glycol, and TEG: triethylene glycol).

<b>Composition</b>	<b>M<sub>w</sub> (g/mol)</b>	<b>M<sub>n</sub> (g/mol)</b>	<b>M<sub>w</sub>/M<sub>n</sub></b>	<b>T<sub>g</sub> (°C)</b>
DMAP + DEG	67,000	44,000	1.53	-47
DMAP + TEG	59,000	27,000	2.22	-49
DMCD + DEG	55,000	35,000	1.56	-12
DMCD + TEG	41,000	19,000	2.13	-25

The peel test results confirmed that low-T<sub>g</sub> polyesters based on DMCD and DEG exhibited higher peel strengths compared to DMAP, DEG, and TEG compositions under applied test conditions. All compositions showed cohesive failure, as suggested by the presence of a residue on the stainless steel substrate after the peel test. The summary of peel test results is shown in Table 3.2.

**Table 3.2.** Summary of molecular weight and peel properties of linear low-T<sub>g</sub> polyesters.

<b>Composition</b>	<b>M<sub>w</sub> (g/mol)</b>	<b>M<sub>n</sub> (g/mol)</b>	<b>M<sub>w</sub>/M<sub>n</sub></b>	<b>Thickness (μm)</b>	<b>Peel Adhesion (lb/in)</b>
DMCD+DEG	55,000	35,000	1.56	24 ± 3	2.41 ± 0.10
DMCD+TEG	41,000	19,000	2.13	27 ± 6	0.07 ± 0.01
DMAP+DEG	67,000	44,000	1.53	22 ± 2	0.23 ± 0.01
DMAP+TEG	59,000	27,000	2.22	30 ± 5	0.28 ± 0.01

In order to evaluate the dependence of the adhesives properties of the DMCD-DEG based low- $T_g$  polyesters, polymers of varying molecular weights were selected based on the molecular weight information obtained from SEC analysis. A summary of the thermal analysis and SEC results of polyesters of varying molecular weights (28,000 to 57,000 g/mol) is shown in Table 3.3. Characterization of the thermal properties of the synthesized polyesters indicated that all polymers were amorphous and the  $T_g$  varied between -15 to -11 °C. This temperature range is slightly higher compared to other adhesive compositions studied in earlier literature; however, it should be noted that these  $T_g$  values correspond to neat polymers in the absence of any tackifiers or plasticizers.

**Table 3.3.** Thermal analysis and SEC results of DMCD and DEG based low- $T_g$  polyesters having various molecular weights.

<i>cis/trans</i>	$M_w$ (g/mol) <sup>2</sup>	$M_n$ (g/mol) <sup>2</sup>	$M_w/M_n$	$T_g$ (°C) <sup>3</sup>
<b>DMCD</b> <sup>1</sup>				
95/5	28,000	13,000	2.14	-15
95/5	34,000	14,000	2.43	-15
95/5	44,000	17,000	2.66	-13
95/5	57,000	21,000	2.71	-11

<sup>1</sup>Calculated from <sup>1</sup>H NMR of the polymer

<sup>2</sup>SEC conducted in THF

<sup>3</sup>DSC, 2<sup>nd</sup> heating cycle

Selected low- $T_g$  polymers utilized in this study were characterized using DMA and adhesive tests to evaluate the influence of molecular weight on adhesive properties. DMA revealed the glass transition temperature, storage modulus at room temperature, and the plateau region, which reflects the holding power of the polymer (Figure 3.2). DMA also confirmed that the peak tan delta value increased as the molecular weight of the polymer increased. DMA analysis indicated a high storage modulus at low temperatures, where the polymer behaved like a glass. As expected, and the storage modulus decreased as the temperature was increased and a short plateau region was observed. It should be noted that these polymers did not yield a long plateau region, which is also typical for acrylic adhesives. This was attributed to the lower molecular weights of these polyesters compared to acrylic adhesives, whose molecular weights were as high as 500,000 g/mol.<sup>45</sup> In comparing the behavior of varying molecular weight polymers, we determined that as molecular weight increased, the storage modulus plateau extended and the storage modulus measured at room temperature increased. The molecular weight demonstrates a strong correlation with the adhesive properties due to its influence on several polymer properties such as modulus and viscosity. An increase in molecular weight is expected to improve adhesive properties and an extended plateau region due to higher degree of entanglements. It is important to note that very high molecular weights results in poor wetting due to reduced flow. Another important measurement, following the Dahlquist's criterion, correlates tack with the compliance of an adhesive. It states that the 1 sec creep compliance of a polymer, which is associated with bonding, must be  $3 \times 10^{-7}$  cm<sup>2</sup>/dyne or larger to exhibit good tack characteristics.

DMA analyses of all of the samples indicated that storage modulus at room temperature was clearly below  $3 \times 10^6$  dynes/cm<sup>2</sup>, which is the Dahlquist criterion for tack.

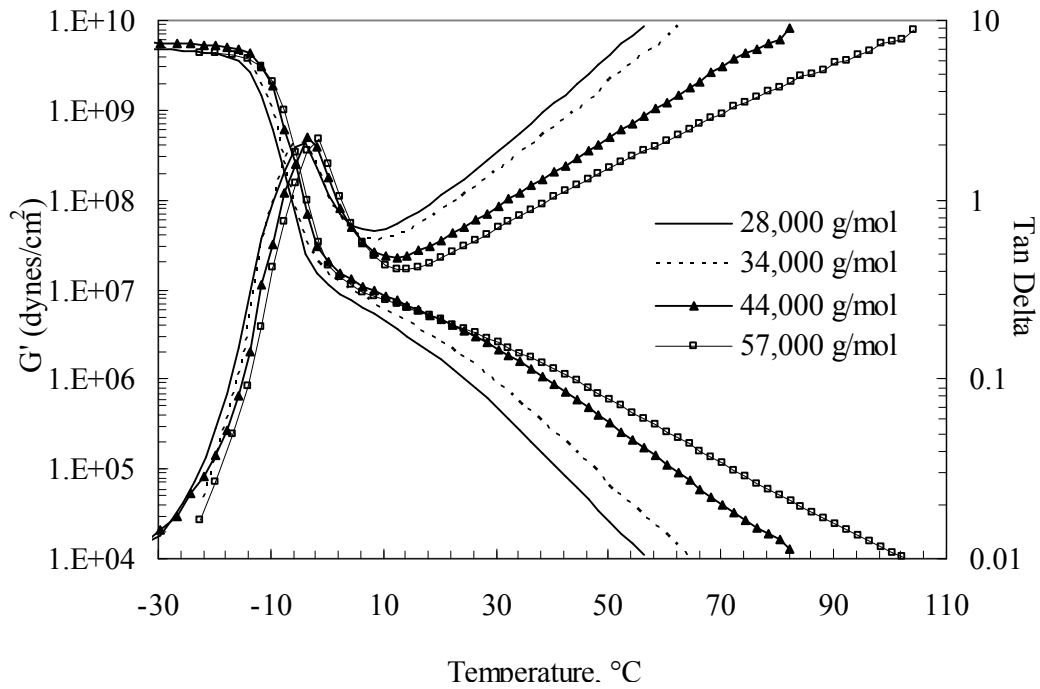


**Figure 3.2.** Dynamic mechanical analysis of molecular weight series.

The influence of molecular weight of the low- $T_g$  polyesters was measured with rolling ball and loop tack methods (Figure 3.3). Tack measurements indicated that as molecular weight increased, tack properties also increased, but then leveled off. The dependence of tack on molecular weight is confirmed in the literature,<sup>46</sup> which shows that as molecular weight increases, the viscosity of the polymer also increases and reaches a high viscosity, thereby efficiently reducing the wetting of the polymer. In some applications, therefore, additives such as tackifiers or plasticizers are required to improve the tack of high molecular weight polymers for adhesive applications.<sup>47,48</sup> However, in the current study all the samples were tested in the absence of plasticizers or tackifiers.

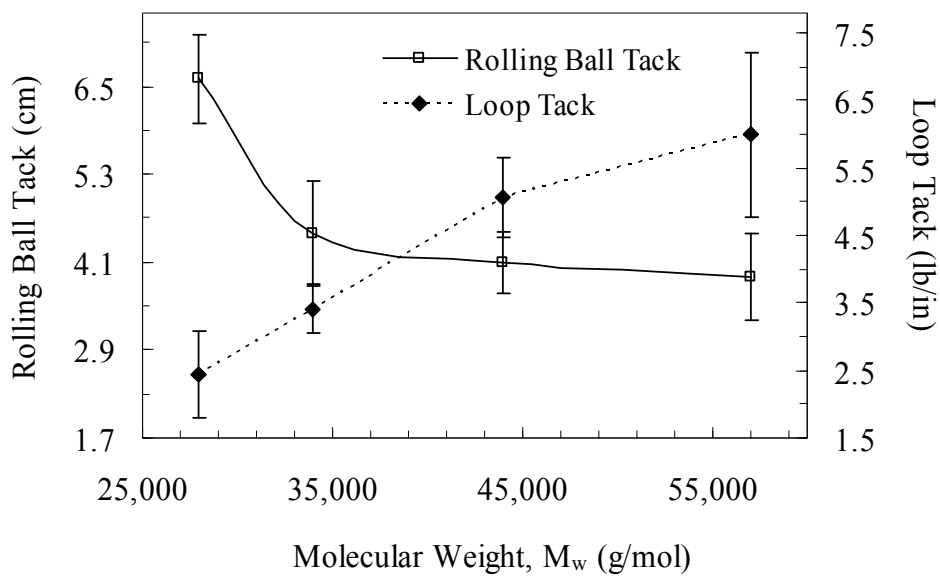


**Figure 3.3.** Tack properties of molecular weight series measured with rolling ball and loop tack techniques.

The resistance-to-shear and peel strength both improved as the molecular weight of the low- $T_g$  polymers increased (Figure 3.4). The polymers exhibited peel strength comparable to commercially available polymers. However, the holding power of the polymers indicated inadequate cohesive strength. The typical holding power for commercially available polymers is reported to be 10,000 min; while the holding power for our low- $T_g$  polyesters was limited to 500 min. It should be noted, however, that the reported adhesive results were determined from characterization of neat samples. Peel performance may be improved through the incorporation of additives such as tackifiers, which are compatible with this polymer composition. Moreover, the molecular weights of the samples under study were lower when compared to conventional polymers typically used as pressure sensitive adhesives. The cohesive strength of these samples may be improved as the molecular weight is increased. Moreover, all these polyesters are linear; therefore, the absence of crosslinking is another factor resulting in low cohesive strength. As reported in the literature<sup>23,49</sup> incorporation of low levels of crosslinking results in enhanced cohesive strength. It is important to note that low crosslink density and high molecular weight between crosslink points is required to attain balanced tack and shear properties.<sup>50</sup>

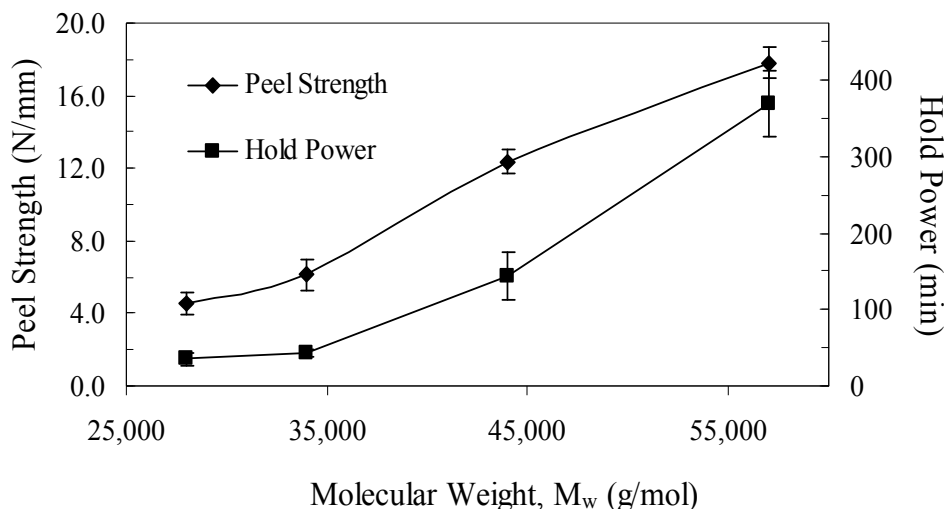


**Figure 3.4.** Peel and shear properties of molecular weight series.

### 3.5 Conclusions

Linear all-aliphatic polyesters having low  $T_g$ s were synthesized using a solvent-free, environmentally friendly melt polycondensation. The polymerization of isomeric mixtures of DMCD, DMAP, and DEG in the melt phase generated a series of polyesters with  $T_g$ s varying from -57 to -11 °C. Rheological studies and the characterization of adhesive properties indicated an influence of molecular weight and polymer composition on adhesive performance. Low- $T_g$  polyesters based on DMCD and DEG exhibited higher peel strengths compared to DMAP, DEG, and TEG compositions. Moreover, peel strength and resistance to shear was enhanced as the molecular weight of low- $T_g$  polyesters increased from 28,000 to 57,000 g/mol. DMCD and DEG based low- $T_g$  polyesters exhibited good tack and peel properties; however, the cohesive strength of the low- $T_g$  polyesters was low compared to polymers used for conventional pressure sensitive applications.

### 3.6 Acknowledgements

This material is based upon work supported by Eastman Chemical Company. The authors would like to thank the Eastman Chemical Company for financial and technical support. The authors also thank Emmet O'Brien, Jeremy Lizotte, and Mark Peters at Eastman Chemical Company for helpful technical discussions.

### 3.7 References

1. Satas, D., *Handbook of Pressure Sensitive Adhesive Technology*. 3rd ed.; Warwick, RI: Satas & Associates: 1999.
2. Tan, H. S.; Pfister, W. R., *Pharm. Sci. Technol. Today* **1999**, 2 (2), 60-69.
3. Ho, K. Y.; Dodou, K., *Int. J. Pharm.* **2007**, 333 (1-2), 24-33.
4. Drzal, P. L.; Shull, K. R., *J. Adhes.* **2005**, 81 (3-4), 397-415.
5. Gower, M. D.; Shanks, R. A., *J. Macromol. Sci. Phys.* **2006**, 44 (8), 1237-1252.
6. Williams, J. A.; Kauzlarich, J. J., *J. Adhes. Sci. Technol.* **2007**, 21 (7), 515-529.
7. Lim, D.-H.; Do, H.-S.; Kim, H.-J., *J. Appl. Polym. Sci.* **2006**, 102 (3), 2839-2846.
8. Romero-Sanchez, M. D.; Pastor-Blas, M. M.; Martin-Martinez, J. M., *Int. J. Adhes. Adhes.* **2003**, 23 (1), 49-57.
9. Romero-Sanchez, M. D.; Pastor-Blas, M. M.; Martin-Martinez, J. M., *J. Adhes.* **2002**, 78 (1), 15-38.
10. Lin, S. B.; Durfee, L. D.; Ekeland, R. A.; McVie, J.; Schalau, G. K., *J. Adhes. Sci. Technol.* **2007**, 21 (7), 605-623.
11. Phillips, J. P.; Deng, X.; Stephen, R. R.; Fortenberry, E. L.; Todd, M. L.; McClusky, D. M.; Stevenson, S.; Misra, R.; Morgan, S.; Long, T. E., *Polymer* **2007**, 48 (23), 6773-6781.
12. Chu, S. G., *Viscoelastic Properties of PSAs*. Van Nostrand-Reinhold Co., New York, 1988.
13. Chang, E. P., *J. Adhes.* **1991**, 34 (1-4), 189-200.
14. Chang, E. P. In *Viscoelastic properties of pressure-sensitive adhesives*, 18th Annual Meeting of the Adhesion-Society, 1995; pp 233-248.
15. Zosel, A., *J. Adhes. Sci. Technol.* **1997**, 11 (11), 1447-1457.
16. Zosel, A., *Int. J. Adhes. Adhes.* **1998**, 18 (4), 265-271.
17. Pasquale, A. J.; Long, T. E.; Truong, H.; Allen, R. D. In *Investigations of the adhesion of maleic anhydride/cyclic olefin alternating copolymers to silicon substrates: Improved materials for 193 nm lithography*, 24th Annual Meeting of the Adhesion-Society, 2001; pp 1-13.
18. Satas, D., *Adhesives Age* **1972**, 12, 19-23.
19. Song, R.; Chiang, M. Y. M.; Crosby, A. J.; Karim, A.; Amis, E. J.; Eidelman, N., *Polymer* **2005**, 46 (5), 1643-1652.
20. Wang, L. C.; Xie, Z. G.; Bi, X. J.; Wang, X.; Zhang, A. Y.; Chen, Z. Q.; Zhou, J. Y.; Feng, Z. G., *Polym. Degrad. Stabil.* **2006**, 91 (9), 2220-2228.

21. Chan, E. P.; Smith, E. J.; Hayward, R. C.; Crosby, A. J., *Adv. Mater.* **2008**, *20* (4), 711-716.
22. Chan, E. P.; Ahn, D.; Crosby, A. J., *J. Adhes.* **2007**, *83* (5), 473-489.
23. Trenor, S. R.; Long, T. E.; Love, B. J., *J. Adhes.* **2005**, *81* (2), 213-229.
24. Lindner, A.; Lestriez, B.; Mariot, S.; Creton, C.; Maevis, T.; Luhmann, B.; Brummer, R., *J. Adhes.* **2006**, *82* (3), 267-310.
25. Czech, Z.; Gsiorowska, M.; Soroka, J., *J. Appl. Polym. Sci.* **2007**, *106* (1), 558-561.
26. Gower, M. D.; Shanks, R. A., *J. Polym. Sci. Pol. Phys.* **2006**, *44* (8), 1237-1252.
27. Wang, T., *Adv. Mater.* **2006**, *18*, 2730.
28. Czech, Z.; Wojciechowicz, M., *Eur. Polym. J.* **2006**, *42*, 2153-2160.
29. Roberge, S.; Dube, M.A., *Polymer* **2006**, *40*, 4094-4104.
30. Doi, Y. F., K., *Biodegradable Plastics and Polymers*. Elsevier: Netherlands, **1994**.
31. Kang, H. Y.; Lin, Q.; Armentrout, R. S.; Long, T. E., *Macromolecules* **2002**, *35* (23), 8738-8744.
32. Unal, S.; Long, T. E., *Macromolecules* **2006**, *39* (8), 2788-2793.
33. McKee, M. G.; Unal, S.; Wilkes, G. L.; Long, T. E., *Prog. Polym. Sci.* **2005**, *30* (5), 507-539.
34. Lin, Q.; Pasatta, J.; Long, T. E., *J. Polym. Sci. Pol. Chem.* **2003**, *41* (16), 2512-2520.
35. Brunelle, D. J.; Jang, T., *Polymer* **2006**, *47* (11), 4094-4104.
36. Berti, C.; Binassi, E.; Celli, A.; Colonna, M.; Fiorini, M.; Marchese, P.; Marianucci, E.; Gazzano, M.; Di Credico, F.; Brunelle, D. J., *J. Polym. Sci. Pt. B-Polym. Phys.* **2008**, *46* (6), 619-630.
37. Kricheldorf, H. R.; Schwarz, G., *Makromol. Chem.* **1987**, *188* (6), 1281-1294.
38. Vanhaecht, B.; Teerenstra, M. N.; Suwier, D. R.; Willem, R.; Biesemans, M.; Koning, C. E., *J. Polym. Sci. Pol. Chem.* **2001**, *39* (6), 833-840.
39. Turner, S. R. S., R. W.; Dombroski, J. R. *Modern polyesters*. Wiley, Chichester: **2003**.
40. American Pressure Sensitive Tape Council, Resistance to peel for single coated pressure-sensitive tapes 180° angle, Norm PSTC-1M. **1986**.
41. American Pressure Sensitive Tape Council, Tack Rolling Ball, Norm PSTC-6M. **1986**.
42. American Pressure Sensitive Tape Council, Loop Tack, Norm PSTC-16. **1986**.
43. American Pressure Sensitive Tape Council, Holding power of pressure-sensitive tape, Norm PSTC-7M. **1986**.
44. Czech, Z., *Int. J. Adhes. Adhes.* **2004**, *24* (2), 119-125.
45. Gower, M. D.; Shanks, R. A., *Macromol. Chem. Physic.* **2005**, *206* (10), 1015-1027.
46. Poh, B. T.; Yong, A. T., *J. Macromol. Sci. Chem.* **2009**, *46* (1), 97-103.
47. Tse, M. F. In *Fundamental understanding in rolling ball tack of tackified block copolymer adhesives*, International Pressure Sensitive Adhesive Technoforum, 1997; pp 95-118.
48. Poh, B. T.; Chow, S. K., *J. Appl. Polym. Sci.* **2007**, *106* (1), 333-337.
49. Czech, Z.; Wojciechowicz, M., *Eur. Polym. J.* **2006**, *42* (9), 2153-2160.

50. Asahara, J.; Hori, N.; Takemura, A.; Ono, H., *J. Appl. Polym. Sci.* **2003**, *87* (9), 1493-1499.

## **Chapter 4: Influence of Long-chain Branching on Adhesive Properties of Aliphatic Low- $T_g$ Polyesters**

### **4.1 Abstract**

Tailoring degree of branching enables control of thermal, mechanical, and rheological properties of polymers. In this study, the influence of long-chain branched topology on adhesive and rheological properties of aliphatic polyesters was investigated. Linear and long-chain branched polyesters with low glass transition temperatures ( $T_g$ s) were synthesized from melt polycondensation of dimethyl-1,4-cyclohexane dicarboxylate (DMCD) and diethylene glycol (DEG). Long-chain branched (LCB) topology was achieved using a trifunctional monomer, trimethyl-1,3,5-benzene tricarboxylate (TMT), as the branching reagent. A series of long-chain branched low- $T_g$  polyester were synthesized using 0.5 to 2 mol% TMT to attain polyesters with different degrees of long-chain branching. Moreover, incorporation of monofunctional monomers including 1-dodecanol and poly(propylene glycol) monobutyl ether was exploited to avoid gel formation at high conversions. Characterization of adhesive properties revealed an improved cohesive strength for long-chain branched low- $T_g$  polyesters. Moreover, the adhesive performances of the linear and long-chain branched polymers were characterized from storage and loss modulus measured that were measured at bonding and debonding frequencies.

## 4.2 Introduction

Pressure sensitive adhesives (PSAs) are widely utilized in medical applications,<sup>1,2</sup> packaging, and electronics.<sup>1,4-6</sup> The literature<sup>3,4</sup> reported that acrylic copolymers,<sup>5</sup> styrene-isoprene-styrene (SIS) and styrene-butadiene-styrene (SBS) block copolymers, and silicones<sup>6,7</sup> are commonly utilized PSAs. In addition, poly(alkylcyanoacrylate)s<sup>8</sup> have been widely exploited as bioadhesives in biomedical applications. As reported in the literature, adhesive properties of polymers are improved through altering the interfacial and bulk properties using crosslinking,<sup>9,10</sup> incorporation of tackifiers<sup>11</sup> and polar groups. More recently, incorporation of carbon nanotubes<sup>12</sup> and fullerenes<sup>13</sup> were investigated to improve the adhesive properties and conductivity of PSAs. In particular, development of conductive adhesives using nano-wires and carbon nanotubes has received interest in microelectronics.<sup>14</sup> Recently, development of new types of polymers<sup>15</sup> and water-borne PSAs have received attention due to environmental concerns.<sup>12</sup>

Several fundamental polymer properties including molecular weight, morphology, chemical composition, and glass transition temperature influence the performance of adhesives.<sup>4,16</sup> In the literature,<sup>10</sup> tailoring polymer topology has been exploited to alter flow properties and adhesive performance of polymers. In particular, incorporation of low levels of crosslinking has been commonly utilized to improve adhesive performance and cohesive strength of acrylic polymers for PSA applications.<sup>17</sup> Several studies<sup>18,19</sup> reported that high levels of crosslinking resulted in improved shear strength. In addition, molecular weight of polymers and entanglement molecular weight have a significant influence on adhesive properties.<sup>19</sup> Benedek and Satas<sup>3,18</sup> reported that increasing the

molecular weight improves the modulus of elasticity and peel strength. However, polymers with high molecular weights exhibit decreased chain mobility and reduced peel strength as a result of inefficient contact with the surface due to of high elastic modulus. Several studies<sup>20,21</sup> reported the influence of molecular weight on tack, peel strength, and hold power. As illustrated in Figure 4.1, tack of a polymeric adhesive is high at low molecular weight region and decreases with increasing molecular weight. In contrast, the increase in peel strength is followed by a decrease as a certain molecular weight is reached. Conversely, shear strength increases with increasing molecular weight. High tack and peel strength are attained at an intermediate molecular weight; therefore, tuning the molecular weight is essential to achieve balanced tack, peel strength, and hold power for improved adhesive performance.<sup>4,22</sup>

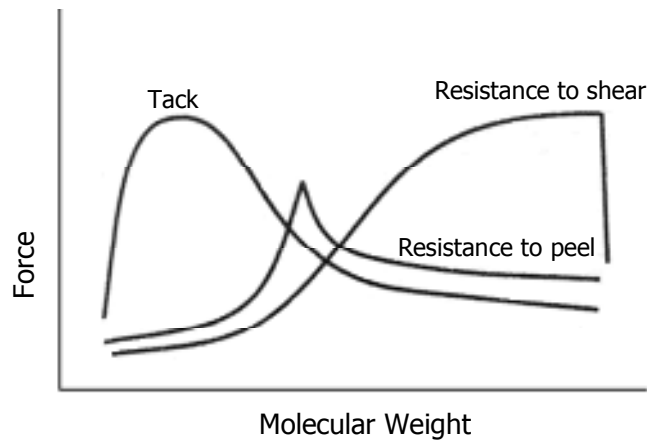


**Figure 4.1.** Effect of molecular weight on adhesive properties.<sup>3</sup>

PSAs possess elastic and viscous properties which highly depend on the temperature and rate of deformation. Loss modulus controls the liquid-like behavior whereas elastic modulus dominates the solid-like character of polymers. The liquid-like property controls the bonding process and promotes contact with surfaces. Moreover,

elastic behavior is important in the debonding process which takes place at higher rates of deformation. Therefore, a balance between solid and liquid-like properties is critical to obtain optimum adhesive performance. Measurement of the storage ( $G'$ ) and loss modulus ( $G''$ ) at bonding and debonding rates provides information about adhesive properties of polymers. Yang and Chang<sup>23</sup> demonstrated the correlation between the storage and loss modulus measured with different adhesive tests. The four-quadrant viscoelastic window concept was reported to classify different types of PSAs based on the storage and loss modulus measured at bonding and debonding frequencies from the rheological master curves (Figure 4.2).

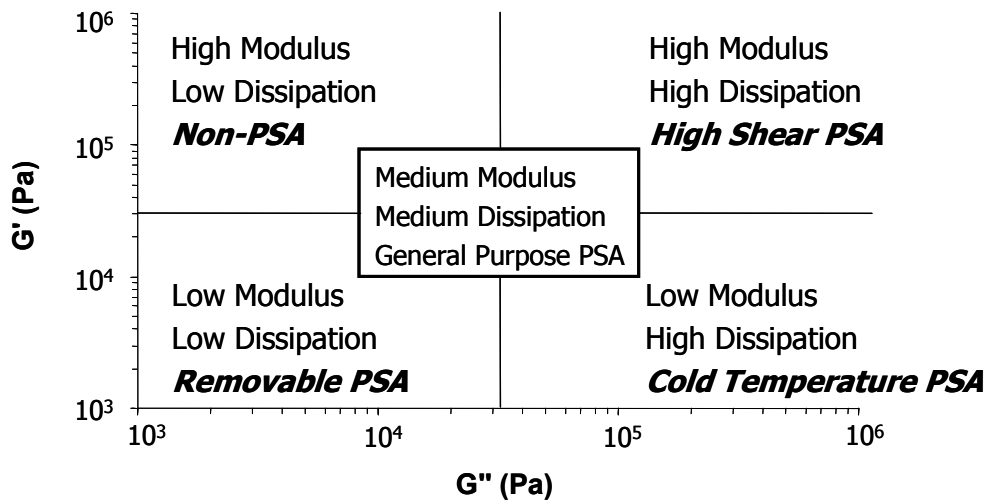


**Figure 4.2.** Four-quadrant viscoelastic window concept proposed by Yang and Chang.<sup>23</sup>

Adhesive performance of PSAs is characterized based on tack,<sup>22,24-26</sup> peel,<sup>27</sup> and shear strength. Tack is commonly measured using loop tack or quick stick methods which measure bond formation and bond separation. Moreover, peel master curves<sup>28</sup> using time temperature superposition principle provide useful information about the influence of peel rate, molecular weight and composition of polymers. Rivals et al.<sup>29</sup>

reported the potential for using a probe test to predict peel and tack properties of PSAs. Chu et al.<sup>30</sup> showed that loss modulus dominated at low frequencies and correlated to tack. In contrast, the storage modulus dominated at high frequencies that were associated with peel testing. It is important to note that sample preparation and testing parameters such as adhesive thickness, backing material, temperature, and humidity influence the measured adhesive properties.

There is a well-established literature<sup>31</sup> showing that tailoring the degree of branching allows controlling thermomechanical and rheological properties of polymers. This study focused on investigating the influence of long-chain branching on adhesive and rheological properties of all-aliphatic low- $T_g$  polyesters. In contrast to hyperbranched polymers, long-chain branched polymers possess branches with molecular weights above the critical molecular weight for entanglement. Gower et al.<sup>32</sup> demonstrated the influence of branching on shear, peel and tack properties of polymers having branches long enough to entangle. In the literature,<sup>31</sup> long-chain branched polymers have been synthesized from polycondensation of difunctional monomers ( $A_2$  and  $B_2$ ) with low levels ( $< 2$  mol%) of trifunctional monomers ( $B_3$ ). Polymers with greater degrees of branching were achieved using higher levels of trifunctional monomers; however incorporation of a branching reagent greater than 2 mol% resulted in crosslinking at high conversions. Our research group<sup>33,34</sup> recently demonstrated synthesis of gel-free highly branched polyester from polymerization of  $A_2$  and  $B_3$  in the melt. Several other studies<sup>30-32</sup> also reported incorporation of a monofunctional alcohol as an endcapper to avoid gel formation and allowed synthesis of polymers with higher degrees of branching.

Our group previously reported synthesis of linear all-aliphatic low- $T_g$  polyesters from melt polycondensation of DMCD and DEG for PSA applications.<sup>35</sup> These low- $T_g$  polyesters exhibited good tack and peel properties for room temperature PSA applications. In this study, synthesis of long-chain branched aliphatic polyesters was investigated to enhance adhesive properties through introduction of long-chain branched topology. Polymers with different levels of branching were synthesized to investigate the influence of long-chain branching on rheological and adhesive properties. Utilization of 1-dodecanol, was investigated to prevent gelation at high conversions. In addition, incorporation of a long-chain monofunctional monomer, poly(propylene glycol) monobutyl ether, was investigated to hinder gel formation and lower the glass transition temperature of the polymers.

## **4.3 Experimental**

### **4.3.1 Materials**

Diethylene glycol (DEG), trimethyl-1,3,5-benzenetricarboxylate (TMT), poly(propylene glycol) monobutyl ether ( $M_n=1000$  g/mol), 1-dodecanol, and titanium tetraisopropoxide (99%) were purchased from Aldrich. Eastman Chemical Company kindly provided dimethyl-1,4-cyclohexane dicarboxylate (DMCD, 60/40 *cis/trans* mixture). All reagents and solvents were used as received without further purification.

### **4.3.2 Characterization**

Molecular weight was determined at 40 °C in THF using a Waters size exclusion chromatograph (SEC) equipped with 3 in-line PLgel 5  $\mu$ m MIXED-C columns with an autosampler, a 410 RI detector, a Viscotek 270 dual detector, and an in-line Wyatt Technologies miniDawn multiple angle laser light scattering (MALLS) detector.  $^1\text{H}$

NMR spectroscopic analysis was performed on a Varian Unity 400 spectrometer at 400 MHz in CDCl<sub>3</sub>. Thermal analysis using TA Instruments Q-100 DSC determined thermal transition temperatures at a heating rate of 10 °C/min under nitrogen. All reported values were obtained from the second heating cycle. Dynamic mechanical analysis (DMA) characterized the temperature and frequency dependence of the polyesters. Samples were characterized using 8 mm plates at an auto-strain of 0.5 to 5%, ramp rate of 6 °C/min, and frequency of 10 rad/sec. Rheological properties of the polymers were characterized using a TA Instruments AR 1000 stress-controlled rheometer with 8 mm parallel plate geometry. Strain amplitudes were limited to the linear viscoelastic regime over a frequency range of 0.1 to 100 Hz. Time temperature superposition method was applied to investigate the frequency dependence over a wide frequency range. Storage modulus (G') and loss modulus (G'') were measured at bonding ( $10^{-2}$  rad/sec) and debonding frequencies ( $10^2$  rad/sec). Viscoelastic windows of the low-T<sub>g</sub> polyesters were constructed from values of G' and G'' measured at bonding and debonding frequencies following the Yang and Chang model.<sup>36</sup> The viscoelastic windows were generated for both linear and long-chain branched samples to investigate the influence of topology on viscoelastic properties and adhesive performance.

### **4.3.3 Adhesive testing**

Polymer solutions (30 wt%) were prepared in toluene and stirred overnight before casting. The polymer solutions were cast on poly(ethylene terephthalate) (Mylar<sup>®</sup>) backing material using a doctor's blade to obtain films with homogeneous coating thickness. Polymer-coated Mylar<sup>®</sup> films were dried at room temperature for 10 min and subsequently dried in a convection oven at 80 °C for 10 min and ramped to 120 °C for an

additional 5 min. The coating weights of the films were measured gravimetrically using the difference between the mass of coated and uncoated Mylar<sup>®</sup> films. The samples were cut into strips with a width of 2.54 cm. The stainless steel substrates were cleaned with acetone prior to each test to remove any impurities on the surface.

#### **4.3.3.1 180° Peel testing**

The sample strips were adhered onto stainless steel substrates and a 2-kg roller was passed over each sample two times under its own weight before each peel testing. The specimens were peeled from the stainless steel substrate at a speed of 300 mm/min and angle of 180°. <sup>37</sup> All the peel tests were performed in controlled temperature (22 °C) and humidity environment (50% R.H.). An average of five peel testing results are reported.

#### **4.3.3.2 Holding power**

The cohesion strength of the low- $T_g$  aliphatic polyesters was estimated from resistance to shear that was measured in a static manner. The sample strips were cut and a square area (2.54 cm x 2.54 cm) of each specimen was placed onto a stainless steel substrate. 2-kg roller was passed over the sample two times under its own weight before each test. The specimen was placed in the test stand and a 1-kg weight was applied to the end of the sample. The time during which the specimen completely separated from the test panel was recorded. <sup>38</sup> The reported values represent an average of five tests.

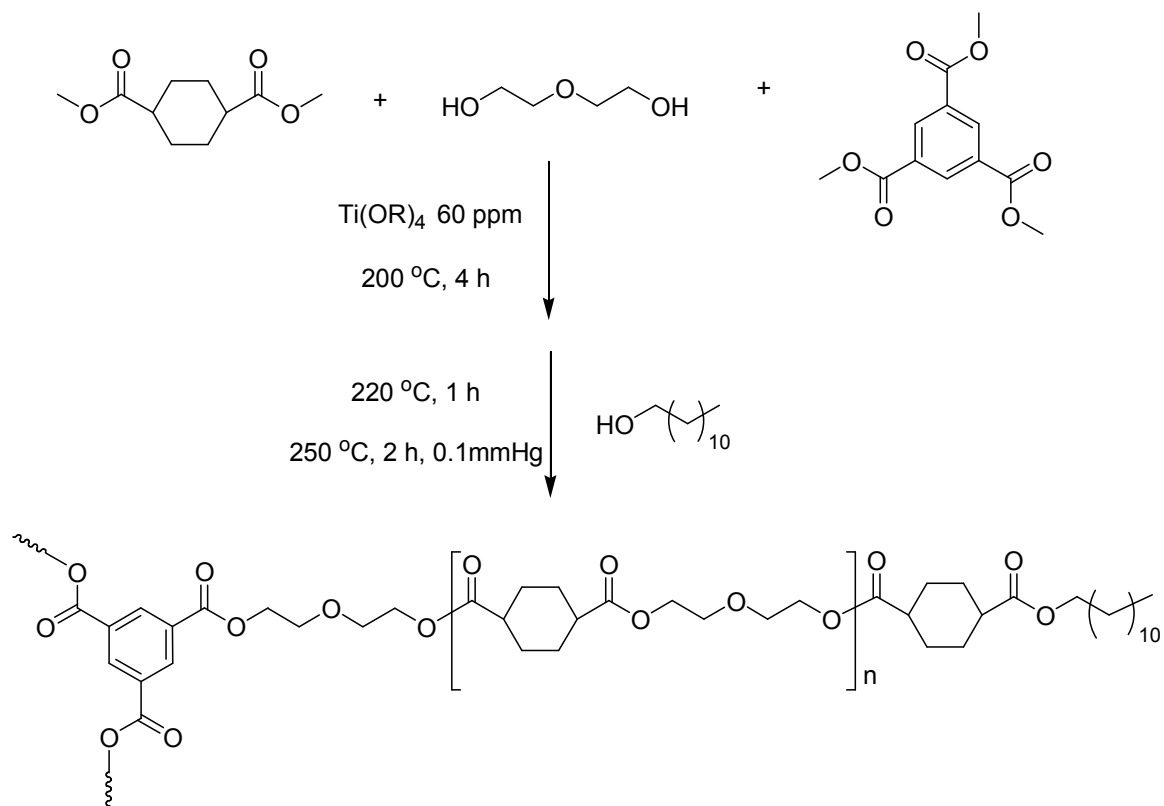
#### **4.3.4 Synthesis of long-chain branched low- $T_g$ polyesters**

Synthesis of long-chain branched polyesters included a pre-reaction of TMT (0.5 mol%) with DEG to prevent TMT loss due to sublimation at the reaction temperatures under nitrogen purge. The branching reagent, TMT, (0.13 g, 0.5 mmol) and DEG (15.92

g, 150 mmol) were charged to a 100-mL, two-necked, round-bottomed flask equipped with a mechanical stirrer, nitrogen inlet, and condenser. Titanium tetraisopropoxide (60 ppm  $\text{Ti}(\text{OR})_4$ ) catalyst was added to facilitate the transesterification reaction. The flask was degassed three times using vacuum and nitrogen flush and subsequently heated to 180 °C. The pre-reaction proceeded under nitrogen atmosphere at 180 °C for 30 min. The diester monomer, dimethyl-1,4-cyclohexanedicarboxylate (DMCD) (20.23 g, 100 mmol), was added to the reaction mixture and the temperature was maintained at 200 °C for 3 h. The temperature was subsequently raised to 220 °C over 2 h. Vacuum (0.1 mmHg) was applied gradually and the temperature was raised to 250 °C. Aliquots of the reaction mixture were removed and the solubility of the products was tested in chloroform. The products were characterized using  $^1\text{H}$  NMR spectroscopy without further purification.

#### **4.3.5 Synthesis of long-chain branched low- $T_g$ polyesters in the presence of monofunctional monomers**

Long-chain branched polyesters were synthesized using monofunctional monomers such as 1-dodecanol and poly(propylene glycol) monobutyl ether to avoid gelation at high conversions. TMT, (0.13 g, 0.5 mmol), was pre-reacted with DEG (15.92 g, 150 mmol) at 180 °C for 30 min. Subsequently, DMCD (20.23 g, 100 mmol) was added and the reaction proceeded under nitrogen atmosphere at 200 °C for 4 h. The monofunctional monomer, 1-dodecanol or poly(propylene glycol), was added and the temperature was raised to 220 °C over 1 h. Vacuum was applied gradually and the temperature was raised to 250 °C over 2 h (Scheme 4.1 and 4.2). Aliquots were removed from the reaction flask to test the solubility of the samples in chloroform.



**Scheme 4.1.** Synthesis of long-chain branched low- $T_g$  polyester in the presence of 1-dodecanol.



## 4.4 Results and Discussion

Long-chain branched low- $T_g$  polyesters with varying degrees of branching were synthesized to probe the influence of topology on adhesive performance and viscoelastic properties. The long-chain branched polyesters were synthesized from solvent-free melt polycondensation of DMCD, DEG, and TMT. Trifunctional branching reagent was pre-reacted with the diethylene glycol during each reaction to prevent TMT sublimation. It was critical to determine the amount of TMT incorporated in the reaction due to its influence on the resulting degree of branching; therefore the amount of TMT incorporated in the polymer was calculated from  $^1\text{H}$  NMR spectroscopic analysis of the products.

Our previous study<sup>35</sup> on synthesis of linear low- $T_g$  polyesters from melt polycondensation of DMCD and DEG showed that the highest attainable molecular weight was limited to 55,000 g/mol under the applied polymerization conditions. As shown in Table 4.1, reaction of DMCD and DEG in the presence of a trifunctional reagent resulted in synthesis of long-chain branched low- $T_g$  polyesters with increased weight-average molecular weights. As shown in Table 4.1, incorporation of TMT increased the polydispersity of the polymers as expected for branched polymers. The weight-average molecular weight of the polymer increased from 54,800 to 130,000 g/mol as 0.5 mol% of TMT was included in the reaction. Incorporation of 0.5 mol% TMT produced long-chain branched polymers with molecular weights of 104,000 and 130,000 g/mol. Increasing the concentration of the branching reagent increased the degree of branching. However, as reported in the literature<sup>31</sup> reaction of higher levels of multifunctional monomers resulted in gelation at high conversions. Incorporation of the

branching reagent greater than 0.5 mol% resulted in crosslinked polymers under applied polymerization conditions.

The degree of branching was characterized using the branching index ( $g'$ ) that was calculated from SEC coupled with viscosity detector. The  $g'$  values close to unity indicated linear topology. Conversely, lower values of  $g'$  indicated higher levels of branching which was consistent with the change in polydispersity of the polymers. As reported in the literature,<sup>31</sup>  $g'$  was calculated using the intrinsic viscosities of branched ( $[\eta]_{\text{branched}}$ ) and linear polymers ( $[\eta]_{\text{linear}}$ ) of equivalent molecular weights. The following equation was used to calculate the branching index of the synthesized long-chain branched polyesters.

$$g' = [\eta]_{\text{branched}}/[\eta]_{\text{linear}}$$

As summarized in Table 4.1,  $g'$  was calculated as 0.96 for linear polyesters. Conversely, the value of  $g'$  decreased to 0.84 and 0.77 for the long-chain branched polyesters indicating different degrees of branching. The final degree of branching highly depended on the reaction conditions including heating rate, reaction temperature, and vacuum levels at the second step of the reaction. Therefore, the difference in molecular weights, polydispersities, and branching index of the two branched samples given in Table 4.1 were attributed to slight changes in experimental conditions. In the presence of equivalent concentrations of TMT, longer reaction times produced polymers having higher weight-average molecular weight with higher degree of branching. Moreover, replicates of reaction revealed the importance of reaction time, temperature, stirring rate, and catalyst concentration on the resulting degree of branching.

**Table 4.1.** Summary of molecular weight of linear and long-chain branched low- $T_g$  polyesters.

<b>Mol % TMT<sup>1</sup></b>	<b>M<sub>w</sub> (g/mol)</b>	<b>M<sub>n</sub> (g/mol)</b>	<b>M<sub>w</sub>/M<sub>n</sub></b>	<b>g'</b>
0.5	130,000	24,000	5.37	0.77
0.5	104,000	37,000	2.81	0.84
0	54,800	35,000	1.56	0.96

Rheological characterization indicated that long-chain branched polymers exhibited enhanced melt stability compared to linear low- $T_g$  polyesters. Moreover, the melt stability of the branched samples highly depended on the degree of branching. As shown in Figure 4.3, the linear polymer exhibited a short plateau region and the melt stability was poor at elevated temperatures. The significant drop in storage modulus at elevated temperatures was attributed to insufficient entangling of the linear low- $T_g$  polyesters due to low weight-average molecular weights. However, long-chain branched samples exhibited a longer plateau region compared to linear low- $T_g$  polyesters. Moreover, the plateau region was further extended for the long-chain branched polymer having higher weight-average molecular weight and lower  $g'$  relating to higher degree of branching. As reported in the literature,<sup>31</sup> long-chain branching allowed control of rheological properties for branches with molecular weights high enough to entangle. In contrast to short-chain branched and hyperbranched polymers, long-chain branched polymers exhibit enhanced melt stability.

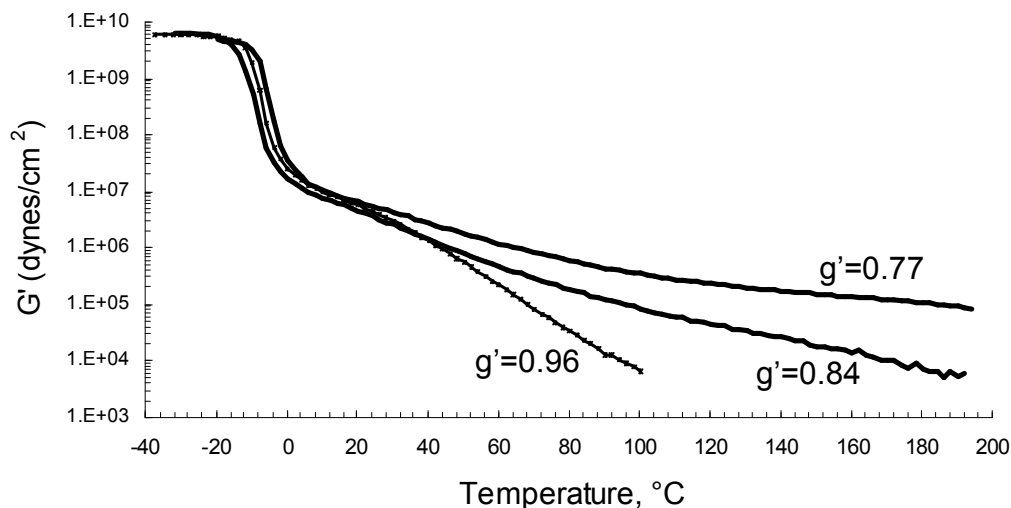


**Figure 4.3.** Temperature sweep of linear and branched polyesters.

Adhesive properties of the linear and long-chain branched low- $T_g$  polyesters were characterized using peel strength and hold power tests. Characterization of the adhesive properties showed that peel and tack properties of linear polymers were comparable to commercial adhesives. However, the hold power measurements revealed an inadequate cohesive strength. Figure 4.3 depicts peel and hold power performance of low- $T_g$  polyesters having linear or long-chain branched topology. Characterization of the peel strength revealed that the peel strength did not change significantly as the molecular weight increased. However, measurement of hold power increased significantly from 300 to 1200 min indicating an enhanced cohesive strength. The improvement in cohesive strength was attributed to higher resistance of the long-chain branched polymers for deformation due to greater number of entanglements and higher weight-average molecular weights. The long-chain branched samples possessed significantly higher weight-average molecular weights compared to the linear polymer. O'Connor et al.<sup>39</sup> also reported that larger numbers of entanglements enhanced the shear strength and hindered the elongation during a static shear test.

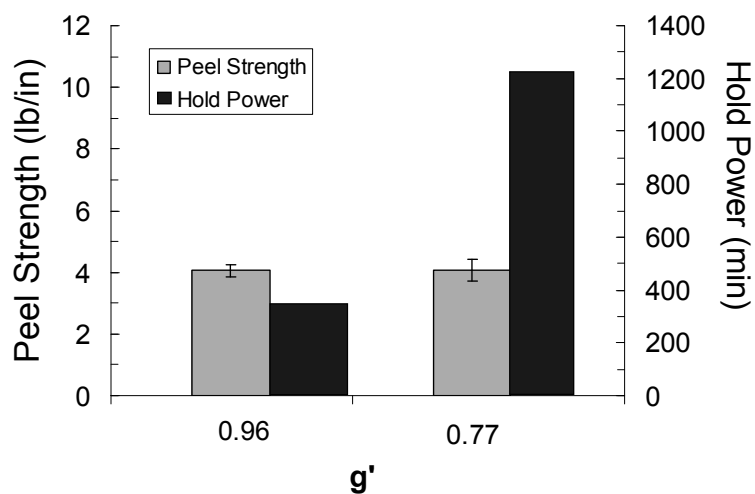


**Figure 4.4.** Peel strength and holding power properties of linear and branched low- $T_g$  polyesters.

In the absence of monofunctional reagents, the amount of branching reagent incorporated in the reaction was limited due to gelation at high conversions. In this study, long-chain branched low- $T_g$  polyesters were synthesized in the presence of 1-dodecanol to hinder gel formation and attain higher degrees of long-chain branching. Use of 1-dodecanol permitted the incorporation of 2 mol% TMT and avoided crosslinking of the polymer at high conversions. Conversely, the highest amount of TMT was limited to 0.5 mol% in the absence of an endcapper.  $^1\text{H}$  NMR spectroscopic analysis verified incorporation of 1-dodecanol (Figure 4.5). For long-chain branched polymers, the degree of branching depended on the reaction conversion and the concentration of the branching reagent. Synthesis of long-chain branched polyesters using 0.5 mol% indicated that  $g'$  value was 0.70. However, synthesis of long-chain branched polyesters in the presence of monofunctional comonomer enabled using 2 mol% and  $g'$  was reduced to 0.59 indicating a higher degree of branching.

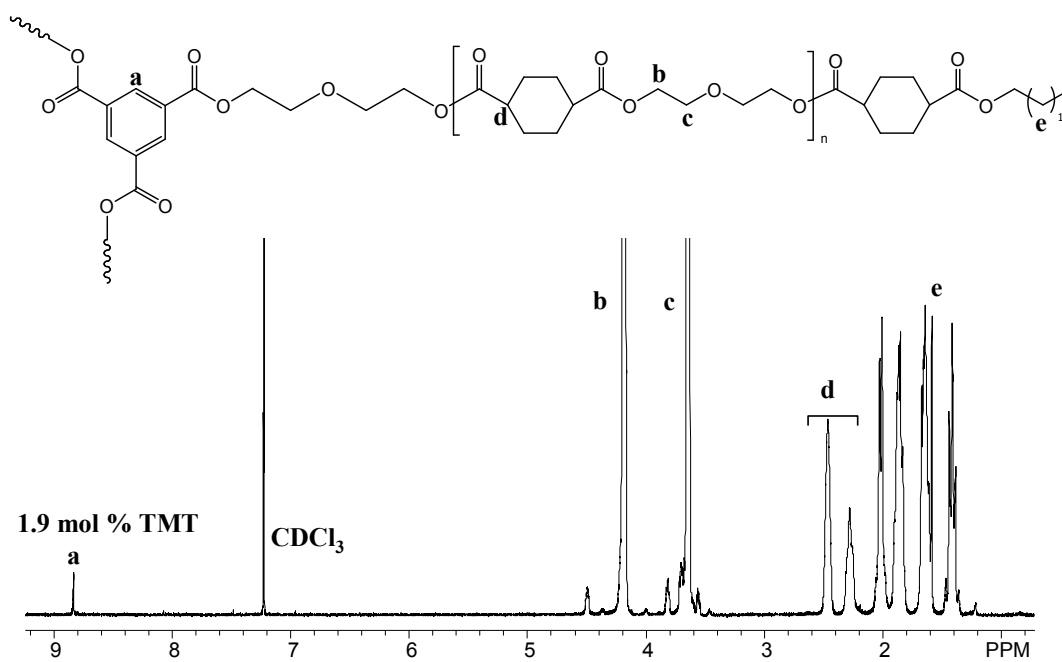


**Figure 4.5.** <sup>1</sup>H NMR of dodecylester endcapped long-chain branched polyester.

Increasing the molecular weight is required to enhance cohesive strength of adhesives. However, as reported in the literature, when the molecular weight is very high, the polymer exhibits poor wetting properties due to reduced flow. Moreover, at very high molecular weights the ability of the polymer to desorb energy is lower and the tack is lowered. Therefore, there is a limit for having high molecular weights to attain balanced cohesive strength while maintaining the tack property. Incorporation of poly(propylene glycol) monobutyl ether endcapper was envisaged to lower the glass transition temperature and enhance flow properties and tack at high molecular weights.  $^1\text{H}$  NMR spectroscopic analysis confirmed the incorporation of targeted amount of branching reagent and endcapper (Figure 4.6).

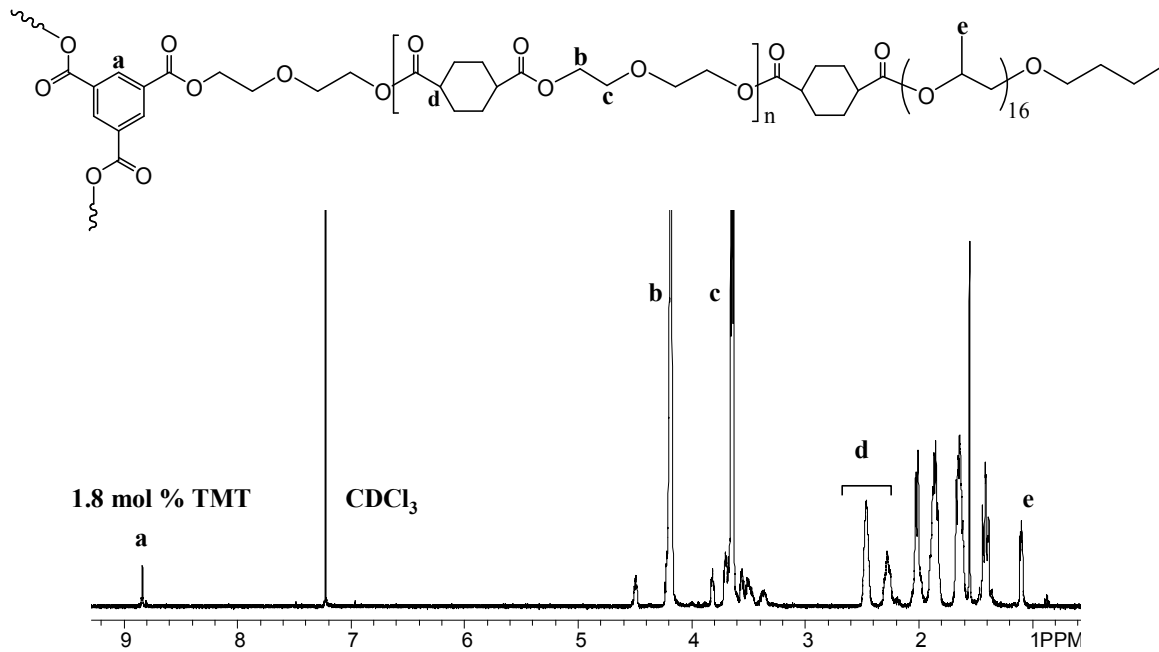


**Figure 4.6.**  $^1\text{H}$  NMR of poly(propylene glycol) monobutyl ether endcapped long-chain branched polyester.

Molecular weights of the long-chain branched low- $T_g$  polyesters were characterized using SEC (Table 4.2). Characterization of the molecular weight and branching index indicated that synthesis of long-chain branched low- $T_g$  polyesters in the presence of monofunctional reagents retarded gel formation and permitted synthesis of gel-free polymers having higher degrees of branching. Moreover, the presence of endcappers allowed incorporation of TMT up to 3.2 mol%. As shown in Table 4.2, reaction of higher levels of trifunctional reagent resulted in synthesis of polymers with higher degrees of branching as depicted from the lower branching index values. Moreover, incorporation of poly(propylene glycol) monobutyl ether as the monofunctional long-chain endcapper resulted in lowering the glass transition temperature of the low- $T_g$  polyesters. Adhesive testing of the samples using peel testing

revealed the dependence of peel strength on molecular weight. Long-chain branched low- $T_g$  polyester having a molecular weight of 150,000 g/mol exhibited the highest peel strength. Despite very high molecular weight, the presence of long-chain endcappers permitted lowering the  $T_g$  and maintaining tack.

**Table 4.2.** Summary of molecular weight and compositional properties of linear and long-chain branched low- $T_g$  polyesters.

Endcapper Type	<sup>1</sup> Mol% endcapper	<sup>1</sup> Mol TMT	$M_w$ (g/mol)	$M_w/M_n$	<sup>2</sup> $T_g$ (°C)	$g'$	Peel Strength (lb/in)
No endcapper	0	0.5	85,000	5.37	-15	0.77	1.96 ± 0.19
DD <sup>2</sup>	2.8	1.9	120,000	7.05	-14	0.59	1.97 ± 0.23
PPG-M <sup>3</sup>	1.3	1.8	104,000	11.1	-22	0.56	1.73 ± 0.13
PPG-M <sup>3</sup>	4	3.2	150,000	13.5	-12	0.54	2.54 ± 0.27

<sup>1</sup>Calculated using <sup>1</sup>H NMR <sup>2</sup>DD: 1-dodecanol

<sup>3</sup>PPG-M: Poly(propylene glycol) monobutyl ether

Temperature and frequency dependence of storage modulus, loss modulus, and of low- $T_g$  polyesters was studied to investigate the influence of long-chain branching on viscoelastic and adhesive properties. The viscoelastic performance windows were constructed for both linear and long-chain branched low- $T_g$  polyesters following Yang and Chang model.<sup>23</sup> Viscoelastic windows of the low- $T_g$  polyesters were constructed plotting storage ( $G'$ ) and loss ( $G''$ ) modulus on a log-log cross plot (Figure 4.7). Storage modulus ( $G'$ ) and loss modulus ( $G''$ ) were measured at bonding and debonding frequencies,  $10^{-2}$  rad/sec and  $10^2$  rad/sec, respectively. The comparison of the

viscoelastic windows of linear and long-chain branched samples revealed that the presence of long-chain branches shifted the performance window to a higher modulus region indicating an improved cohesive strength. The point  $G'$  (0.01 rad/sec),  $G''$  (100 rad/sec) on the plot was shifted to a higher modulus, lower dissipation region as the topology was changed from linear to long-chain branched architecture.

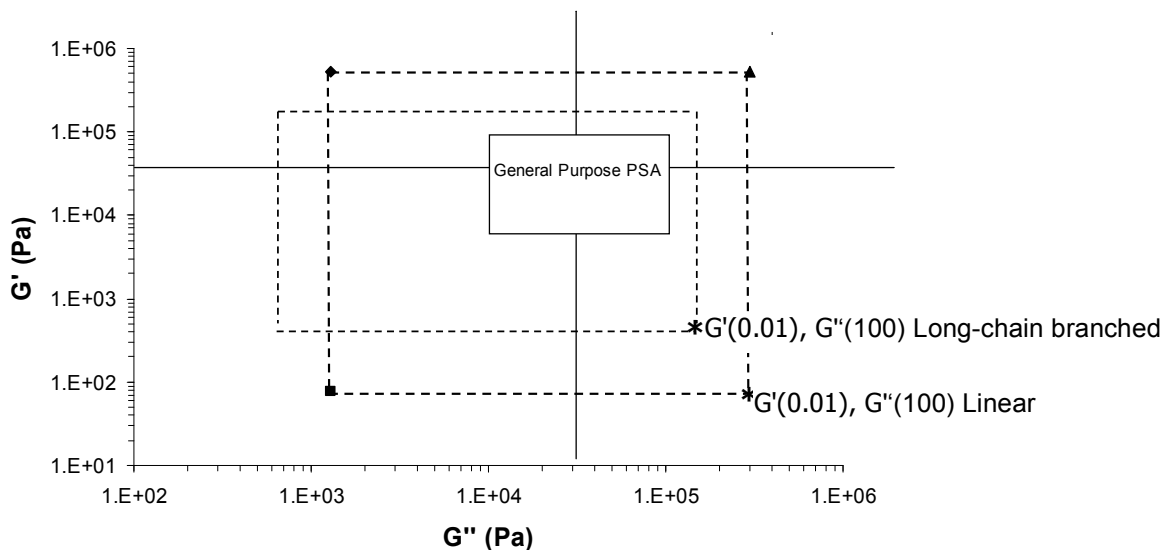


**Figure 4.7.** Viscoelastic window of linear and long-chain branched polyesters.

## 4.5 Conclusions

Synthesis and characterization of linear and long-chain branched, low- $T_g$  polymers based on DMCD and DEG were investigated for PSA applications. Synthesis of long-chain branched polymers based on DMCD, DEG, and TMT showed that pre-reaction of TMT with DEG efficiently prevented TMT sublimation and maintained the stoichiometric balance. Characterization of adhesive properties revealed that long-chain branched polymers exhibited an enhanced cohesive strength. Incorporation of endcappers, 1-dodecanol or poly(propylene glycol) monobutyl ether, allowed synthesis of polymers having higher degrees of branching without gel formation at high conversions.

Viscoelastic performance windows that were constructed using Yang and Chang model indicated that adhesive behavior of linear and long-chain branched low- $T_g$  polyesters was similar to removable adhesives. Incorporation of different degrees of branching indicated a shift in the adhesive performance towards a higher shear region in the adhesive performance window.

## 4.6 Acknowledgements

This material is based upon work supported by Eastman Chemical Company. The authors also thank Eastman Chemical Company for financial and technical support. The authors acknowledge Emmet O'Brien, Jeremy Lizotte, and Mark Peters at Eastman Chemical Company for helpful discussions.

## 4.7 References

1. Renvoise, J.; Burlot, D.; Marin, G.; Derail, C., *Int. J. Pharm.* **2009**, *368* (1-2), 83-88.
2. Kim, J. H.; Lee, C. H.; Choi, H. K., *Drug Dev. Ind. Pharm.* **2002**, *28* (7), 833-839.
3. Satas, D., *Handbook of Pressure Sensitive Adhesives*. Warwick, Satas & Associates: 1999.
4. Benedek, I., *Pressure Sensitive Adhesives and Applications*. Marcel Dekker, 2004.
5. Gower, M. D.; Shanks, R. A., *J. Polym. Sci. Pt. B-Polym. Phys.* **2006**, *44* (8), 1237-1252.
6. Lin, S. B.; Durfee, L. D.; Ekeland, R. A.; McVie, J.; Schalau, G. K., *J. Adhes. Sci. Technol.* **2007**, *21* (7), 605-623.
7. Ho, K. Y.; Dodou, K., *Int. J. Pharm.* **2007**, *333* (1-2), 24-33.
8. Vauthier, C.; Dubernet, C.; Fattal, E.; Pinto-Alphandary, H.; Couvreur, P., *Adv. Drug Deliv. Rev.* **2003**, *55* (4), 519-548.
9. Trenor, S. R.; Long, T. E.; Love, B. J., *J. Adhesion* **2005**, *81* (2), 213-229.
10. Czech, Z.; Gsiorowska, M.; Soroka, J., *J. Appl. Polym. Sci.* **2007**, *106* (1), 558-561.
11. Poh, B. T.; Yong, A. T., *J. Macromol. Sci. Part A-Pure Appl. Chem.* **2009**, *46* (1), 97-103.
12. Wang, T.; Lei, C. H.; Dalton, A. B.; Creton, C.; Lin, Y.; Fernando, K. A. S.; Sun, Y. P.; Manea, M.; Asua, J. M.; Keddie, J. L., *Adv. Mater.* **2006**, *18* (20), 2730.

13. Phillips, J. P.; Deng, X.; Stephen, R. R.; Fortenberry, E. L.; Todd, M. L.; McClusky, D. M.; Stevenson, S.; Misra, R.; Morgan, S.; Long, T. E., *Polymer* **2007**, *48* (23), 6773-6781.
14. Lu, D. D.; Li, Y. G.; Wong, C. P., *J. Adhes. Sci. Technol.* **2008**, *22* (8-9), 815-834.
15. Bunker, S. P.; Wool, R. P., *J. Polym. Sci. Pol. Chem.* **2002**, *40* (4), 451-458.
16. Chu, S. G., *Viscoelastic Properties of PSAs*. Van Nostrand-Reinhold Co., New York, 1988.
17. Czech, Z.; Loclair, H.; Wesolowska, M. In *Photoreactivity adjustment of acrylic PSA*, 3rd Workshop on Functional Materials, 2006; pp 141-150.
18. Benedek, I., *Pressure-sensitive Adhesives and Applications*. Second Edition ed.; Marcel Dekker 1996.
19. Do, H. S., Kim, S.E., Kim H.J., *Preparation and characterization of UV-crosslinkable pressure-sensitive adhesives in adhesion* Wiley-VCH, Weinheim, 2005.
20. Lakrout, H.; Creton, C.; Ahn, D. C.; Shull, K. R., *Macromolecules* **2001**, *34* (21), 7448-7458.
21. Krencieski, M. A.; Johnson, J. F., *Polym. Eng. Sci.* **1989**, *29* (1), 36-43.
22. Satas, D., *Adhes. Age* **1972**, *12*, 19-23.
23. Yang, H. W. H.; Chang, E. P., *Trends Poly. Sci.* **1997**, *5* (11), 380-384.
24. Zosel, A., *J. Adhes. Sci. Technol.* **1997**, *11* (11), 1447-1457.
25. Zosel, A., *Int. J. Adhes. Adhes.* **1998**, *18* (4), 265-271.
26. Pasquale, A. J.; Long, T. E.; Truong, H.; Allen, R. D. In *Investigations of the adhesion of maleic anhydride/cyclic olefin alternating copolymers to silicon substrates: Improved materials for 193 nm lithography*, 24th Annual Meeting of the Adhesion-Society-Inc, 2001; pp 1-13.
27. Zhang, L.; Wang, J., *Int. J. Adhes. Adhes.* **2009**, *29* (3), 217-224.
28. Gower, M. D.; Shanks, R. A., *J. Appl. Polym. Sci.* **2004**, *93* (6), 2909-2917.
29. Rivals, I.; Personnaz, U.; Creton, C.; Simal, F.; Roose, P.; van Es, S., *Meas. Sci. Technol.* **2005**, *16* (10), 2020-2029.
30. Chu, S. G., *Viscoelastic Properties of PSAs*. Van Nostrand-Reinhold Co., New York, , 1988.
31. McKee, M. G.; Unal, S.; Wilkes, G. L.; Long, T. E., *Prog. Polym. Sci.* **2005**, *30* (5), 507-539.
32. Gower, M. D.; Shanks, R. A., *Macromol. Chem. Phys.* **2005**, *206* (10), 1015-1027.
33. Oguz, C.; Unal, S.; Long, T. E.; Gallivan, M. A., *Macromolecules* **2007**, *40* (18), 6529-6534.
34. Unal, S.; Long, T. E., *Macromolecules* **2006**, *39* (8), 2788-2793.
35. Ozturk, G., Paquale, A. J., Long, T. E., *J. Adhesion* **2009**, (In Press).
36. Chang, E. P., *Trends Poly. Sci.* **1997**, 380-384.
37. American Pressure Sensitive Tape Council, N. P.-M., Resistance to peel for single coated pressure-sensitive tapes 180° angle. **1986**.
38. American Pressure Sensitive Tape Council, N. P.-M., Holding power of pressure-sensitive tape. 1986.
39. O'Connor, A. E.; Willenbacher, N., *Int. J. Adhes. Adhes.* **2004**, *24* (4), 335-346.

## **Chapter 5: Melt Synthesis and Characterization of Aliphatic Copolyesters for Pressure Sensitive Adhesive Applications**

### **5.1 Abstract**

Aliphatic polyesters having low glass transition temperatures ( $T_g$ s) were synthesized from melt polycondensation of dimethyl-1,4-cyclohexane dicarboxylate (DMCD) with various diols including diethylene glycol (DEG), 1,4-butanediol, and 1,4-cyclohexanedimethanol (CHDM). Polyesters having different compositions were attained from incorporation of comonomers at varying molar ratios. The influence of polymer composition on thermal and mechanical properties was determined using differential scanning calorimetry (DSC) and dynamical mechanical analysis (DMA). Relationships between thermal properties and molar ratio of the comonomers were established for a series of low- $T_g$  polyesters containing DEG, 1,4-butanediol, and CHDM. The adhesive properties were characterized using peel strength and hold power tests. The composition of the copolyesters greatly influenced the adhesive properties and the rheological behavior. Characterization of adhesive properties revealed an improved cohesive strength for copolyesters containing CHDM.

### **5.2 Introduction**

Pressure-sensitive adhesives (PSAs) are utilized in several applications such as tapes, labels, packaging, and medical devices.<sup>1,2</sup> Acrylic copolymers, styrene-isoprene-styrene (SIS) block copolymers, styrene-butadiene-styrene (SBS) block copolymers, and styrene-butadiene rubber (SBR) are important families of polymers that are commonly as PSAs.<sup>3,4</sup> Recently, investigation of new types of polymers has received attention due to

increased costs and reduced availability of raw materials.<sup>5,6</sup> Our research group reported synthesis of linear and long-chain branched aliphatic low- $T_g$  polyesters from melt polycondensation of DMCD and DEG for PSA applications.<sup>7</sup> In contrast, this study involves synthesis of low- $T_g$  polyesters from melt polycondensation of DMCD with various diols including diethylene glycol (DEG), 1,4-butanediol, and 1,4-cyclohexanedimethanol (CHDM) to probe the influence of comonomers on adhesive properties.

Literature reports several examples for synthesis of polyesters from 1,4-cyclohexane dicarboxylic acid (CHDA).<sup>8,9</sup> Sanchez-Arrieta et al.<sup>10</sup> reported synthesis of poly(ethylene terephthalate-co-1,4-cyclohexane dicarboxylate) copolymer.<sup>10-12</sup> Poly(ethylene terephthalate) copolyesters containing cyclohexylene rings exhibited high tensile strength, stiffness, and impact properties. Moreover, several studies investigated the influence of *cis* and *trans* geometrical isomers of DMCD on physical properties of the resulting polymer.<sup>13-15</sup> Berti et al.<sup>14</sup> showed that the *trans* isomer produced a more crystalline structure compared to the *cis* isomer. Conversely, the *cis* isomer was less symmetrical and more flexible. *Cis* isomer introduced kinks to the polymer backbone and lowered the  $T_g$ . In this study, the ratio of *cis* to *trans* isomers was calculated to ensure that the ratio remained constant. <sup>1</sup>H NMR spectroscopic analysis of the products revealed that low- $T_g$  polyesters contained a thermodynamic equilibrium mixture of *cis* and *trans* isomers.

One of the essential molecular requirements for polymers to serve as PSAs for room temperature applications is the flexibility of the polymer backbone which correlates to low  $T_g$ s.<sup>16</sup> In addition to having a low  $T_g$ , polarity of the polymer is important in terms

of adhesion to surfaces. Zosel<sup>19</sup> stated that the surface energy of a polymer should be smaller than the substrate surface to have adhesion. Moreover, the adhesion of a polymer on a surface takes place through mechanical interlocking and molecular interfusion. When the adhesive is applied on a surface, it flows into the cavities of the rough surface. Therefore, surfaces with increased surface roughness improve adhesion as a result of enhanced interlocking due to increased contact area. Another accepted mechanism of adhesion is molecular interfusion which results in interlocking at the molecular level. Improved molecular interfusion is desired to accomplish better adhesion on the surface. Moreover, electrostatic attraction between adhesive and substrate has been utilized to improve adhesion. However, chemical and physical modification of the surfaces is beyond the scope of this study. This chapter focused on achieving optimum peel and cohesive strength properties by tuning the chemical composition and thermal properties of a series of low- $T_g$  polyesters.

Important properties of PSAs that define its performance are tack, peel strength, and shear. Tack measures the ability of an adhesive to adhere quickly. Peel resistance measures the ability to resist removal through peeling. Holding power measures the ability to hold position when shear forces are applied. Moreover, rheological analysis of polymers reveals important information on the influence of molecular weight, composition, and the presence of additives on adhesive properties.<sup>2,17</sup> Dahlquist criterion relates tack to modulus where the storage modulus of a polymer for PSA application must be smaller than  $10^6$  dynes/cm<sup>2</sup> at low frequencies. High elastic properties results in lack of flow and results in unfavorable bonding step. High storage modulus ( $G'$ ) and low dissipation properties are required in high shear applications.<sup>18</sup> Moreover, molecular

weight has an important influence on adhesive properties. Polymers having low molecular weights have high tack, however the mechanical strength is not sufficient to hold the bond together. Therefore, tailoring the molecular weight and the chemical composition of a polymer is essential to attain optimum adhesive performance.

Current research investigated synthesis of a series of low- $T_g$  polyesters containing different molar ratios of 1,4-butanediol and CHDM to alter the thermomechanical and adhesive properties. Incorporation of different comonomer compositions allowed tailoring the  $T_g$ s over a wide range. Relationship between adhesive properties and polymer composition was analyzed using differential scanning calorimetry (DSC),  $^1\text{H}$  NMR spectroscopy, and adhesive testing methods.

## **5.3 Experimental**

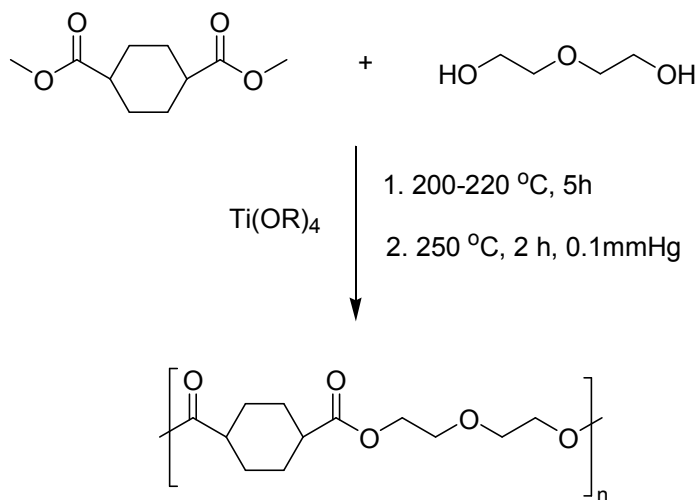
### **5.3.1 Materials**

Diethylene glycol (DEG) and 1,4-butanediol were purchased from Aldrich. Eastman Chemical Company graciously provided dimethyl-1,4-cyclohexane dicarboxylate (DMCD, 90/10 *cis/trans* mixture) and 1,4-cyclohexanedimethanol (CHDM, 30/70 *cis/trans* mixture). All reagents and solvents were used as received without further purification.

### **5.3.2 Synthesis of low- $T_g$ polyesters**

Synthesis of low- $T_g$  polyesters was conducted at Eastman Chemical Company research laboratories. DMCD (200 mmol, 40.05 g) and 50 mol% excess DEG (300 mmol, 31.83 g) were added to a 250-mL, round-bottomed flask equipped with a mechanical stirrer, nitrogen inlet, and condenser. Titanium tetraisopropoxide (60 ppm,  $\text{Ti}(\text{OR})_4$ ) catalyst was added to facilitate transesterification. The flask was degassed three

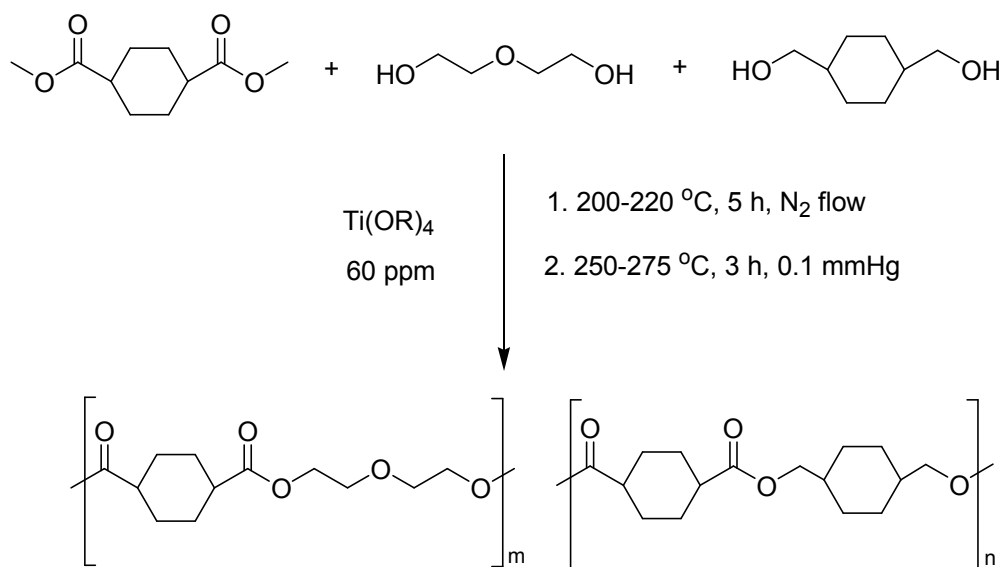
times using vacuum and nitrogen flushes and subsequently heated to 200 °C. The reaction proceeded under nitrogen atmosphere at 200 °C for 2 h and the temperature was raised to 220 °C over 3 h. Finally, vacuum (0.1 to 0.2 mmHg) was gradually applied for 2 h at 250 °C (Scheme 5.1). The products were characterized using <sup>1</sup>H NMR spectroscopy without further purification.



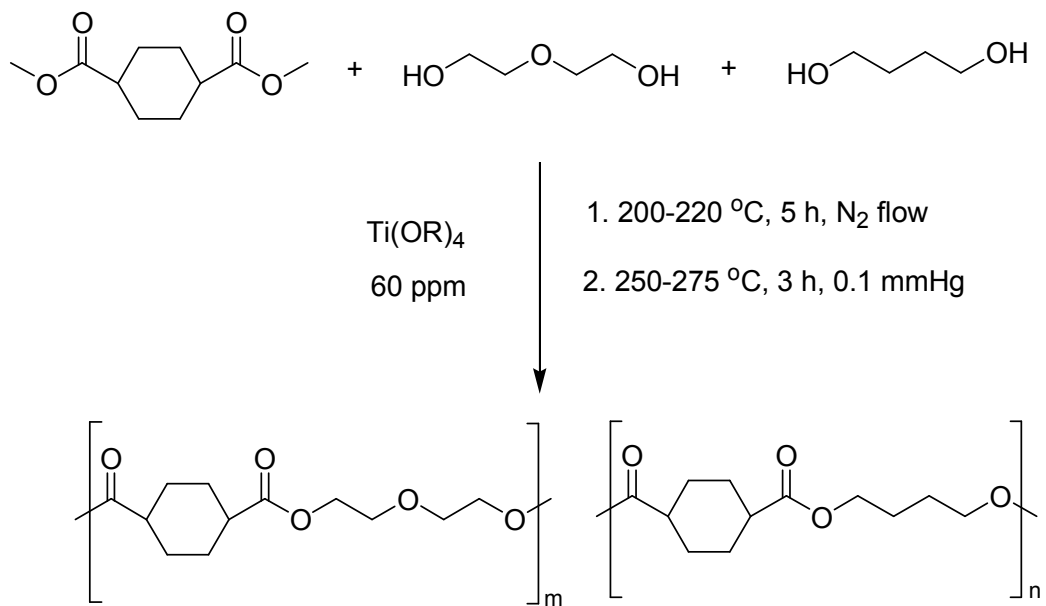
**Scheme 5.1.** Synthetic scheme for polycondensation of DMCD and DEG.

### 5.3.3 Synthesis of low- $T_g$ polyesters in the presence of comonomers

A series of low- $T_g$  polyesters were synthesized using CHDM or 1,4-butanediol as the comonomers. Polymerizations were conducted following the procedure explained above. CHDM was added to the reaction at 5 to 25 mol% with respect to DMCD (Scheme 5.2). Another series of low- $T_g$  polyesters were synthesized using DEG as the main diol and 5 to 20 mol% 1,4-butanediol as the secondary diol (Scheme 5.3). The products were characterized using <sup>1</sup>H NMR spectroscopy without further purification.



**Scheme 5.2.** Polycondensation of dimethyl-1,4-cyclohexane dicarboxylate (DMCD), diethylene glycol (DEG), and 1,4-cyclohexanedimethanol (CHDM).



**Scheme 5.3.** Polycondensation of dimethyl-1,4-cyclohexane dicarboxylate (DMCD), diethylene glycol (DEG), and 1,4-butanediol.

### 5.3.4 Characterization

Size exclusion chromatography (SEC) was performed at 30 °C in THF at a flow rate of 1mL/min using an Agilent series 1100 system chromatograph equipped with an autosampler, Polymer Laboratories PLgel Mixed-C, Oligopore 5- $\mu$ m guard columns, and a refractive index (RI) detector.  $^1\text{H}$  NMR spectroscopic data were collected on a Varian 400 MHz spectrometer at ambient temperature. Dynamic mechanical analysis (DMA) characterized the temperature and frequency dependence of the polyesters. Samples were characterized using 8 mm plates at an auto-strain of 0.5 to 5%, ramp rate of 6 °C/min, and frequency of 10 rad/sec. The thermal properties of the polymers were characterized using differential scanning calorimetry (DSC) and thermal gravimetric analysis (TGA) at a heating rate of 10 °C/min. The reported  $T_g$  values are obtained from the second heating cycle.

### 5.3.5 Characterization of adhesive properties

Polymer solutions of 30 wt% in toluene were cast on poly(ethylene terephthalate) (Mylar<sup>®</sup>) backing material using an automated coater to obtain uniform thickness. Coated films were dried at room temperature for 10 min, and then dried in a convection oven at 80 °C for 10 min. The coating weight of the films was determined from the difference of the coated and uncoated Mylar<sup>®</sup> films (12.8 cm x 12.8 cm). A coating weight of 20 g/m<sup>2</sup> was targeted for each specimen. All adhesive testing was performed in controlled temperature (22 °C) and humidity (50% R.H.) environment.

#### 5.3.5.1 180° peel testing

Peel resistance of the polymers was measured according to 180° peel test method.<sup>19</sup> Strips having a width of 2.56 cm were cut from the coated Mylar<sup>®</sup> films using

a cutting template and coating weight of the each strip was measured. Stainless steel panel was used as the substrate from which the sample was peeled. The substrates were cleaned thoroughly prior to each test to remove any residue on the surface. The specimen strip (2.56 cm x 30 cm) was placed on the stainless steel panel and a 2-kg roller was passed over two times under its own weight. The specimens were pulled immediately after preparation at an angle of 180° using an Instron at 300 mm/min. Average of 5 specimens was reported.

#### **5.3.5.2 Holding power**

Specimens were cut into strips of 2.56 cm x 10.24 cm and a square area (2.56 x 2.56 cm) of the adhesive specimen was centered on the stainless steel panel. 2-kg roller was passed over it two times under its own weight. A clamp was placed on the free end of the specimen ensuring that the clamp extended completely across the width and was properly aligned to distribute the load uniformly. The specimen was then placed in the test stand and a 1-kg weight was applied to the end of the sample. The time during which the specimen completely separated from the test panel was recorded.<sup>20</sup> The reported values represent an average of 5 tests.

### **5.4 Results and Discussion**

A series of low- $T_g$  copolyesters containing different amounts of 1,4-butanediol was synthesized and characterized as alternatives to DMCD and DEG based polyesters for PSA applications. Melt polycondensation of DMCD and DEG with 1,4-butanediol comonomers is depicted in Scheme 5.3. The amount of secondary diol incorporated in the resulting polymers was calculated using  $^1\text{H}$  NMR spectroscopic analysis. As shown in Table 5.1, 5, 10, 15, and 20 mol% of 1,4-butanediol was incorporated in the reaction to

tune the thermal and adhesive properties. Characterization of thermal transitions using DSC revealed that  $T_g$  of the polymers increased from -11 to -7 °C as 1,4-butanediol was added as the comonomer. The resulting polymers exhibited weight-average molecular weights ranging from 40,000 to 60,000 g/mol. It is important to note that molecular weight has a significant influence on adhesive properties. Therefore, copolyesters having similar molecular weights were selected for characterization of adhesive properties to probe the influence of comonomer ratio on the resulting adhesive performance of the low- $T_g$  polyesters.

**Table 5.1.** Summary of thermal, compositional, and molecular weight characterization of copolyesters containing 1,4-butanediol.

1,4-butanediol		$M_w$	$M_n$	$M_w/M_n$	$T_g$ (°C)
Feed	By $^1H$ NMR	(g/mol)	(g/mol)		
0	0	57,000	28,000	2.04	-11
5	10	50,000	18,800	2.65	-11
10	12	40,000	18,000	2.22	-10
15	19	60,000	21,000	2.85	-7
20	24	54,000	20,600	2.62	-8

DMA curves shown in Figure 5.1 exhibited an increase in  $G'$  measured at room temperature as higher levels of 1,4-butanediol were incorporated in the copolyester composition. Comparison of the storage moduli of the copolyesters at temperatures higher than room temperature indicated that the melt stability of the polymers highly depended on the molar ratio of 1,4-butanediol comonomer. An increase in the melt stability corresponded to enhanced cohesive strength. DMA analyses of all of the samples indicated that storage modulus at room temperature was around  $10^6$  dynes/cm<sup>2</sup>, which is the Dahlquist criterion for tack.<sup>1</sup>

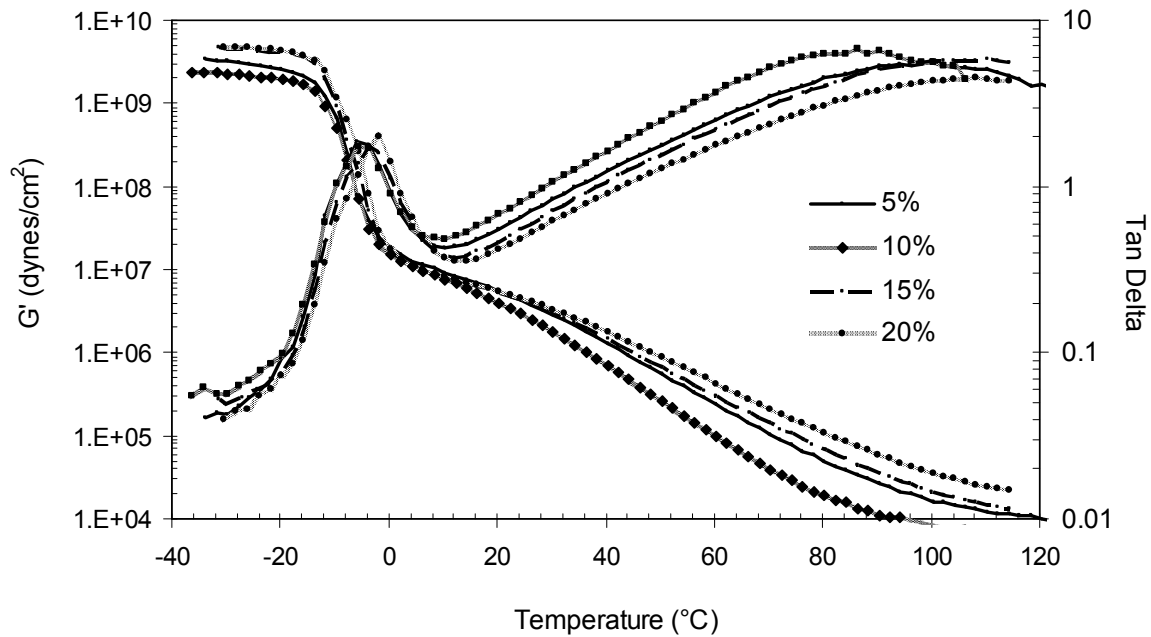


**Figure 5.1.** Dynamic mechanical analysis of polyesters having various amounts of 1,4-butanediol.

The adhesive performance of the low- $T_g$  copolyesters was evaluated using 180° peel and holding power tests. Characterization of adhesive properties indicated an improvement in peel strength and holding power as the amount of 1,4-butanediol incorporated in the polymer was increased. Peel strength and shear adhesion was measured using 180° peel test and holding power tests at room temperature and controlled humidity. Comparison of the peel strength of polyesters synthesized using 100 mol% DEG and 80/20 mol% DEG/1,4-butanediol showed that the peel strength increased from 2.83 ( $\pm$  0.14) to 3.74 ( $\pm$ 0.18) lb/in (Figure 5.2). Characterization of resistance-to-shear using a holding power test indicated an enhanced cohesive for the copolyesters containing higher levels of the comonomer (Figure 5.3). These results are in agreement with DMA which indicated that  $G'$  of the copolyesters were higher at elevated temperatures. However, the holding power of the samples was limited to approximately 900 min which is significantly lower compared to the typical values for commercially available polymers.

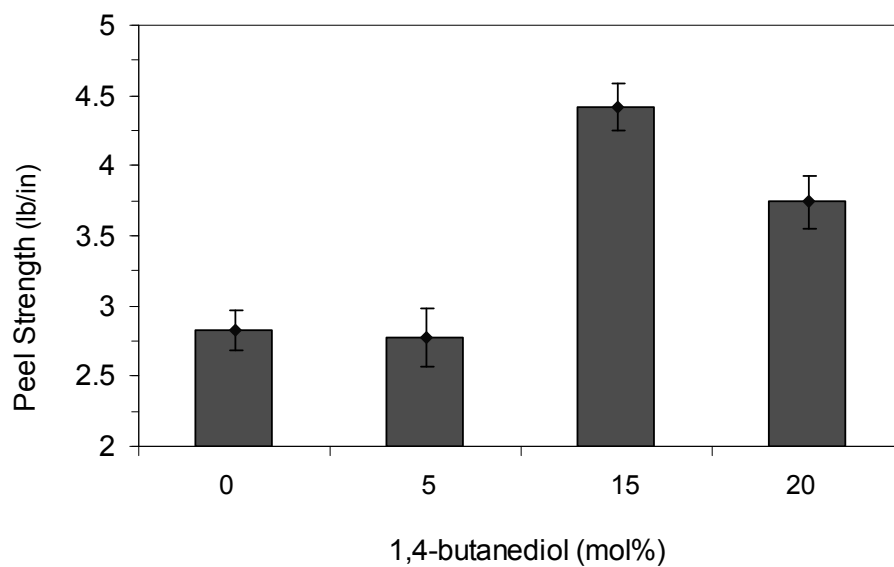


**Figure 5.2.** Peel strength results of low- $T_g$  copolyester containing different amounts of 1,4-butanediol.

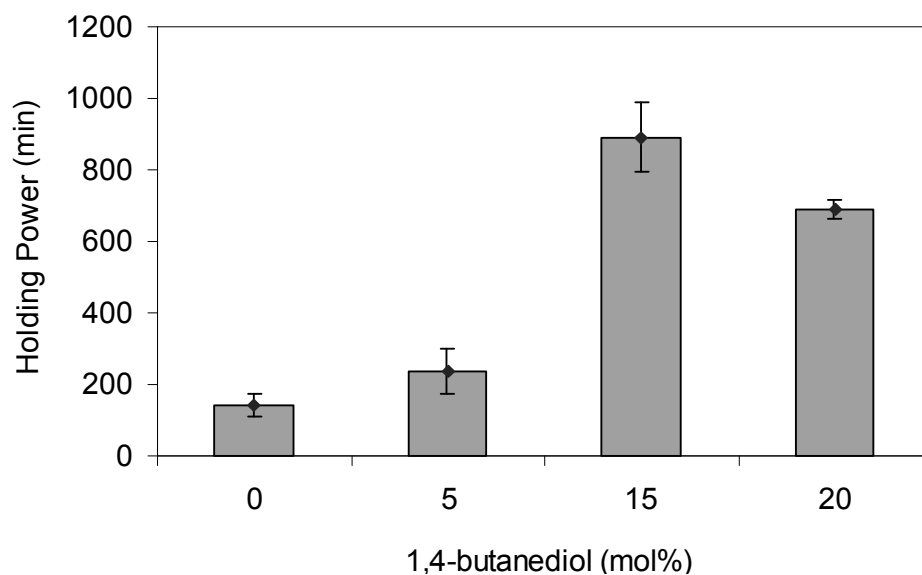


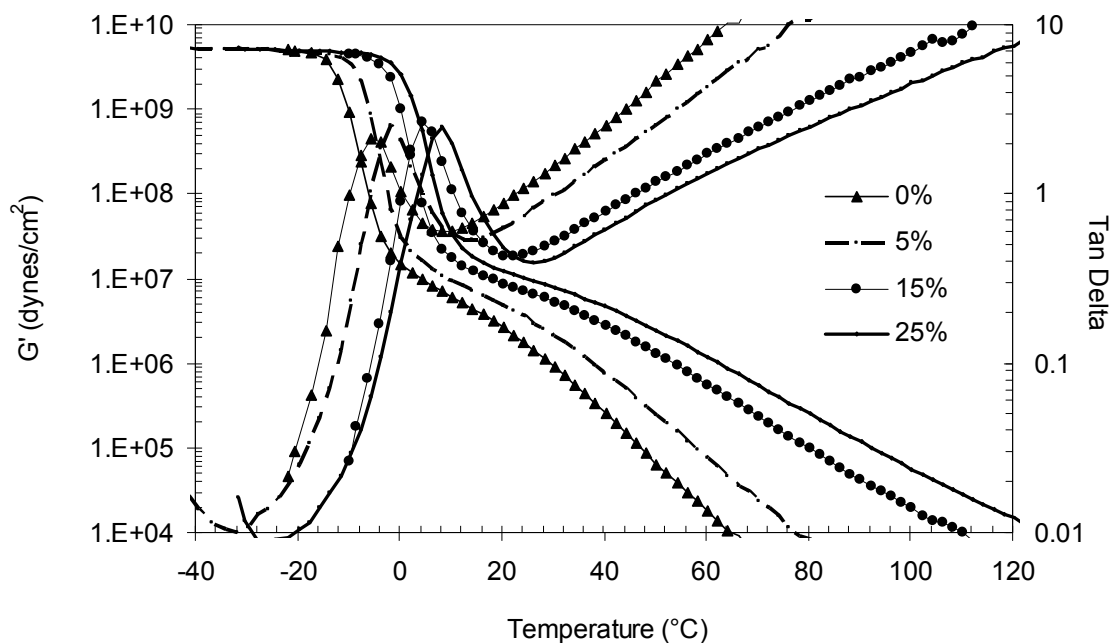
**Figure 5.3.** Holding power results of copolymers containing different amounts of 1,4-butanediol.

Another series of copolyester were synthesized using CHDM as the secondary diol to achieve tunable thermal and adhesive properties. Synthesis of copolyesters from melt polycondensation of DMCD and DEG with CHDM is depicted in Scheme 5.2. As listed in Table 5.2, 5, 15, 20, and 25 mol% of CHDM was used to synthesize polymers with different chemical compositions.  $^1\text{H}$  NMR spectroscopic analysis determined the amount of CHDM incorporated into the polymer. The calculations revealed that the amount of CHDM incorporated in the reaction was lower compared to the feed ratios. The differences in the feed and actual molar ratios were attributed to the differences in the reactivity of the DEG and CHDM monomers. Characterization of thermal transitions using DSC revealed that all the polymers were amorphous and  $T_g$  of the copolyesters increased from -11 to -6 °C depending on the amount of the comonomer included in the reaction. Weight-average molecular weights of the copolyesters ranged from 38,900 to 55,200 g/mol.

**Table 5.2.** Summary of thermal, compositional, and molecular weight characterization of copolyesters containing CHDM.

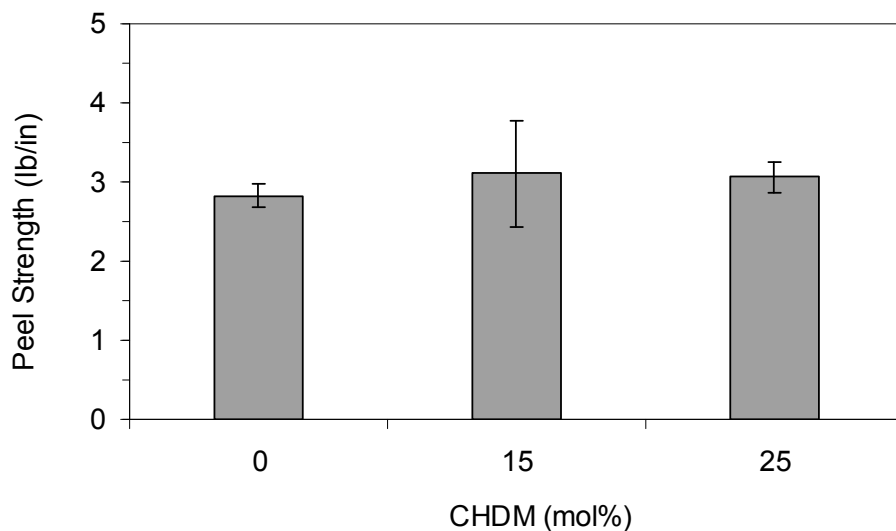
<b>CHDM mol%</b>					
<b>Feed</b>	<b>By NMR</b>	<b><math>M_w</math> (g/mol)</b>	<b><math>M_n</math> (g/mol)</b>	<b><math>M_w/M_n</math></b>	<b><math>T_g</math> (°C)</b>
0	0	57,000	28,000	2.04	-11
15	16	48,200	20,300	2.37	-3
20	19	46,100	19,500	2.36	-2
25	22	55,200	22,200	2.48	-6

Figure 5.4 illustrates DMA of low- $T_g$  polyesters containing different molar ratios of CHDM. Comparison of the storage moduli of the copolyesters at elevated temperatures revealed that the melt stability of the polymers increased with increasing molar ratio of CHDM. Higher  $G'$  values at elevated temperatures related to the melt stability and corresponded to the enhanced cohesive strength. However, the rubbery plateau region was short for all the samples due to low molecular weights. Moreover, DMA analyses indicated that the storage modulus at room temperature increased for polymers containing higher amounts of CHDM. The samples exhibited  $G'$  values around  $6 \times 10^6$  dynes/cm<sup>2</sup>, which is slightly above the Dahlquist criterion for tack.<sup>1</sup>



**Figure 5.4.** Temperature dependence of copolyesters having different amounts of 1,4-cyclohexanedimethanol.

Adhesive properties of low- $T_g$  copolyesters containing CHDM were characterized using 180° peel and holding power tests to probe the influence of polymer composition on adhesive performance. As shown in Figure 5.5, the peel strength did not change within experimental error with increasing the CHDM molar ratio. However, holding power test indicated a dramatic increase in shear strength for polymers containing higher amounts of CHDM. Addition of 25 mol% CHDM into the polymer increased holding power from 370 to 7000 min (Figure 5.6). The enhanced resistance to shear was attributed to the presence of the cyclohexane ring of CHDM.



**Figure 5.5.** Peel strength results of copolyesters containing different amounts of CHDM.

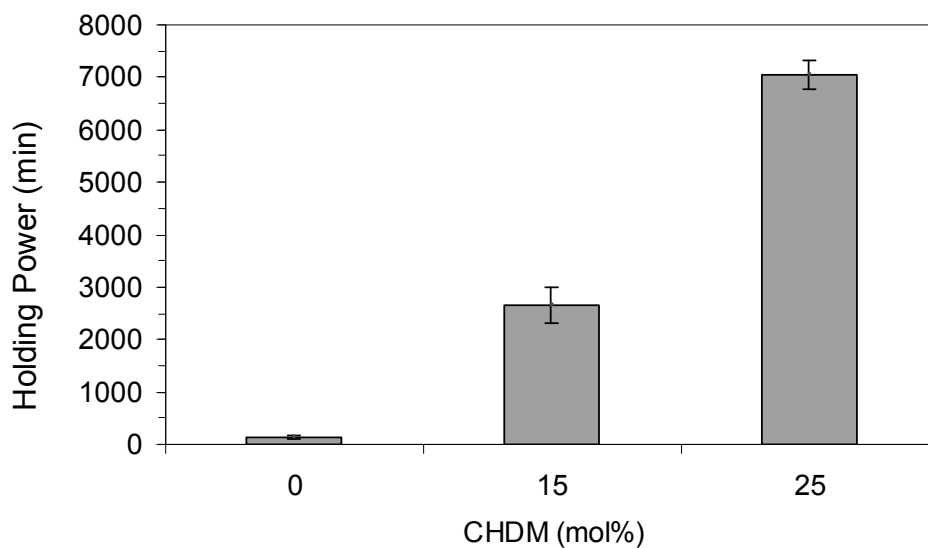


**Figure 5.6.** Holding power results of copolyesters containing different amounts of CHDM.

Figure 5.7 compares holding power of low- $T_g$  polyesters of varying chemical compositions. The cohesive strength of adhesives depends on the molecular weight and composition. Therefore, copolyesters having similar weight-average molecular weights and different chemical compositions were characterized to determine the influence of the comonomer type on the cohesive strength. As depicted in Figure 5.7, the holding power increased dramatically for the copolyester containing 25 mol% CHDM.

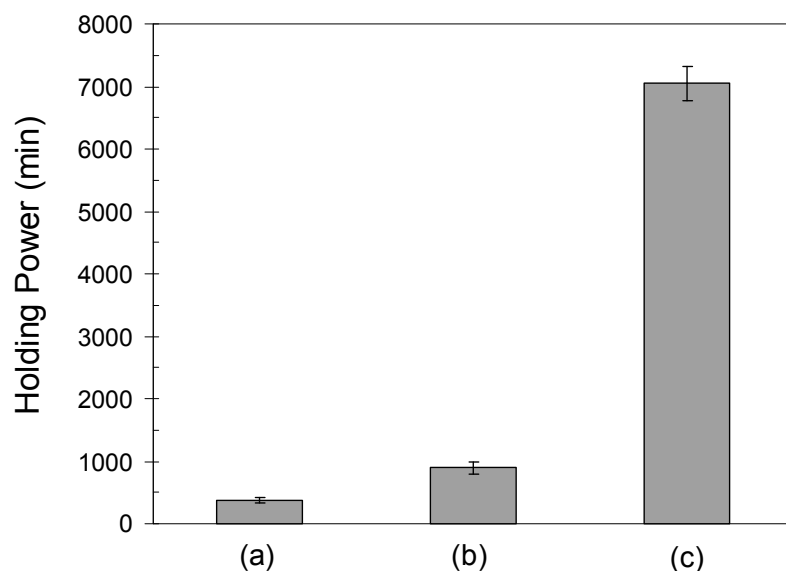


**Figure 5.7.** Influence of diol type on holding power of low- $T_g$  polyesters containing a) 100 mol% DEG, b) 15 mol% 1,4-butanediol, and c) 25 mol% CHDM

## 5.5 Conclusions

In this study, synthesis of low- $T_g$  polyesters having different compositions was investigated to tailor adhesive properties. Melt polycondensation of a variety of monomers allowed synthesis of linear low- $T_g$  polyesters with various compositions. Influence of chemical composition of low- $T_g$  polyester containing different amounts of DEG, CHDM and 1,4-butanediol on adhesive properties was investigated using peel and holding power tests. The comonomer type significantly influenced the adhesive properties and the rheological behavior. Incorporation of CHDM improved the cohesive strength significantly and increased the holding power from 370 minutes to 7,000 minutes.

## 5.6. Acknowledgements

The authors would like to thank the Eastman Chemical Company for financial and technical support. The authors also thank Emmet O'Brien, Jeremy Lizotte, and Mark Peters at Eastman Chemical Company for helpful technical discussions.

## 5.7 References

1. Satas, D., *Handbook of Pressure Sensitive Adhesive Technology*. Satas & Associates, Warwick, 1999.
2. Ho, K. Y.; Dodou, K., *Int. J. Pharm.* **2007**, *333* (1-2), 24-33.
3. Tan, H. S.; Pfister, W. R., *Pharm. Sci. Technol. Today* **1999**, *2* (2), 60-69.
4. Trenor, S. R.; Long, T. E.; Love, B. J., *J. Adhesion* **2005**, *81* (2), 213-229.
5. Chan, E. P.; Ahn, D.; Crosby, A. J., *J. Adhesion* **2007**, *83* (5), 473-489.
6. Chan, E. P.; Smith, E. J.; Hayward, R. C.; Crosby, A. J., *Adv. Mater* **2008**, *20* (4), 711-716.
7. Ozturk G. I.; Pasquale, A. J. L., T. E., *J. Adhesion* **2009**, *In Press*.
8. Jackson Jr W. J., D., W. R. 1982.
9. Jackson Jr W. J., D. W. R. 1982.
10. Sanchez-Arrieta, N.; de Ilarduya, A. M.; Alla, A.; Munoz-Guerra, S., *Eur. Polym. J.* **2005**, *41* (7), 1493-1501.
11. Brunelle, D. J.; Jang, T., *Polymer* **2006**, *47* (11), 4094-4104.
12. Turner, S. R.; Dombroski, J. R., *Modern polyesters*. Chichester, 2003.
13. Berti, C.; Binassi, E.; Celli, A.; Colonna, M.; Fiorini, M.; Marchese, P.; Marianucci, E.; Gazzano, M.; Di Credico, F.; Brunelle, D. J., *J. Polym. Sci. Pol. Phys* **2008**, *46* (6), 619-630.
14. Berti, C.; Celli, A.; Marchese, P.; Marianucci, E.; Barbiroli, G.; Di Credico, F., *Macromol. Chem. Physic.* **2008**, *209* (13), 1333-1344.
15. Wang, L. C.; Xie, Z. G.; Bi, X. J.; Wang, X.; Zhang, A. Y.; Chen, Z. Q.; Zhou, J. Y.; Feng, Z. G., *Polym. Degrad. Stabil.* **2006**, *91* (9), 2220-2228.
16. Zosel, A., *J. Adhes. Sci. Technol.* **1997**, *11* (11), 1447-1457.
17. Benedek, I., *Pressure Sensitive Adhesives and Applications*. Marcel Dekker, 2004.
18. Yang, H. W. H.; Chang, E. P., *Trends Polym. Sci* **1997**, *5* (11), 380-384.
19. American Pressure Sensitive Tape Council, N. P.-M., Resistance to peel for single coated pressure-sensitive tapes 180° angle. **1986**.
20. American Pressure Sensitive Tape Council, N. P.-M., Holding power of pressure-sensitive tape. **1986**.

## Chapter 6: Michael Addition Crosslinking of Poly(caprolactone)s

**Partially taken from:** Ozturk, G.I.; Long, T.E. *Journal of Polymer Science Part A: Polymer Chemistry*, submitted, 2009.

### 6.1 Abstract

Poly(caprolactone) networks have received significant attention in the literature due to many emerging potential applications as biodegradable materials. In this study, the Michael addition reaction was utilized for the first time to synthesize biodegradable networks using crosslinking of acetoacetate-functionalized poly(caprolactone) oligomers with neopentyl glycol diacrylate. Hydroxyl-terminated poly(caprolactone) (PCL) telechelic oligomers with number-average molecular weights ranging from 1000 to 4000 g/mol were quantitatively functionalized with acetoacetate groups using transacetoacetylation. In addition to difunctional PCL oligomers, hydroxyl-terminated trifunctional star-shaped PCL oligomers were functionalized with acetoacetate groups. Derivatization of the terminal hydroxyl groups with acetoacetate groups was confirmed using FTIR spectroscopy, <sup>1</sup>H NMR spectroscopy, mass spectrometry, and base titration of hydroxyl end groups. Acetoacetate-functionalized PCL precursors were reacted with neopentyl glycol diacrylate in the presence of an organic base at room temperature. The crosslinking reactions yielded networks with high gel contents (> 85%). The thermomechanical properties of the networks were analyzed to investigate the influence of molecular weight between crosslink points. The glass transition and the extent of crystallinity of the PCL networks were dependent on the molecular weight of the PCL segment. Dynamic mechanical analysis (DMA) indicated that the plateau modulus of the

networks was dependent on the molecular weight of PCL, which was related to the crosslink density of the networks.

## 6.2 Introduction

Biodegradable polymers have received significant attention in the literature due to their potential for a variety of medical and environmental applications. Aliphatic polyesters and their copolymers are important classes of polymers that both degrade in the body and produce non-toxic byproducts when used for environmental applications.<sup>1</sup> For that reason, aliphatic polyesters such as poly(hydroxybutyrate)s,<sup>2,3</sup> poly(caprolactone),<sup>4,5</sup> poly(lactide), poly(glycolide), and their copolymers<sup>6,7</sup> are widely used for a variety of applications such as food packaging, as well as in medical applications that include tissue engineering, surgical fixation procedures, and controlled drug delivery.

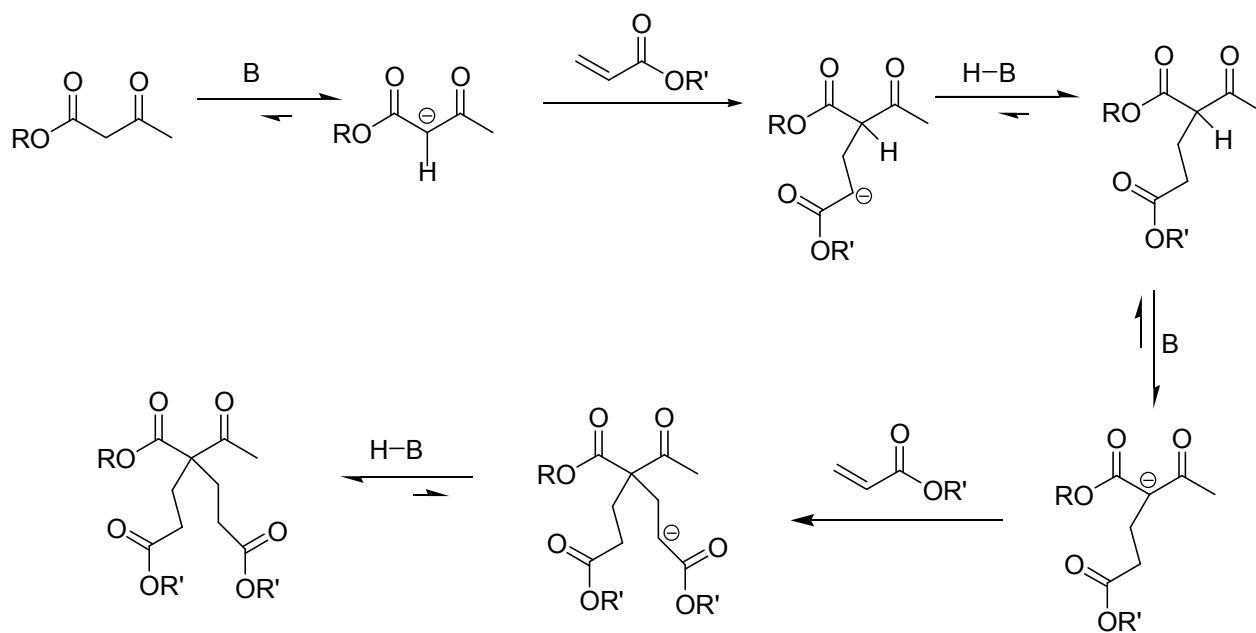
The synthesis and characterization of a diverse group of linear, branched, and crosslinked biodegradable polyesters have probed the influence of topology on biodegradation rates and biocompatibility.<sup>6</sup> Recently, crosslinking biodegradable polymers that form three-dimensional networks offered potential for improving mechanical properties, such as enhanced drug delivery.<sup>8</sup> The incorporation of crosslinking improves thermal and mechanical properties compared to linear or branched thermoplastics.<sup>9</sup> Moreover, both the biodegradation and release rates of the networks are successfully manipulated with variations in crosslink density and crystallinity.

The literature reports several examples of biodegradable thermoset<sup>1</sup> and thermoplastic<sup>10</sup> elastomers. Biodegradable thermoplastic elastomers contain either a crystalline or high  $T_g$  segment that acts as a physical crosslink. The relative resistance of

crystalline segments to hydrolytic degradation results in a heterogeneous degradation and non-linear loss of mechanical properties, which may lead to mechanical failure. Conversely, amorphous thermosets provide control over degradation rates and mechanical loss. Therefore, amorphous biodegradable elastomers are preferred in several applications, such as drug delivery, due to their homogeneous degradation behavior.<sup>9</sup>

The literature also describes several biodegradable polymers including poly(butylene succinate), poly(caprolactone),<sup>9</sup> and poly(lactide)s,<sup>11</sup> which are crosslinked using a number of techniques, including UV-radiation,<sup>12</sup> reaction with peroxides and polycondensation of multifunctional carboxylic acids.<sup>6</sup> Literature<sup>9,11,12</sup> reports UV-crosslinking as a rapid, effective, and well controlled curing technique that takes place with low heat production. Therefore, *in-situ* crosslinking of polymers with pendant photo-functional groups was investigated for several biomedical applications including bioadhesive applications.<sup>11</sup> Recently, the Michael addition reaction was utilized in the chemical crosslinking of polymers for crosslinkable waterborne coatings,<sup>13</sup> hydrogels, and thermoset applications.<sup>14-16</sup> In addition to crosslinking, Michael addition was used in the literature to synthesize hyperbranched polymers.<sup>17</sup> Michael addition crosslinking offers several advantages such as functional group tolerance, availability of the precursors, mild reaction conditions, and elimination of solvent and side-products.<sup>16</sup> Michael addition involves the reaction of an enolate-type nucleophile, such as an acetoacetate, and unsaturated carbonyl groups such as acrylate esters in the presence of a base (Scheme 6.1). The reaction is catalyzed with either inorganic or organic bases (e.g., amidine or hydroxide) and carbonate.<sup>18,19</sup> In the reaction, deprotonation of the acetoacetate ester is in equilibrium; therefore, the strength of the basic catalyst is

important for determining the rate of the reaction. In the presence of a strong base, a nucleophilic and resonance stabilized enolate anion is formed upon deprotonation of the  $\beta$ -keto ester.<sup>19</sup> This intermediate reacts with a  $\beta$ -unsaturated ester and forms a second intermediate. This second intermediate reacts with another unsaturated ester. It should be noted that the  $pK_a$  values for the hydrogens on the acetoacetate functionality are different ( $pK_{a1} \approx 12$ ,  $pK_{a2} \approx 13$ ), therefore the type and strength of the base determines the final network structure. Bowman et al.<sup>20</sup> showed that the reactivity of the acrylate groups is enhanced upon functionalization of the acrylates with carbamates, hydroxyl or cyano groups. Hydroxyl telechelic polymers are readily functionalized with acetoacetate groups upon esterification of hydroxyl groups with *tert*-butyl acetoacetate or diketene.<sup>18</sup> Therefore, the hydroxyl end groups of any aliphatic polyester are readily derivatized with acetoacetate groups and further crosslinked with a variety of diacrylate groups. This process facilitates the synthesis of a variety of networks having different chemical compositions, which display a range of biodegradation rates and thermomechanical properties.



**Scheme 6.1.** Mechanism of carbon-Michael addition reaction of acetoacetates and acrylates.

Poly(caprolactone) (PCL) is a semicrystalline polyester that degrades enzymatically and hydrolytically. It is widely utilized in several biomedical applications such as drug delivery,<sup>21,22</sup> suture coatings, and microporous intravascular stents.<sup>23</sup> The degradation product, 6-hydroxycaproic acid, is completely metabolized in a citric acid cycle.<sup>4</sup> PCL biodegradation rates are slower compared to PLA and PGA due to enhanced hydrophobicity.<sup>6</sup> As expected, the crystallinity of PCL depends on molecular weight, and therefore, low molecular weight PCL is less prone to crystallization. Although low molecular weight PCL oligomers are generally amorphous, PCL oligomers become semicrystalline as their molecular weight approaches 2000 g/mol. Furthermore, topological changes dramatically influence the crystallization behavior of PCL.<sup>24</sup> The introduction of branching is also known to disrupt symmetry; in fact, a single branch will result in amorphous PCL. Therefore, the introduction of branching or crosslinking was investigated as a means to suppress the crystallinity of PCL and tailor its degradation rates.

In this study, the synthesis of covalently crosslinked poly(caprolactone) based biodegradable networks using Michael addition was investigated. The crosslinking of PCL using a Michael addition is promising for biomedical applications due to the elimination of organic solvents, crosslinking at physiological temperatures, and the absence of undesirable byproducts. Moreover, the availability of different diacrylates such as poly(ethylene glycol) diacrylate and poly(propylene diacrylate) enables one to tailor the hydrophilicity of the networks. In addition, the biodegradation rates are controlled with morphology changes, which are achieved with controlling molecular weight of the PCL segment. In the present study, poly(caprolactone) oligomers having

molecular weights ranging from 1000 to 4000 g/mol were crosslinked with neopentyl glycol diacrylate to study the effect of the molecular weight of PCL on thermal and mechanical properties. Crosslinking a trifunctional PCL oligomer enabled tailoring the morphology of the networks, which will facilitate greater control of degradation rates and thermomechanical properties. The thermal and mechanical properties were dependent on PCL molecular weight due to crosslinking density as well as degree of crystallinity.

## **6.3 Experimental**

### **6.3.1 Materials**

Neopentylglycol diacrylate, *tert*-butyl acetoacetate (*t*-BAA, 98%), acetic anhydride ( $\geq 99\%$ ), pyridine ( $\geq 99\%$ ), 1,8-diazabicyclo[5.4.0]undec-7-ene (DBU, 98%), 0.1 N KOH in methanol, and tetrahydrofuran (THF) were purchased from Aldrich. Solvay Chemicals generously donated poly(caprolactone) diol oligomers (1000, 2000, and 4000 g/mol) and poly(caprolactone) triol oligomer (2000 g/mol). All chemicals were used as received without further purification.

### **6.3.2 Characterization**

Molecular weights were determined at 40 °C in THF (HPLC grade) on a Waters size exclusion chromatograph (SEC) equipped with an autosampler, a 410 RI detector and an in-line Wyatt Technologies miniDawn multiple angle laser light scattering (MALLS) detector. <sup>1</sup>H NMR analyses were performed on a Varian Unity 400 spectrometer at 400 MHz in CDCl<sub>3</sub>. Thermal analysis using a TA Instruments Q-100 DSC determined thermal transition temperatures at a heating rate of 10 °C/min under nitrogen flow and all reported values were obtained from a second heating cycle. The thermal stability of the networks was measured using a TA Instruments Hi-

ResThermogravimetric Analyzer 2950, under N<sub>2</sub> flow with a temperature ramp of 10 °C/min. MALDI-TOF MS analyses were performed using a Kratos Kompact SEQ instrument equipped with nitrogen laser (337.1 nm), using 100-180 power setting in the positive ion linear mode. The accelerating voltage was 20 kV in delayed extraction mode. The targets were prepared from a solution of acetonitrile with dihydroxy benzoic acid as the matrix. The samples were dissolved in acetonitrile at 1 mg/mL, and approximately 0.5 µL of this solution was mixed with matrix solution. The instrument was calibrated using endohedral metallofullerene sample as the reference compound. The characterization of the hydroxyl end-functionality was carried out for each poly(caprolactone) diol and triol. The samples were dissolved in solution of acetic anhydride/pyridine (1:3 v:v) and reacted overnight at room temperature under constant mixing. Following this, 10 mL of distilled water, and 10 mL of pyridine was added to hydrolyze the excess acetic anhydride. The samples were titrated with 0.1 N KOH solution using phenolphthalein as an indicator. Gel fraction analysis was performed using Soxhlet extraction in refluxing in THF for 3 h and drying the samples under reduced pressure for 24 h at ambient temperature until constant weight was obtained. *In-situ* FTIR spectroscopic analysis was performed using an ASI ReactIR 1000 attenuated total reflectance (ATR) spectrometer. Dynamic mechanical analysis was performed on a TA instruments Q-800 DMA under nitrogen at a heating rate of 3 °C/min at 1 Hz frequency in film-tension mode. The tensile properties of the networks were characterized using a 5500R Instron universal testing instrument at room temperature with a cross-head speed of 10 mm/min using dog-bone shaped films.

The degree of swelling was determined gravimetrically from swelling of the samples in THF. Prior to swelling experiments, the sol fractions of the crosslinked samples were removed using a Soxhlet extraction in refluxing. The samples were dried under reduced pressure until a constant weight was reached. The rectangular samples (11x6x0.4 mm) were stored in THF and the weight was measured after the samples were equilibrated at  $37 \pm 0.1$  °C. The swelling ratio was expressed as the weight of the swollen sample per weight of the dry sample.

### **6.3.3 Synthesis of acetoacetate-functionalized poly(caprolactone) (PCL bisacac)**

Hydroxyl functional oligomeric poly(caprolactone) (5 g, 5 mmol) and 50 mol% excess *t*-BAA (2.37 g, 15 mmol) were charged to a 100-mL flask. The flask was flushed with nitrogen and the mixture was subsequently heated to 150 °C for 3 h. The byproduct *tert*-butanol and excess *t*-BAA were removed under reduced pressure (100 mmHg) using a short-path distillation head and receiving flask under vacuum. Additional *t*-BAA (2.37 g, 15 mmol) was added and the flask was heated for 3 h at 150 °C to ensure complete functionalization of the PCL oligomer. Reaction byproducts and unreacted starting materials were removed under modest vacuum (0.1 mmHg) at 150 °C for 1 h. The products were characterized using  $^1\text{H}$  NMR spectroscopy and MALDI-TOF MS analysis.

### **6.3.4 Synthesis of poly(caprolactone) networks: crosslinking reactions**

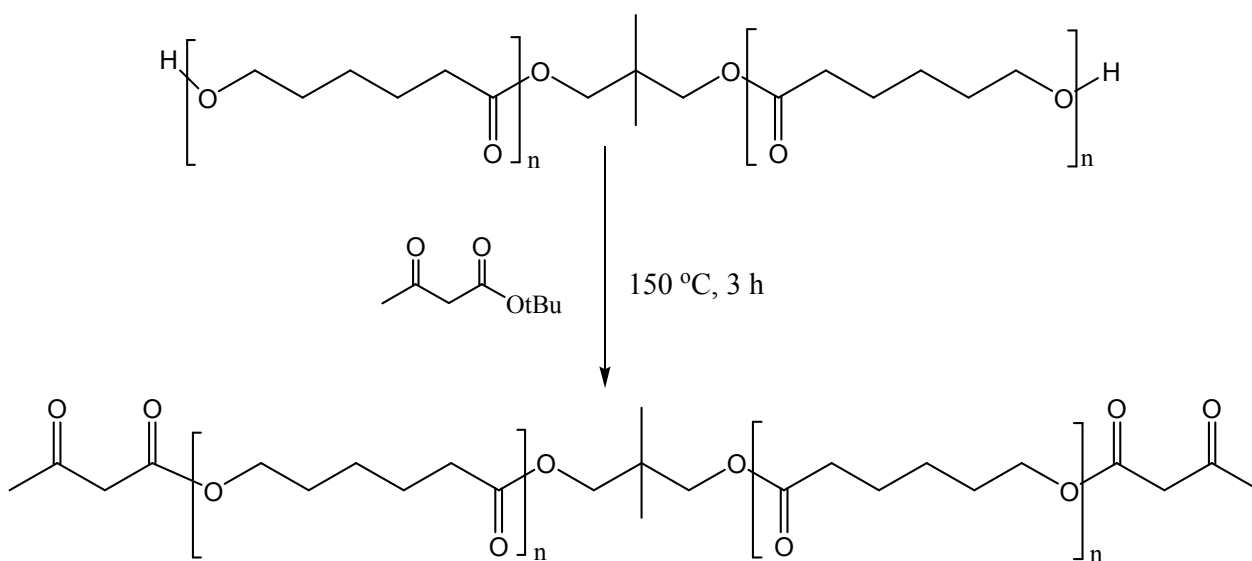
Acetoacetate functionalized poly(caprolactone) (PCL bisAcAc) precursors having various molecular weights were reacted with neopentylglycol diacrylate in the presence of an organic base. PCL bisAcAc and neopentylglycol diacrylate were mixed in a sample vial to obtain a homogeneous blend. An organic base catalyst, DBU (0.05 wt% relative to bisAcAc precursor), was added and mixed at room temperature. The mixture was

transferred to a Teflon<sup>TM</sup> mold and cured at room temperature for 48 h. The films were kept under vacuum overnight before analysis.

## 6.4 Results and Discussion

### 6.4.1 Synthesis of acetoacetate-functionalized poly(caprolactone) (PCL bisacac)

Hydroxyl terminated poly(caprolactone) oligomers were characterized using <sup>1</sup>H NMR spectroscopy, MALDI-TOF analysis, and end group titration prior to transacetoacetylation reaction to confirm the hydroxyl functionality. Poly(caprolactone) oligomers were successfully functionalized with acetoacetate groups in the absence of any catalyst or solvent using transacetoacetylation (Scheme 6.2). The product was purified with a one-step vacuum distillation.



**Scheme 6.2.** Synthesis of bisacetoacetate functionalized poly(caprolactone).

Mass spectrometry and <sup>1</sup>H NMR spectroscopic analyses confirmed telechelic acetoacetate functionality. Figure 6.1 illustrates <sup>1</sup>H NMR spectra showing the chemical compositions of oligomeric poly(caprolactone)s bisacetoacetate. The presence of

acetoacetate functionality was confirmed using the peaks corresponding to the AcAc methyl resonance ( $\delta = 2.26$  ppm) and the AcAc methylene resonance ( $\delta = 3.22$  ppm). The molecular weights of the bisacetoacetate-functional polyesters were calculated using the integrations of the AcAc methyl resonances from the  $^1\text{H}$  NMR analysis.

MALDI-TOF MS is an important analytical technique to characterize end functionality and the molecular weight of polymers with narrow polydispersity.<sup>25,26</sup> The molecular weight and polydispersity of the poly(caprolactone) precursors having molecular weight of 1000 and 2000 g/mol were calculated using MALDI-TOF analysis, as summarized in Table 6.1. The MALDI-TOF MS spectrum consisted of several peaks which corresponded to different degrees of polymerization, therefore the difference between each peak is 114, corresponding to the mass of repeating unit of poly(caprolactone) (Figure 6.2). The difference between the mass obtained from mass spectra of the poly(caprolactone) diol and the acetoacetate-functional analog provided the mass of the end groups. For each calculation, 170 m/z was obtained which is equal to the mass of two acetoacetate groups. Poly(caprolactone) oligomers (4000 g/mol) was not characterized using MALDI-TOF MS due to lowered accuracy of the measurement and instrumental limitations as the molecular weight of the samples approached 4000 g/mol.

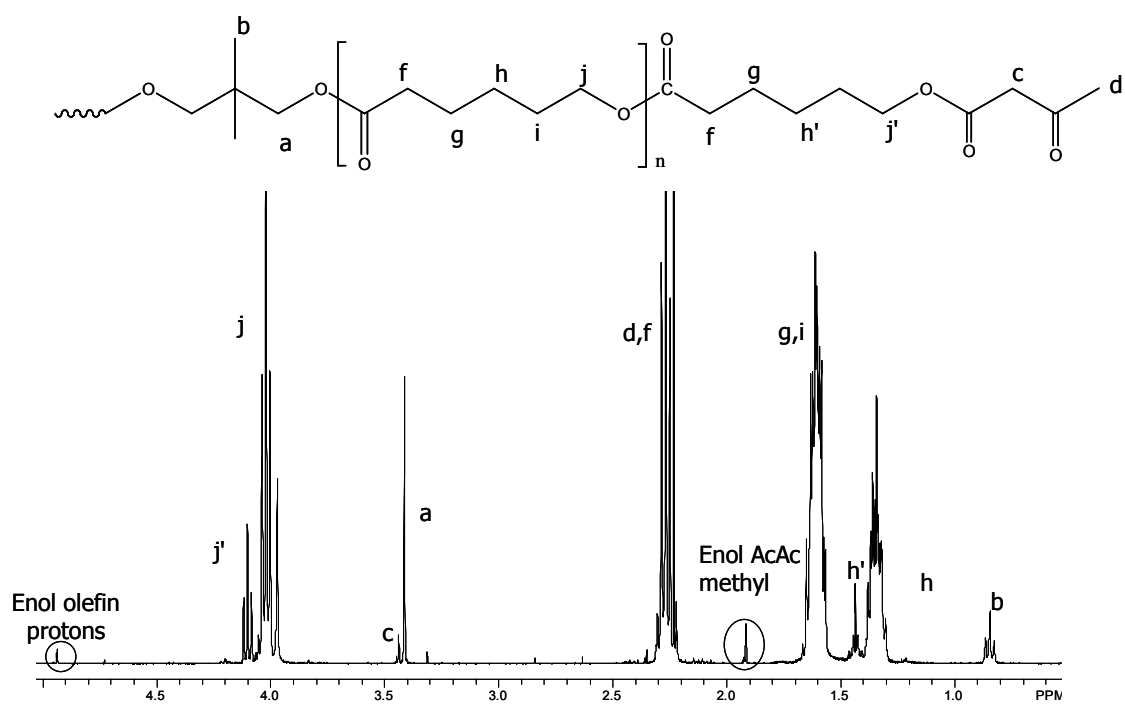


**Figure 6.1.** <sup>1</sup>H NMR spectra of acetoacetate functionalized poly(caprolactone) (PCL bisacac).

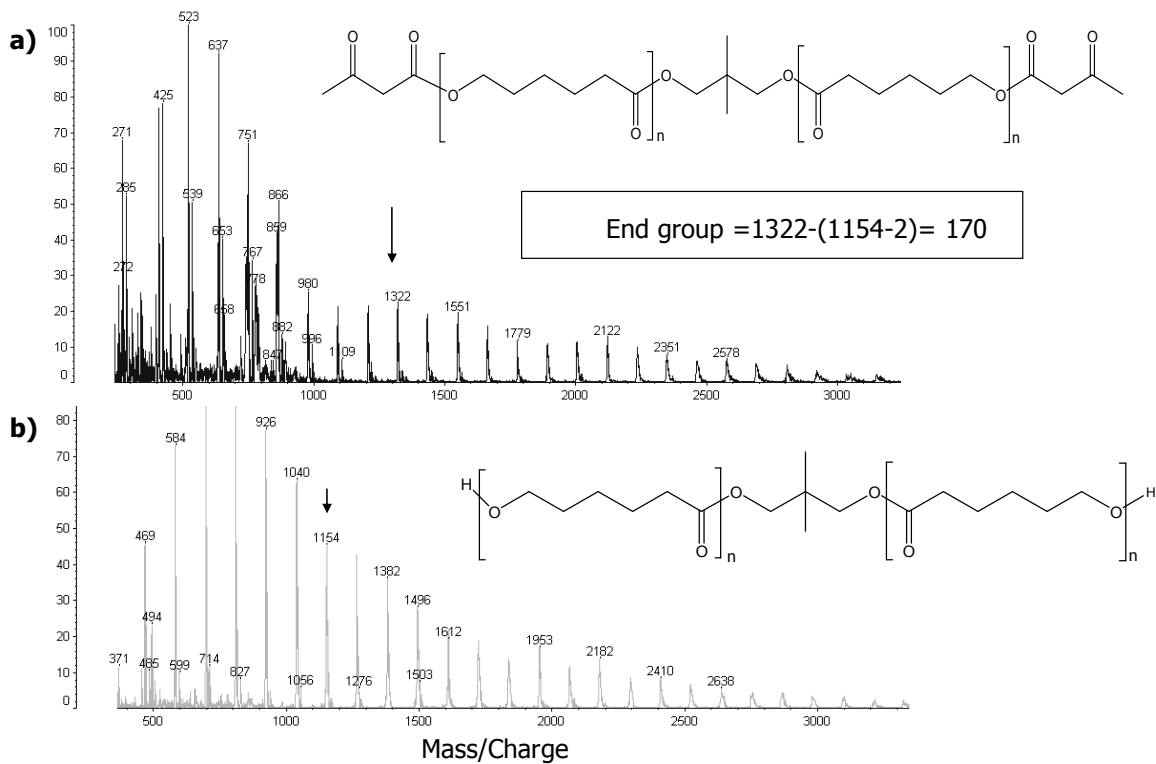


**Figure 6.2.** MALDI-TOF MS of a) acetoacetate-functionalized poly(caprolactone) (PCL bisAcAc) and b) poly(caprolactone) diol.

Base titration of the hydroxyl end groups of the PCL polyols was utilized to quantify the hydroxyl end group. In addition, the acetoacetate-functional samples were titrated following the same procedure to ensure that all of the hydroxyl end groups were consumed. The titration of acetoacetate-functionalized poly(caprolactone) precursor indicated the absence of hydroxyl end functionality. Moreover, number average molecular weights of the polyols were calculated from titration using the amount of acid required for titration, the concentration of the based used, and the sample weight.

Characterization of the molecular weight using SEC did not indicate any change in the molecular weight of the PCL after transacetoacetylation except for the slight increase due to end groups. As shown in Figure 6.3, comparison of SEC refractive index traces of PCL before and after a transacetoacetylation reaction indicates the traces are nearly identical. Moreover,  $^1\text{H}$  NMR analysis did not indicate any change in the composition of the backbone, which may arise from side reactions or possible attack to the ester functionality along the backbone. These results are in agreement with MALDI-TOF MS analysis indicating that the molecular weight of the precursor was retained upon transacetoacetylation. Table 6.1 displays a comparison of the molecular weight of PCL precursors and acetoacetate-functionalized PCL measured with SEC,  $^1\text{H}$  NMR, titration of the end groups, and MALDI-TOF MS.

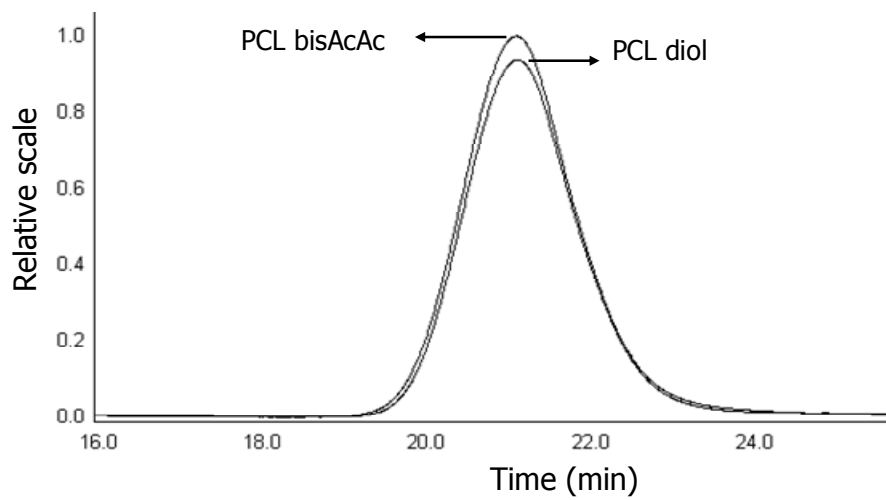


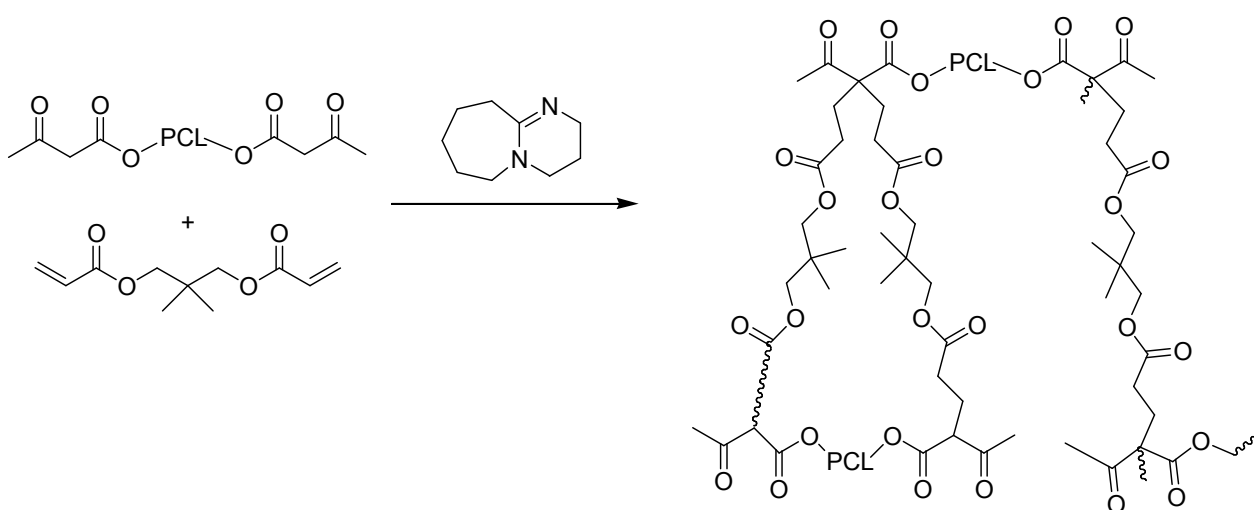
**Figure 6.3.** Comparison of SEC refractive index trace of PCL diol and PCL bisacetoacetate.

**Table 6.1.** Molecular weight characterization of PCL diol and PCL bisacetoacetate precursors using  $^1\text{H}$  NMR, hydroxyl-end titration, and MALDI-TOF MS.

Type of PCL oligomers	$M_n$ (g/mol) (NMR)	$M_n$ (g/mol) (Titration)	$M_w$ (g/mol) (MALDI)	PDI (MALDI)
1000 g/mol PCL	1,240	1,010	1,120	1.10
1000 g/mol PCL bisAcAc	1,470	---	1,390	1.20
2000 g/mol PCL	2,400	2,010	1,310	1.02
2000 g/mol PCL bisAcAc	2,600	---	1,880	1.08
4000 g/mol PCL diol	4,200	4,080	ND	ND
4000 g/mol PCL bisAcAc	4,800	---	ND	ND
2000 g/mol PCL triol	2,000	1,970	1,300	1.13
2000 g/mol PCL trisAcAc	2,150	---	1,580	1.21

#### 6.4.2 Crosslinking of PCL bisacetoacetate and neopentyl glycol diacrylate

Acetoacetate-functionalized PCL oligomers were successfully crosslinked with neopentyl glycol diacrylate in the presence of DBU (Scheme 6.3). The molar ratio of acetoacetate to acrylate was 1.4 to 1.0 for all networks based on our earlier studies.<sup>18,19</sup> Gel fraction analysis confirmed the effectiveness of oligomer incorporation into the networks and high gel fractions were achieved for all the networks (85%). The crosslinking reaction was monitored with *in-situ* FTIR spectroscopy following the intensity of the peak at 810 cm<sup>-1</sup>. As illustrated in 2-D *in situ* FTIR spectra (Figure 6.4), the absorbance of the peak corresponding to the vinyl stretching of the diacrylate groups decreased as the crosslinking reaction progressed. It confirmed that the acrylate groups were gradually and quantitatively consumed throughout the reaction.



**Scheme 6.3.** Crosslinking of poly(caprolactone) bisacetoacetate with neopentyl glycol diacrylate.

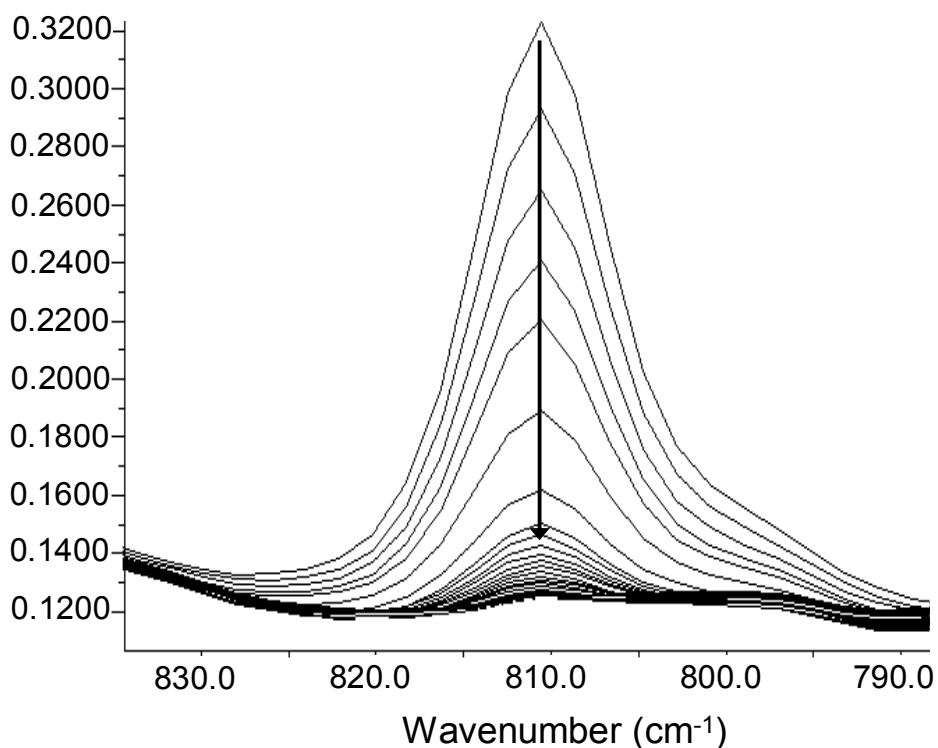


**Figure 6.4.** Stacked *in situ* FTIR spectra of crosslinking of PCL bisAcAc with neopentyl glycol diacrylate showing 810  $\text{cm}^{-1}$  ( $\text{CH}_2=$  twist).

These networks demonstrated glass transition temperatures below body temperature with high gel contents (> 85%). Moreover, our results confirmed that the networks were easily processed into a variety of geometries, and mechanical properties were altered with changing the molecular weight of the poly(caprolactone) segment. The covalently crosslinked networks demonstrated higher thermal stability compared to PCL oligomers (Figure 6.5), presumably due to removal of the nucleophilic, hydroxyl chain ends.

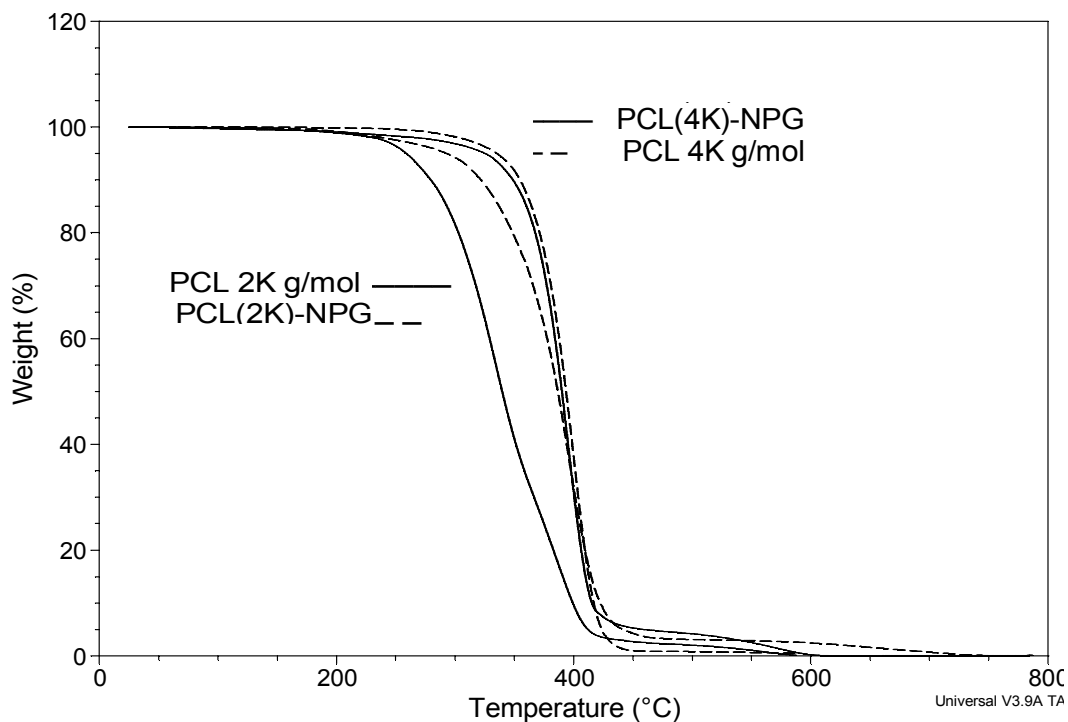


**Figure 6.5.** Thermogravimetric analysis of PCL precursors and networks.

The influence of PCL molecular weight on the crystallinity of the networks was investigated using DSC. The glass transition temperature of the networks increased from -64 to -42 °C as the molecular weight of the PCL segment in the networks increased from 1000 to 4000 g/mol. The  $T_g$  was highly dependent on PCL molecular weight due to the effect of crosslink density. Specifically, networks having PCL segments with molecular weights of 1000 g/mol were amorphous, while higher molecular weight PCL segments (2000 and 4000 g/mol) were semicrystalline (Figure 6.6). As shown in Figure 6.7, DSC analysis of PCL(1K)-NPG networks measured after 2 months of storage did not indicate development of crystallinity. The glass transition temperatures, melting point, heat of fusion ( $\Delta H$ ), and crystallinity of the networks are summarized in Table 6.2. The crystallinity of the networks were calculated using heat of fusion measured using DSC relative to the heat of fusion of 100% crystalline PCL (135 J/g), as reported in the

literature.<sup>8</sup> As shown in Table 6.2, PCL molecular weight demonstrated influence on the crystallinity of the crosslinked networks. The PCL(4K)-NPG network exhibited a higher degree of crystallinity compared to PCL(2K)-NPG, which suggests that the higher crosslink density suppressed the crystallization.

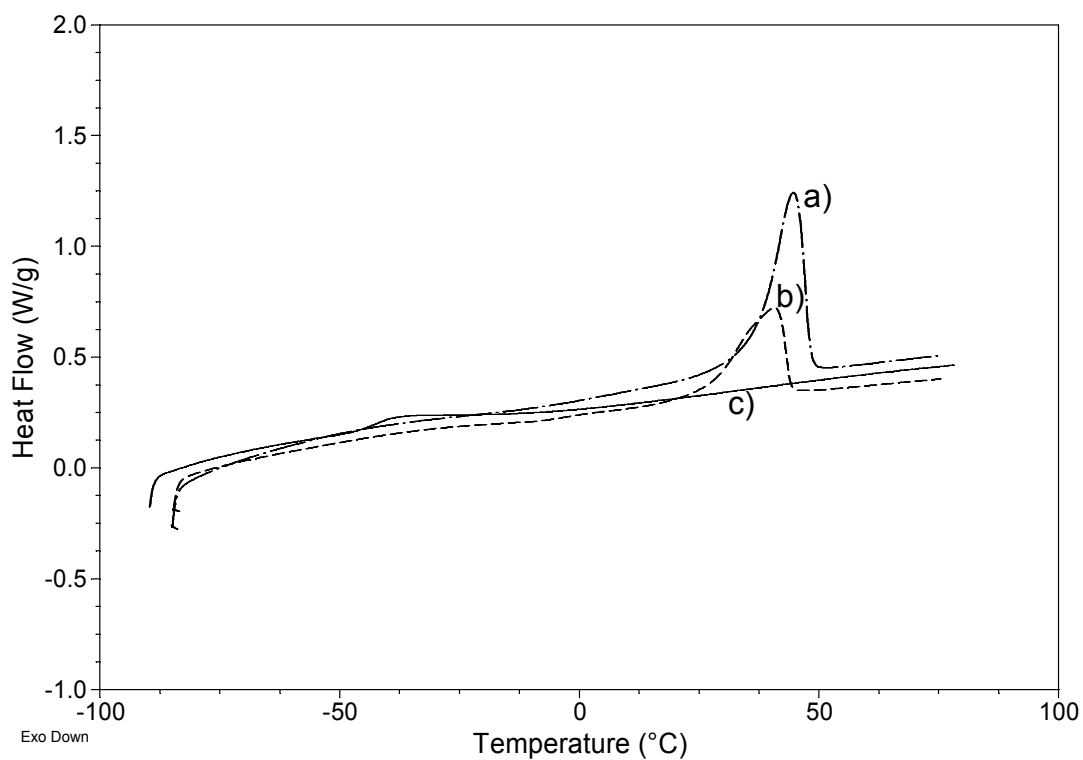


**Figure 6.6.** DSC analysis of networks from crosslinking of NPGDA with PCL bisacetoacetate a) 4000, b) 2000, and c) 1000 g/mol.

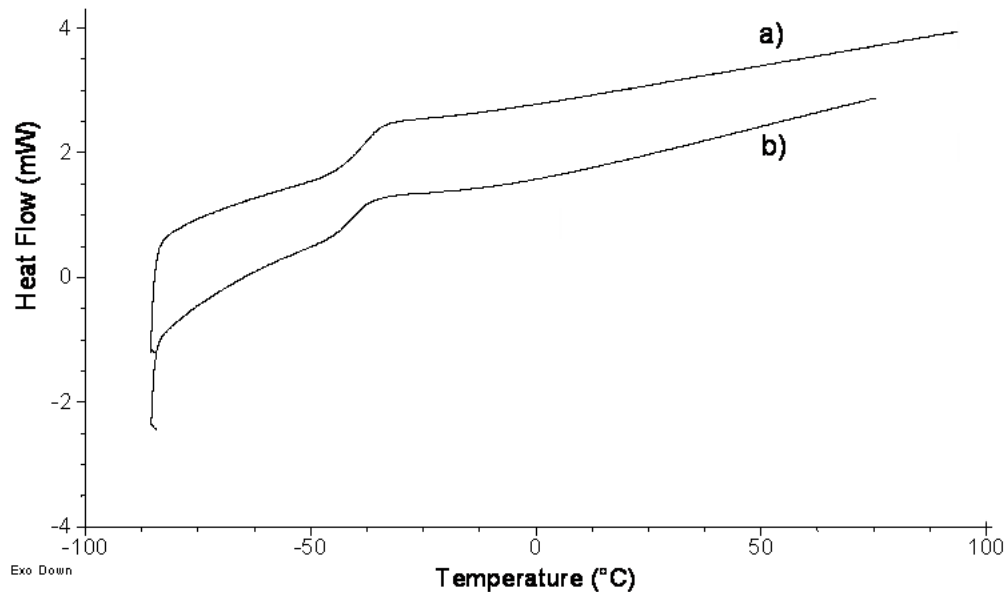


**Figure 6.7.** DSC of PCL(1K)-NPGDA networks a) after 1 week of storage b) after 2 months of storage.

**Table 6.2.** Glass transition temperatures, melting point, heat of fusion, and crystallinity of the networks.

Precursor Type	$T_g$ (°C)	$T_m$ (°C)	Heat of Fusion (J/g)	Crystallinity (%)
1000 g/mol PCL bisAcAc	-43	ND	ND	ND
2000 g/mol PCL bisAcAc	-54	41	26	19
4000 g/mol PCL bisAcAc	-64	45	44	33
2000 g/mol PCL trisAcAc	-25	ND	ND	ND

ND= not detected

DMA revealed that the storage modulus, plateau modulus, and glass transition of the networks were dependent on the molecular weight of the PCL segment due to the difference in crosslink density and the degree of crystallinity. DMA results supported the presence of a crystalline phase for the networks with higher molecular weight PCL (Figure 6.8). Networks having longer PCL segments exhibited lower  $T_g$  due to decreased crosslink density despite of the presence of crystallinity. The crystalline domains act as physical crosslink points and result in increased  $T_g$  values due to hindered segmental motion. However, in this case the  $T_g$  of the networks did not increase in the presence of crystallinity. This result was attributed to the fact that crystalline domains are connected with amorphous phase, and in this particular example the crystalline phase did not significantly influence the amorphous phase. It should be also noted that dangling ends in the networks also contribute to the resulting thermomechanical behavior. Networks having longer PCL segments (2000 and 4000 g/mol) exhibited melting transitions around 54 and 60 °C due to the presence of crystallinity. DMA demonstrated a higher plateau modulus for the PCL(1K)-NPG network due to increased crosslink density resulting from the shorter PCL segment. For semicrystalline networks, the moduli measured above their melting point demonstrated dependence on the crosslink density. The plateau moduli of the network having longer PCL segments were lower due to lower crosslink density.

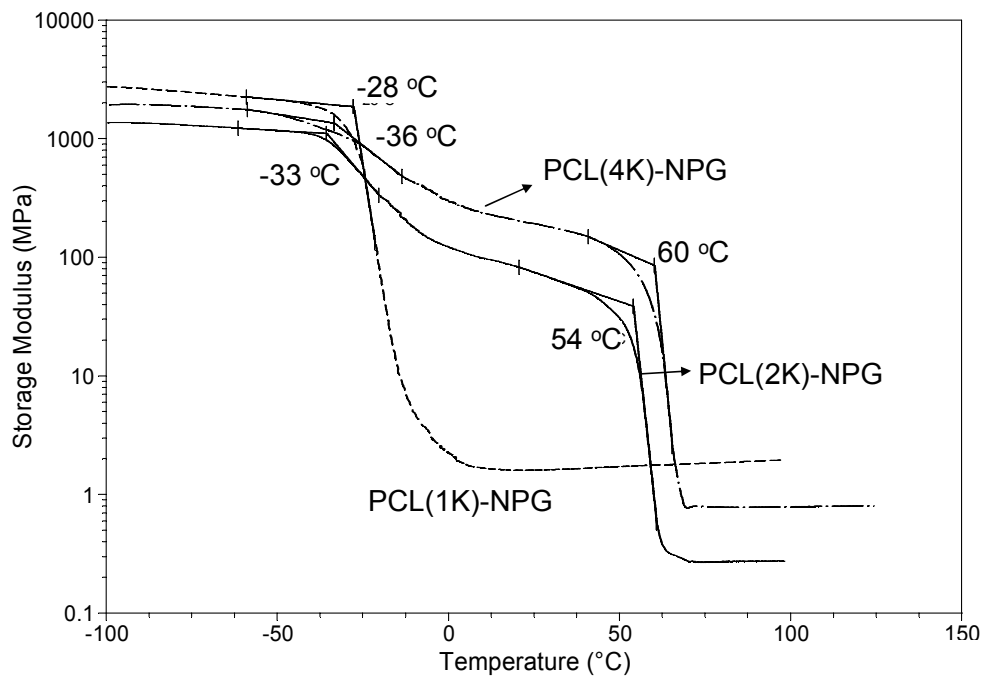


**Figure 6.8.** DMA of networks with varying PCL molecular weight.

Figure 6.9 shows the stress-strain curves corresponding to the networks obtained from reaction of NPGDA with poly(caprolactone) bisacetoacetate precursors with molecular weights of 1000, 2000, and 4000 g/mol. Tensile testing revealed dependence of mechanical properties on the molecular weight of the PCL segment due to its influence on crosslink density and crystallinity. The tensile properties of the networks are tabulated in Table 6.3. The networks obtained from PCL segments with molecular weights of 2000 and 4000 g/mol demonstrated higher Young's modulus due to the presence of crystallinity. While the crosslink density was theoretically highest for the PCL(1K)-NPG network, the modulus, stress, and stress at break values were lower due to the absence of crystallinity. The lower elongation was attributed to the higher crosslink density that restricted the extension of the network. Moreover, the modulus of the semicrystalline network increased as the molecular weight of the PCL increased to 4000 g/mol due to a higher degree of crystallinity. The networks obtained from poly(caprolactone) precursors having molecular weights 2000 and 4000 g/mol demonstrated a yield point that was followed by further elongation. The higher moduli and the yield points observed for these networks were attributed to the presence of crystallinity that was confirmed using DSC and DMA. The yield point was more distinctive in PCL(4K)-NPG networks due to higher degrees of crystallinity. In the literature, similar trends in tensile properties were obtained for poly(caprolactone) based networks having different crosslink densities and degrees of crystallinity.<sup>27</sup> It is well known that the biodegradation behavior of polymers is strongly associated with both molecular weight and morphology. During degradation, the amorphous phase degrades first, followed by the highly crystalline phase.<sup>28</sup> Therefore, controlling the molecular weight of the PCL segment enables control of the

crystallinity of these networks, as well as control of the biodegradation rate. Moreover, specific mechanical properties are attainable with controlled crystallinity.

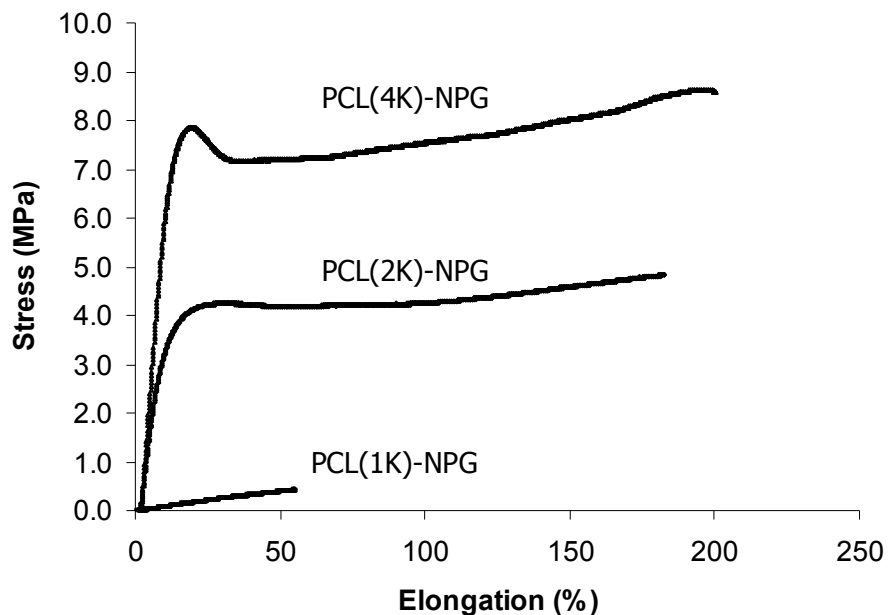


**Figure 6.9.** Tensile testing of PCL networks.

**Table 6.3.** Summary of tensile data for PCL bisacetoacetate-NPG based networks.

<b>M<sub>n</sub> of PCL bisacac (g/mol)</b>	<b>Gel Fraction (%)</b>	<b>Stress at Break (MPa)</b>	<b>Strain at Break (%)</b>	<b>Modulus (MPa)</b>
1000	86	0.45 ± 0.03	34 ± 9	6 ± 2
2000	85	4.25 ± 0.05	162 ± 36	48 ± 1
3000	84	7.38 ± 0.78	232 ± 35	107 ± 37

In addition to functionalizing and crosslinking PCL diol oligomers, oligomeric PCL triol (2000 g/mol) was successfully functionalized with acetoacetate groups and crosslinked with NPGDA.  $^1\text{H}$  NMR spectroscopy and MALDI-TOF analysis of the PCL trisacetoacetate precursor confirmed the presence of telechelic acetoacetate functionality. As shown in Figure 6.10, the comparison of SEC refractive index traces of PCL triol and PCL trisacetoacetate confirms that the molecular weight did not change after transacetoacetylation. Oligomeric PCL trisacetoacetate Michael donor was crosslinked with NPGDA following the synthetic route as explained in the experimental section. Thermogravimetric analysis indicated an enhanced upon crosslinking (Figure 6.11). The increase in the thermal stability was attributed to the absence of nucleophilic hydroxyl end groups in the crosslinked networks.

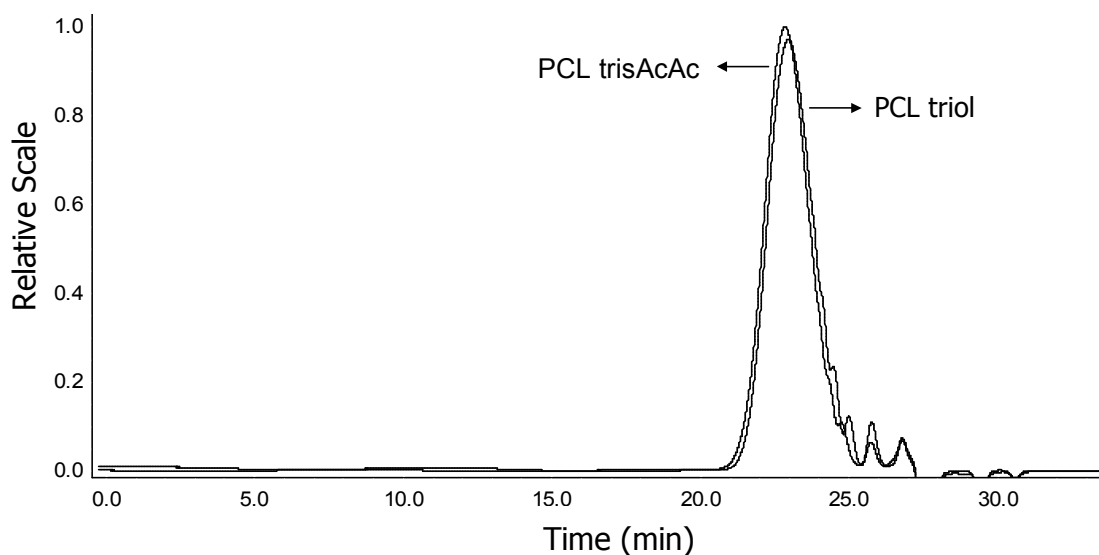


**Figure 6.10.** Comparison of SEC refractive index trace of PCL diol and PCL bisacetoacetate.

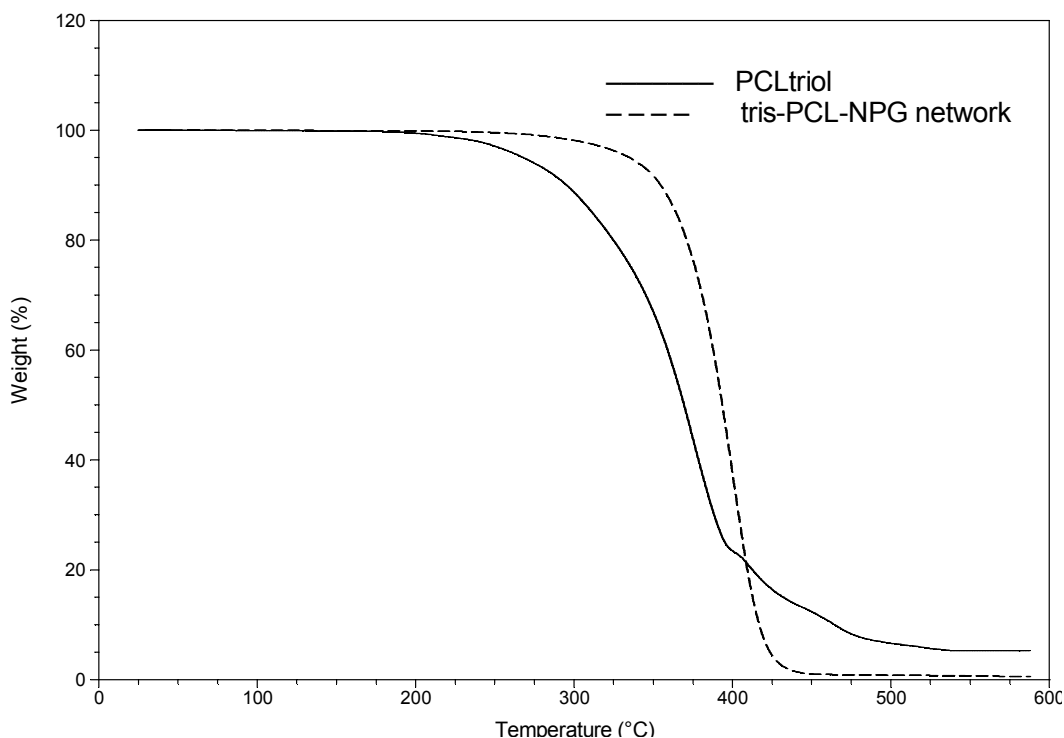


**Figure 6.11.** Thermogravimetric analysis of PCL triol and the corresponding network.

The thermomechanical properties of the networks were investigated using DSC and DMA to probe the influence of branching on crystallinity and mechanical properties. Thermal analysis using first scan DSC showed that PCL trisacetoacetate (2000 g/mol) and NPGDA networks were amorphous in contrast to the networks synthesized from PCL bisacetoacetate (2000 g/mol) (Figure 6.12). As the topology of the precursor was changed from linear to branched architecture, the symmetry was disrupted due to presence of branch points and the crystallization was suppressed. This result agrees with previous literature that reports dependence of the crystallization behavior on topology of PCL.<sup>24</sup> The glass transition of the network was increased from -42 to -25 °C as the trifunctional PCL precursor was incorporated to the network. The increase in the glass

transition was attributed to the presence of branching point which further restricts the motion.

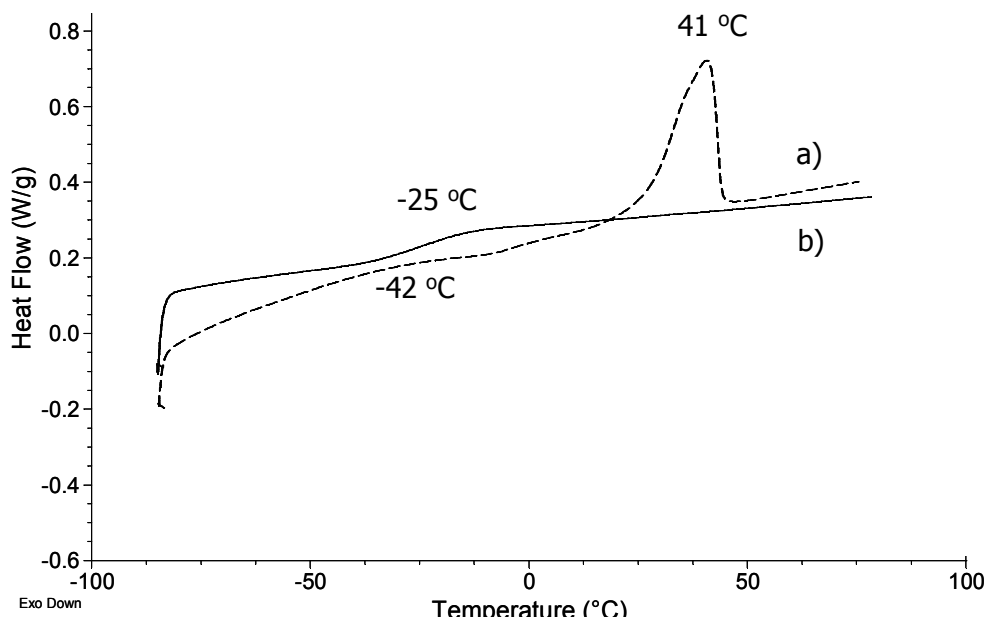


**Figure 6.12.** DSC analysis of PCL networks from crosslinking of NPGDA with a) PCL bisacetoacetate and b) PCL trisacetoacetate.

DMA also demonstrated the influence of precursor topology on final thermomechanical properties of the networks. As shown in Figure 6.13, DMA confirmed that the PCL trisacetoacetate network was amorphous. The modulus of the network is higher compared to networks obtained from PCL bisacetoacetate at temperatures greater than 50 °C, which is above the melting point of the semicrystalline network. The enhanced plateau modulus was attributed to higher crosslink density and the presence of branching in the star-shaped PCL trisacetoacetate precursor (Figure 6.13).

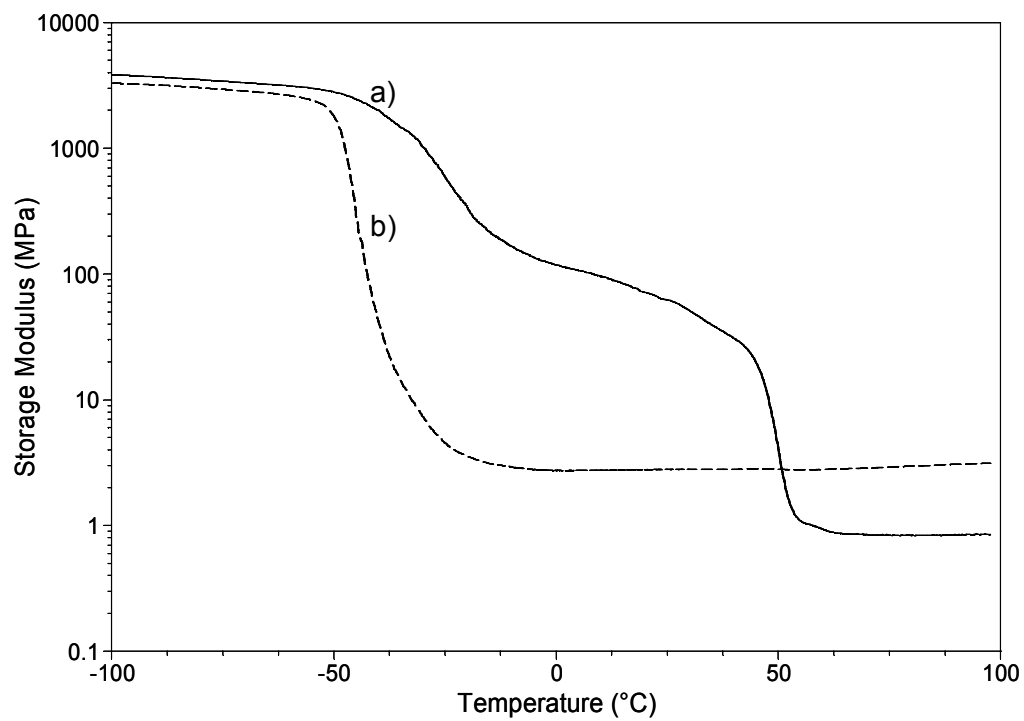


**Figure 6.13.** DMA analysis of PCL networks from crosslinking of NPGDA with a) PCL bisacetoacetate and b) PCL trisacetoacetate.

The crosslink density of the networks was characterized from swelling of the networks in THF at room temperature. As shown in Figure 6.14, the networks synthesized from PCL precursor with a number-average molecular weight of 1000 g/mol exhibited the lowest swelling ratio due to shorter chain lengths between crosslink points and increased crosslinking density. The results revealed an increase in swelling ratio as the molecular weight of the segment increased to 4000 g/mol. These results also demonstrate the correlation of the PCL precursor molecular weight and the crosslink density. These results support the earlier discussion on the dependence of mechanical properties on the PCL precursor molecular weight that was presumed to influence the crosslink density of the networks.

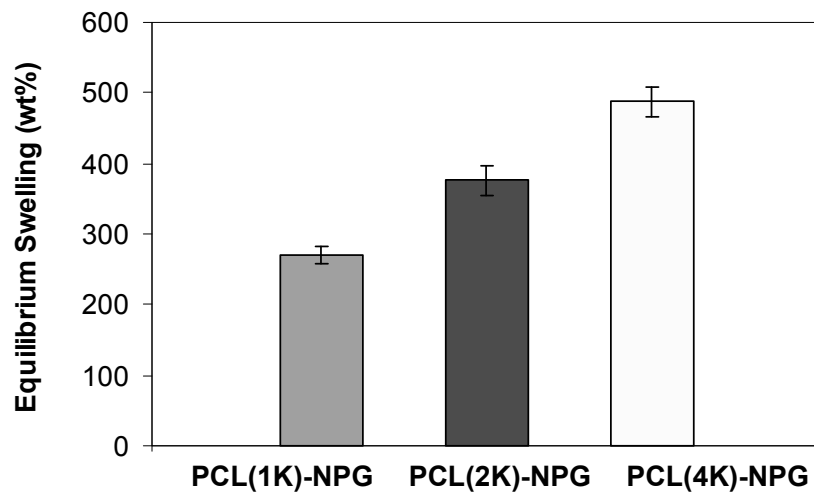


**Figure 6.14.** Swelling properties of PCL networks in THF.

The molecular weight between crosslink points ( $M_c$ ) was calculated for amorphous networks using the relationship between elastic modulus and crosslink density based on rubbery elasticity theory.<sup>29</sup> The  $M_c$  was calculated following Equation (1) using Young's modulus, gas constant, and room temperature.

$$E = 3\rho RT / M_c \quad (1)$$

$M_c$  was calculated for amorphous networks obtained from reaction of NPGDA with 1000 g/mol PCL BisAcAc and 2000 g/mol PCL TrisAcAc (Molecular weight of each arm estimated at 700 g/mol). The calculated  $M_c$  values were 1300 g/mol and 1060 g/mol for PCL BisAcAc and PCL TrisAcAc. These values agreed fairly well with PCL precursor molecular weights with efficient crosslinking.

## 6.5 Conclusions

In this study, the Michael addition reaction was utilized to prepare covalently crosslinked networks based on poly(caprolactone) and neopentyl glycol diacrylate. Hydroxyl terminated poly(caprolactone) (PCL) telechelic oligomers with molecular weights ranging from 500 to 4000 g/mol were successfully functionalized with acetoacetate groups. FTIR, <sup>1</sup>H NMR analysis, and titration studies confirmed end functionalization. Bis(acetoacetate) functionalized PCL precursors were reacted with neopentyl glycol diacrylate in the presence of an organic base at room temperature. The crosslinking reaction was monitored using *in situ* FTIR. PCL networks demonstrated higher thermal stability compared to PCL oligomers. Differential scanning calorimetry (DSC) results indicated that PCL based networks were either amorphous or semicrystalline depending on the molecular weight of the PCL segment. Dynamic mechanical analysis (DMA) confirmed the dependence of plateau modulus on the

molecular weight of the PCL unit, which also influenced the crystallinity and crosslink density of the network. Tensile testing results indicated a higher modulus for the semicrystalline network compared to its amorphous analog. Future work will include investigating the effect of PCL molecular weight on the biodegradation behavior of the crosslinked networks.

## 6.6 Acknowledgements

This material is based upon work supported by Eastman Chemical Company. The authors would like to thank A. J. Pasquale at Eastman Chemical Company for helpful discussions. Authors acknowledge Sharlene Williams and Brian Mather for helpful discussions.

## 6.7 References

1. Olson, D. A.; Gratton, S. E. A.; DeSimone, J. M.; Sheares, V. V., *J. Am. Chem. Soc.* **2006**, *128* (41), 13625-13633.
2. Cheng, M. L.; Lin, C. C.; Su, H. L.; Chen, P. Y.; Sun, Y. M., *Polymer* **2008**, *49* (2), 546-553.
3. Cool, S. M.; Kenny, B.; Wu, A.; Nurcombe, V.; Trau, M.; Cassady, A. I.; Grondahl, L., *J. Biomed. Mater. Res.* **2007**, *82A* (3), 599-610.
4. Garcia-Giralt, N.; Izquierdo, R.; Nogues, X.; Perez-Olmedilla, M.; Benito, P.; Gomez-Ribelles, J. L.; Checa, M. A.; Suay, J.; Caceres, E.; Monllau, J. C., *J. Biomed. Mater. Res.* **2008**, *85A* (4), 1082-1089.
5. Lee, S. J.; Liu, J.; Oh, S. H.; Soker, S.; Atala, A.; Yoo, J. J., *Biomaterials* **2008**, *29* (19), 2891-2898.
6. Amsden, B., *Soft Matter* **2007**, *3* (11), 1335-1348.
7. Simioni, A. R.; Vaccari, C.; Re, M. I.; Tedesco, A. C., *J. Mater. Sci.* **2008**, *43* (2), 580-584.
8. Kweon, H.; Yoo, M. K.; Park, I. K.; Kim, T. H.; Lee, H. C.; Lee, H. S.; Oh, J. S.; Akaike, T.; Cho, C. S., *Biomaterials* **2003**, *24* (5), 801-808.
9. Amsden, B. G.; Misra, G.; Gu, F.; Younes, H. M., *Biomacromolecules* **2004**, *5* (6), 2479-2486.
10. Cohn, D.; Salomon, A. F., *Biomaterials* **2005**, *26* (15), 2297-2305.
11. Karikari, A. S.; Williams, S. R.; Heisey, C. L.; Rawlett, A. M.; Long, T. E., *Langmuir* **2006**, *22* (23), 9687-9693.

12. Karikari, A. S.; Edwards, W. F.; Mecham, J. B.; Long, T. E., *Biomacromolecules* **2005**, *6* (5), 2866-2874.
13. Edgar, K. J.; Arnold, K. M.; Blount, W. W.; Lawniczak, J. E.; Lowman, D. W., *Macromolecules* **1995**, *28* (12), 4122-4128.
14. Geurink, P. J. A.; vanDalen, L.; vanderVen, L. G. J.; Lamping, R. R., *Prog. Org. Coat.* **1996**, *27* (1-4), 73-78.
15. Mather, B. D.; Miller, K. M.; Long, T. E., *Macromol. Chem. Physic.* **2006**, *207* (15), 1324-1333.
16. Mather, B. D.; Viswanathan, K.; Miller, K. M.; Long, T. E., *Prog. Polym. Sci.* **2006**, *31* (5), 487-531.
17. Lin, Y. Z., K.Y.; Dong, Z.M., *J. Polym. Sci. Pol. Chem.* **2007**, *45*, 4309-4321.
18. Williams, S. R.; Mather, B. D.; Miller, K. M.; Long, T. E., *J. Polym. Sci. Pol. Chem.* **2007**, *45* (17), 4118-4128.
19. Williams, S. R.; Miller, K. M.; Long, T. E., *Prog. React. Kinet.* **2007**, *32* (4), 165-194.
20. Kilambi, H.; Stansbury, J. W.; Bowman, C. N., *J. Polym. Sci. Pol. Chem.* **2008**, *46* (10), 3452-3458.
21. Luong-Van, E.; Grondahl, L.; Chua, K. N.; Leong, K. W.; Nurcombe, V.; Cool, S. M., *Biomaterials* **2006**, *27* (9), 2042-2050.
22. Prabu, P.; Chaudhari, A. A.; Aryal, S.; Dharmaraj, N.; Park, S. Y.; Kim, W. D.; Kim, H. Y., *J. Mater. Sci.* **2008**, *19* (5), 2157-2163.
23. Cho, H. H.; Han, D. W.; Matsumura, K.; Tsutsumi, S.; Hyon, S. H., *Biomaterials* **2008**, *29* (7), 884-893.
24. Choi, J.; Chun, S. W.; Kwak, S. Y., *J. Polym. Sci. Polym. Phys.* **2007**, *45* (5), 577-589.
25. Allgaier, J.; Martin, K.; Rader, H. J.; Mullen, K., *Macromolecules* **1999**, *32* (10), 3190-3194.
26. Rader, H. J.; Schrepp, W., *Acta Polym.* **1998**, *49* (6), 272-293.
27. Nagata, M.; Kato, K.; Sakai, W.; Tsutsumi, N., *Macromolecular Bioscience* **2006**, *6* (5), 333-339.
28. Kim, E. K.; Bae, J. S.; Im, S. S.; Kim, B. C.; Han, Y. K., *J. Appl. Polym. Sci.* **2001**, *80* (9), 1388-1394.
29. Calvet, D.; Wong, J. Y.; Giasson, S., *Macromolecules* **2004**, *37* (20), 7762-7771.

## **Chapter 7: Michael Addition Crosslinking of Acetoacetate-functionalized Poly(trimethylene adipate)s and Poly(trimethylene succinate)s**

**Partially taken from:** Ozturk, G.I.; Long, T.E. *Macromolecular Chemistry and Physics*, to be submitted, 2009.

### **7.1 Abstract**

Covalently crosslinked, biodegradable networks were synthesized from reaction of acetoacetate-functional oligomeric poly(trimethylene succinate)s and poly(trimethylene adipate)s with neopentylglycol diacrylate using a Michael addition reaction. Oligomeric polyesters with telechelic hydroxyl functionality were synthesized from renewable monomers, adipic and succinic acid, using solvent-free melt polycondensation. Molecular weights of the polyols were varied systematically to probe the influence of the molecular weight on the thermomechanical properties of the networks. The polyols were subsequently end-functionalized with acetoacetate groups using an environmentally friendly, facile transacetoacetylation reaction in the bulk.  $^1\text{H}$  NMR spectroscopy and MALDI-TOF MS analysis verified the presence of telechelic acetoacetate groups. Acetoacetate-functionalized polyesters were subsequently reacted with neopentyl glycol diacrylate in the presence of a basic catalyst at room temperature, and networks with approximately 90% gel were obtained. The thermomechanical properties of the networks and the oligomeric polyester precursors confirmed the influence of molecular weight on both the crystallinity of the oligomeric polyesters and the glass transition temperatures of the resulting networks. DSC analyses showed that the

extent of crystallinity depended on the molecular weight of the precursor, which also impacted crosslink density.

## 7.2 Introduction

Biodegradable polymers<sup>1</sup> are widely utilized in a number of biomedical applications to replace non-biodegradable polymers, thereby reducing the need to surgically remove implants<sup>1</sup> and sutures.<sup>2-4</sup> Additionally, in drug delivery applications,<sup>6,7</sup> targeted drug release rates are achieved through controlled polymer degradation. Several researchers<sup>5-7</sup> focused on developing new types of polymers as well as modifying existing polymers to tailor mechanical properties and degradation rates and improve polymer performance for several biomedical applications. For example, several studies showed that tailoring polymer topology through the introduction of branching<sup>7,8</sup> and crosslinking<sup>5,6,9</sup> enabled control over thermomechanical properties and biodegradation rates.

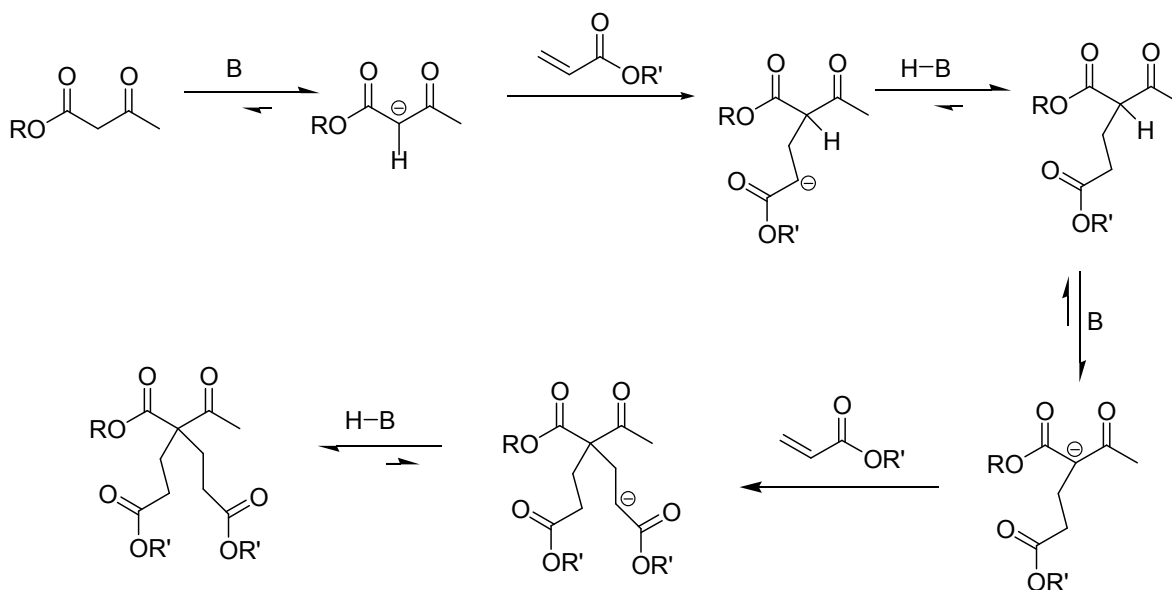
Biodegradable, aliphatic polyesters such as poly(caprolactone)s,<sup>10</sup> poly(lactide)s,<sup>11</sup> poly(glycolide)s<sup>12,13</sup> and their copolymers<sup>14</sup> with linear topology have been extensively studied. Moreover, altering the molecular structure and the morphology of polymers were exploited to control the degradation behavior. Bikiaris<sup>15</sup> reported the influence of glass transition temperature and hydrophilicity on the water penetration and rate of hydrolysis in novel biodegradable polyesters. In an earlier study, West et al.<sup>16</sup> incorporated enzyme cleavable peptide segments into polymer networks to overcome random hydrolysis and achieve controllable polymer degradation. Despite these reported improvements, a number of important biomedical applications require the use of

polyesters with enhanced physical and mechanical properties, which involves tailoring the topology of these materials.

As reported in the literature,<sup>17</sup> branched polymers exhibit significantly different solubility, crystallinity, viscosity, and mechanical properties compared to linear polymers with similar molecular weights. In particular, branched<sup>8,19</sup> polyesters featuring both hyperbranched and star shape<sup>7,9,20</sup> have attracted attention as a result of their unique physiochemical properties, which result from their low intrinsic viscosity and the presence of a large number of end groups. Moreover, several studies<sup>5,9,18</sup> investigated tailoring the biodegradation rates and mechanical properties of branched polyesters through introduction of different levels of crosslinking. The resulting crosslinked polyesters exhibited improved thermal and mechanical properties compared to linear and branched polyesters.<sup>9</sup> Crosslinking has also been widely utilized to fabricate degradable scaffolds. Several biodegradable aliphatic polyesters including poly(butylene succinate), poly(caprolactone), and poly(lactide)s<sup>19</sup> polyesters were crosslinked using UV-radiation,<sup>6</sup> hydrolysis and condensation of triethoxysilane end groups, and the polycondensation of multifunctional carboxylic acids.<sup>20</sup> Additionally, reactions of thiol groups with acrylates, as well as amines with aldehydes and other activated sites have been utilized to crosslink polymers. For example, Amsden et al.<sup>9</sup> studied the influence of topology on the properties of biodegradable polyesters with a particular emphasis on star shaped and crosslinked polyesters.

Recent studies investigated utilization of Michael addition<sup>21</sup> for synthesis of hyperbranched<sup>22</sup> polymers as well as chemical crosslinking<sup>23,24</sup> of a variety of polymers for coatings,<sup>25</sup> hydrogels, and thermoset applications.<sup>26,27</sup> Michael addition crosslinking

offers several advantages over other crosslinking methods in terms of availability of the precursors, mild reaction conditions, and elimination of solvent and side products.<sup>25,27,28,32</sup> Specifically, Michael addition involves the reaction of an enolate-type nucleophile, such as an acetoacetate, and unsaturated carbonyl groups in the presence of a base<sup>21</sup> (Scheme 7.1). Williams et al.<sup>25,26</sup> demonstrated that hydroxyl functionality is readily derivatized with acetoacetate groups using transacetoacetylation in the bulk.



**Scheme 7.1.** Mechanism of Michael addition with acetoacetates and acrylates.

Although early studies of biodegradable polyesters focused on poly(ethylene succinate)s and poly(butylene succinate)s to enhance mechanical properties without losing biodegradation performance, the synthesis of biodegradable polyesters from monomers obtained from renewable feedstocks has recently received considerable attention.<sup>16,30-33</sup> For example, several studies<sup>15,28-30</sup> reported the synthesis of sustainable polyesters and copolyesters using renewable monomers such as adipic acid,<sup>39,40</sup> succinic acid,<sup>28,31-35</sup> and 1,3-propanediol.<sup>18,46</sup> Bikiaris et al.<sup>15,31,32,35,36</sup> reported the synthesis and characterization of poly(alkylene succinate)s<sup>36, 38</sup> with a particular emphasis on the

influence of distance between ester groups on biodegradation behavior.<sup>36</sup> Moreover, advances and improvements in industrial scale production of 1,3-propanediol have increased its use in the synthesis of a variety of polyesters. New techniques such as the hydration of acrolein,<sup>37</sup> the hydrogenation of the intermediate 3-hydroxypropionaldehyde, or the hydroformylation of ethylene oxide were reported to produce high purity 1,3-propanediol in large scale. Haveren et al.<sup>38</sup> studied the synthesis of renewable polyesters as well as renewable monomers such as succinic acid, isosorbide, and 1,3-propanediol and reported novel polyesters for coating applications. Moreover, recent studies investigated the use of natural polymers such as chitosan for enhancing mechanical and biological performance.<sup>39</sup>

In this study, Michael addition was utilized to synthesize renewable and potentially biodegradable networks from poly(trimethylene adipate) and poly(trimethylene succinate)s. As discussed, Michael addition reactions offer advantages over photocrosslinking and free radical routes due to the elimination of organic solvents, crosslinking at physiological temperatures, and the absence of byproducts. In addition, one can control the morphology and thermomechanical properties of the networks through controlling the molecular weight of the polyester precursors. In this study, oligomeric poly(trimethylene adipate) and poly(trimethylene succinate) polyols were synthesized in the melt phase from solvent-free polycondensation in the absence of a catalyst. The resulting polyester polyols were subsequently end-functionalized with acetoacetate and reacted with neopentyl glycol diacrylate to form crosslinked networks. Polyesters with different molecular weights were crosslinked to probe the effect of molecular weight on thermal and mechanical properties of the networks.

## 7.3 Experimental

### 7.3.1 Materials

Neopentylglycol diacrylate, succinic acid ( $\geq 99\%$ ), adipic acid ( $\geq 99\%$ ), *tert*-butyl acetoacetate (*t*-BAA, 98%), 1,8-diazabicyclo[5.4.0]undec-7-ene (DBU, 98%), 1,3-propanediol ( $\geq 99.6\%$ ), 0.1 N KOH in methanol, acetic anhydride ( $\geq 99\%$ ), pyridine ( $\geq 99\%$ ), and tetrahydrofuran (THF) were purchased from Aldrich. All chemicals were used as received without further purification.

### 7.3.2 Characterization

Molecular weight was determined using a Waters size exclusion chromatograph at 40 °C in THF (HPLC grade). SEC was equipped with a 410 RI detector, a Viscotek 270 dual detector, and an in-line Wyatt Technologies miniDawn multiple angle laser light scattering (MALLS) detector. The samples were run at a flow rate of 1 mL/min using an autosampler. The instrument was calibrated using polystyrene standards, and reported SEC traces were obtained from the refractive index detector. The chemical compositions of the polymer backbone and end group functionality were characterized using  $^1\text{H}$  NMR spectroscopy conducted on a Varian Unity 400 spectrometer at 400 MHz in  $\text{CDCl}_3$ . Thermal analysis using a TA Instruments Q-100 DSC determined thermal transition temperatures at a heating rate of 10 °C/min under nitrogen. MALDI-TOF MS analyses were performed using a Kratos Kompact SEQ instrument equipped with nitrogen laser with a wavelength of 337.1 nm. The accelerating voltage was 20 kV in delayed extraction mode using 100-180 power setting in the positive ion linear mode. The targets were prepared from a solution of acetonitrile with 2,5-dihydroxybenzoic acid as the matrix. The samples were dissolved in acetonitrile at 1 mg/mL, and approximately 0.5

$\mu\text{L}$  of this solution was mixed with matrix. The instrument was calibrated using endohedral metallofullerene sample as the reference compound.

The hydroxyl end-functionality of the polyols was quantified using a base titration. The samples were dissolved in acetic anhydride/pyridine mixture (1:3 v:v) and reacted overnight at room temperature under constant mixing. 10 mL of distilled water and 10 mL of pyridine were added and allowed to react for 30 min to hydrolyze the excess acetic anhydride. The samples were titrated with 0.1 N KOH solution. Base titration of hydroxyl end groups was also used to calculate the number average molecular weight of the polyester polyols.

Gel fraction of the networks was measured gravimetrically using Soxhlet extraction in refluxing THF for 3 h. Dynamic mechanical analysis was performed on a TA instruments Q-800 DMA under nitrogen at a heating rate of 3  $^{\circ}\text{C}/\text{min}$  at 1 Hz frequency in the film-tension mode.

### **7.3.3 Synthesis of oligomeric polyester polyols**

Adipic acid (14.61 g, 100 mmol) or succinic acid (11.81 g, 100 mmol) and 50 mol% excess (with respect to the diacid) 1,3-propanediol (11.41 g, 150 mmol) were reacted in a 100-mL, round-bottomed flask equipped with a mechanical stirrer and a condenser under constant nitrogen flow. The flask was degassed three times using vacuum and nitrogen flush and subsequently heated to 200  $^{\circ}\text{C}$ . The reaction proceeded under nitrogen atmosphere at 200  $^{\circ}\text{C}$  for 2 h and the temperature was raised to 220  $^{\circ}\text{C}$  over 5 h. The byproduct was removed under vacuum (0.1 mm Hg) for 2 h at 250  $^{\circ}\text{C}$ . Oligomeric polyesters having different molecular weights were synthesized using the stoichiometric imbalance of the monomers. The diol was charged in 10, 20, and 40

mol% excess with respect to the diacid monomer to obtain the targeted molecular weights. The reaction products were characterized without further purification.

#### **7.3.4 Acetoacetate end-functionalization of polyesters polyols**

Hydroxyl-functional oligomeric poly(trimethylene adipate) (5 g, 5 mmol) and 50 mol% excess *t*-BAA (2.37 g, 15 mmol) were charged to a 100-mL flask. The flask was flushed with nitrogen and the mixture was subsequently heated to 150 °C for 3 h. Additional *t*-BAA (2.37 g, 15 mmol) was added and the flask was heated for an additional 3 h at 150 °C to ensure complete functionalization of the polyester oligomer. The byproduct *tert*-butanol and excess *t*-BAA were removed under moderate vacuum (100 mmHg) at 150 °C for 1 h using a short-path distillation system. The products were characterized using <sup>1</sup>H NMR spectroscopy and MALDI-TOF MS.

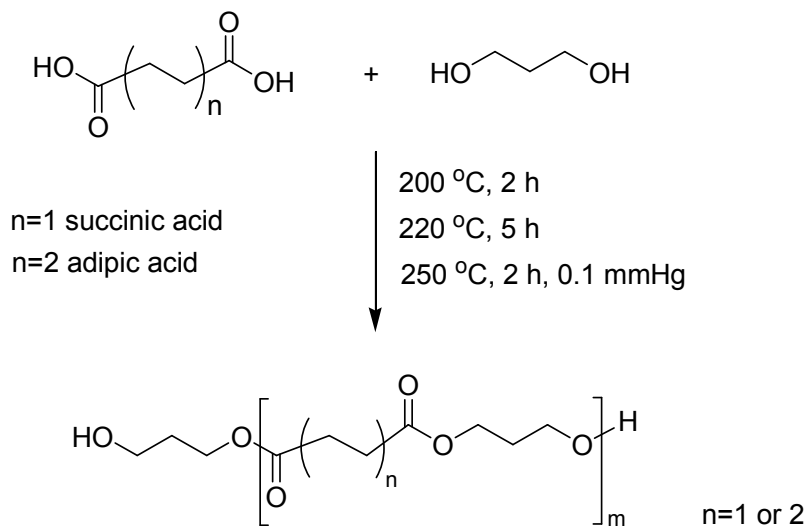
#### **7.3.5 Synthesis of crosslinked networks**

Acetoacetate-functionalized oligomeric poly(trimethylene adipate) and poly(trimethylene succinate) precursors having various molecular weights were reacted with neopentylglycol diacrylate in the presence of DBU. The acetoacetate functionalized polyesters and the diacrylate were reacted at a mole ratio of 1.0 to 1.4, respectively. Acetoacetate-functionalized polyester and neopentylglycol diacrylate were mixed in a sample vial to obtain a homogeneous blend. The organic base catalyst, DBU (0.05 wt% relative to bisacac precursor), was added and mixed at room temperature. The mixture was transferred to a Teflon<sup>TM</sup> mold and allowed to cure at ambient temperature. The films were kept under vacuum overnight before conducting thermomechanical analyses.

## 7.4 Results and Discussion

### 7.4.1 Synthesis of hydroxyl telechelic polyesters

Hydroxyl-functional oligomeric poly(trimethylene adipate)s and poly(trimethylene succinate)s were synthesized from the melt polycondensation of adipic acid, succinic acid, and 1,3-propanediol in the absence of a catalyst, as depicted in Scheme 7.2. For this study, the use of titanium isopropoxide, which is a catalyst commonly used for polyester synthesis, was eliminated to prevent the unwanted influence of any residual titanium catalyst on the subsequent transacetoacetylation step. Specifically, prior experiments using titanium isopropoxide and *t*-butyl acetoacetate indicated that the presence of titanium catalyst hindered end group functionalization due to the coordination of titanium with acetoacetate units. Literature studies also supported the coordination of transition metals with acetoacetate groups.<sup>40,41</sup>



**Scheme 7.2.** Synthesis of poly(trimethylene adipate) and poly(trimethylene succinate) diol.

Oligomeric poly(trimethylene adipate)s and poly(trimethylene succinate)s of different molecular weights were synthesized using stoichiometric imbalances of the

diacid and the diol monomer. The diacid monomers, succinic and adipic acid, were reacted with 10, 20, and 40 mol% excess of 1,3-propanediol to achieve theoretical molecular weights of 4000, 2000, and 1000 g/mol, respectively. The progress of the reaction was monitored according to the amount of water produced from the direct esterification of the diacid and diol. In addition, aliquots were removed from the reaction medium for titration with base to determine the acid number. As expected, the acid number decreased sharply in the beginning of the reaction due to consumption of the diacid monomer. The reaction was terminated when the measured acid number of the polymer was lower than 0.5 mg KOH/g and a theoretical amount of water was collected in the receiving flask. In addition, MALDI-TOF MS analysis of the oligomers confirmed the completion of the esterification reaction due to the absence of acid end groups (Figures 7.2 and 7.3). The resulting oligomeric polyesters were characterized using  $^1\text{H}$  NMR spectroscopy and MALDI-TOF MS. The hydroxyl-end groups were titrated prior to the transacetoacetylation reaction to confirm hydroxyl functionality and to determine molecular weight. Table 7.1 summarizes the molecular weight of poly(trimethylene adipate)s as calculated from  $^1\text{H}$  NMR spectroscopy, MALDI-TOF MS, and base titration. These complementary techniques confirmed that targeted molecular weights were achieved from melt polycondensation. The molecular weights of the poly(trimethylene succinate)s were also shown to be within the targeted range (Table 7.2).

**Table 7.1.** Molecular weight data of poly(trimethylene adipate) measured using  $^1\text{H}$  NMR spectroscopy, MALDI-TOF MS, and base titration.

<b>Adipic acid:1,3- propanediol</b>	<b><sup>a</sup>Targeted <math>M_n</math> (g/mol)</b>	<b><sup>b</sup><math>M_n</math> (g/mol)</b>	<b><sup>c</sup><math>M_n</math> (g/mol)</b>	<b><sup>d</sup><math>M_n</math> (g/mol)</b>
1:1.4	1,210	931	1,040	1022
1:1.2	2,048	1,800	1,900	1,667
1:1.1	3,910	4,200	5,500	ND

<sup>a</sup> Calculated from  $X_n=(1+r)/(1-r)$  <sup>b</sup> $^1\text{H}$  NMR <sup>c</sup> Titration <sup>d</sup> MALDI-TOF MS

ND= not determined

**Table 7.2.** Molecular weight data of poly(trimethylene succinate) measured using  $^1\text{H}$  NMR spectroscopy, MALDI-TOF MS, and base titration.

<b>Succinic acid:1,3- propanediol</b>	<b><sup>a</sup>Targeted <math>M_n</math> (g/mol)</b>	<b><sup>b</sup><math>M_n</math> (g/mol)</b>	<b><sup>c</sup><math>M_n</math> (g/mol)</b>	<b><sup>d</sup><math>M_n</math> (g/mol)</b>
1:1.4	949	990	1,100	1,400
1:1.17	2,019	1,970	1,800	1,800
1:1.08	4,112	3,100	3,200	ND

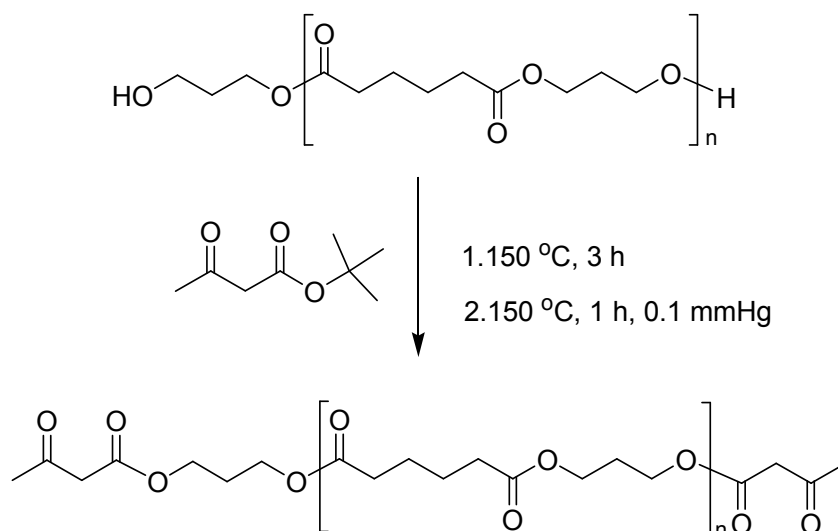
<sup>a</sup> Calculated from  $X_n=(1+r)/(1-r)$  <sup>b</sup> $^1\text{H}$  NMR <sup>c</sup> Titration <sup>d</sup> MALDI-TOF MS

ND= not determined

#### 7.4.2 Synthesis of bisacetoacetate functionalized polyesters

The hydroxyl end groups of the oligomeric polyesters were derivatized with acetoacetate groups using a method reported previously by our research group.<sup>27,28</sup> The polyesters were end-functionalized with acetoacetate groups using transacetoacetylation of hydroxyl groups with *t*-butyl acetoacetate in the bulk and in the absence of any catalyst

(Scheme 7.3). The final product was purified after removing the byproduct *t*-butanol and excess *t*-butyl acetoacetate using a one-step vacuum distillation.



**Scheme 7.3.** Transacetoacetylation of poly(trimethylene adipate) diol.

Telechelic acetoacetate functionality was confirmed using  $^1\text{H}$  NMR spectroscopy and MALDI-TOF MS analysis. Figure 7.1a and 7.1b show the  $^1\text{H}$  NMR spectra of the oligomeric poly(trimethylene adipate)s diol and the poly(trimethylene adipate)s bisacetoacetate, respectively. In Figure 7.1, both spectra depict peaks at  $\delta=2.63$  and  $1.62$  ppm, corresponding to methylene protons in the adipate unit, while the central and terminal methylene protons of 1,3-propanediol appear at  $\delta=1.98$  and  $4.11$  ppm, respectively. The spectrum of the polyol shows a peak at  $\delta=3.62$  ppm, which corresponds to the methylene adjacent to the hydroxyl end group. A comparison of the two spectra showed that this peak disappeared when the hydroxyl groups were converted to acetoacetate functionality. The absence of this peak in Figure 7.1a suggests that all hydroxyl end groups were derivatized with the acetoacetate groups. Moreover,  $^1\text{H}$  NMR spectra (shown in Figure 7.1b) confirmed the presence of acetoacetate functionality as

indicated by the peaks at  $\delta=2.26$  and 3.22 ppm, which correspond to the AcAc methyl and AcAc methylene resonances, respectively.

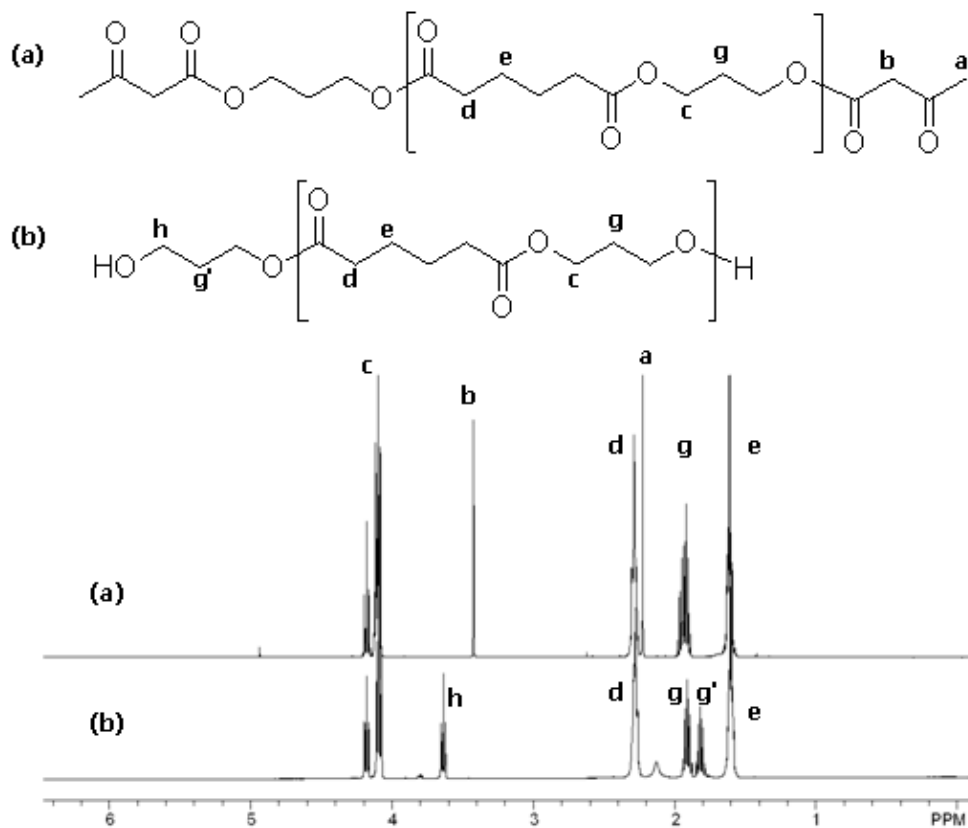


**Figure 7.1.**  $^1\text{H}$  NMR spectroscopy comparison of a) poly(trimethylene adipate) diol and b) poly(trimethylene adipate) bisacac.

Since polyesters have ester functionality along the backbone, which is prone to hydrolytic degradation, it is important to characterize the molecular weight of the precursors and chemical structure after transacetoacetylation. Comparison of  $^1\text{H}$  NMR spectra before and after transacetoacetylation confirmed that there were no changes in the composition of the polyester backbone after end group modification. Moreover, due to the fact that any attack to the ester functionality on the polyester backbone would result in a dramatic decrease of molecular weight, precursor molecular weights were characterized before and after the reaction to detect any degradation. Subsequent SEC analysis of the oligomeric polyester indicated that the molecular weight did not change after the transacetoacetylation reaction. As shown in Figure 7.2, the representative SEC traces of poly(butylene adipate) oligomers obtained from refractive index detector are approximately identical. The molecular weights of the bisacetoacetate-functional polyesters were also calculated using the integrations of the AcAc methyl resonances from  $^1\text{H}$  NMR analyses. The calculated molecular weights for the precursors are consistent with SEC molecular weights.

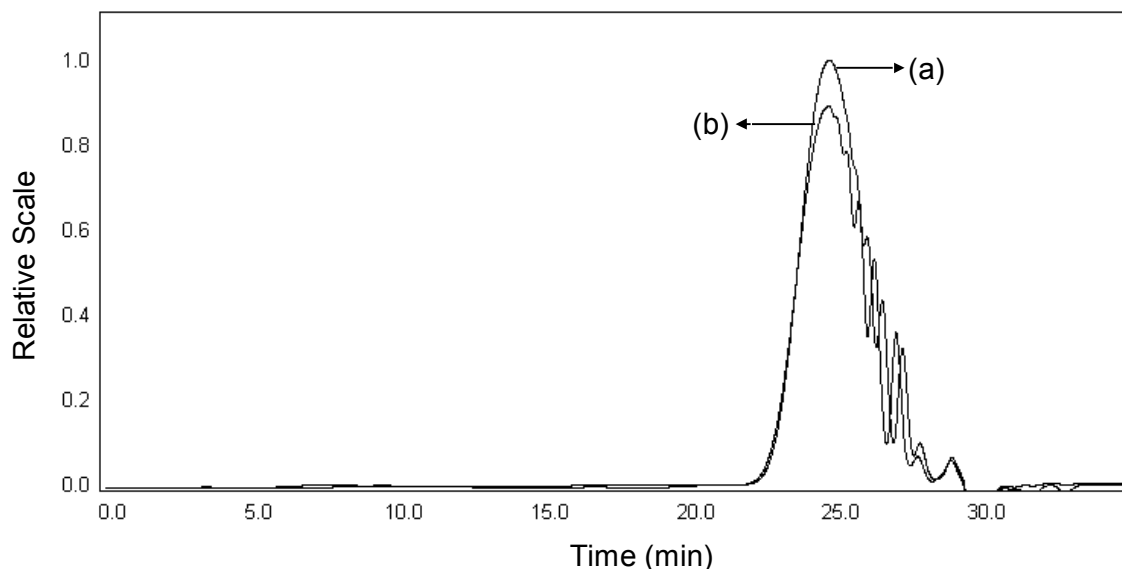


**Figure 7.2.** SEC RI detector traces of a) poly(trimethylene adipate) diol and b) poly(trimethylene adipate) bisacac.

As reported, MALDI-TOF MS is a powerful analytical technique for characterizing end-functionality and the molecular weight of polymers with narrow polydispersities.<sup>47-49</sup> In this study, oligomeric polyester polyols and bisacetoacetate analogs with molecular weights of approximately 1000-2000 g/mol were also characterized using mass spectroscopy. Analysis of the oligomers with higher molecular weights was limited due to the analytical limitations of the instrument. MALDI-TOF spectra of the poly(trimethylene adipate) and poly(trimethylene succinate) diols, as well as their acetoacetate-functional analogs, confirmed anticipated molecular weight distributions for step growth polymers. The mass difference between the polyester diols and acetoacetate-functionalized polyesters was then investigated to confirm the presence of acetoacetate end-functionality. MALDI-TOF MS results, shown in Figures 7.3 and 7.4, revealed several peaks, each of which corresponds to poly(trimethylene adipate) and

poly(trimethylene succinate) oligomers with different degrees of polymerization. The difference between each peak in the mass spectra corresponds to the mass of the repeat unit. The peak-to-peak difference was calculated as 189 m/z for the poly(trimethylene adipate) and 158 m/z for the poly(trimethylene succinate). The difference between the mass of the acetoacetate relative to the hydroxyl-functional polymer provided information about the mass of the end groups. For the poly(trimethylene adipate) and poly(trimethylene succinate) oligomers, this calculation was 170 m/z, which corresponded to the mass of the two acetoacetate groups. Moreover, MALDI-TOF MS spectra confirmed the absence of acidic end-groups in both the poly(trimethylene adipate) and poly(trimethylene succinate) diols. These results are in agreement with the titration of the polyols and the  $^1\text{H}$  NMR spectroscopic characterization.

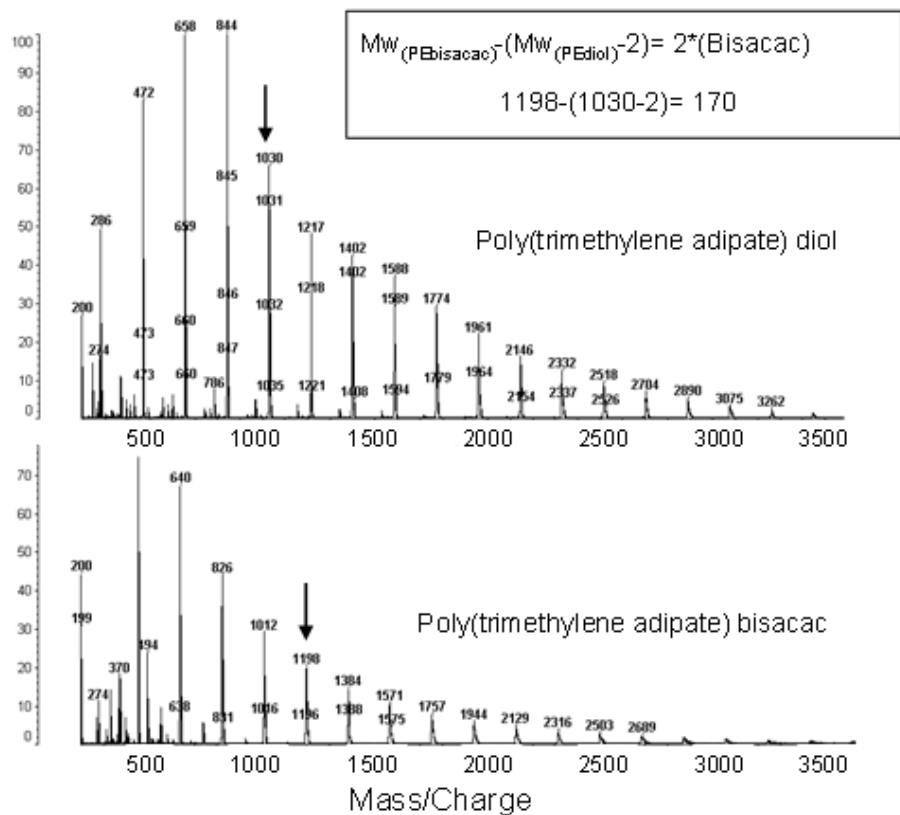


**Figure 7.3.** MALDI-TOF MS comparison of poly(trimethylene adipate) diol and poly(trimethylene adipate) bisacac.

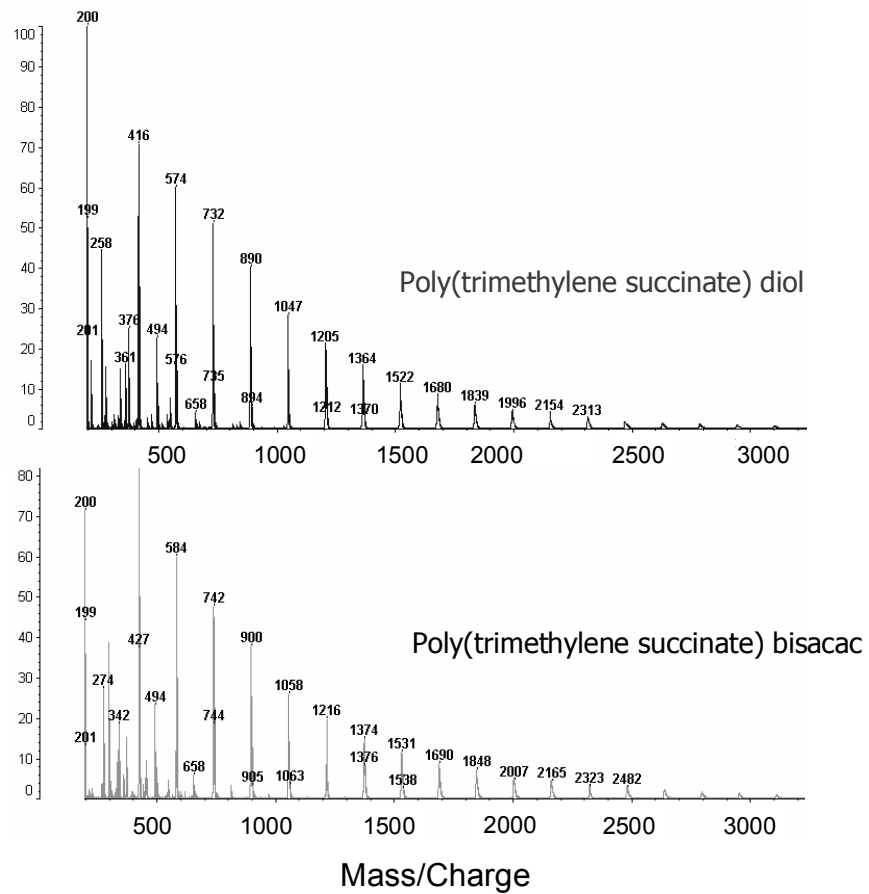


**Figure 7.4.** MALDI-TOF MS comparison of poly(trimethylene succinate) diol and poly(trimethylene succinate) bisacac.

DSC characterization of the oligomeric polyesters revealed that thermal behavior was significantly dependent on molecular weight, the number of methylene groups in the repeat unit, and thermal history. Thermal analysis of the oligomeric polyesters using first scan DSC indicated that all the polyester polyols were semicrystalline. As expected, the glass transition temperature of the oligomers increased with increasing molecular weight. The  $T_g$ s of the poly(trimethylene succinate)s increased from  $-49$  to  $-42$  °C as the molecular weight increased from 1000 to 3000 g/mol (Figure 7.5), while the  $T_g$ s of the oligomeric poly(trimethylene adipate)s increased from  $-63$  to  $-43$  °C as the molecular weight increased from 1000 to 4000 g/mol (Figure 7.5). Moreover, the poly(trimethylene adipate) and poly(trimethylene succinate) oligomers with the highest molecular weight exhibited melting points at  $42$  and  $49$  °C, respectively. As the molecular weight of the polyol decreased to 1000 g/mol, however, a melting shoulder peak was observed for both the poly(trimethylene adipate) and poly(trimethylene succinate) oligomers. The presence of this shoulder peak was attributed to the presence of lower molecular weight oligomers that influenced the packing of the polyester chain. Table 7.3 shows that melting temperature ( $T_m$ ) and heat of fusion ( $\Delta H_f$ ) for the poly(trimethylene succinate)s decreased with decreasing molecular weight, which was attributed to the presence of low molecular weight segments that act as an impurity and disturb crystallization, which results in the formation of less perfect crystals. A similar trend was observed for poly(trimethylene adipate) oligomers (Table 7.4). Moreover, the decrease in the breadth of the melting peak with increasing molecular weight suggests the presence of more organized crystals.

**Table 7.3.** Glass transition temperatures, melting point, and heat of fusion of poly(trimethylene succinate) diol oligomers.

Poly(trimethylene succinate)	T <sub>g</sub> (°C)	T <sub>m</sub> (°C)	Heat of Fusion (J/g)
1000 g/mol	-49	44	20
2000 g/mol	-46	48	47
4000 g/mol	-42	49	64

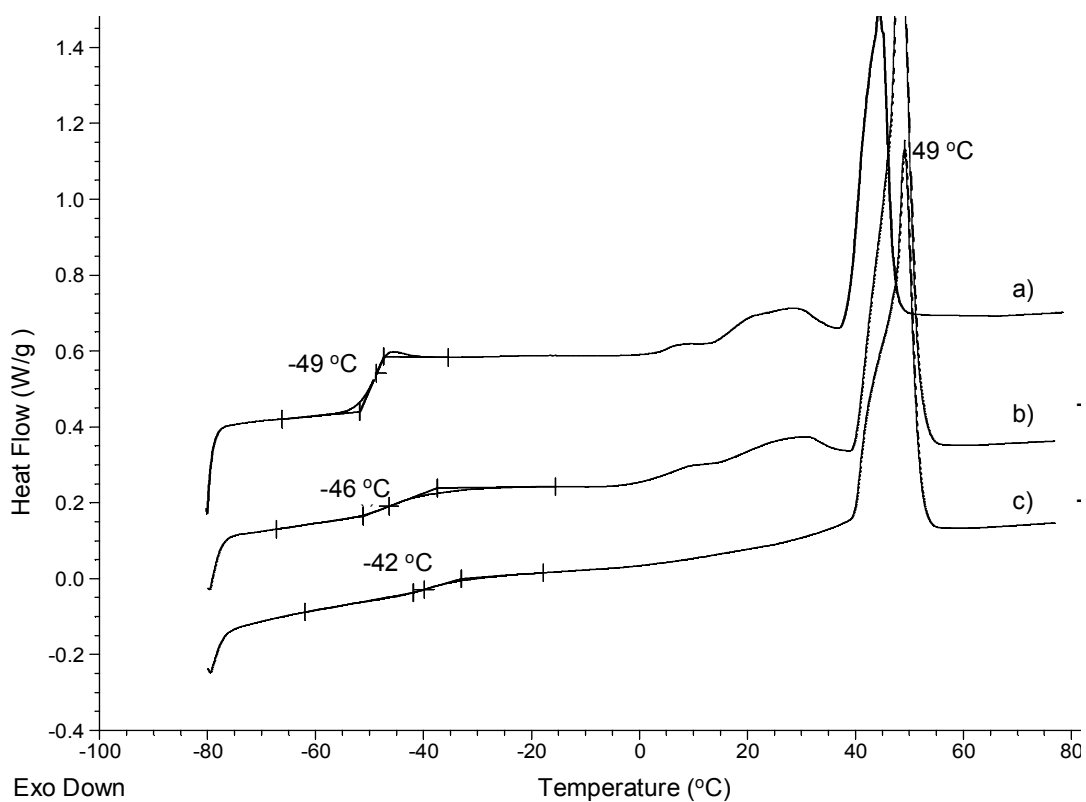


**Figure 7.5.** DSC of poly(trimethylene succinate) diol oligomers with molecular weights of a) 1000, b) 2000, and c) 4000 g/mol.

A comparison of DSC thermograms of poly(trimethylene adipate) and poly(trimethylene succinate) oligomers of similar molecular weight revealed the influence of methylene spacers on the thermal properties of these aliphatic polyesters. This finding is supported by earlier research<sup>16,41</sup> describing how the number of in a diacid or diol segment impact thermal properties. In our studies, as the number of methylene groups increased from 2 to 4 in the diacid monomer, the melting point of the polyester decreased, which agrees well with literature studies by Bikiaris.<sup>18</sup> Moreover, as the number of methylene groups increased from the poly(trimethylene succinate) to the poly(trimethylene adipate), the  $T_g$  decreased due to enhanced chain flexibility. As the samples were cooled from the melt at a cooling rate of 5 °C/min, cold crystallization was not detected for poly(trimethylene succinate)s. In contrast, the poly(trimethylene adipate) oligomers displayed slow crystallization behavior and broad crystallization exotherms at 0, -11, and -14 °C, corresponding to molecular weights of 4000, 2000, and 1000 g/mol, respectively.

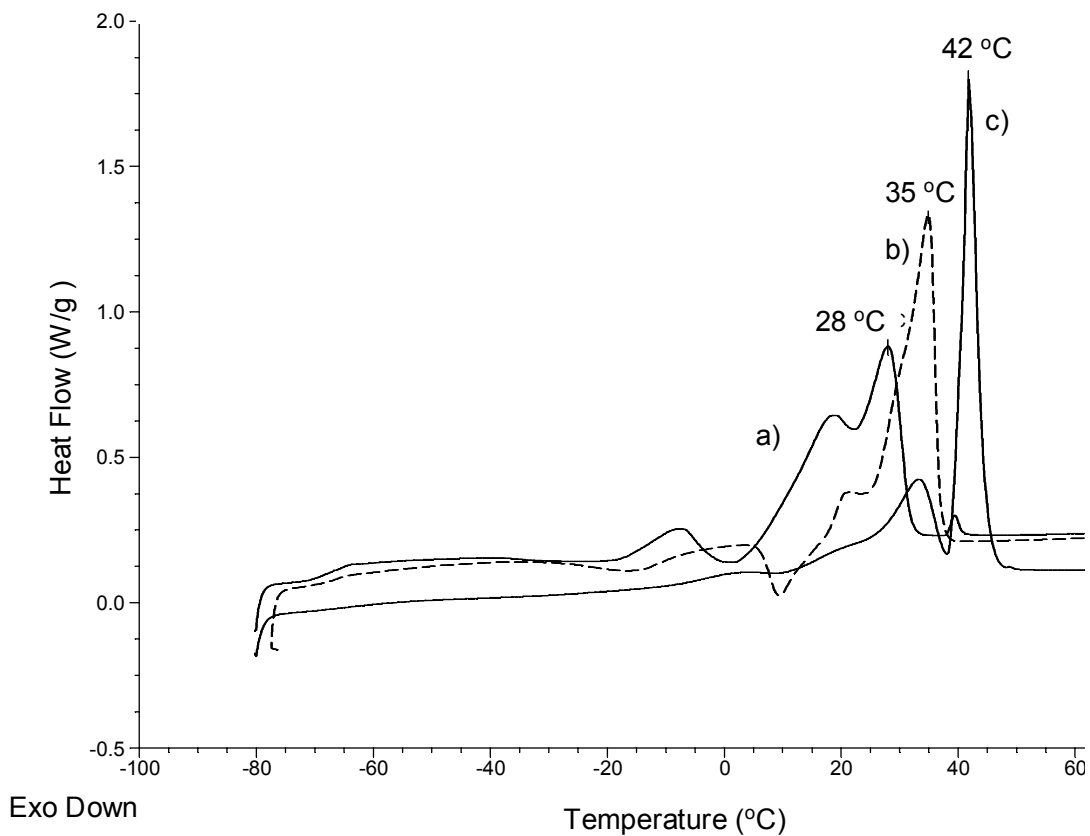


**Figure 7.6.** DSC of poly(trimethylene adipate) diol oligomers having molecular weight of a) 1000, b) 2000, and c) 4000 g/mol.

**Table 7.4.** Glass transition temperatures, melting point, and heat of fusion of poly(trimethylene adipate) diol oligomers

Poly(trimethylene succinate)	$T_g$ (°C)	$T_m$ (°C)	$T_c$ (°C)	Heat of Fusion (J/g)
1000 g/mol	-63	28	-14	55
2000 g/mol	-60	35	-11	56
4000 g/mol	-43	42	1	109

### 7.4.3 Network synthesis

Acetoacetate-functional oligomeric poly(trimethylene adipate) and poly(trimethylene succinate) precursors were reacted with neopentyl glycol diacrylate in the presence of the strong base catalyst DBU to form crosslinked networks (Scheme 7.3). The acetoacetate to acrylate molar ratio was 1.0 to 1.4 for all networks, with an acetoacetate functionality of  $f=1-2$  based on our earlier studies.<sup>23,24,42</sup> Acetoacetate-functional polyesters having molecular weights of 1000 to 4000 g/mol were reacted with NPGDA and high gel fractions were achieved for all networks (> 90%). As the molecular weight of the polyester precursor increased, lower gel fractions were obtained. The reduced crosslinking efficiency of the precursors with higher molecular weights was attributed to the reduced concentration of end groups and the formation of linear segments due to the mono-addition of AcAc methylene. Similar results have been observed for the Michael addition crosslinking of poly(propylene oxide) bisacetoacetate with NPGDA, during which the molecular weight of the poly(propylene oxide) based precursor increased from 1000 to 6000 g/mol.<sup>23</sup>

DSC revealed the thermal properties of the crosslinked poly(trimethylene succinate)s and poly(trimethylene adipate)s networks to investigate the influence of polyester molecular weight on the  $T_g$  and crystallinity of the networks. While all the polyester precursors were initially semicrystalline, the resulting networks were amorphous as a result of restricted segmental motion due to presence of crosslinking points. Networks synthesized from polyester precursors with molecular weights of 1000 and 2000 g/mol remained amorphous. However, the network synthesized from the precursor with 4000 g/mol slowly crystallized over time (Figure 7.6). The resulting

crosslinked film was semicrystalline and exhibited a melting point of 47 °C after two months. When the molecular weight of the polyester segment reached 4000 g/mol, even though in the crosslinked state, the polyester unit between the crosslink points was long enough to pack and form an ordered state. Conversely, polyester segment of 1000 to 2000 g/mol has restricted motion in the crosslinked state, which hinders packing of the polyester chain thereby preventing crystallization.

DSC analysis also showed that the glass transition temperature of the networks was dependent on the molecular weight of the polyester precursor. Specifically, the  $T_g$  of the networks decreased as the molecular weight of the poly(trimethylene succinate) and poly(trimethylene adipate) based precursors increased. The  $T_g$  of the networks increased from -51 to -31 °C as the molecular weight of the poly(trimethylene adipate) segment in the networks was decreased from 4000 to 1000g/mol (Figure 7.8). A similar trend was observed for the poly(trimethylene succinate) based networks, which was attributed to the difference in molecular weight between crosslink points. As one increases the molecular weight of the polyester precursor, the molecular weight between crosslink points of the corresponding network will presumably be higher, thereby producing less hindered segmental motion relating to reduced  $T_g$  values.

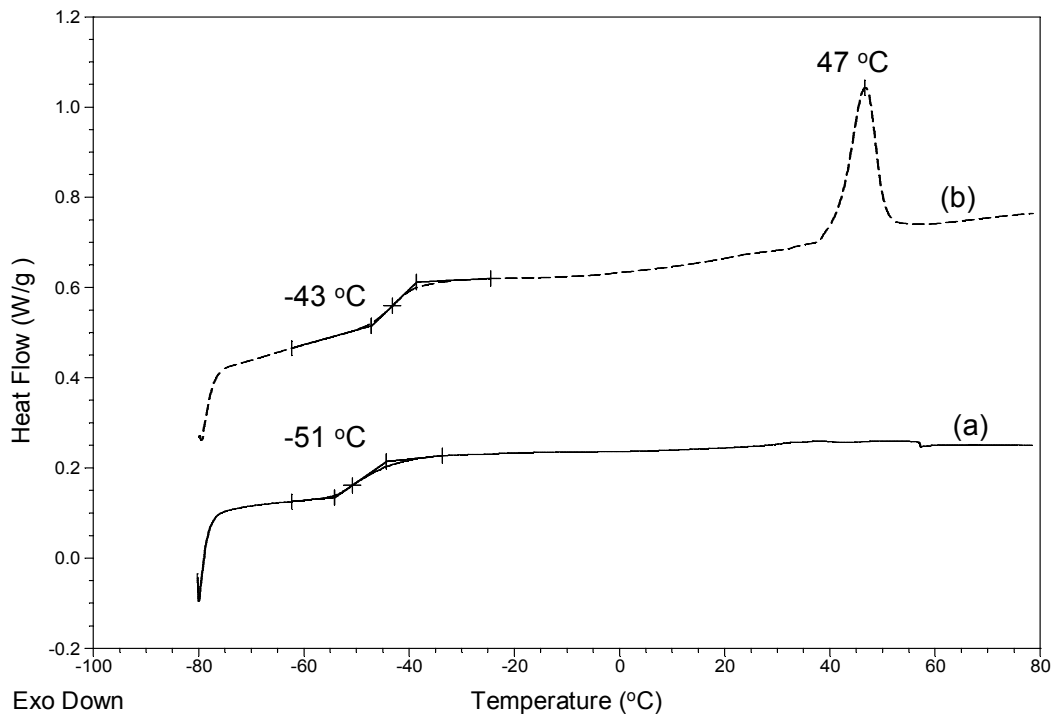


**Figure 7.7.** DSC analysis of networks synthesized from NPGDA and poly(trimethylene adipate) 4000 g/mol after a) a week and b) after two months.

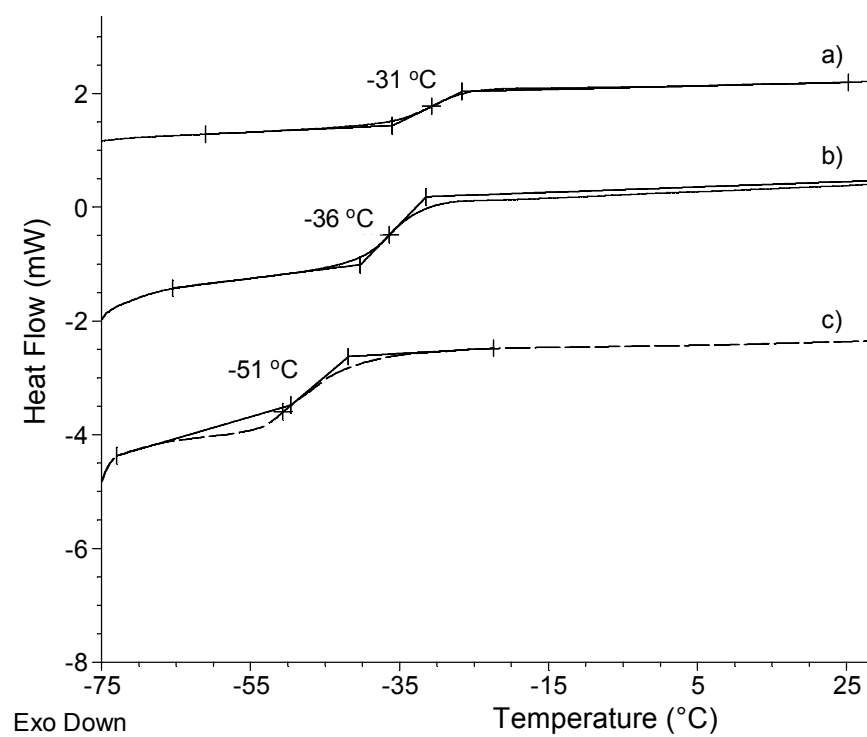


**Figure 7.8.** DSC comparison of poly(trimethylene adipate)-NPG networks

DMA was utilized to determine the influence of precursor molecular weight on the thermomechanical properties of the networks. Although all the networks were initially amorphous, after two months of storage, the network synthesized from the poly(trimethylene adipate) precursor with higher molecular weight (4000 g/mol) exhibited a crystalline phase (Figure 7.9). The DMA of this crosslinked poly(trimethylene adipate) exhibited melting transition at 45 °C, which is in good agreement with DSC analysis that confirmed the formation of crystallinity over time.

DMA analysis demonstrated a higher rubbery plateau modulus for the networks synthesized from polyesters with molecular weight of 1000 g/mol (Figure 7.10). This increase was attributed to increased crosslink density resulting from the shorter polyester segment between crosslink points. As expected, the plateau modulus of the networks decreased with increasing polyester precursor molecular weight. The comparison of the storage modulus at temperatures greater than 50 °C, indicated that, the modulus dropped more dramatically for the network synthesized from the 4000 g/mol precursor, suggesting that this network had a lower gel fraction and lower crosslink density than expected. This finding agrees with our earlier study,<sup>23</sup> which confirmed that as the molecular weight of an acetoacetate functionalized precursor increases, the concentration of functional end groups decrease, and the resulting networks feature reduced crosslink density.

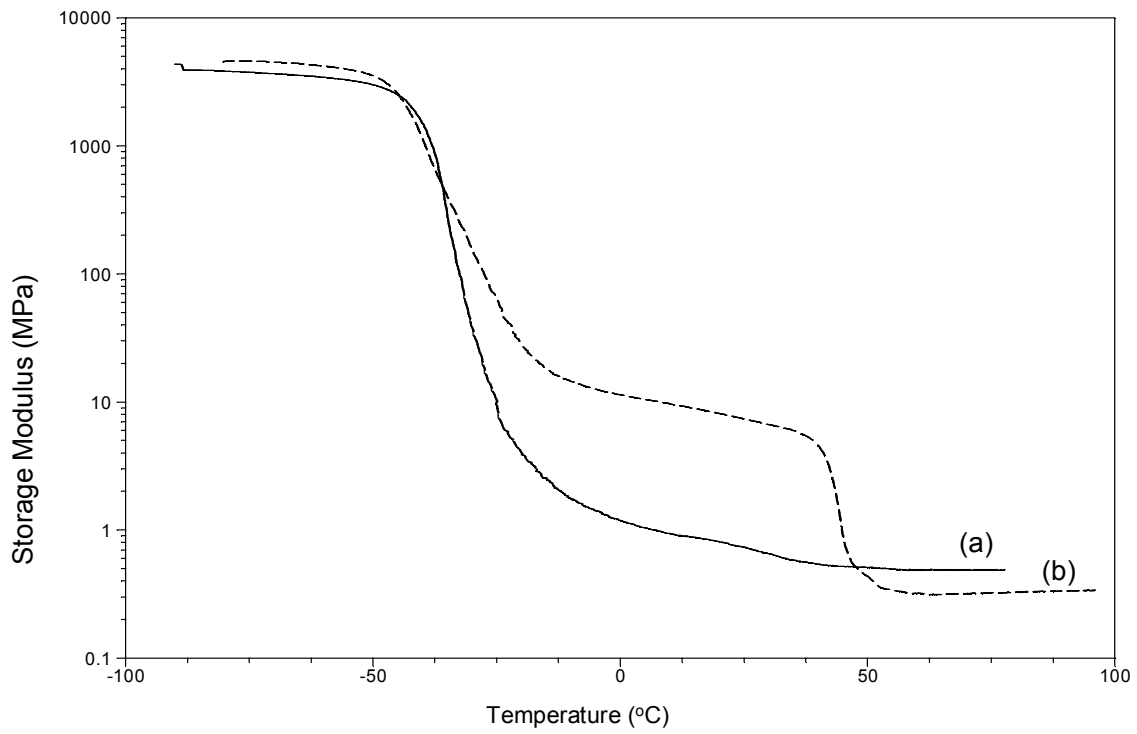


**Figure 7.9.** DMA of networks synthesized from NPGDA and poly(trimethylene adipate) 4000 g/mol after a) a week and b) after two months.

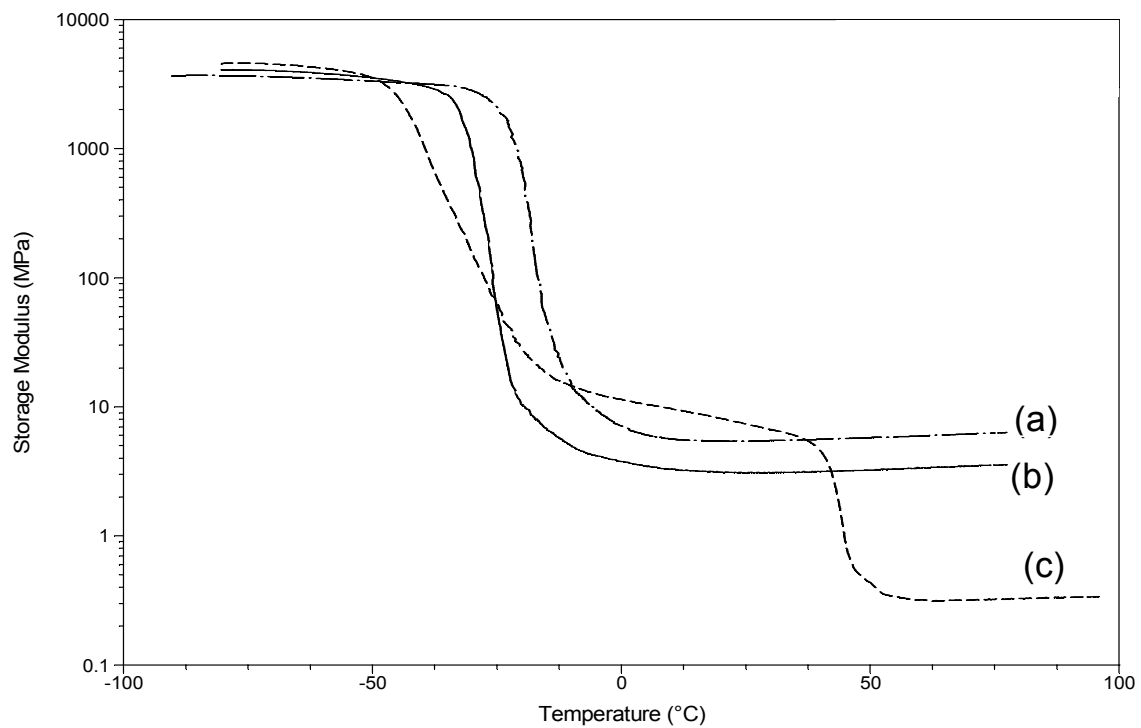


**Figure 7.10.** DMA of networks synthesized from NPGDA and poly(trimethylene adipate) a) 1000 b) 2000, and c) 4000 g/mol

## 7.5 Conclusions

In this study, Michael addition chemistry was utilized to synthesize biodegradable networks based on poly(trimethylene succinate) and poly(trimethylene adipate). Hydroxyl-terminated oligomeric polyesters were synthesized in the melt phase via polycondensation. The polyols were functionalized with acetoacetate groups which were confirmed using  $^1\text{H}$  NMR spectroscopy, MALDI-TOF analysis, and titration of end groups. Acetoacetate-functionalized precursors were subsequently reacted with neopentyl glycol diacrylate in the presence of an organic base at room temperature. The crosslinking reactions yielded networks with high gel contents ( $> 90\%$ ). The thermomechanical properties of the networks were analyzed to investigate the influence of molecular weight between crosslink points. The glass transition temperatures, crystallinities, rubbery plateau moduli, and gel fractions were dependent on the molecular weight of the polyester precursor. Specifically, as the molecular weight of the polyester bisacetoacetates changed, the  $T_g$ s of the networks ranged from  $-51$  to  $-31$   $^{\circ}\text{C}$  for the poly(trimethylene adipate) based networks, and from  $-30$  to  $-24$   $^{\circ}\text{C}$  for the poly(trimethylene succinate) based networks. DMA revealed that the rubber plateau modulus was dependent on the crosslink density, which was determined by the molecular weight of the precursor.

## 7.6 Acknowledgements

This material is based on work supported by Eastman Chemical Company. The author acknowledges Laurie Good and Prof. Judy Riffle for manuscript editing. The author acknowledges Kim Harich for MALDI-TOF MS analysis.

## 7.7 References

1. Hong, Y.; Ye, S. H.; Nieponice, A.; Soletti, L.; Vorp, D. A.; Wagner, W. R., *Biomaterials* **2009**, *30* (13), 2457-2467.
2. Chooprayoon, P.; Siripitayananon, J.; Molloy, R.; Bunkird, S.; Soywongsa, T.; Tariyawong, A. In *Processing, Mechanical Property Development and In Vitro Hydrolytic Degradation Studies of a Poly(L-lactide-co-epsilon-caprolactone) Monofilament Fibre for Potential Use as an Absorbable Surgical Suture*, 2008; pp 693-696.
3. Ueda, H.; Tabata, Y., *Adv. Drug Deliver. Rev* **2003**, *55* (4), 501-518.
4. Andrade, M. G. S.; Weissman, R.; Reis, S. R. A., *J. Mater. Sci-Mater. M.* **2006**, *17* (10), 949-961.
5. Amsden, B. G.; Misra, G.; Gu, F.; Younes, H. M., *Biomacromolecules* **2004**, *5* (6), 2479-2486.
6. Karikari, A. S.; Edwards, W. F.; Mecham, J. B.; Long, T. E., *Biomacromolecules* **2005**, *6* (5), 2866-2874.
7. Kim, E. K.; Bae, J. S.; Im, S. S.; Kim, B. C.; Han, Y. K., *J. Appl. Polym. Sci* **2001**, *80* (9), 1388-1394.
8. Karikari, A. S.; Mather, B. D.; Long, T. E., *Biomacromolecules* **2007**, *8* (1), 302-308.
9. Amsden, B., *Soft Matter*. **2007**, *3* (11), 1335-1348.
10. Cohn, D.; Salomon, A. F., *Biomaterials* **2005**, *26* (15), 2297-2305.
11. Venkatraman, S.; Boey, F.; Lao, L. L., *Prog. Polym. Sci.* **2008**, *33* (9), 853-874.
12. Nair, L. S.; Laurencin, C. T., *Prog. Polym. Sci.* **2007**, *32* (8-9), 762-798.
13. Okada, M., *Prog. Polym. Sci.* **2002**, *27* (1), 87-133.
14. Nguyen, J.; Steele, T. W. J.; Merkel, O.; Reul, R.; Kissel, T., *J. Control. Release* **2008**, *132* (3), 243-251.
15. Bikiaris, D. N.; Papageorgiou, G. Z.; Giliopoulos, D. J.; Stergiou, C. A., *Macromol. Biosci.* **2008**, *8* (8), 728-740.
16. West, J. L.; Hubbell, J. A., *Macromolecules* **1999**, *32* (1), 241-244.
17. McKee, M. G.; Unal, S.; Wilkes, G. L.; Long, T. E., *Prog. Polym. Sci.* **2005**, *30* (5), 507-539.
18. Amsden, B. G.; Tse, M. Y.; Turner, N. D.; Knight, D. K.; Pang, S. C., *Biomacromolecules* **2006**, *7* (1), 365-372.
19. Karikari, A. S.; Williams, S. R.; Heisey, C. L.; Rawlett, A. M.; Long, T. E., *Langmuir* **2006**, *22* (23), 9687-9693.
20. Fawcett, A. H.; Hania, M.; Lo, K. W.; Patty, A., *J. Polym. Sci. Pol. Chem.* **1994**, *32* (5), 815-827.
21. Mather, B. D.; Viswanathan, K.; Miller, K. M.; Long, T. E., *Prog. Polym. Sci.* **2006**, *31* (5), 487-531.
22. Kim, Y. B.; Kim, H. K.; Nishida, H.; Endo, T., *Macromol. Mater. Eng.* **2004**, *289* (10), 923-926.
23. Williams, S. R.; Mather, B. D.; Miller, K. M.; Long, T. E., *J. Polym. Sci. Pol. Chem.* **2007**, *45* (17), 4118-4128.
24. Williams, S. R.; Miller, K. M.; Long, T. E., *Prog. React. Kinet.* **2007**, *32* (4), 165-194.

25. Edgar, K. J.; Arnold, K. M.; Blount, W. W.; Lawniczak, J. E.; Lowman, D. W., *Macromolecules* **1995**, *28* (12), 4122-4128.
26. Geurink, P. J. A.; vanDalen, L.; vanderVen, L. G. J.; Lamping, R. R. In *Analytical aspects and film properties of two-pack acetoacetate functional latexes*, 20th International Conference in Organic Coatings Science and Technology, 1994; pp 73-78.
27. Metters, A.; Hubbell, J., *Biomacromolecules* **2005**, *6* (1), 290-301.
28. Xu, Y. X.; Xu, J.; Liu, D. H.; Guo, B. H.; Xie, X. M., *J. Appl. Polym. Sci* **2008**, *109* (3), 1881-1889.
29. Tserki, V.; Matzinos, P.; Pavlidou, E.; Panayiotou, C., *Polym. Degrad. Stabil.* **2006**, *91* (2), 377-384.
30. Lindblad, M. S.; Liu, Y.; Albertsson, A. C.; Ranucci, E.; Karlsson, S., Polymers from renewable resources. In *Degradable Aliphatic Polyesters*, Springer-Verlag Berlin: Berlin, 2002; Vol. 157, pp 139-161.
31. Bikiaris, D. N.; Achilias, D. S., *Polymer* **2006**, *47* (13), 4851-4860.
32. Bikiaris, D. N.; Achilias, D. S., *Polymer* **2008**, *49* (17), 3677-3685.
33. Papageorgiou, G. Z.; Bikiaris, D. N., *Polymer* **2005**, *46* (26), 12081-12092.
34. Liu, Y.; Ranucci, E.; Lindblad, M. S.; Albertsson, A. C., *J. Bioact. Compat. Polym.* **2002**, *17* (3), 209-219.
35. Achilias, D. S.; Bikiaris, D. N. In *Synthesis and biodegradation of three poly(alkylene succinate)s: mathematical modelling of the esterification reaction and the enzymatic hydrolysis*, 1st International Conference on Environmental Toxicology, 2006; pp 309-318.
36. Bikiaris, D. N.; Papageorgiou, G. Z.; Achilias, D. S., *Polym. Degrad. Stabil.* **2006**, *91* (1), 31-43.
37. Haas, T.; Jaeger, B.; Weber, R.; Mitchell, S. F.; King, C. F., *Appl. Catal. A-Gen.* **2005**, *280* (1), 83-88.
38. Noordover, B. A. J.; van Staalduinen, V. G.; Duchateau, R.; Koning, C. E.; van Benthem, R.; Mak, M.; Heise, A.; Frissen, A. E.; van Haveren, J., *Biomacromolecules* **2006**, *7* (12), 3406-3416.
39. Coutinho, D. F.; Pashkuleva, I. H.; Alves, C. M.; Marques, A. P.; Neves, N. M.; Reis, R. L., *Biomacromolecules* **2008**, *9* (4), 1139-1145.
40. Czech, Z.; Wojciechowicz, M., *Eur. Polym. J.* **2006**, *42* (9), 2153-2160.
41. McNeill, I. C.; Liggat, J. J., *Polym. Degrad. Stabil.* **1992**, *37* (1), 25-32.
42. Mather, B. D.; Williams, S. R.; Long, T. E., *Macromol. Chem.Physic.* **2007**, *208* (18), 1949-1955.

# Chapter 8: Crosslinking of Aliphatic Low- $T_g$ Polyesters for Adhesive and Coating Applications

## 8.1 Abstract

In this study, crosslinking of aliphatic polyesters having low glass transition temperatures ( $T_g$ s) was investigated to improve cohesive strength for pressure sensitive adhesive (PSA) applications. Oligomeric low- $T_g$  polyesters with telechelic hydroxyl functionality were synthesized from melt polycondensation of 1,4-cyclohexane dicarboxylic acid (CHDA) and diethylene glycol (DEG) in the absence of catalyst. The telechelic hydroxyl functionality of the polyester polyols was derivatized with acetoacetate groups and subsequently reacted with neopentyl glycol diacrylate in the presence of an organic base at ambient temperature. Networks having different levels of gel fractions were investigated to probe the influence of degree of crosslinking on thermomechanical and adhesive properties of low- $T_g$  polyesters. The influence of catalyst concentration on the efficiency of crosslinking and gelation time was investigated using measurement of loss and storage modulus during crosslinking. Monitoring the crosslinking reactions using rheological measurements revealed the significant influence of catalyst levels on crosslinking time.

## 8.1 Introduction

Crosslinking of adhesives have been utilized to improve adhesive performance of PSAs for several applications ranging from microelectronics to bioadhesives.<sup>1-3</sup> Literature<sup>1-5</sup> reported a detailed investigation on incorporation of low levels of chemical crosslinking to improve cohesive strength of adhesives. Photocrosslinking of polymers

has been investigated extensively for PSA applications.<sup>1,2,6-8</sup> Moreover, metal chelates have been utilized for crosslinking polymers to improve cohesive strength.<sup>7</sup>

Bioadhesives or tissue adhesives received significant attention as alternatives to suturing and stapling in biomedical applications.<sup>9-11</sup> Bioadhesives are utilized to bind tissues and provide a tight closure until the wound is healed.<sup>12</sup> In the literature,<sup>10,13</sup> poly(alkyl cyanoacrylate)s have been widely exploited as surgical adhesives. Poly(alkyl cyanoacrylate)s<sup>10</sup> are capable of adhering on several polar substrates including tissues and skin.<sup>14</sup> They have been reported as the strongest tissue adhesives; however, the applications are restricted to external use due to the toxicity of the monomer and release of heat during the polymerization. Conversely, long-chain alkyl cyanoacrylates such as n-butylcyanoacrylate and octylcyanoacrylate are non-toxic promising alternatives that have been used for topical skin use in commercial bioadhesives such as Indermil<sup>®</sup>, Liquiband<sup>®</sup>, and Dermabond<sup>®</sup>.<sup>10,13</sup> In addition to poly(alkylcyanoacrylate)s, low-T<sub>g</sub> polyester based adhesives offer potential to develop new alternative bioadhesives due their biocompatibility, biodegradability, and non-toxicity. Moreover, biodegradable and biocompatible tissue adhesives based on methacrylate and acrylate functional biodegradable polyesters have attracted attention to overcome the limitations associated with cyanoacrylates. *In-situ* photo-polymerizable poly(lactide) copolymers<sup>9</sup> were reported as biodegradable and biocompatible bioadhesives.<sup>11,15</sup> Young et al.<sup>9</sup> demonstrated synthesis of adhesives from poly(lactic acid) and poly(propylene glycol) based ABA triblocks with controlled drug release property. Several literature studies<sup>11,16</sup> reported synthesis of bioadhesives from UV-curable branched oligomers consisting of a core molecule and biodegradable arms.

PSA applications require balanced viscous and elastic properties to attain optimum adhesive performance. For crosslinked PSAs, the degree of crosslinking determines the balance between the adhesive and cohesive strength.<sup>1</sup> Therefore, controlling the degree of crosslinking is essential to attain high shear strength while maintaining the tack and peel strength. Crosslinking of self-adhesive polymers having low viscosity results in improved adhesion.<sup>3,17</sup> Moreover, introduction of different levels of crosslinking using patterned UV-curing permits generation of adhesive coatings having different zones of adhesive and cohesive properties.<sup>18</sup>

Our earlier studies demonstrated synthesis of linear and long-chain branched all-aliphatic low- $T_g$  polyesters from melt polycondensation of DMCD and DEG.<sup>19</sup> These polyesters exhibited fine tack and peel properties for room temperature PSA applications. However, the cohesive strength was inadequate for conventional pressure sensitive applications. The low cohesive strength was attributed to molecular weights of these polyesters which were lower compared to acrylic based adhesives that have very high molecular weights.<sup>20</sup> In this study, Michael addition chemistry was utilized as an alternative route to UV-curing to attain crosslinking and improve cohesive strength of low- $T_g$  oligomers. In the literature,<sup>21-24</sup> Michael addition reaction was utilized in several studies to synthesize covalently crosslinked polymer networks under mild conditions. Moreover, Michael addition was utilized in synthesis of high performance coatings and laminates.<sup>25,26</sup> This reaction benefits from absence of solvents, mild reaction conditions, and non-toxic by-products.<sup>22</sup> In this study, Michael addition chemistry was utilized to achieve different levels of crosslinking in low- $T_g$  polyesters to enhance cohesive strength and adhesive properties. Oligomeric low- $T_g$  polyesters were synthesized in comparison

to previously synthesized linear<sup>19</sup> and long-chain branched<sup>27</sup> low- $T_g$  polyesters having higher molecular weights. Incorporation of different levels of crosslinking was targeted to probe the efficiency of crosslinking and its influence on the thermal properties.

## 8.3 Experimental

### 8.3.1 Materials

Diethylene glycol ( $\geq 99\%$ ), neopentylglycol diacrylate, *tert*-butyl acetoacetate (*t*-BAA, 98%), 1,8-diazabicyclo[5.4.0]undec-7-ene (DBU, 98%), 0.1 N KOH in methanol, acetic anhydride ( $\geq 99\%$ ), pyridine ( $\geq 99\%$ ), and tetrahydrofuran (THF) were purchased from Aldrich. Eastman Chemical Company kindly provided cyclohexane dicarboxylic acid (60/40 *cis/trans*, CHDA) monomer. All the chemicals were used as received without further purification.

### 8.3.2 Characterization

Molecular weight was determined at 40 °C in THF (HPLC grade) using a Waters size exclusion chromatograph (SEC) equipped with 3 in-line PLgel 5  $\mu\text{m}$  MIXED-C columns with an autosampler, a 410 RI detector and an in-line Wyatt Technologies miniDawn multiple angle laser light scattering (MALLS) detector. <sup>1</sup>H NMR spectroscopic analyses were performed on a Varian Unity 400 spectrometer at 400 MHz in CDCl<sub>3</sub>. Thermal analysis using a TA Instruments DSC Q-100 determined thermal transition temperatures at a heating rate of 10 °C/min under nitrogen. All reported values were obtained from a second heating cycle. The hydroxyl end-functionality of the polyols was quantified using base titration. The polyester polyols were dissolved in a solution of acetic anhydride and pyridine (1:3 v:v) and stirred overnight at room temperature. Subsequently, 10 mL of distilled water and 10 mL of pyridine were added

and allowed to react for an additional 30 min. All the samples were titrated using 0.1 N KOH solution and phenolphthalein as the indicator. Number average molecular weights of the polyester polyols were calculated from the base titration of the hydroxyl end groups.

Gel fractions of the networks were determined gravimetrically from Soxhlet extraction of the networks in refluxing THF for 3 h. The samples were dried under reduced pressure at ambient temperature. Dynamic mechanical analysis was performed using a TA instruments Q-800 DMA under nitrogen at a heating rate of 3 °C/min at 1 Hz frequency in film-tension mode.

### **8.3.3 Synthesis of oligomeric low- $T_g$ polyester polyols**

Oligomeric low- $T_g$  polyester polyols were synthesized from melt polycondensation of CHDA and DEG in the absence of catalysts. CHDA (14.61 g, 100 mmol) and 50 mol% excess diethylene glycol (11.41 g, 150 mmol) were charged to a 100-mL, two-necked round-bottomed flask. The melt polycondensation set-up was equipped with a metal bath, mechanical stirrer, nitrogen inlet, and condenser. The flask was degassed three times using vacuum and nitrogen prior to the reaction. The reaction flask was heated to 200 °C and the reaction proceeded under nitrogen atmosphere for 18 h. The temperature was raised to 220 °C over 3 h and vacuum (0.1 to 0.2 mm Hg) was gradually applied for 2 h at 275 °C. The amount of water produced from the direct esterification of the diacid and diol was measured throughout the reaction. Reaction progress was monitored using base titration of the aliquots. The acid numbers of the intermediate reaction products were determined from titration of acid end groups with KOH. The polymerization was stopped when the amount of water collected in the

receiving flask reached the theoretical amount. In addition, oligomeric low- $T_g$  polyesters having different molecular weights of 1200, 2600, and 5000 g/mol were synthesized from polycondensation of CHDA with 10, 20, and 40 mol% excess DEG, respectively. All the products were characterized without further purification.

#### **8.3.4 Acetoacetate functionalization of oligomeric low- $T_g$ polyesters**

Oligomeric low- $T_g$  polyester polyols were functionalized with bisacetoacetate groups using transesterification of hydroxyl groups with *tert*-butyl acetoacetate in the bulk, following the procedure reported previously by our research group.<sup>21,24</sup> Oligomeric polyester polyols were reacted with 50 mol% excess *tert*-butyl acetoacetate. The reagents were charged to a 100-mL, round-bottomed flask, sealed with a rubber septum, and flushed with nitrogen prior to the reaction. The flask was heated at 150 °C for 3 h using a silicon oil bath. The byproduct, *tert*-butanol and excess *tert*-butyl acetoacetate were removed under reduced pressure. Additional *tert*-butyl acetoacetate was added and the flask was heated for an additional 3 h at 150 °C. Reaction byproducts and excess *tert*-butyl acetoacetate were removed under reduced pressure (0.1 mmHg) at 150 °C for 1 h. The products were dried under reduced pressure overnight before thermal analysis. The acetoacetate-functionalized low- $T_g$  polyesters were characterized using  $^1\text{H}$  NMR spectroscopy.

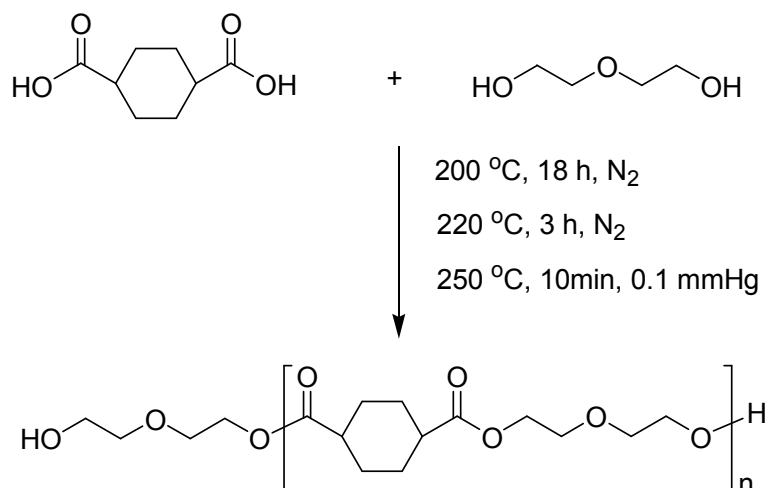
#### **8.3.5 Synthesis of crosslinked networks**

Acetoacetate-functionalized oligomeric low- $T_g$  polyester was reacted with neopentylglycol diacrylate in the presence of a base catalyst. Acetoacetate-functionalized polyester (1 mmol, 1.2 g) and neopentylglycol diacrylate (1.4 mmol, 0.24 g) were added to a sample vial and mixed to obtain a homogeneous blend. Low viscosity of the low- $T_g$

polyester precursor allowed synthesis of crosslinked networks in the absence of solvents. An organic base catalyst, DBU (0.05 wt% relative to bisacac precursor), was added and mixed at room temperature. The mixture was transferred to a Teflon<sup>TM</sup> mold and allowed to cure at ambient temperature. The crosslinked samples were stored under vacuum overnight before thermal analysis. Networks having various levels of crosslinking were synthesized from crosslinking of acetoacetate-functionalized polyesters in the presence of different levels of catalyst and NPGDA. The crosslinking reactions were conducted in the presence of 0.025, 0.050, and 0.075 wt% DBU to probe the influence of catalyst levels on gel time and the degree of crosslinking.

## **8.4 Results and Discussion**

Oligomeric low- $T_g$  polyester polyols were synthesized from direct esterification of CHDA and DEG in the melt phase in the absence of titanium catalyst (Scheme 8.1). Melt polycondensation method permitted synthesis of low- $T_g$  polyesters in the absence of solvents. The products exhibited  $T_g$ s well below the room temperature and were readily removed from the reaction flask.



**Scheme 8.1.** Synthesis of oligomeric low- $T_g$  polyester polyol from polycondensation of CHDA and DEG.

As shown in Figure 8.1,  $^1\text{H}$  NMR spectrum of the polyester polyol exhibited peaks at  $\delta=2.8\text{-}1.5$  ppm region corresponding to the cycloaliphatic protons of the cyclohexane in the repeating unit. The calculation revealed that the ratio of *cis* to *trans* isomer did not change upon polycondensation under applied reaction conditions. The peaks at  $\delta=3.7$  and  $3.6$  ppm corresponded to the methylene protons in the DEG unit of the repeating unit and the protons of the methylenes at the end groups adjacent to the hydroxyl group.

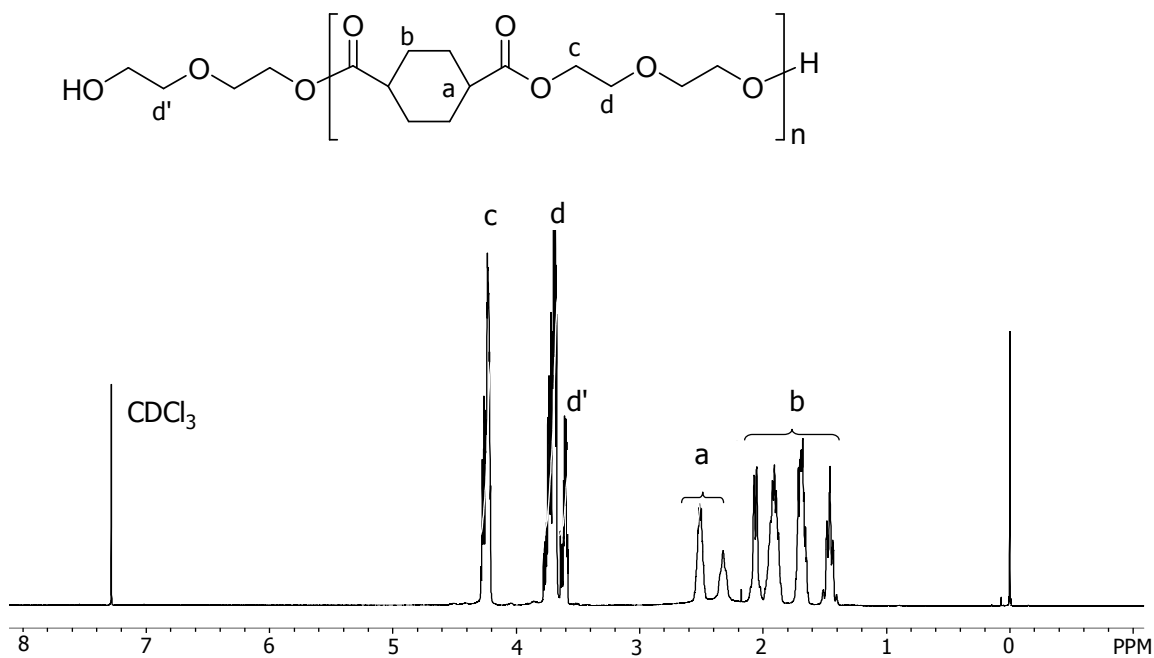


**Figure 8.1.**  $^1\text{H}$  NMR spectroscopy comparison of polyester polyol synthesized from polycondensation of CHDA and DEG.

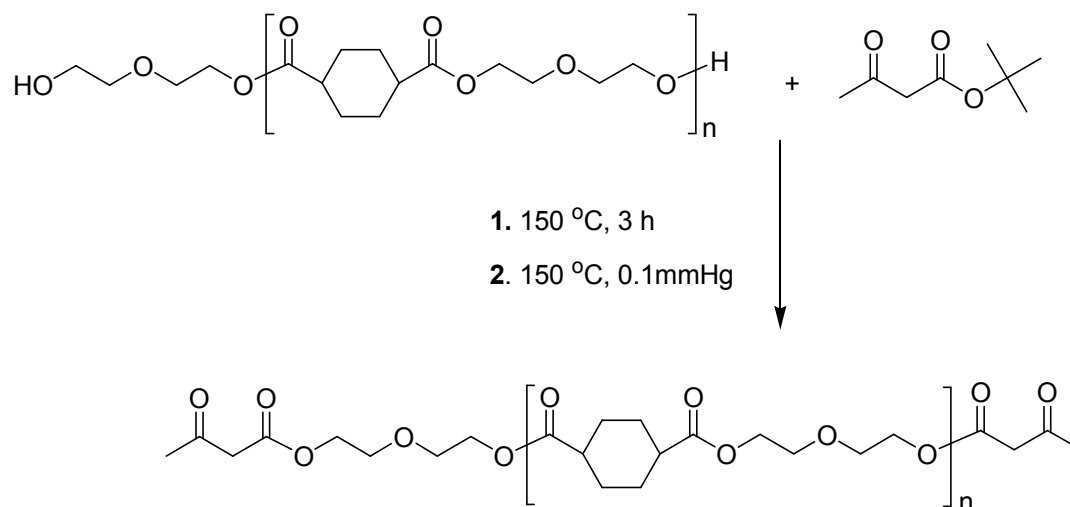
Oligomeric low- $T_g$  polyesters having different molecular weights were synthesized using stoichiometric imbalance of the diacid and the diol monomers. The diacid monomer, CHDA, was reacted with 10, 20, and 50 mol% excess DEG to attain oligomeric polyester polyols having theoretical molecular weights of 5000, 2600, and 1200 g/mol, respectively. The progress of the reaction was monitored following the amount of water produced from the reaction. As summarized in Table 8.1, the molecular weights of the oligomers are close to the theoretical targeted molecular weights that were calculated based on the stoichiometric imbalance. These results showed that the targeted molecular weights were achieved. Characterization of thermal properties using DSC indicated that  $T_g$ s of the oligomers increased with increased molecular weight.

**Table 8.1.** Summary of molecular weight and thermal characterization of low- $T_g$  polyols.

<b>CHDA:DEG mol ratio</b>	<b>Targeted molecular weight (g/mol)</b>	<b><sup>a</sup>M<sub>w</sub> (g/mol)</b>	<b><sup>a</sup>M<sub>n</sub> (g/mol)</b>	<b><sup>a</sup>PDI</b>	<b><sup>b</sup>T<sub>g</sub> (°C)</b>
1:1.5	1,210	2,500	1,600	1.56	-43
1:1.2	2,660	5,100	3,200	1.60	-30
1:1.1	5,082	16,000	7,700	2.08	-19

<sup>a</sup>SEC RI detector <sup>b</sup>DSC

Low- $T_g$  polyester oligomers were functionalized with acetoacetate groups in the absence of any catalyst and solvents (Scheme 8.2).  $^1\text{H}$  NMR analysis did not indicate any degradation or scission of the backbone which may arise from side reactions or any possible attack to the ester functionality along the backbone during transacetoacetylation reaction. Figure 8.2 demonstrates  $^1\text{H}$  NMR spectra of the oligomeric polyester polyol before and after transacetoacetylation. The peaks at  $\delta=2.8\text{-}1.5$  ppm region indicated the cycloaliphatic protons in the cyclohexane dicarboxylate unit. Integrations of the peaks corresponding to the *cis* and *trans* cyclohexanedicarboxylate isomers indicated that the *cis* to *trans* ratio did not change after polycondensation. As discussed earlier,  $^1\text{H}$  NMR spectra of the polyol indicated the presence of the peak at  $\delta=3.62$  ppm corresponding to the methylene adjacent to the hydroxyl end group. Comparison of the two spectra showed that this peak disappeared as the hydroxyl groups were converted to acetoacetate functionality.



**Scheme 8.2.** Acetoacetate functionalization of low- $T_g$  polyols.

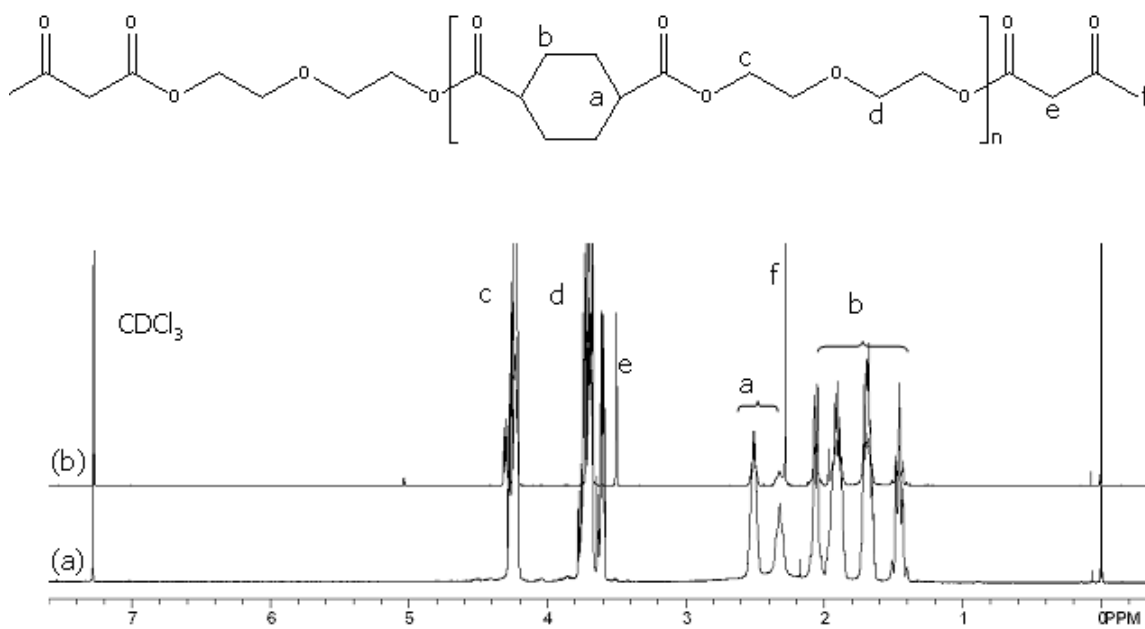


**Figure 8.2.**  $^1\text{H}$  NMR spectra of polyester polyol a) before and b) after transacetoacetylation.

In addition to characterization of chemical composition it is critical to characterize the molecular weight of the polyester oligomers upon transacetoacetylation. Comparison of SEC refractive index traces of the low- $T_g$  polyesters polyol before and after acetoacetate functionalization indicated that the molecular weight of the polyester changed slightly after transacetoacetylation due to added mass. As shown in Figure 8.3, the refractive index traces of the oligomeric low- $T_g$  polyesters before and after transacetoacetylation are similar.

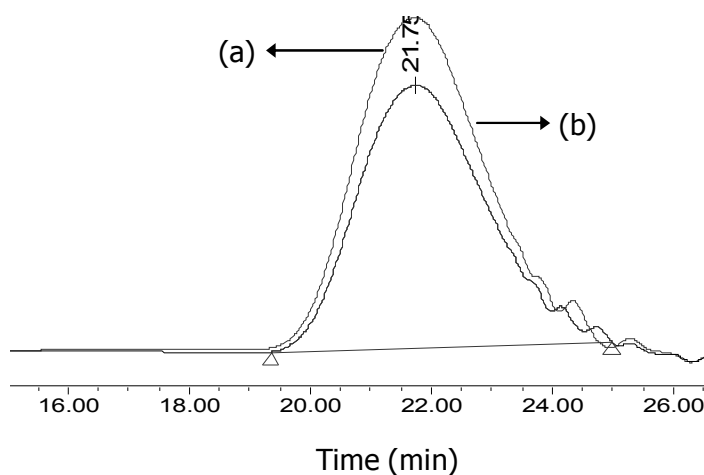
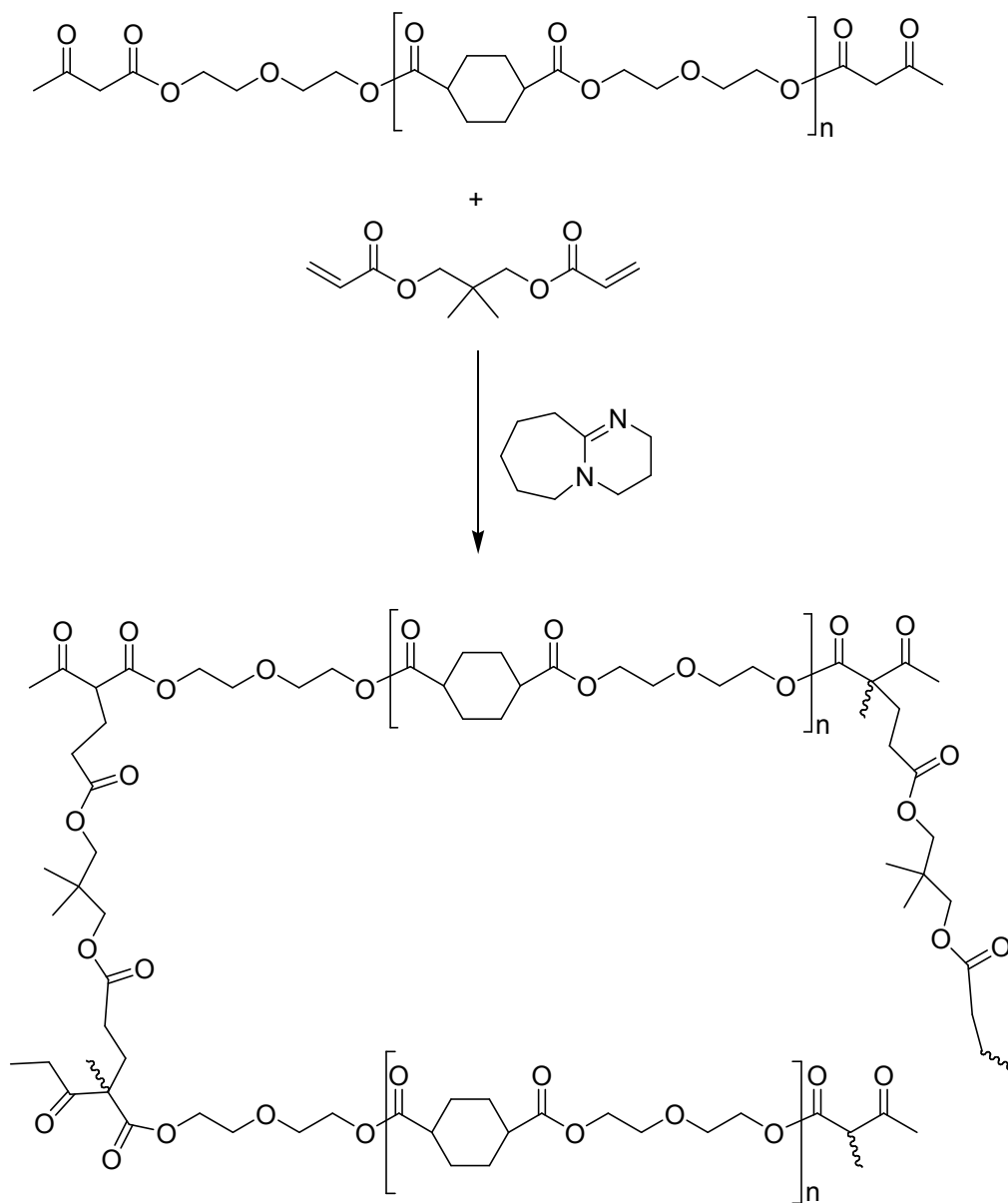


**Figure 8.3.** SEC RI detector traces of polyester polyol a) after and b) before transacetoacetylation.

Acetoacetate-functionalized oligomers were successfully crosslinked with neopentyl glycol diacrylate (Scheme 8.3). The molar ratio of acetoacetate to acrylate was 1.4 to 1.0 based on our earlier studies. Gel fraction analysis was conducted to measure the effectiveness of oligomer incorporation into the networks. High gel fractions were obtained for all networks synthesized using 0.05 wt% DBU. Moreover, crosslinked networks with varying gel fractions were obtained using different levels of DBU. Reaction of acetoacetate-functionalized polyester with NPGDA using 0.05, 0.025, and 0.10 wt% DBU produced networks with gel fractions of 81, 61, and 21%, respectively.

In addition, the polyester precursor and NPGDA were reacted at a mol ratio of 1.0:1.2 as opposed to 1.0:1.4 in order to probe the influence of Michael donor and acceptor ratio on the resulting gel fractions.



**Scheme 8.3.** Crosslinking of acetoacetate-functionalized low- $T_g$  polyester with NPGDA in the presence of DBU.

Thermal properties of the networks were characterized using DSC to investigate the influence of gel fraction on  $T_g$  of the networks. DSC analysis indicated that all the

networks were amorphous. The glass transition of the networks increased from -27 to -9 °C as the gel fraction increased from 10 to 80% (Figure 8.4). Moreover, the plot of  $T_g$  versus gel fraction indicated that the  $T_g$  of the networks increased from -27 to -9 °C as the gel fraction increased from 10 to 80%. The increase in gel fraction increased the  $T_g$ , and as the gel fraction increased further a significant enhancement was observed. These results showed that controlling the degree of crosslinking enables tailoring the  $T_g$ s of these crosslinked low- $T_g$  networks as different levels of catalysts are utilized in the reaction. These results are promising in terms of demonstrating the ability to control the degree of crosslinking and glass transition of the resulting low- $T_g$  polyester with various concentrations of crosslinking sites.

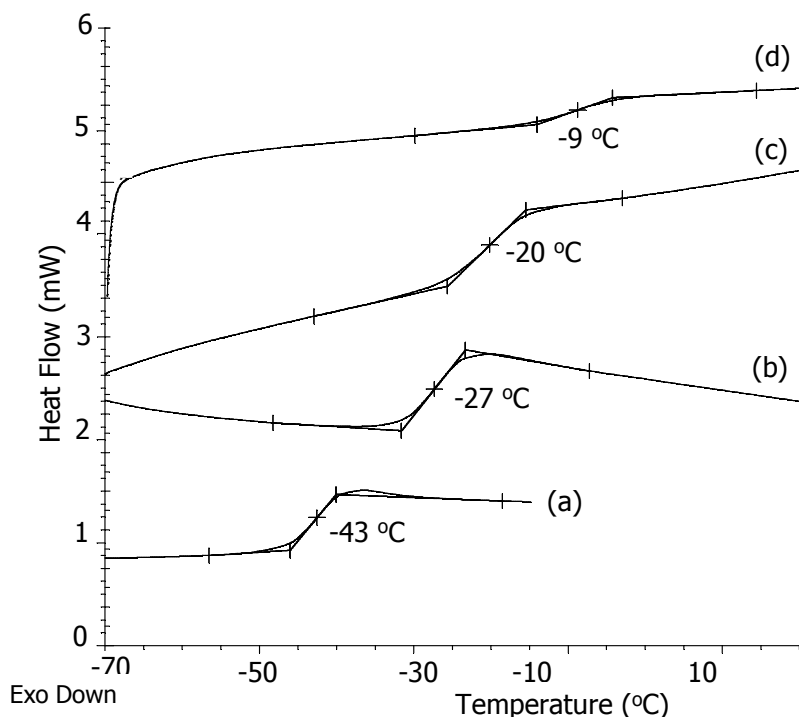


**Figure 8.4.** DSC analysis of (a) polyester precursor and the networks synthesized from NPGDA and acetoacetate-functionalized low- $T_g$  polyester having gel fractions of (b) 10, c) 60, and d) 80%.

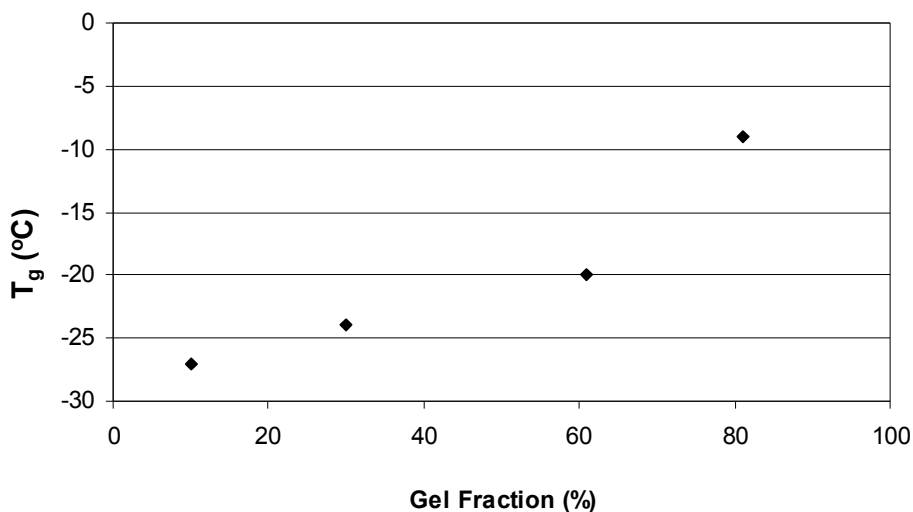


**Figure 8.5.** Dependence of  $T_g$  of the networks on gel fraction.

The influence of catalyst level on crosslinking time was evaluated using rheological analysis. Storage and loss modulus was measured as a function of time and the gel times were determined from the crossover point of  $G'$  and  $G''$ . Gel times were reported as the time when the  $G'$  was equal to  $G''$  (Figure 8.6). Michael addition reactions of acetoacetate-functionalized low- $T_g$  polyester with NPGDA were conducted using various catalyst concentrations and the reactions were monitored using melt rheological analysis. The acetoacetate functionalized polyester, NPGDA, and the catalyst was mixed and placed between parallel plates of the rheometer and the storage and loss modulus. Figure 8.5 illustrates time sweep rheological analysis of the crosslinking using 0.075 wt% DBU. The gel time was determined as 6, 19, and 180 min for the crosslinking reactions that utilized 0.075, 0.05, and 0.25 wt% DBU, respectively. Significantly, longer gel time was observed for the network synthesized using lowest level of DBU catalyst.

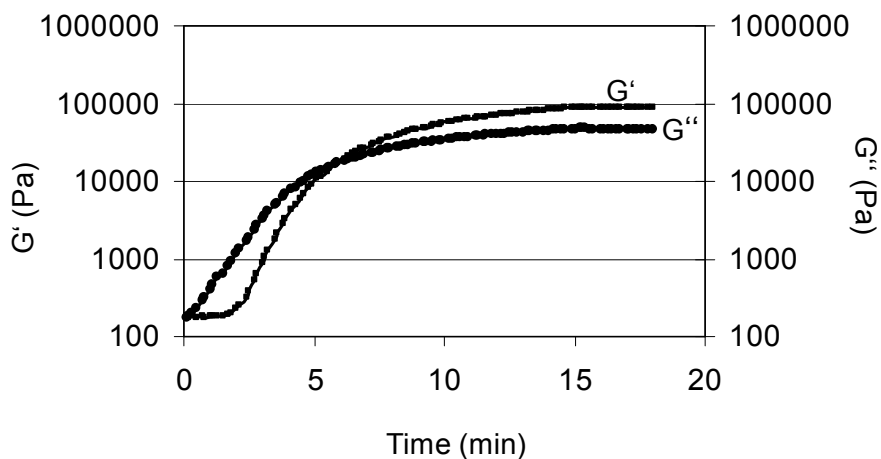


**Figure 8.6.** Rheological analysis of crosslinking at using 0.075 w% DBU.

In addition, the increase in viscosity during crosslinking reaction was measured as a function of reaction time. Figure 8.7 demonstrates the change in viscosity as a function of reaction time. Crosslinking of acetoacetate functional low- $T_g$  polyester with NPGDA was conducted using 0.025, 0.05, and 0.75 wt% DBU. As expected, the viscosity increased upon crosslinking. However, depending on the level of DBU the viscosity increased at different rates. For crosslinking reactions using 0.025 wt% DBU, the viscosity increased slowly over 180 min. The results revealed that the influence of catalyst should be taken into consideration for crosslinking low- $T_g$  polyesters for adhesive and coating applications.

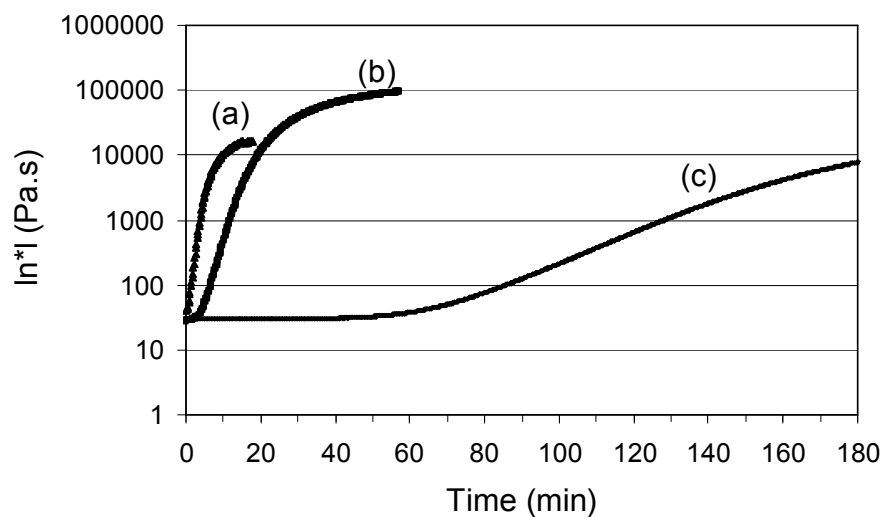


**Figure 8.7.** Rheological analysis of crosslinking at 40 °C using a) 0.75, b) 0.05, and c) 0.025 wt% DBU catalyst.

## 8.5 Conclusions

In this study, Michael addition reaction was utilized to crosslink low- $T_g$  polyols for adhesive applications. Hydroxyl-terminated low- $T_g$  oligomeric polyesters were synthesized in the melt phase using the melt polycondensation method. Acetoacetate-functionalized precursors were subsequently reacted with neopentyl glycol diacrylate in the presence of an organic base at room temperature. The crosslinking reactions yielded networks with varying from 10 to 80% gel fractions depending on the concentration of basic catalyst. Thermal analysis indicated that changing the gel fraction of the networks allows tailoring the  $T_g$ s ranging from -27 to -9 °C. The crosslinking reaction was monitored following measurement of storage and loss modulus using rheological analysis. The rheological analyses revealed that gel time changed from 180 to 6 min depending on the concentration of the basic catalyst. The ability to control the  $T_g$  and the gel fraction of the networks offered potential for adhesive and coating applications.

## 8.6 Acknowledgements

This material was based upon work supported by Eastman Chemical Company.

## 8.7 References

1. Kajtna, J.; Golob, J.; Krajnc, M., *Int. J. Adhes. Adhes.* **2009**, *29* (2), 186-194.
2. Ferreira, P.; Coelho, J. F. J.; Gil, M. H., *Int. J. Pharm.* **2008**, *352* (1-2), 172-181.
3. Benedek, I., *Pressure-sensitive Adhesives and Applications*. Marcel Dekker, 1996.
4. Saiki, N.; Yamazaki, O.; Ebe, K., *J. Appl. Polym. Sci.* **2008**, *108* (2), 1178-1183.
5. Czech, Z.; Goracy, K., *Polimery* **2005**, *50* (10), 762-764.
6. Do, H. S.; Kim, S.E.; Kim H.J., *Preparation and characterization of UV-crosslinkable pressure-sensitive adhesives in adhesion* Wiley-VCH, Weinheim, 2005.
7. Czech, Z.; Wojciechowicz, M., *Eur. Polym. J.* **2006**, *42* (9), 2153-2160.
8. Kim, J. K.; Kim, W. H.; Lee, D. H., *Polymer* **2002**, *43* (18), 5005-5010.
9. Young, A. M.; Ho, S. M., *J. Control. Release* **2008**, *127* (2), 162-172.
10. Vauthier, C.; Dubernet, C.; Fattal, E.; Pinto-Alphandary, H.; Couvreur, P., *Adv. Drug Deliv. Rev.* **2003**, *55* (4), 519-548.
11. Cohn, D.; Lando, G., *Biomaterials* **2004**, *25* (27), 5875-5884.
12. Kao, F. J.; Manivannan, G.; Sawan, S. P., *J. Biomed. Mater. Res.* **1997**, *38* (3), 191-196.
13. Katti, D.; Krishnamurti, N., *J. Appl. Polym. Sci.* **1999**, *74* (2), 336-344.
14. Ellman, P. I.; Reece, T. B.; Maxey, T. S.; Tache-Leon, C.; Taylor, J. L.; Spinosa, D. J.; Pinerros-Fernandez, A. C.; Rodeheaver, G. T.; Kern, J. A., *J. Surg. Res.* **2005**, *125* (2), 161-167.
15. Viljanmaa, M.; Sodergard, A.; Tormala, P., *Int. J. Adhes. Adhes.* **2002**, *22* (3), 219-226.
16. Karikari, A. S.; Edwards, W. F.; Mecham, J. B.; Long, T. E., *Biomacromolecules* **2005**, *6* (5), 2866-2874.
17. Czech, Z., *Int. J. Adhes. Adhes.* **2007**, *27* (3), 195-199.
18. Czech, Z.; Gsiorowska, M.; Soroka, J., *J. Appl. Polym. Sci.* **2007**, *106* (1), 558-561.
19. Ozturk, G. I. P., A.J.; Long, T.E., *J. Adhesion* **2009**, *In Press*.
20. Gower, M. D.; Shanks, R. A., *Macromol. Chem. Physic.* **2005**, *206* (10), 1015-1027.
21. Mather, B. D.; Miller, K. M.; Long, T. E., *Macromol. Chem. Physic.* **2006**, *207* (15), 1324-1333.
22. Mather, B. D.; Viswanathan, K.; Miller, K. M.; Long, T. E., *Prog. Polym. Sci.* **2006**, *31* (5), 487-531.
23. Mather, B. D.; Williams, S. R.; Long, T. E., *Macromol. Chem. Physic.* **2007**, *208* (18), 1949-1955.
24. Williams, S. R.; Mather, B. D.; Miller, K. M.; Long, T. E., *J. Pol. Sci. Pol. Chem.* **2007**, *45* (17), 4118-4128.
25. Narayan, R.; Raju, K., *Prog. Org. Coat.* **2002**, *45* (1), 59-67.

26. Edgar, K. J.; Arnold, K. M.; Blount, W. W.; Lawniczak, J. E.; Lowman, D. W., *Macromolecules* **1995**, 28 (12), 4122-4128.
27. Ozturk, G. I. P., A.J.; Long, T.E. , *Polym. Prep. (Am. Chem. Soc., Div. Polym. Chem.)* **2008**, 49, 34-35.

## Chapter 9: Overall Conclusions

The synthesis of linear, long-chain branched, and crosslinked polyesters were described focusing on tailoring polymer topology and functionality to alter thermomechanical, rheological, and adhesive properties of polyesters. Aliphatic polyesters were synthesized using a melt polycondensation methodology. Tailoring the topology and the chemical composition enabled modification of thermomechanical and adhesive properties.

Aliphatic polyesters having linear and long-chain branched topology were synthesized for adhesive applications. Synthesis of a series of linear and long-chain branched aliphatic low- $T_g$  polyesters was investigated to determine the influence of molecular weight and branching on adhesive performance. Low- $T_g$  polyesters having different degrees of branching were explored to investigate the influence of long-chain branching on melt rheology and adhesive properties. Long-chain branched low- $T_g$  polyesters displayed an enhanced cohesive strength compared to linear samples. Moreover, changing the polymer composition allowed tailoring the adhesive properties. Low- $T_g$  copolyesters were synthesized from melt polycondensation of DMCD with various molar ratios of DEG, 1,4-butanediol, and CHDM to investigate the relationship between polymer composition and adhesive properties. Low- $T_g$  copolyesters containing CHDM exhibited a holding power of 7000 min which correlated to significant improvement in cohesive strength

Michael addition chemistry was utilized to chemically crosslink oligomeric polyesters with different chemical compositions and molecular weights. The influence of molecular weight between crosslink points on thermal and mechanical properties of the

crosslinked networks was investigated for networks having a varying chemical composition and crosslink density. Poly(caprolactone) (PCL) based oligomers with telechelic acetoacetate functionality was obtained from transacetoacetylation of PCL diol and triols with different molecular weights. Controlling the molecular weight and topology of PCLs allowed controlling the thermal and mechanical properties of the resulting networks. Thermal and mechanical properties of the networks were highly dependent molecular weight of the PCL precursor due to the effect of crosslink density. The glass transition temperature of the networks increased from -64 to -42 °C as the molecular weight of the acetoacetate functionalized PCL precursor increased from 1000 to 4000 g/mol. Moreover, the degree of crystallinity of the networks was dependent on the molecular weight of the PCL segment due to influence of crosslink density. Networks having PCL segments with molecular weights of 2000 and 4000 g/mol were semicrystalline. Conversely, the crystallinity was suppressed for the networks synthesized from acetoacetate-functional PCL with molecular weight of 1000 g/mol. Differences in tensile properties of the networks were attributed to the differences in crystallinity and crosslink density. The crosslink density was theoretically highest for the PCL(1K)-NPG network, however the modulus was lower due to the absence of crystallinity. Moreover, lower elongation was obtained due to the higher crosslink density that restricted the extension of the network. Despite of their lower crosslink density, the networks synthesized from poly(caprolactone) precursors having molecular weights 2000 and 4000 g/mol demonstrated higher moduli and the yield points due to the presence of crystallinity. Moreover, controlling the topology of the PCL segment enabled control of the crystallinity and tensile properties. As the topology of the

precursor was changed from linear to branched architecture, the crystallinity was suppressed due to presence of branch points. Crosslinking of acetoacetate-functional star-shaped PCL and NPGDA produced networks amorphous networks. The glass transition of the network was increased from -42 to -25 °C. Moreover, the modulus was increased compared to the network synthesized from a linear PCL analog with similar molecular weight. The increase in mechanical properties was attributed to higher crosslink density and the presence of branch points in the star-shaped PCL segment of the network.

The Michael addition chemistry was also utilized to form covalently crosslinked networks using acetoacetate-functional oligomeric poly(trimethylene succinate)s and poly(trimethylene adipate)s. Oligomeric polyesters with telechelic hydroxyl functionality were synthesized from melt polycondensation of adipic and succinic acid with 1,3-propanediol. Molecular weights of the polyols were varied systematically to probe the influence of the molecular weight on the thermomechanical properties of the networks. The influence of precursor molecular weight on the thermomechanical properties was investigated. The polyols were then end-functionalized with acetoacetate groups and reacted with neopentyl glycol diacrylate in the presence of a basic catalyst at room temperature. DMA and DSC analyses indicated the influence of molecular weight of the oligomeric polyesters on the thermal and mechanical properties. DSC analyses showed that the extent of crystallinity depended on the molecular weight of the precursor, which also impacted crosslink density.  $T_g$ s of the poly(trimethylene succinate)s increased from -49 to -42 °C as the molecular weight increased from 1000 to 3000 g/mol. Similarly, the  $T_g$ s of the oligomeric poly(trimethylene adipate)s increased from -63 to -43 °C as the

molecular weight increased from 1000 to 4000 g/mol. DSC analysis also showed that the glass transition temperature of the networks was dependent on the molecular weight of the polyester precursor.  $T_g$  of the networks decreased as the molecular weight of the poly(trimethylene succinate) and poly(trimethylene adipate) precursors increased. The  $T_g$  of the networks increased from -51 to -31 °C as the molecular weight of the poly(trimethylene adipate) segment in the networks was decreased from 4000 to 1000g/mol. Poly(trimethylene succinate) based networks displayed similar change in  $T_g$  which was attributed to the difference in molecular weight between crosslink points.

In addition to linear and long-chain branched topologies, crosslinking of low- $T_g$  polyesters as investigated to potentially improve the adhesive properties. Hydroxyl-terminated low- $T_g$  oligomeric polyesters were synthesized in the melt phase using the melt polycondensation method and subsequently functionalized with acetoacetate groups. Crosslinking of acetoacetate-functional low- $T_g$  polyesters with NPGDA using different levels of catalyst produced networks with 10, 60, and 80% gel fractions.  $T_g$ s of the networks varied from -27 to -9 °C depending on the gel fraction. Furthermore, measurement of storage and loss modulus during the reaction enabled characterization of gel time. Investigation of the relationship between catalyst concentration and gel time revealed that gel time decreased from 180 to 6 min depending on catalyst concentration. The ability to control the gel fraction, gel time, and  $T_g$  of the networks offered potential for utilization of crosslinked low- $T_g$  polyesters for adhesive and coating applications.

## Chapter 10: Suggested Future Work

### 10.1 Synthesis of Low- $T_g$ Polyesters for PSA Applications

Synthesis and characterization of aliphatic polyesters having linear and long-chain branched topologies indicated that the adhesive performance highly depended on the molecular weight of and composition the low- $T_g$  polyesters. The polymers displayed peel strengths comparable to commercial adhesives. However, the cohesive strength was low compared to acrylic based adhesives due several reasons including absence of non-covalent interactions and low molecular weight of the synthesized polyesters. Hydrogen bonding and high molecular weight contributes to the cohesive strength acrylic adhesives. One possible approach to enhance the cohesive strength of low- $T_g$  polyesters is the introduction of pendant ionic groups that would lead to intermolecular non-covalent interactions. Synthesis of low- $T_g$  polyesters with different levels of the dimethyl-5-sulfoisophthalate sodium salt is a possible route to increase the cohesive strength through aggregation of pendant ionic groups (Figure 10.1).

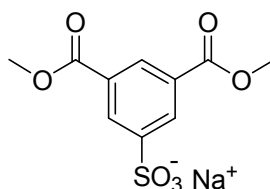


**Figure 10.1.** Chemical structure of dimethyl-5-sulfoisophthalate sodium salt.

The adhesive properties of low- $T_g$  polyesters that were discussed in several chapters were characterized in the absence of tackifiers and plasticizers. A detailed analysis of compatibility of tackifiers and characterization of adhesive properties of formulations containing different levels of additives could be beneficial in terms of enhancing the adhesive performance.

## 10.2 Synthesis of Polyester Based Michael Addition Networks

Polyesters are promising biodegradable polymers due to the susceptibility of the ester bond to biological attack and hydrolysis, predictable biodegradation kinetics, and the potential to tailor the polymer structure to adjust degradation rates for specific applications. Changing the chemistry of the structural units on the polyester backbone permits tailoring thermomechanical properties and biodegradation behavior. In chapters 7 and 8 synthesis and characterization of polyester networks with various compositions were described in detail focusing on structure-property relationships. Furthermore, relationship between thermomechanical properties and biodegradation should be investigated.

Poly(caprolactone) based Michael addition networks show promise for biocompatible and biodegradable systems due to the susceptibility towards hydrolysis or enzymatic degradation. Characterization of the thermomechanical properties of the networks as a function of molecular weight indicated that the extent of crystallinity highly depended on the molecular weight of the precursor. Changing the molecular weight of the polyester precursor allowed synthesis of amorphous or semicrystalline networks. Moreover, changing the topology of the precursor permitted altering the thermal properties. Therefore, the influence of topology and crosslink density on the biodegradation behavior of poly(caprolactone) based networks should be investigated. Biodegradation occurs in the amorphous phase rather than the crystalline phase, therefore the topology and the molecular weight of the precursor is expected to have a significant influence on the biodegradation behavior of these networks. Biodegradation of the



Synthesis and characterization of crosslinked networks using polyester precursors with varying molecular weight indicated that thermomechanical properties of these networks highly depend on the precursor molecular weight. For PCL based networks, crosslinking of the acetoacetate functionalized precursor (1000 g/mol) produced amorphous networks. As the molecular weight of the precursor reached 2000 g/mol, semicrystalline networks were obtained. Moreover, the tensile properties significantly changed. The properties of the networks can be further altered using a mixture of polyester precursors with different molecular weights. Moreover, changing the weight percentages could allow fine tuning the resulting mechanical properties.

### **10.3 UV-curing of Michael Addition Networks**

Crosslinking of polymers using UV-radiation received significant attention in the literature due to fast cure rates and low emission of volatile organic compounds.<sup>1</sup> UV-initiated crosslinking was utilized in synthesis of crosslinked networks for many applications including membranes, hydrogels,<sup>1</sup> adhesion barriers, *in-situ* crosslinkable adhesives, and scaffolds.<sup>2</sup> Our research group<sup>3,4</sup> previously investigated *in-situ* crosslinking of polyesters with pendant photo-functional groups received bioadhesive applications due fast curing rates at physiological temperatures with minimal production of heat. UV-curing is a rapid, effective, and well-controlled curing technique that can be performed at low temperatures in the presence of a light source and an appropriate initiator with minimal heat production.<sup>5</sup> However, the presence of photoinitiators in UV-curable systems is undesirable in applications such as food packaging due to potential migration of the photoinitiator to the surface. The literature reported undesired color and odor upon UV-curing due to formation of byproducts from photolysis of the initiators.

Recently, UV-curing of polymers in the absence of photoinitiators received interest in medical applications. Wang et al.<sup>6</sup> showed that oligomers prepared from Michael addition of  $\beta$ -diketones,  $\beta$ -ketoesters (Figure 10.3) and multifunctional acrylates can undergo UV-curing in the absence of photoinitiator. As depicted in Figure 10.4, alpha-cleavage upon UV exposure as proposed for Michael addition oligomers to explain the formation of radical species. Alpha-cleavage and subsequent decomposition with loss of carbon monoxide is proposed to form radicals that may initiate further polymerization. It should be noted that it is important to characterize the absorbance of the initiating species and to select the light source with an appropriate wavelength.

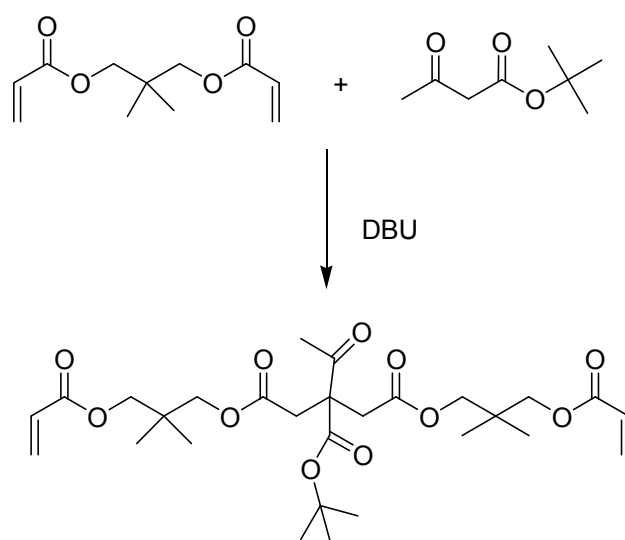


**Figure 10.3.** Synthesis of Michael addition oligomer.



applications including food packaging would benefit from a UV-curable system that works in the absence of catalysts.

Initial UV-curing studies of Michael addition oligomers showed promise for crosslinking of in the absence of photoinitiators. In this work, initially model oligomers were synthesized using Michael addition reaction of *t*-butyl acetoacetate and neopentyl diacrylate and cured using UV-radiation in the absence of initiators. Thermal analysis of the oligomers before and after UV-curing indicated a significant increase in the glass transition temperature. The glass transition temperature of the sample increased from -31 to -24 °C upon curing (Figure 10.5). Moreover, measurement of  $T_g$  from different heating cycles did not indicate increase in the thermal properties of the networks.

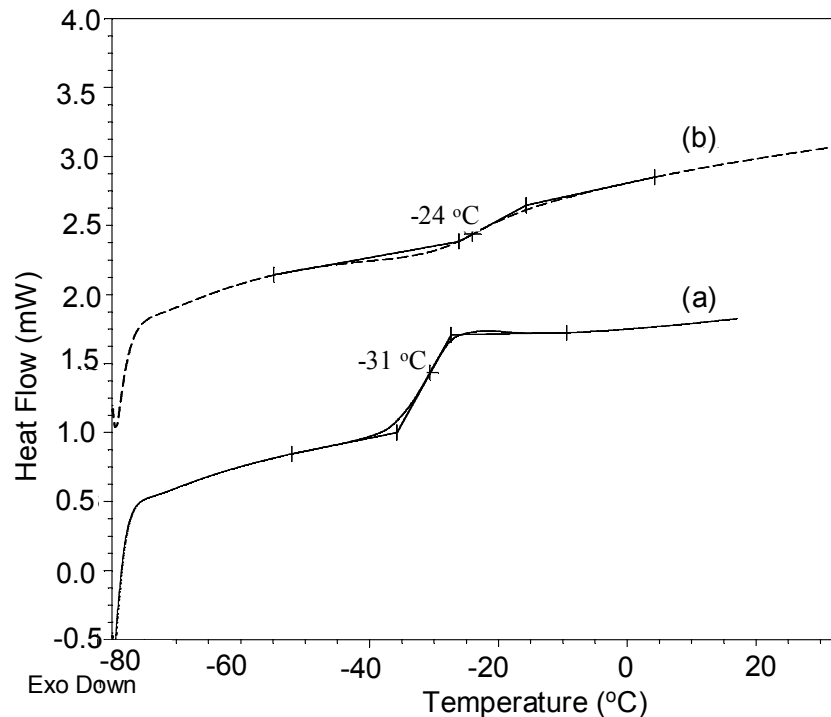


**Figure 10.5.** DSC analysis of Michael addition oligomer a) neat oligomer (before UV radiation) and b) after UV radiation.

Moreover, UV curing of poly(trimethylene succinate) based biodegradable networks were studied to investigate the potential to further crosslink without photoinitiators and enhance the resulting thermomechanical properties. Self-initiating UV curing facilitated the synthesis of a variety of networks having different crosslink density, which display different thermal and mechanical properties. UV-curing of the networks in the absence of photoinitiator indicated increase in gel fractions. Michael addition oligomers and networks were successfully crosslinked and various gel contents were obtained. The glass transition temperature of networks increased from -28 to -15 °C as the gel fraction increased from 70 to 99%. These initial experiments indicated that the networks can be further crosslinked upon UV-irradiation. Further characterization should

be performed to elucidate the use of photocrosslinking of a variety of polyesters in the absence of photoinitiators.

#### **10.4 References**

1. Nguyen, K. T.; West, J. L., *Biomaterials* 2002, 23 (22), 4307-4314.
2. Burdick, J. A.; Philpott, L. M.; Anseth, K. S., *J. Polym. Sci. Pol. Chem.* 2001, 39 (5), 683-692.
3. Karikari, A. S.; Mather, B. D.; Long, T. E., *Biomacromolecules* 2007, 8 (1), 302-308.
4. Karikari, A. S.; Williams, S. R.; Heisey, C. L.; Rawlett, A. M.; Long, T. E., *Langmuir* 2006, 22 (23), 9687-9693.
5. Fisher, J. P.; Tirnmer, M. D.; Holland, T. A.; Dean, D.; Engel, P. S.; Mikos, A. G., *Biomacromolecules* 2003, 4 (5), 1327-1334.
6. Zhang, X. H.; Yang, J. W.; Zeng, Z. H.; Wu, Y. W.; Huang, L.; Chen, Y. L.; Wang, H. H., *Polym. Eng. Sci.* 2007, 47 (7), 1082-1090.